LAND USE LAND COVER CHANGE ANALYSIS OF AFŞİN ELBİSTAN COAL BASIN WITH TWO DIFFERENT CLASSIFICATION METHODS

A THESIS SUBMITTED TO
THE GRADUATE SCHOOL OF NATURAL AND APPLIED SCIENCES
OF
MIDDLE EAST TECHNICAL UNIVERSITY

BY

İLKE ARICAN

IN PARTIAL FULFILLMENT OF THE REQUIREMENTS
FOR
THE DEGREE OF MASTER OF SCIENCE
IN
MINING ENGINEERING

SEPTEMBER 2015

Approval of the thesis:

LAND USE LAND COVER CHANGE ANALYSIS OF AFŞİN ELBİSTAN COAL BASIN WITH TWO DIFFERENT CLASSIFICATION METHODS

submitted by **İLKE ARICAN** in partial fulfillment of the requirements for the degree of **Master of Science in Mining Engineering Department, Middle East Technical University** by,

Prof. Dr. Gülbin Dural Ünver _____
Dean, Graduate School of **Natural and Applied Sciences**

Prof. Dr. Ali İhsan Arol _____
Head of Department, **Mining Engineering**

Prof. Dr. H. Şebnem Düzgün _____
Supervisor, **Mining Engineering Dept., METU**

Examining Committee Members:

Prof. Dr. Ali İhsan Arol _____
Mining Engineering Dept., METU

Prof. Dr. H. Şebnem Düzgün _____
Mining Engineering Dept., METU

Prof. Dr. Bahtiyar Ünver _____
Mining Engineering Dept., Hacettepe University

Assoc. Prof. Dr. Arzu Erener _____
Geomatics Engineering Dept., Kocaeli University

Prof. Dr. Suphi Ural _____
Mining Engineering Dept., Çukurova University

Date: _____

I hereby declare that all information in this document has been obtained and presented in accordance with academic rules and ethical conduct. I also declare that, as required by these rules and conduct, I have fully cited and referenced all material and results that are not original to this work.

Name, Last name : İlke Arıcan

Signature :

ABSTRACT

LAND USE LAND COVER CHANGE ANALYSIS OF AFŞİN ELBİSTAN COAL BASIN WITH TWO DIFFERENT CLASSIFICATION METHODS

Arıcan, İlke

M.S., Department of Mining Engineering

Supervisor : Prof. Dr. H. Şebnem Düzgün

September 2015, 161 pages

Surface coal mining is one of the most widespread energy and economic source for the communities and if implemented inappropriately, causes negative short and long term environmental, social and economic effects (such as loss of vegetation, migration, decreasing water resources, etc.). In order to detect, minimize and avoid all of these impacts, affected areas should be monitored and mapped, constantly. Monitoring surface mining activities by using land use land cover (LULC) maps is one of the effective methods for large areas. However, finding the suitable method for constructing LULC maps for monitoring has been a challenge. Remote Sensing (RS) and Geographical Information Systems (GIS) have been helpful for generation of LULC maps. In this study, two change detection methods, namely, the post-classification change detection based on Support Vector Machine (SVM) and Change-Detection-Driven Transfer Learning Approach (CDTL) are used to monitor change detection in LULC classes in the Afşin-Elbistan Coal Basin, which is one of the largest surface coal mines in Turkey. The Landsat imageries of Afşin-Elbistan Coal Basin for the years of between 1984 and 2014 are utilized for the analyses. The progressive change in the LULC classes since the beginning of the mining activities are obtained quantitavely.

The LULC change detection maps reveal that the vegetation class increases by 3.2%, forest class increases by 55.9%, agriculture class decreases by 5.9%, settlement class decreases by 96.2%, water class increases by 608.1% and soil class decreases by 8.1% between the years 1984 and 2014. It is found that the most and the least effected classes are water and vegetation, respectively. The comparison of post classification change detection based on SVM and CDTL shows that difference in the results are not significantly high. Nevertheless, post classification change detection based on SVM results in higher accuracies than CDTL for each year.

Keywords: Surface Coal Mine, Land Use Land Cover (LULC) Classification, Remote Sensing (RS) Support Vector Machine (SVM), Change-Detection-Driven Transfer Learning Approach (CDTL), Change Detection

ÖZ

AFŞİN ELBİSTAN KÖMÜR HAVZASININ İKİ FARKLI SINIFLANDIRMA YÖNTEMİ İLE ARAZİ ÖRTÜSÜ KULLANIMI DEĞİŞİM ANALİZİ

Arıcan, İlke

Yüksek Lisans, Maden Mühendisşiği Bölümü

Tez Yöneticisi : Prof. Dr. H. Şebnem Düzgün

Eylül 2015, 161 sayfa

Açık ocak kömür madenciliği en çok kullanılan enerji ve ekonomik kaynaklardan biridir. Uygunsuz yapıldığı zaman kısa ve uzun vadeli çevresel, sosyal ve ekonomik olumsuz etkilere yol açabilir (bitki örtüsü kaybı, göç, su kaynaklarının azamlası vb.). Tüm bu olumsuz etkilerin tespit edilmesi azaltılması ve önlenmesi için etkilenen alanların sürekli bir biçimde kontrol edilmesi ve haritalanması gerekmektedir. Açık ocak mandecilik aktivitelerinin Arazi Örtüsü ve Arazi Kullanımı (AÖK) haritaları ile izlenmesi en etkin yöntemlerden biridir. AÖK haritalarını oluşturabilmek için en uygun yöntemi bulmak çözülmesi gereken bir sorun olagelmiştir. Uzaktan Algılama (UA) ve Coğrafi Bilgi Sistemleri (CBS) ise bu adımda devreye girmektedir. Araştırmacılar yıllardır UA ve CBS yöntemlerini kullanaraktan AÖK haritaları oluşturmaktadır. Çalışmada sınıflandırma sonrası fark haritalarını elde etmek için iki farklı yöntem karşılaştırılarak hangisinin daha tutarlı olduğu incelenmiştir. Yöntemlerden biri geleneksel destek vektör makineleri sınıflandırma sonrası arazi değişim metodu ve diğeri de Değişim Belirlemeye Dayalı Transfer Öğrenme yaklaşımıdır. Çalışma alanı Türkiye'nin en büyük açık ocak kömür madenciliğinin uygulandığı Afşin-Elbistan Kömür Havzası olarak belirlenmiştir. Afşin-Elbistan Kömür Havzası'nın 1984 ve 2014 yılları arasındaki Landsat görüntüleri kullanılarak AÖK değişim haritaları çıkarılmıştır.

Analizler sonrası AÖK değişim haritaları incelendiğinde, bitki örtüsünün %3.2 arttığı, ormanların %55.9 arttığı, tarım alanlarının %5.9 azaldığı, yerleşim yerlerinin %96.2 azaldığı, su alanlarının %608.1 arttığı ve toprak alanların %8.1 azaldığı gözlemlenmiştir. En fazla etkilenen sınıf su sınıfı olup, en az etkilenen sınıf ise bitki örtüsü olmuştur. Sınıflandırma yöntemleri karşılaştırma sonuçlarında ise her yıl, her sınıflandırma yöntemi için ayrı ayrı hesaplanılan doğruluk değerlendirmeleri arasında çok fark gözlemlenmemiştir. Geleneksel destek vektör makineleri ile sınıflandırılan görüntülerin doğruluk değerlendirmeleri sürekli olarak daha yüksek çıkmıştır.

Anahtar kelimeler: Açık Ocak Kömür Madeni, Arazi Örtü ve Kullanımı (AÖK) Sınıflandırması, Uzaktan Algılama (UA), Destek Vektör Makinaları, Değişim Belirlemeye Dayalı Transfer Öğrenme Yaklaşımı, Değişim haritaları

To my mother and my father

ACKNOWLEDGEMENTS

I would like to express my sincere appreciation and thanks to my supervisor Prof. Dr. H. Şebnem Düzgün for providing me an opportunity to research under her supervision and to take part at a TÜBİTAK supported 113M463 project. I am highly indebted for her constant encouragement, continuous support and guidance. I feel privileged to be a graduate student of her.

This thesis had its roots from 113M463 numbered TÜBİTAK project. Therefore, I would also like to express my thanks to Prof. Dr. Suphi Ural, from Çukurova University, Prof. Dr. Sibel Kalaycıoğlu, Assoc. Prof. Dr. Emre Alp and Assoc. Prof. Dr. Elçin Kentel, for their valuable contributions during the project.

Also, I am grateful to my colleague Mr. Evren Deniz Yaylacı for his support and help for my studies, and dedicated work for the 113M463 numbered project.

I would like to acknowledge TÜBİTAK for providing financial support for my study.

I would like to express my sincere gratitude to my mother Fahriye Arıcan and my father Ahmet Arıcan for their love, and for their endless patience, encouragement and support for everything I have chosen to do.

My sincere thanks also go to my friends Aylin Acar, Fırat Olcay, Hüseyin Ali Bolat, Burcu Ünlütürk and my other friends for their ideas, support and patience for my loquaciousness.

I would like to thank to my significant other Aykut Tuğrul Bulut for his endless support, patience and love.

Finally I would like to express my love to the cats who settled in my house, Admin and Toma, for just being there.

TABLE OF CONTENTS

LIST OF TABLES

TABLES

LIST OF FIGURES

FIGURES

ABBREVIATIONS

CDTL	Change-Detection-Driven Transfer Learning Approach
CORINE	Coordination of Information on the Environment
DEM	Digital Elevation Model
ETKB	Turkish abbreviation for the Ministry of Energy and Natural Resources
ETM+	Enhanced Thematic Mapper Plus
EUAŞ	Turkish abbreviation for the Electricity Generation Company
GIS	Geographical Information Systems
HGK	Turkish abbreviation for the General Command of Mapping
LULC	Land Use Land Cover
NIR	Near Infrared
OA	Overall Accuracy
OGM	Turkish abbreviation of the General Directorate of Forestry
OLI	Operational Land Imager
PA	Producer's Accuracy
RS	Remote Sensing
SVM	Support Vector Machine
SWIR	Short Wave Infrared
TM	Thematic Mapper
TUBİTAK	Turkish abbreviation of the Scientific and Technological Research Council of Turkey
USGS	United States Geological Survey

CHAPTER 1

INTRODUCTION

1.1 Introduction

Coal had been one of the most consumed product in mining industry, especially in Turkey and it had been an important energy source (electricity, heating, manufacturing, etc.) to the countries for years. Total coal production of the world was 8687 million short tons in 2012 and, for Turkey, the production was 76 million short tons (U.S. Energy Information Administration, 2012).

There are two ore extraction methods; surface and underground mining. Coal mining, particularly surface coal mining, generates significant impacts due to its nature, such as disturbing the topography, and decreasing value of biological and economical attributes on the surrounding environment of the mine (Rathore and Wright, 2007). Also, the surface coal mining accounts for about 40% of world coal production (World Coal Institute, 2009). Therefore sustainable approaches for the mining activities have been searched. As the communities increased their focus on sustainable development, mining companies begun to prioritize conserving the environment. Effective management of surface mining operations for environmental responsibility can be accomplished with intensive monitoring of surface mine areas and disturbed land and earth observation technology can play a central role in this

process (Düzgün and Demirel, 2011). In order to accomplish a successful monitoring for evaluating surface activities and their dynamics at a regional scale, researchers require observations with frequent temporal coverage over a long period of time in order to separate natural changes from human related changes (Latifovic *et al.*, 2005). Land disturbance monitoring for the mining areas can be achieved by the data obtaining the land use land cover (LULC) information. Remote Sensing (RS) and Geographical Information Systems (GIS) tools provides efficient ways of representing the spatial data like LULC maps while easing the process of monitoring. Unlike the site focused studies, satellite data grants a broad territorial analysis, which seldom performed with field methods alone (Moran *et al.*, 1994). LULC change detection analyses help monitoring the disturbed areas resulted from surface mining activities, such as, exploitation of ore, stripping, and dumping overburden. In the same fashion, LULC change detection provides valuable information for planning and management. In addition, temporal resolution of remote sensing satellites captures historical timeline for estimation of LULC changes. There are various change detection methods in the literature with their merits and flows. Lu *et al.* (2004) divided the LULC change detection methods having common characteristics into following five main categories; algebra, transformation, classification, advanced models, and visual analysis (Table 1).The most utilized method for LULC change detection monitoring in the literature is post-classification change detection technique due to its reliability, and ability to extract change matrices. For post-classification change detection, multi-temporal images are individually classified into thematic maps. Then the classified images put into comparison pixel-by-pixel, consecutively. This method minimizes effects of environmental, atmospheric, sensor, and sun angle differences between the multi-temporal images (Lu *et al.*, 2004).

Classification techniques of satellite images are investigated to improve pre-mapping products that enable the user to identify the distribution of the land units within the area with relatively limited field study. These classification methods are divided into two categories as unsupervised and supervised classifications. The

supervised classification method, Support Vector Machine (SVM), is a very popular method designating the classes within the research area. SVM classification results very promising outcomes for creating classification maps and minimizes the classification errors empirically (Tso and Mather, 2009).

Table 1. Change detection methods

Techniques	**Specific Methods**
Image Enhancement (Algebra)	• Image differencing • Vegetation index differencing • Change vector analysis (CVA) • Image regression • Image Ratioing
Image Enhancement (Transformation)	• Principal component analysis (PCA) • Tasseled Cap (KT) • Gramm-Schmidt (GS) • Chi square
Classification	• Artificial neural networks (ANN) • Unsupervised change detection • Hybrid Change Detection • Post-classification comparison
Advanced Models and Visual Analysis	

Lately, instead of obtaining the classification steps manually, users began to automate the classification procedure. There is a new method that is developed by Demir *et al.* (2012), called Change-Detection-Driven Transfer Learning (CDTL). CDTL as being a newly developed approach, offers a vast chance by classifying remote sensing images acquired on the same area at different times with active learning when compared to the traditional way of change detection. The approach classifies an image for which no ground truth information is available by using the

existing information for an image acquired on the same area of interest at a different time (Demir *et al.,* 2012). In this study, post-classification change detection with classified multi-temporal images is adopted. Classification methods chosen as the traditional supervised SVM classification technique and CDTL method.

1.2 Objectives of the Study

The main objective of the thesis is to compare post classification change detection approach based on SVM classification and Change-Detection-Driven Transfer Learning Approach (CDTL) in monitoring the surface coal mining activities. In order to evaluate the performance of the two change detection algorithms, Afşin-Elbistan Coal Basin is selected as it is one of the largest surface coal mines in Turkey.

1.3 Outline of the Thesis

In Chapter 2, a literature survey given in detail, which are environmental impacts of mining, introduction on geospatial information technologies and their related literature research. After overviewing the backgrounds in Chapter 1 and 2, research methodology is presented step by step in Chapter 3. Following Chapter 4 includes the study area, how the methodology is implemented, and results of analyzes. Finally, conclusions and recommendations are given in Chapter 5.

CHAPTER 2

LITERATURE SURVEY

2.1 Monitoring Environmental Impacts of Surface Coal Mining Activities

Mining operations inherently cause various negative environmental effects, mainly as land disturbance, water and air pollution (Table 2). If not managed appropriately, these effects might decrease living standards of people, disturb the habitat and overall environment in a local, regional, or global scale. The impacts of mining activities can be grouped into three main categories according to the level of affected environmental components as land, water, and air disturbances (Düzgün and Demirel, 2011).

Monitoring of the surface mining activities is required to manage the impacts on the environment. Geospatial information technologies, such as RS and GIS, provide for time and cost efficient tools for monitoring the large area. Rathore *et al.* (2007) overviewed the literature studies on the use of geospatial information technologies for monitoring environmental impacts of surface mining activities. They investigated performance of several satellite images on different monitoring conditions, which are monitoring land disruption due to surface coal mining, detection of mine fires, mine revegetation and reclamation monitoring, water pollution assessment, and detection

of subsidence. Moreover, use of Landsat TM data had been found to be superior to Landsat MSS due to the higher spectral resolution, and Landsat TM data favored over SPOT data for monitoring surface mining activities. The importance and efficiency of the incorporation of remotely sensed data with GIS for monitoring, and developing effective long term plans for environmental management and reclamation were also emphasized.

Table 2. List of impacts and essential level of monitoring for surface mining (Düzgün and Demirel, 2011)

Land	
Impact	Monitoring Scale/Level
• Land use change • Removal of top soil • Removal of sub soil • Huge holes and scars on the Earth's surface • Deforestation • Reduced agricultural area	• Regional monitoring on the basis of years and decades
Water	
Impact	Monitoring Scale/Level
• Acid mine drainage • Heavy metal contamination of water resources • Extensive use of water • Chemical contamination • Drainage network destruction and transportation of sediments	• Regional monitoring on the basis of years and decades
Air	
Impact	Monitoring Scale/Level
• Dust • Air blast • Particulate matter • Emissions to atmosphere	• Local monitoring on the basis of days to months

2.2 Geographical Information Systems (GIS)

GIS is a system that captures, stores, controls, manipulates, analyzes and displays data which are spatially referenced to the Earth (Department of Environment, 1987). GIS analyzes data layers that simulates real world as seen in Figure 1. General hardware requirements for GIS are a computer, input devices (plotter, digitizer) and output devices (printer, monitor). The suitable GIS software can be split into five functional groups (Burrough and McDonnell, 1998):

- Data input and verification
- Data storage and database management
- Data output and presentation
- Data transformation
- Interaction with the user.

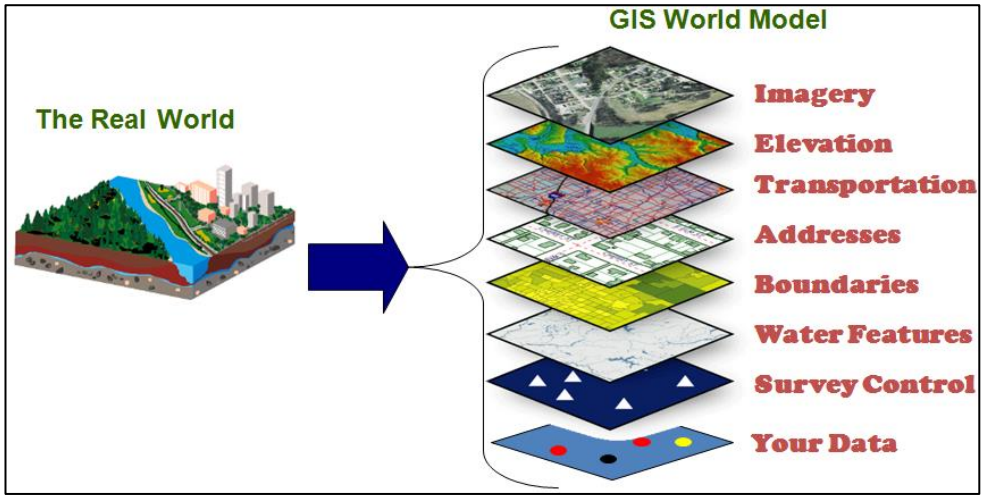

Figure 1. Layer structure of GIS (Henrico County, 1997)

2.3 Remote Sensing (RS)

As defined by Lillesand *et al.* (2004) "Remote sensing is the science and art of obtaining information about an object, area, or phenomenon through the analysis of data acquired by a device that is not in contact with the object, area, or phenomenon under investigation." There are many fields using remote sensing such as, mineral exploration, city and regional planning, monitoring, meteorology, land use land cover observations, disaster monitoring, etc. RS have been used since 1914's. At first, the images taken were the aerial photos and, since then, the technology and the methods are rapidly developed. Nowadays, there are many RS satellites and airborne imagers having specific sensors and different features. Remote sensing systems involve various elements as illustrated in Figure 2.

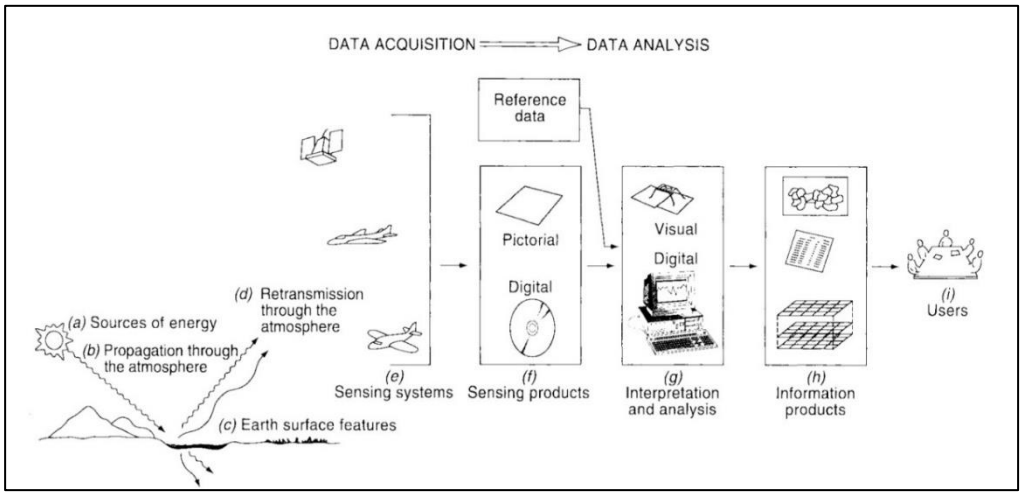

Figure 2. Elements of Remote Sensing (Lillesand *et al.*, 2004)

Images obtained, in other words remotely sensed data, by remote sensing are in raster form and the elements forming the raster are called pixels. Pixels of satellite images used in image analyses represent brightness values and called as digital number (DN) as seen from Figure 3. In color spectrum, each color has a wavelength interval and

satellites record each color with different sensor. Image taken with a sensor having a specific wavelength interval is called band or channel (blue band, red band, green band, etc.).

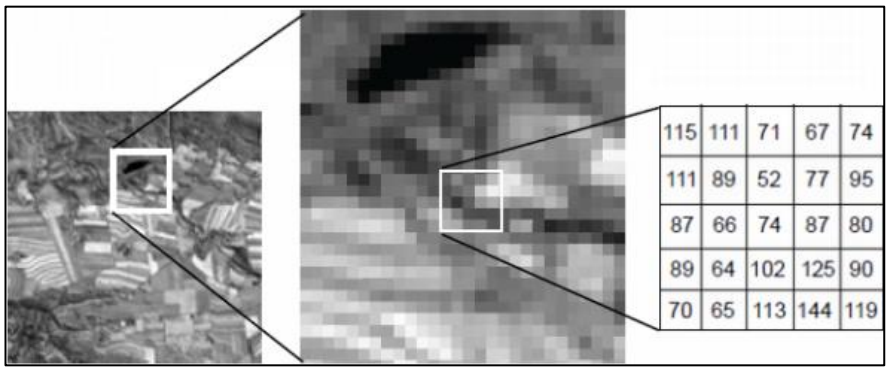

Figure 3. Pixels and digital numbers (DN) in a remotely sensed image

2.2 Land Use Land Cover Change Detection Monitoring for Mining Activities

Land Use Land Cover (LULC) can be described as the materials on the surface and utilizations of the Earth's surface, respectively. Land cover maps produced by utilizing remotely sensed data are an important source of information for monitoring purposes of the LULC across large areas (Aspinall and Hill, 1997). In order to determine LULC change in the study area, two basic methods can be employed (Singh, 2010):

1. Post-classification comparison of independently produced classifications between two images taken on the same area at different times
2. Contemporaneous comparison of multitemporal data

The overall goals in change detection and monitoring are comparing spatial representations of two points in time by controlling all variance caused by

differences in variables not of interest and measuring change caused by differences in the variables of interest (Green *et al.*, 1994).

Researchers began to utilize remotely sensed data for monitoring mining activities with successful launch of the Landsat in 1972. Coker (1977) and Collins (1991) differentiated bare lands from vegetated areas. Parks and Petersen (1987) compared Spot MSS and Landsat TM data for delineation of vegetation and reclamation success in a surface coal mining are in central Pennsylvania. Image analysis and digital techniques emphasized classification of vegetation and coal spoil surfaces. Different vegetation species, age classes, and cover densities are separated with accuracy values ranging from 92% to 115% by maximum likelihood classification. The research demonstrates the potential role of high resolution remotely sensed data in creation of an integrated database that can be used by surface mining regulation enforcement personnel during field inspections. Chaterjee *et al.* (1996) performed a geomorphological classification for Jharia open cast mine covering a relatively large area (about 480 km^2) based on Landsat TM images. In terms of reclamation of mining areas in Turkey, few studies conducted by Erener (2010) and Bascetin (2007) for Seyitömer open cast coal mine, and Pamukçu and Simsir (2006) for limestone quarries located in İzmir. Intensive and constant monitoring of disturbed areas by the use of remote sensing systems is a must to accomplish effective management and control of the mining activities. New satellite platforms having higher spectral and spatial resolution are and will be essential tools for monitoring environmental impacts and reclamation with their cost and time effective characteristics. As mentioned in section 1.1, there are several change detection methods with specific categories, which are described in the following sections. Lu *et al.* (2004) performed an extensive research on LULC change detection methods, which are methods based on algebra (category I), transformation (Category II), classification (Category III) and advanced models (Category IV).

2.2.1 Category I. Algebra

The first category of the change detection methods includes image differencing, vegetation index differencing, change vector analysis (CVA), image regression and image rationing. Common characteristic of these methods is use of distinguishing thresholds to identify the changes. Characteristics, advantages, disadvantages, and the key factors affecting the results are explained in following sections. The majority of these techniques are utilized for change detection with satellite imagery having relatively fine spatial resolution such as Landsat MSS, TM, SPOT, or radar (Lu *et al.*, 2004).

Image Differencing

Image differencing method determines changes in the brightness values between two or more data sets by cell-by-cell subtraction of co-registered image datasets (Muchoney and Haack, 1994). Subtraction produces positive and negative values in changed areas, and zero in areas of no change. A constant is normally added to keep output values in the positive range. The process is expressed mathematically as:

$$\Delta x_{ijk} = x(1)_{ijk} - x(2)_{ijk} + C \qquad (1)$$

where Δx is the change pixel value, x(1) is the value at time 1, x(2) is the value at time 2, C is constant, i=1...*nl* number of lines, j=1...*nc* number of columns, and *k* is a single band (Sohl, 1999). Method cannot provide a detailed change matrix, thus the accuracy assessments cannot be computed. It is simple, straightforward, and the results are easy to interpret. Prakash and Gupta (1998), and Macleod and Congalton (1998) utilized image-differencing method with other algebra related algorithms in order to observe LULC changes.

Vegetation Index Differencing

Vegetation index is an indicator that represents the relative density and health of vegetation for each pixel in a remotely sensed image. Many satellites carry sensors which measuring red and near-infrared wavelength ranges reflected by the surfaces, and with these wavelength ranges, analysts transform raw images into vegetation indices. One of the most widely used vegetation index is Normalized Difference Vegetation Index (NDVI) (U.S. Geological Survey, 2015). The algorithm is expressed by mathematically as NDVI = (NIR — VIS)/(NIR + VIS) where NIR is near infrared radiation and VIS is visible radiation. Calculations of NDVI for a given pixel result in a range from minus one (-1) to plus one (+1); however, no green leaf gives a value close to zero. A zero value means no vegetation and close to +1 (0.8 - 0.9) indicates the highest possible density of green leaves (NASA, 2000). The method reduces effects of illumination and topographic structure.

A remote sensing based LULC change assessment methodology is utilized by Latifovic *et al.* (2004) for the Oil Sands Mining Development in Athabasca, Alta., Canada. Two Landsat images from 2001 and 1992 are analyzed for the study. Researchers applied two LULC change detection methods for each image. The first one is post-classification change detection, and the second one is based on a key resources indicator (KRI), calculated using normalized difference vegetation index. For the post-classification change detection, images are classified with K-means classifier with 15 land cover classes and overall accuracy is calculated as 87%. Post-classification change detection showed a decrease of natural vegetation in the study area (715,094 ha) for 2001 approximately - 8.64% relative to 1992. KRI trend analysis indicated a slightly decreasing trend in vegetation greenness in close distance to the mining development.

Change Vector Analysis (CVA)

A change vector can be described as vector length change and an angle of change from time 1 to time 2 (Jensen, 1996). If a pixel's grey-level values in two images on

dates t1, t2 are given with $G=(g_1, g_2, g_3, \ldots, g_n)^T$ and $H=(h_1, h_2, h_3, \ldots, h_n)^T$, respectively, and n is the number of bands, a change vector is defined as shown in Eq. (2).

$$\Delta G = H - G \tag{2}$$

where ΔG includes all the change information between the two dates for a given pixel, and the change magnitude $//\Delta G//$ is computed as the Euclidean distance in multidimensional space based on the Pythagorean theorem (Eq. 3) (Siwe and Koch, 2008):

$$\|\Delta G\| = \sqrt{(h_1 - g_1)^2 + (h_2 - g_2)^2 + \cdots + (h_n - g_n)^2} \tag{3}$$

CVA has the ability to produce detailed change detection maps but it is difficult to observe and identify the LULC change trajectories. Chen *et al.* (2003) utilized LULC change detection with CVA for Beijing, China from year 1991 to 1997 and with some modifications to the algorithm, researchers concluded that CVA is a reliable LULC change detection method. Other CVA applications are change detection for landscape variables in a region across Mali, Senegal and Guinea (Lambin, 1996), land-cover changes in various regions (Johnson and Kasischke, 1998), and disaster assessment of Hurricane Andrew (Johnson, 1994), disaster assessment of Chernobyl (Schoppmann and Tyler, 1996).

Image Regression

Image regression method establishes relationships between bitemporal images, time 1 and time 2, while estimating pixel values of the time 2 image by the use of an accurate regression function. Then the regressed image is subtracted from the time 1 image. The method reduces the sensor, environmental, and atmospheric differences between the remotely sensed images. Important part of the method is requirement of developing accurate regression functions for the selected bands before performing the change detection (Lu *et al.*, 2004).

Image regression method was utilized by Jha and Unni (1994) in order to detect forest conversion of dry tropical regions consisting Sonbhadra district, Uttar Pradesh, as well as adjoining portions of the Singrauli coal fields, in the Sidhi district, and a part of Sarguja district, Madhya Pradesh, India. Singh (1996) analyzed tropical forest change in the northeastern part of India using Landsat satellite imageries with image regression. Ridd and Liu (1998) compared four different methods, which are image differencing, image regression, tasseled cap transformation (KT), and Chi-square transformation for urban LULC change detection in the Salt Lake Valley area using Landsat TM imagery. The researchers concluded that for band 3 of Landsat TM imagery, image differencing and image regression were the best methods, but none of the algorithms or band selections utilized were superior to the others.

Image Rationing

Image rationing calculates the ratio between the bitemporal images, band by band. Areas of no change have values near wholeness, and changed areas have values less than or greater than one, as the case may be. Observation results showed that the image rationing give a slight overestimation in results (Prakash and Gupta, 1998). This method reduces the effects of shadow, sun angle, and topography, as well .

There are various conclusions regarding the effectiveness of the algebra based change detection methods. This diversity occurs due to the different characteristics of the utilized data and study areas. Additionally, image differencing is the most commonly utilized method among these.

2.2.2 Category II. Transformation

The second category in change detection methods includes principal component analysis (PCA), Tasseled Cap (KT), Gramm-Schmidt (GS), and Chi-square. Methods reduce the data redundancy, but they are lack of change matrices. This is a great

disadvantage for the transformation change detection methods. The GS and chi-square methods are relatively less used in practice due to their complexity compared to PCA and KT transformations (Lu *et al.*, 2004).

Principal Component Analysis (PCA)

Principal component analysis (PCA) is another general tool for coordinate transformation and data reduction in image processing. The new axes formed by PCA are not specified by the user's prior definition of the transformation matrix, but are derived from the correlation matrix computed from the data analysis. The process of PCA can be divided into three steps (Tso and Mather, 2009):

- Calculation of the correlation matrix of multiband images (e.g., in case of a four band image, the covariance matrix has dimension 4 x 4),
- Extraction of the eigenvalues and eigenvectors of the matrix, and
- Transformation of the feature space coordinates using eigenvectors.

PCA reduces data redundancy between the bands and puts emphasis on different information in derived constituents. Also, the algorithm cannot yield a change matrix of class information.

Byrne *et al.* (1980) analyzed land-cover change of Batemas Bay Township by PCA with four channel Landsat images. Ingebritsen and Lyon (1985) performed PCA method in order to detect and monitor LULC change of the area of an open cast uranium mine located in the northwest of Washington, and a wetland area in the Carson Desert, Nevada. Forest mortality of Lake Tahoe Basin, located in the central Sierra Nevada Mountains in the California/Nevada border is analyzed by Collins and Woodcock (1996). In the study, PCA, Tasseled Cap (KT) and Gramm-Schmidt (GS) methods applied to Landsat TM imageries, and results showed that PCA and KT preforms better when compared to GS algorithm.

Tasseled Cap (KT)

Tasseled cap transform (KT) introduced by Kauth and Thomas (1976) uses four band Landsat MSS images. The axes of this four-dimensional feature space are transformed into new four-dimensional coordinates defined by the concepts of brightness, greenness, yellowness, and nonesuch. The transformation involves rotation of the axes of feature space and translation of the origin of the coordinate system (Tso and Mather, 2009). In other words, principle of KT is similar to PCA with the difference of scene dependency. KT transformation is not dependent on the image scene (Lu *et al.*, 2004). Also, the algorithm cannot yield a change matrix of class information.

Coppin *et al.* (2001) utilized KT method for monitoring green biomass change of central Cass County, Minnesota with Landsat TM data. Seto *et al.* (2002) used change vectors of KT to monitor LULC change of Pearl River Delta located in China with Landsat TM data. Forest mortality of Lake Tahoe Basin, located in the central Sierra Nevada Mountains in the California/Nevada border is analyzed by Collins and Woodcock (1996). In the study, PCA, Tasseled Cap (KT) and Gramm-Schmidt (GS) methods applied to Landsat TM imageries, and researchers concluded that PCA and KT performs better when compared to GS algorithm.

Gramm-Schmidt (GS)

Gramm-Schmidt (GS) method was originally used by Kauth and Thomas (1976) in order to derive KT transformation for single date imagery. This method allows subtracting information related to attributes of the study area, which would not be allowed with KT and PCA. Collins and Woodcock (1994) applied the GS transformation to Landsat TM images of Lake Tahoe Basin in order to map forest mortality of the area. Researchers concluded that the GS transformation algorithm is a reliable method for change detection and critical point of this approach is initial identification of the stable subspace of the multitemporal data.

Chi-square

Chi-square method was explored by Ridd and Liu (1998) while comparing the method with three other algorithms to detect changes by utilizing the six bands to create a single band change image. Transformation formula can be seen in Eq (4).

$$Y = (X - M)^T \sum^{-1} (X - M) \quad (4)$$

where Y is digital value of change image, X is vector of the difference of the six digital values between the two dates, M is vector of the mean residuals of each band, T is transverse of the matrix, Σ^{-1} is inverse covariance matrix of the six bands. As a result of the study, accuracy of the chi-square method was calculated above 95% in detecting green-farmland to dry farmland changes. The researchers concluded that none of the methods are superior to the others, and choice of change detection algorithms and band selection depends on environmental conditions.

PCA and KT are most often utilized algorithms among transformation-based change detection methods. When PCA and KT methods compared, PCA is dependent on the image scenes, while KT transformation coefficients are independent of the image scenes. The GS and Chi-square methods are relatively less frequently used in practice due to their relative complexity compared to PCA and KT transforms (Lu *et al.*, 2004).

2.2.3 Category III. Classification

The third category of change detection methods includes artificial neural network (ANN), unsupervised change detection, expectation maximization (EM), hybrid change detection, and post-classification comparison. These methods perform change detection by utilizing classified images. Classification requires sample sets (or training sets), which represents the ground truth information. In order to obtain qualified classification maps, training set selection must be made carefully. If training set is in good quality, resultant classification, and change-detection maps

would be reliable. This category can provide change matrix of difference maps, where the transitions between classes can be observed. Major shortcoming of this category is, time consuming, and difficulty to obtain highly accurate classification maps.

Artificial neural networks (ANN)

Artificial neural networks (ANN) do not demand any assumptions about statistical distribution of the data while using a neural network. The input is utilized in order to train the neural network which is spectral data of the period of change. The performance of a neural network to a specific extent depends on how well the training set is selected, and not on the adequacy of assumptions concerning statistical distribution of the data. Neural network learns from capabilities present in the training data, and with these regularities, constructs rules that can be extended to the unknown data. However, the user must determine the architecture of the network, and also define parameters such as learning rate, which affect the training time, performance, and the rate of convergence of a neural network. There are no clear rules to help with the design of the network, only the rule of thumbs exist (Tso and Mather, 2009).

Woodcock *et al.* (2001) monitored forest change in the Cascade Range of Oregon with Landsat TM and ETM+ images. Bandibas (1998) and Fauzi *et al.* (2001) compared the maximum likelihood (ML) classifier and artificial neural networks (ANN) in the mapping of the land-use/land cover types of Aurora province, Philippines and a tropical rainforest in Indonesia respectively. Overall accuracies of ANN and ML classification methods were compared and results showed that ANN has better accuracy than ML classifier.

Unsupervised change detection

Unsupervised change detection distinguishes spectrally matching groups of pixels in image belonging to time 1 and clusters image into major clusters, then selects similar pixel groups in image belonging to time 2 and clusters image into major clusters. For the final step, the changes are detected between images time 1 and time 2. The unsupervised change detection algorithm is not frequently preferred due to the difficulties in labeling change trajectories (Lu *et al.*, 2004).

Forest change detection with unsupervised change detection for Korkeakoski district of the National Board of Forestry in Finland was performed by Hame *et al.* (1998) with two Landsat TM images from years 1984 and 1985. Remote sensing and GIS technologies were utilized by Manu *et al.* (2004) in order to examine the temporal and spatial extent of environmental degradation from 1986 to 2000 in the Tarkwa gold mining area. In the study, Landsat TM image obtained in June 1986 and Landsat ETM image obtained in June 2001 were used. Landsat images pre-processed and classified with unsupervised classification method. From the observations, for 1986, four LULC classes were identified, and for 2001, the LULC classes increased to six. The results of the classifications showed that most of the agricultural lands were destroyed, and almost 60% of the land was destroyed.

Hybrid Change Detection

The hybrid change detection method combines the advantages of the algebra and classification categories. The algebra methods such as image differencing are often utilized to detect the changed areas, and then classification methods are utilized to classify and analyze detected change areas using the threshold method. In other words, steps of this method are; first step is isolation of changed pixels, second step is applying supervised classification to multi-temporal images, third step is constructing binary change mask from classified thematic maps, and finally sieving out the changed areas from LULC maps generated for each date (Lu *et al.*, 2004). Petit *et al.* (2001) combined image differencing and post-classification change

detection in order to obtain LULC change in the southeastern Zambia. The researchers concluded that this kind of hybrid change detection is better than post-classification change detection methods. Luque (2000) analyzed LULC change detection for New Jersey Pinelands with Landsat MSS and TM satellite imageries by using supervised maximum-likelihood classification technique.

Post-classification comparison

For post-classification change detection, multi-temporal images individually classified into thematic maps, then consecutive classified images put into comparison pixel-by-pixel. This method minimizes effects of environmental, atmospheric, sensor, and sun angle differences between the multi-temporal images (Lu *et al.*, 2004). Other advantage of post-classification LULC change detection is that it provides the change matrix of the multi-temporal thematic maps.

Dimyati *et al.* (1996), Miller *et al.* (1998), Mas (1999), and Foody (2001) monitored LULC changes for Yogyakarta in Indonesia, the northern forest of New England, the southeast of Mexico, southern areas of Sahara, respectively. Munyati (2000) utilized Landsat MSS and TM images to detect wetland change of Kaufe Lats in Zambia with maximum likelihood classification. Kavzaoğlu *et al.* (2009) studied LULC change detection with post-classification method for Gebze district of Turkey with two classification techniques. The experiments in the study pointed out the high urbanization rate in the region. In the comparison of the percentages of LULC classes, it is found that pasture lands and the areas covered by deciduous trees were degraded and transformed into urban lands. In the period between 1997 and 2000, increase in the urban lands reached to around 30%, a substantial change for a five-year period. Emil (2010) utilized multi-temporal high resolution satellite imageries to monitor land degradation of abandoned Ovacık surface coal mine. Historic aerial photos utilized to obtain topography of the pre-mining state of the research area and the LULC classes were determined and mapped with two supervised classification methods. After post-classification LULC change detection analyses, the research

revealed that 63% of the study area had been changed from 1951 to 2008. The changes had been listed as; 37,595 m^2 forest area damaged because of the open pit excavation, 88,046 m^2 forest area disturbed because of the dump sites, 106,012 m^2 forest area recovered due to forestation of old dump sites and 34,877 m^2 forest area converted to agricultural land. Demirel *et al.* (2010) examined LULC changes for an open cast lignite coal mine in Bolu, Turkey. Images of Ikonos in September 2008 and Quickbird in 2004 were utilized in order to analyze the impacts of the surface mining activities on the environment. Six LULC classes were used. SVM was chosen as the classification method and radial basis function was used. For the change detection, post-classification change detection method is utilized, and it was found that mine and dump area decreased by 192.5 ha, forest area increased by 57.4 ha, agriculture area increased by 68.6 ha and water and coal stockpile areas also significantly increased.

2.2.4 Category IV. Advanced Models

Advanced methods transform the image reflectance values to physically based parameters or fractions through linear or non-linear models. Converted parameters allow analyst for better interpretation capabilities. Major disadvantage of the advanced methods are time-consuming and difficulty of developing suitable models for conversion of image reflectance values to biophysical parameters (Lu *et al.*, 2004).

In this category, linear spectral mixture analysis (LSMA) is the most frequently used approach for detection of land-cover change (Adams *et al.*, 1995, and Roberts *et al.*, 1998), Ustin *et al.* (1998) and Rogan *et al.* (2002) utilized this algorithm to observe vegetation change, Radeloff *et al.* (1999) used this method to detect defoliation, Piwowar *et al.* (1998) used advanced methods to visualize environmental change. In studies, researchers concluded that the advanced models can only provide vegetation

change and they are not suitable for other LULC classes. Additionally they are time-consuming and difficult to perform.

2.2.5 Category VI. Visual Analysis

Visual analysis method involves visual interpretation of multi-temporal images and on-screen digitizing of changed regions, while completely utilizing experience and knowledge of the user. Visual interpretation includes observing shape, texture, size and patterns of the remotely sensed images. The disadvantages of visual analysis are; time consuming application of a large area change detection, difficulty to updating the change detection maps of time-series, and difficulty to provide detailed change trajectories. With the rapid development of computer technologies and RS techniques, digital computer processing mainly replaced the visual analysis method (Lu *et al.*, 2004).

All of the LULC change detection methods have advantages and disadvantages. However, post-classification change detection algorithm is the most commonly used one due its reliability (Jensen *et al.*, 1993). For this reason, post-classification change detection method is chosen for the purpose this thesis study. The other reasons are: They provide accuracy measures for the classification results for each image, which provide in-depth understanding of classification performance for each LULC classes, in these methods, image distortions before LULC change detection analyses are minimized.

2.3 Image Classification

Classification is applied to images in order to differentiate the LULC classes. There are two mostly used classification algorithms, which are supervised and unsupervised

classifications. For unsupervised classification approach, it is assumed that there is little knowledge of the characteristics of the data set, and the user is required to input required number of clusters (classes). Finally, classifier automatically constructs the clusters and extracts the thematic maps. In theory, users do not need to interact with automatically operating classifier. Nevertheless, in practice, results of the classifier are modified (accepted and/or rejected) on the basis of user's demands (Tso and Mather, 2009). Iso-data and k-means algorithms are mostly used two unsupervised classification methods. Supervised classification methods are based on statistical learning theory that requires auxiliary information containing knowledge of the area and/or the objects. These methods require some input from the user before classification related to the area to be classified. The input obtained by the user is called a training set and it contains the samples of pixels representing the classes. The validity of the classifications depends on two factors – the size and the representativeness of the training set (Mather, 2004). Therefore, training set selection is the most crucial part of the classification process. Supervised statistical classification carried out in three major steps (Tso and Mather, 2009):

(i) Determination of the LULC classes
(ii) Generation of training sets for each LULC classes
(iii) Utilizing a proper classification technique

The most common supervised classification methods are Maximum Likelihood (ML), Parallelpiped, Minimum Distance, Support Vector Machine (SVM), and Spectral Angle Mapper classifications. Main classes for study area are known from field studies and satellite imageries, and with proper training sets, classification accuracies improve drastically compared to unsupervised classification methods. Therefore supervised classification method is utilized for this study.

Kavzaoğlu, *et al.* (2009) studied LULC change detection with post-classification method of Gebze district of Turkey with two classification techniques, which are Support Vector Machine (SVM) and Maximum Likelihood (ML) classifications. A Landsat ETM+ image acquired in 1997 and a Terra ASTER image acquired in 2002

were used in this study to determine the LULC classes. Training and validation test sets for the two images were formed with randomly selected pixels, thus guaranteeing the maximum variation and representativeness available for each class. All data sets were created with equal numbers of samples for each class, which is important for the estimation of overall accuracy. One-against-one multiclass classification approach and two kernels, which are polynomial and radial basis functions, were used for the classification of the two images with SVM. The quality of the LULC maps obtained from different classification algorithms were compared with the accuracy analyzes. There were six classes, which are water, deciduous, coniferous, pasture, bare soil and urban. Overall accuracies were calculated as 86.95% for ML, 90.81 for SVM-1, 89.71% for SVM-2 in 1997, and 88.0% for ML, 92.81% for SVM-1, 90.93% for SVM-2 in 2002. The study demonstrated that SVM, which has important advantages over the ML classifier, can produce higher classification accuracies. As a result, they appear to be a good alternative to conventional classification techniques. Emil (2010) utilized multi-temporal high resolution satellite imageries to monitor land degradation of abandoned Ovacık surface coal mine. Historic aerial photos utilized to obtain topography of the pre-mining state of the research area and the LULC classes were determined and mapped. In order to construct LULC map, SVM and maximum likelihood classifications carried out and it was concluded that SVM classification creates more homogeneous LULC map than the maximum likelihood classification.

There are various supervised classification algorithms and success of Support Vector Machines (SVMs) suppresses other supervised classification methods (Düzgün and Demirel, 2011). Therefore, SVM classification for post-classification LULC change detection analyses is utilized for this study.

Support Vector Machine Classification

The SVM classification technique is based on the principle of "optimal separation". Process of optimal separation operates as; if the classes are separable, the decision

surface which provides maximum separation between the classes is chosen (Brown *et al.*, 1999). Decision surface is usually called as optimal hyperplane and the data closest to the optimal hyperplane are called support vectors. Users can modify SVM to become a nonlinear classifier through the use of training sets. SVM applies a threshold, which eliminates the certain degree of misclassifications caused by the similar training sets. The threshold creates a soft margin that permits some misclassifications, such as allowing some training points on the wrong side of the hyperplane and eliminates the others. For higher accuracy, threshold should be properly selected (ENVI5.0 Help Menu, 2012). Given a training set of instance label pairs (x_i, y_i), $i = 1, \ldots, l$ where $x_i \in R^n$ and $y \in \{1, -1\}^l$, the support vector machines (SVM) (Boser *et al.*, 1992, and Cortes and Vapnik, 1995) require the solution of the following optimization problem:

$$\min_{w,b,\xi} \frac{1}{2} w^T w + C \sum_{i=1}^{l} \xi_i ,$$

$$\text{Subject to } y_i(w^T \phi(x_i) + b) \geq 1 - \xi_i, \tag{5}$$

$$\xi_i \geq 0.$$

In Eq (5), training vectors x_i are mapped into a higher (maybe infinite) dimensional space by the function ϕ. SVM finds a linear separating hyperplane with the maximal margin in this higher dimensional space. C > 0 is the penalty parameter of the error term. Besides, $K(x_i, x_j) \equiv \phi(x_i)^T \phi(x_j)$ is called kernel function. The basic four kernels are linear, polynomial, radial basis function (RBF) and sigmoid. In this study RBF is utilized (Eq (6)) (Hsu *et al.*, 2010).

$$K(x_i, x_j) = \exp\left(-\gamma \left\| x_i - x_j \right\|^2\right), \gamma > 0. \tag{6}$$

Change Detection Driven Transfer Learning Method

CDTL renews the land use land cover maps with classification of the satellite images acquired for the same area in different times. Main approach of the technique is constructing a primary training set for the first image in the timeline and deriving other training sets with the primary one by using the information between the before and after images. Unsupervised change detection is applied to the source and target images, changed and unchanged areas are determined and the primary training set is transformed with these information. Transformed training set becomes the new training set of the target image to use in classification. Methodology for the CDTL classification approach can be seen from **Figure 4**. Users can determine the supervised classification method for the classification step (Demir *et al.*, 2012). In the proposed method, authors utilized the SVM method for the supervised classifications; therefore SVM is used in this study as well.

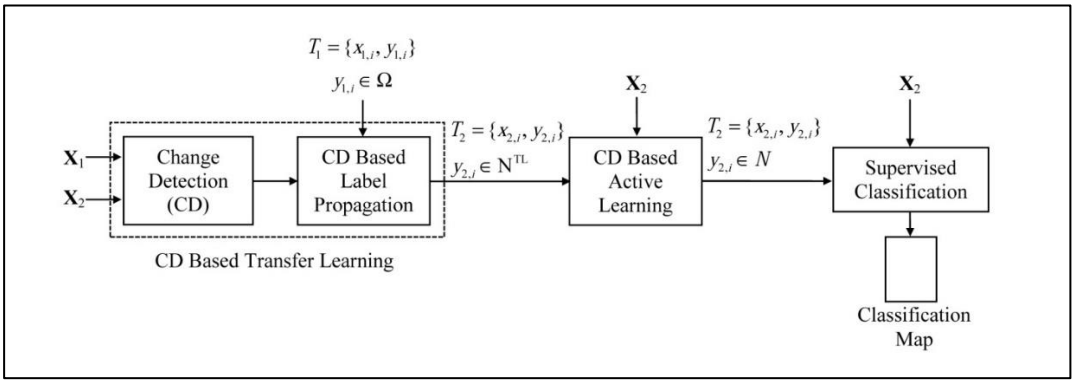

Figure 4. Methodology of change-detection-driven transfer learning (CDTL) approach. (Demir *et al.*, 2012)

Accuracy Assessments

Accuracy is assessed in order to determine whether the classification is valid or not. One of the most commonly used method to calculate accuracy is constructing a classification error matrix (Lillesand *et al.*, 2004). After generation of the error matrix, other important accuracy assessment metrics are calculated, such as

producer's accuracy which controls the accuracy of algorithm, user's accuracy which controls the validity of the training set, overall accuracy which represents the precision of the classification process and kappa coefficient which controls the validity of the overall accuracy. Output of classification is used in post classification comparison algorithm of change detection. An example of error matrix is given in **Figure 5**. In Figure 5, there are six main LULC classes like water, sand, forest, urban and hay, and 1992 random points (pixels) selected from the image. The most successful class is water with 100% producer's accuracy, and the overall accuracy is calculated as 84%.

Error Matrix Resulting from Classifying Training Set Pixels

	Training Set Data (Known Cover Types)[a]						
	W	S	F	U	C	H	Row Total
Classification data							
W	480	0	5	0	0	0	485
S	0	52	0	20	0	0	72
F	0	0	313	40	0	0	353
U	0	16	0	126	0	0	142
C	0	0	0	38	342	79	459
H	0	0	38	24	60	359	481
Column total	480	68	356	248	402	438	1992

Producer's Accuracy	**User's Accuracy**
W = 480/480 = 100%	W = 480/485 = 99%
S = 052/068 = 76%	S = 052/072 = 72%
F = 313/356 = 88%	F = 313/353 = 87%
U = 126/248 = 51%	U = 126/142 = 89%
C = 342/402 = 85%	C = 342/459 = 74%
H = 359/438 = 82%	H = 359/481 = 75%

Overall accuracy = (480 + 52 + 313 + 126 + 342 + 359)/1992 = 84%

[a]W, water; S, sand; F, forest; U, urban; C, corn; H, hay.

Figure 5. Error matrix resulting from classifying training set pixels (Lillesand *et al.*, 2004)

CHAPTER 3

RESEARCH METHODOLOGY

The research methodology followed in this study has three main parts, namely, data collection, Geographical Information Systems (GIS) analyses for the selection of study area and Remote Sensing (RS) studies (Figure 6).

In data collection phase (Figure 6), several different satellite imageries, Ground Control Points (GCPs), digital topographical contour maps and Corine map were gathered. Corine map was obtained in order to observe the classes on the area. GCPs were collected during the field surveys and used for the accuracy assessments.

The GIS analyses mainly serve for delineating the boundary of the study region (Figure 6). Moreover these analyses complement the image processing analyses like collecting GCPs from the field survey. In order to obtain a study area, morphological boundary of a watershed, in which the license area of the mine locates, is used. For this purpose the GIS analyses namely, obtaining Digital Elevation Models (DEMs) from the topographical data, generating slope and aspect maps, establishing the stream network, creating watershed from the slope, aspect and stream network data, and generating the basin boundary.

RS part (Figure 6) consists of image processing analyses, which are pre-processing for correcting any distortions from the raw data, image enhancement for improving

the visual appearance of objects in the images, training set selection for the classifications, performing SVM and CDTL classifications, carrying out accuracy assessments for the classified images, post processing of the classified images by using contrast enhancement and finally conducting change detection analyses.

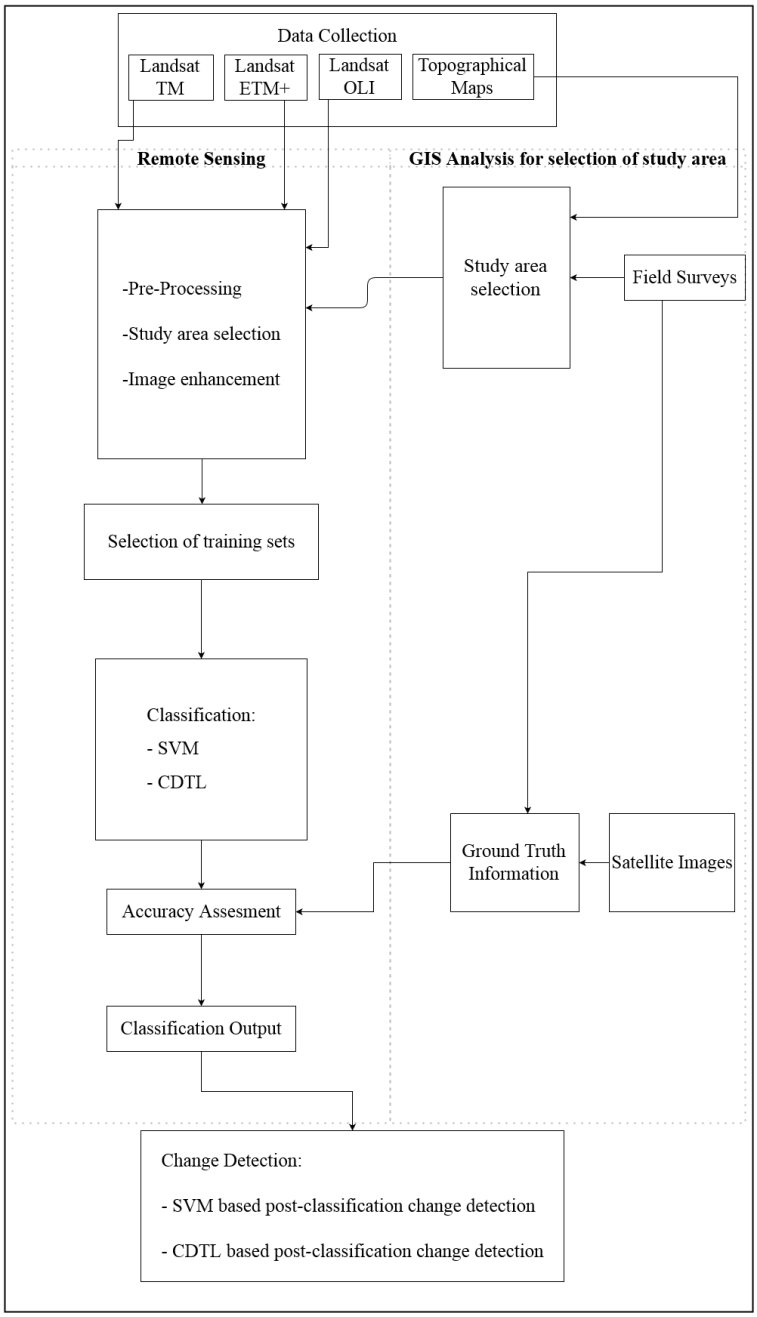

Figure 6. Flow diagram of research methodology

CHAPTER 4

IMPLEMENTATION OF METHODOLOGY: CASE STUDY

4.1 General Information about the Research Area

The study site has 3550 km^2 area entailing Afşin and Elbistan districts in Kahramanmaraş Province, which is located in the South Eastern Turkey (Figure 7). Afşin Elbistan towns are neighbor to Kayseri in the west, Malatya in the east, Sivas in the north and, Nurhak and Göksun in the south. The general topography of the region consists of hills with an average elevation of 1500 m. and the climate of the area is continental with a mean annual rainfall of 570 mm. Ceyhan river, one of the biggest and important rivers in Turkey, passes through the Afşin-Elbistan Coal Basin, having 8 m^3/s flow rate on the average (Mert, 2010). In the basin, a lignite coal mine has been actively working since 1981. In 1973, underground mining trials conducted and it was decided that open cast mining is more appropriate method for the extraction of lignite. Therefore, their operation is open cast mining and there are two power plants located in the basin. The basin has 4.8 billion tonnes of proven lignite reserve and this reserve constitutes 38% of the total lignite reserves in Turkey (Electricity Generation Company of Turkish Republic, 2014). The Plants are established at approximately 15 km. northeast from the Afşin town. The

morphological formations in the basin are 16.3% plains, 59.7% mountains, and 24% plateaus (Ministry of Environment and Urbanization, 2011). Elbistan has the fourth biggest plain with 1000-1300 km^2 surface area and 1100-1150 m average height (Governor's Office of Kahramanmaraş, 2014). Monitoring the surface mining activities and LULC changes in this basin is crucially important due to its potential impacts on large agricultural areas.

Afşin-Elbistan Coal Basin has a 3550.4 km^2 area and the license area covers 296.7 km^2 of the basin. There still are houses with families living and working in their agricultural lands inside the license area of the mine even though there had been expropriations. These expropriations had been done piece by piece, such as only a part of the farm. Therefore there are still changes in settlements and agricultural lands in the license area of the mine.

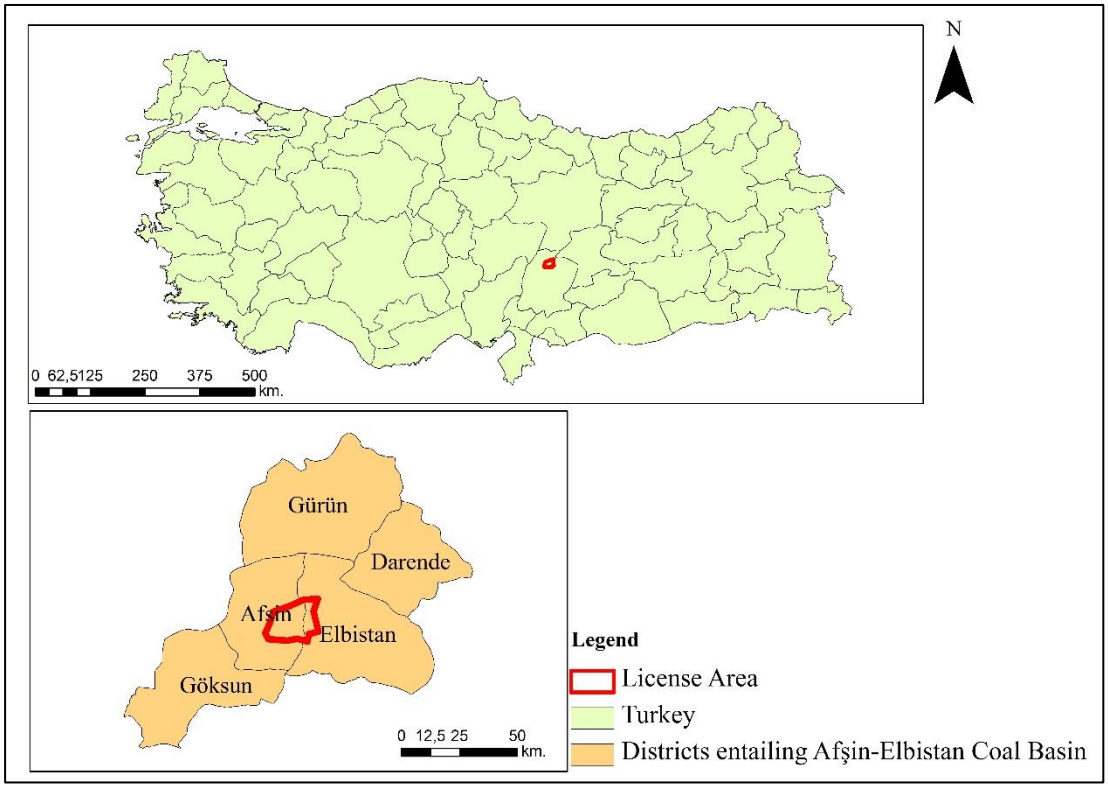

Figure 7. Location of Afşin-Elbistan Coal Basin

Exploration phase in the Afşin-Elbistan Coal Basin began in 1966 by the association of Otto Gold GmbH and General Directorate of Mineral Research and Exploration of Turkish Republic (MTA). The first lignite detected in 1967 and feasibility studies were performed between the years of 1969 and 1970. A summary of activities in the Afşin-Elbistan Coal Basin is provided in Figure 8 (Yaylacı, 2015). As the result of the feasibility analyses, license area divided into five parts and called Sector A, Sector B, Sector C, Sector D and Sector E (Figure 9).

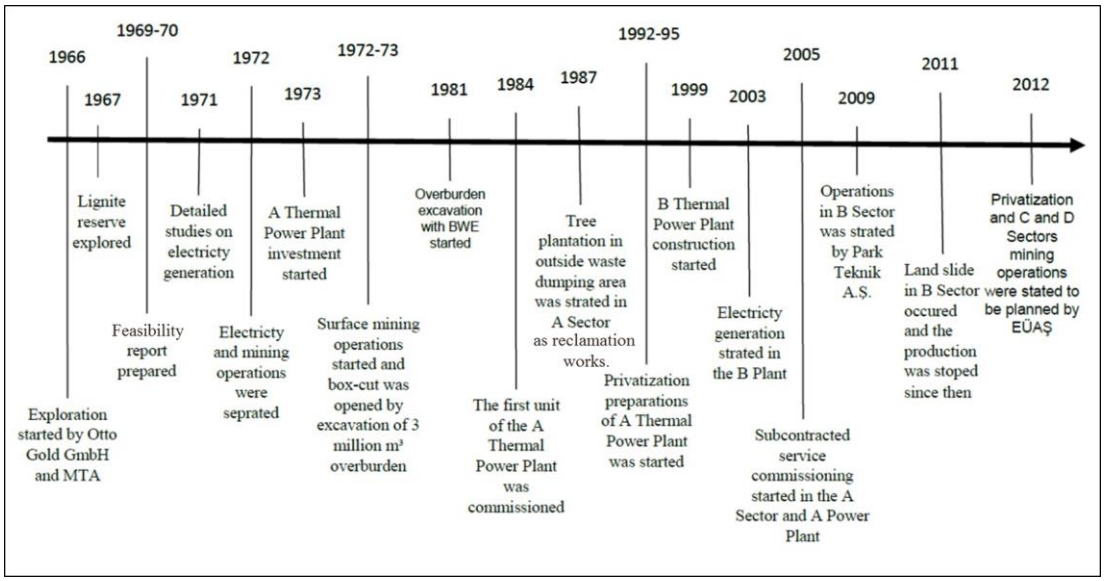

Figure 8. History and Progress of the Mining and Energy Sector Operations in the Afşin-Elbistan Coal Basin

Overburden excavation activities began in 1973, and ore excavation activities began in 1981 in sector A for extraction of 581 million tonnes of lignite. As mentioned before, there are two thermal power plants in the license area, (Figure 9) called A and B power plants having capacities of 1376 MW and 1440 MW, respectively (TKİ, 2011). The first power plant (A) began its activities in 1984 with feed of lignite extracted from the sector A. The second power plant (B) began its activities in 2003 in order to increase electricity production. In 2011 a landslide occurred in sector B and production was stopped since then.

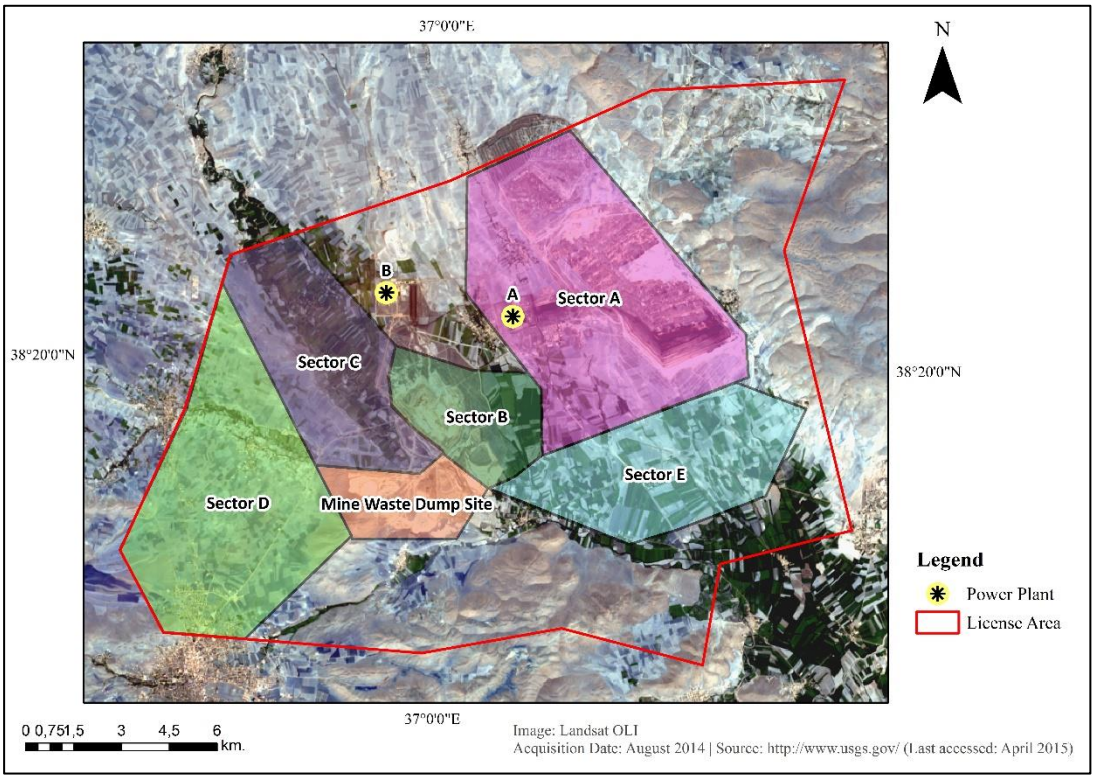

Figure 9. Power plants and sectors of the mine

Potential LULC disturbances for this area are decrease in agricultural areas, increase in water bodies, decrease in settlement, and increase in forested areas. The agricultural lands inside the license area have decreased due to surface mining activities. The agricultural lands outside the license area has decreased due to ash plume carried by wind from power plants as well as expropriation and resettlement activities, which led owner of these lands to move to urban areas and leave the agricultural activities. Change in water bodies inside the license area has potential to affect other connected waterways. Settlement inside the license area can decrease while outside the license area increasing, forested areas can increase due to reclamation works and uncontrolled growth.

4.2 Data Collection and Database

All the data that were gathered and used can be seen from Table 3 with their format, source and dates. Landsat imageries are available for downloading from USGS database, Corine and topographical maps were requested from related departments and Ground Control Points were recorded with handheld GPS device during the field surveys (Figure 10).

Table 3. Collected data

Data Type	Format	Source	Date
Landsat 5 TM Imagery	TIFF	USGS*	21.08.1984
			27.06.1987
			22.08.1990
Landsat 7 ETM+ Imagery	TIFF	USGS*	22.06.2000
			18.08.2003
			23.08.2005
			15.08.2008
			09.09.2011
Landsat 8 OLI Imagery	TIFF	USGS*	24.08.2014
Aerial Photos	TIFF	ETKB***	2001
			2013
Corine Map	SHP	OGM**	1995
Topographic Contour Map	SHP	ETKB***	2014
Topographic Contour Map	SHP	HGK****	-
Mine License Boundary	SHP	HGK****	-
Mine Sector Map	SHP	EUAŞ*****	
Ground Control Points (GCPs)	SHP	Field Works	30.11.2013
			05.04.2014
			06.07.2014

* United States Geological Survey
** General Directorate of Forestry (OGM)
*** Ministry of Energy and Natural Resources (ETKB)
**** General Command of Mapping (HGK)
***** Electricity Generation Company (EUAŞ)

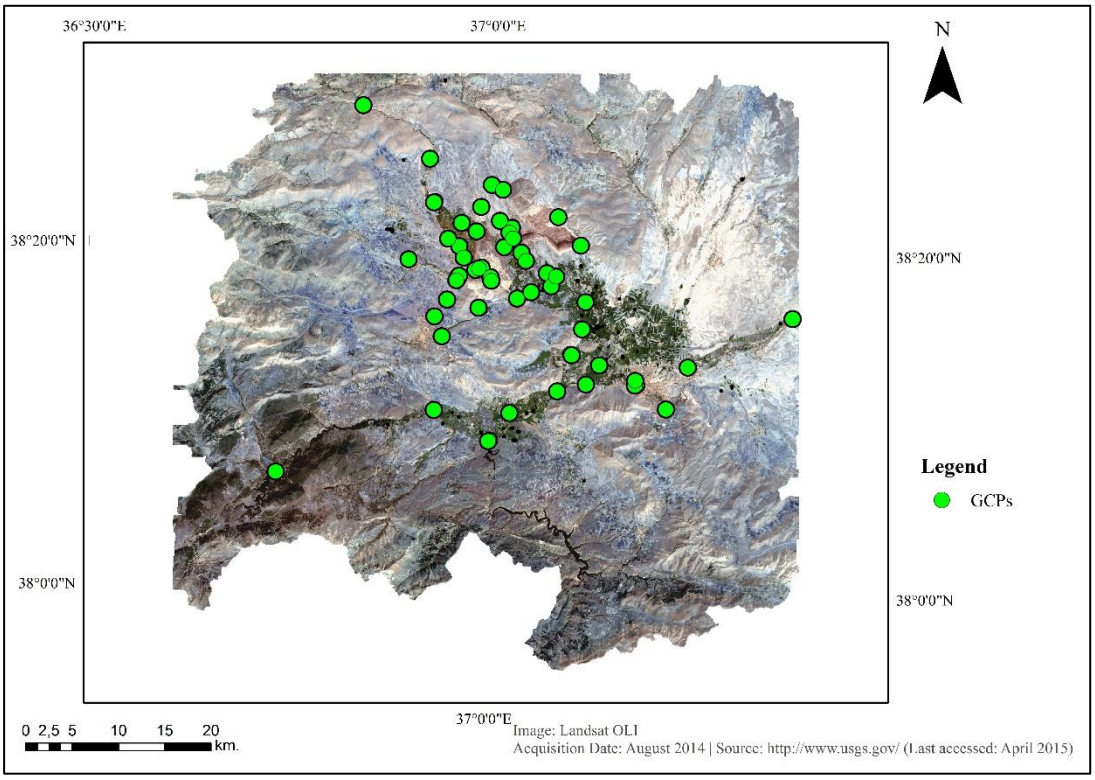

Figure 10. Ground Control Points (GCPs)

Satellite Imagery

In order to detect LULC change, all the Landsat satellite images available between 1970 and 2015 were downloaded from USGS website, which are free for research purposes (U.S. Geological Survey, EarthExplorer, 2014). These images were reviewed and the most suitable ones were chosen for classification analyses. When choosing the years for images, timeline in Figure 8 was taken as reference. Surface mining operations began on 1972 but Landsat images between 1970 and 1984 were unusable due to distortions and sensor errors. Therefore 1984 was taken as the first image of the time series. In order to reduce the problems from Sun angle differences and vegetation phenology changes, images selected were acquired in summer season and had less than 10% cloud cover (Singh, 2010). In order to observe the LULC changes on Afşin-Elbistan Coal Basin, images have three year gaps between them, and most of the milestones in mining activities correspond to the chosen years. No images were found for the study area in the database for the years between 1990 and

1998. Timeline and preview of some of the images can be seen in Figure 11. Detailed band, wavelength and resolution information of the Landsat images, and all the Landsat images utilized in the analyses are given in Appendix A.

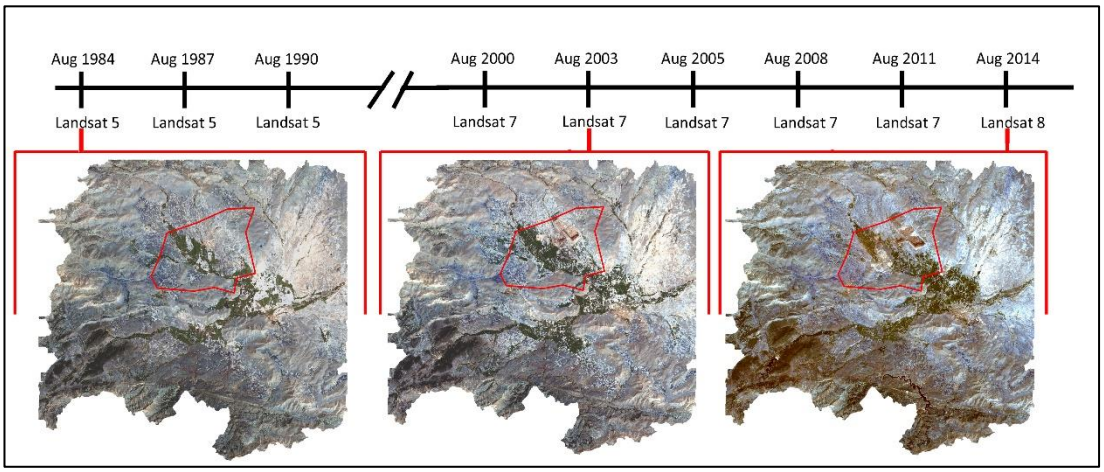

Figure 11. Boundary of study area and previews of satellite imageries: True color displays of (a) TM 1984, (b) ETM+ 2003 (c) OLI 2014

Topographical Maps

Topographical contour maps were obtained from General Command of Mapping (HGK), which includes a very large coverage, (Afşin-Elbistan Coal Basin and the neighboring regions) and the map obtained from Ministry of Energy and Natural Resources (ETKB) was restricted with the license area of mine. Their scale is 1:25000. Topographical maps were utilized to obtain Digital Elevation Models (DEMs) and watershed.

Ancillary Data

Obtained aerial photos are for the years of 2001 and 2013, and cover the license area. The photos were useful when combined with the GCPs, taken during the field surveys, to be used for accuracy assessment of the classifications. Corine map accommodates LULC data from 13 different countries and the section involving

Afşin-Elbistan Coal Basin can be seen from Figure 12. In 1985 the Corine program was started by the European Union. Corine means 'coordination of information on the environment' and it is a prototype research project about many different environmental issues (European Environment Agency, 1995). All of the data is listed in Table 3 and additional data from the analyses are stored and organized using ArcGIS 10 software.

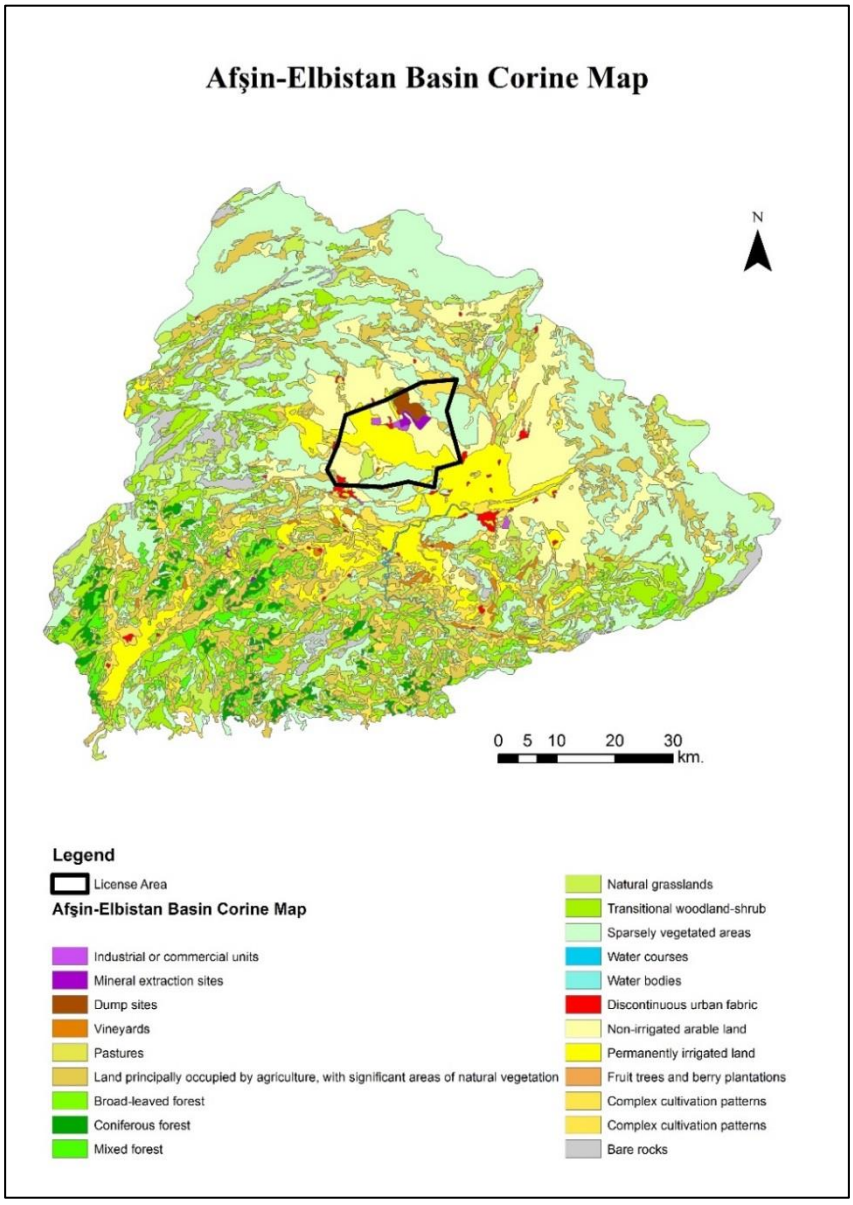

Figure 12. Corine map of the Afşin-Elbistan Basin

4.3 Data Processing

4.3.1 Digital Elevation Model generation for Pre-mining and Mining Terrain

Topographical contour map (obtained from General Command of Mapping) having the scale of 1:25000 was transformed into Digital Elevation Model (DEM) using ArcGIS 10 software. First, contour maps were joined with each other from the end points. After joining, the new polylines were converted to a point cloud with coordinates and elevation data, then extreme elevation values (-9999 or 9999 meters) were eliminated from the point cloud. Finally, Inverse Distance Weighting (IDW) technique was applied to the final layer and digital elevation model of pre-mining terrain was obtained. Elevations alternate between 3025 meters and 440 meters and, average elevation is 1456 meters (Figure 13). The highest elevations represent mountains, which are Binboğa, Berit, and Engizek mountains shown in Figure 13 and Figure 14.

The changes in the topography of Afşin-Elbistan Coal Basin generally occur in the extent of the surface coal mine. Therefore, the license area extracted from topographical contour map obtained from General Command of Mapping (HGK), and the contour map acquired from Ministry of Energy and Natural Resources (ETKB) was located on the extracted part. Join function was applied in ArcGIS 10 software and the new topographic contour map was transformed into DEM with IDW technique. With the surface mining activities, minimum elevation was decreased from 440 meters to 164 meters. Maximum and average elevations did not change (Figure 14). The dark (black and dark grey) colors represent the lower elevations and the bright (white and light grey) colors represent the higher elevations in Figure 14.

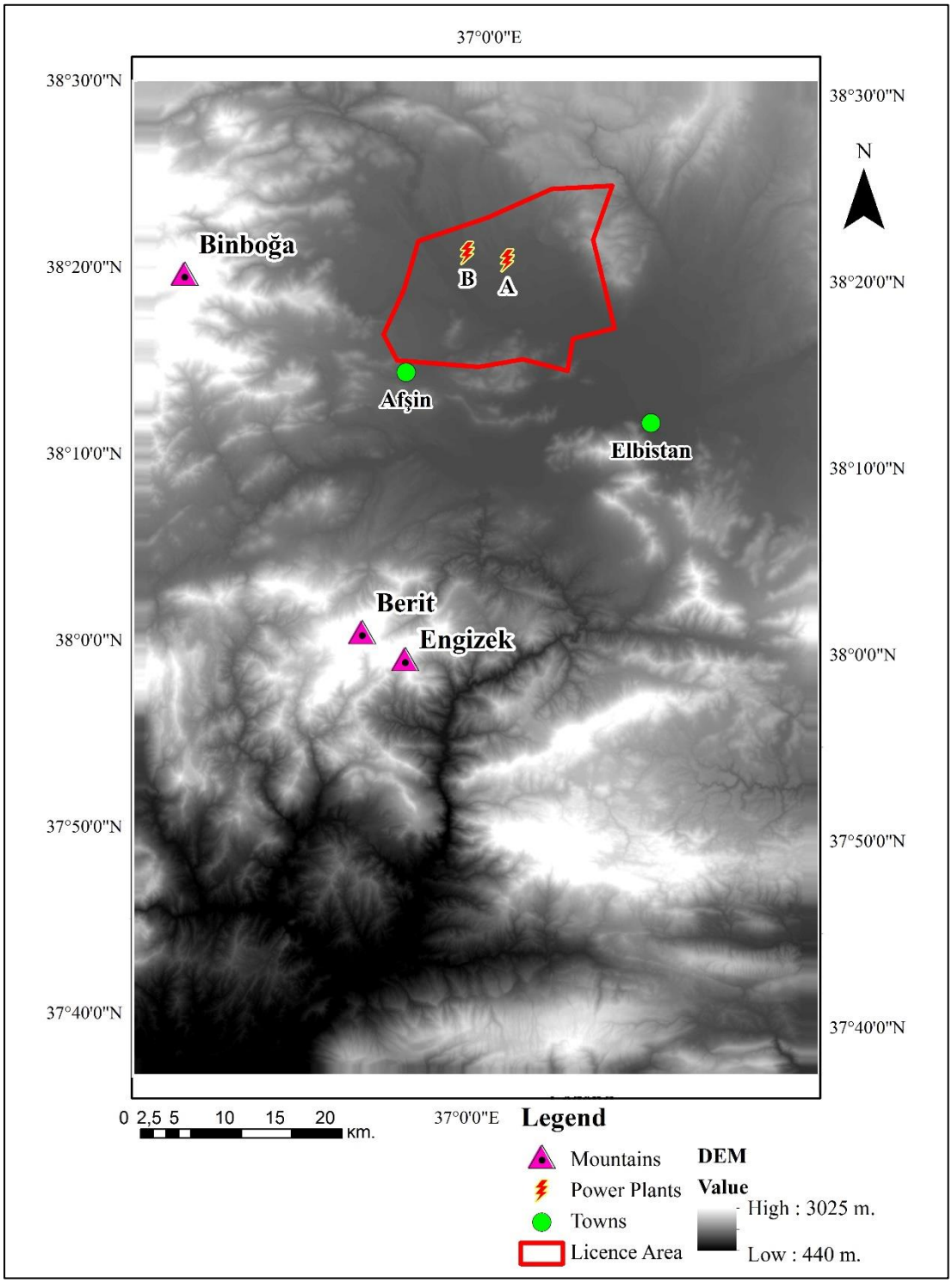

Figure 13. Digital Elevation Model of the pre-mining terrain

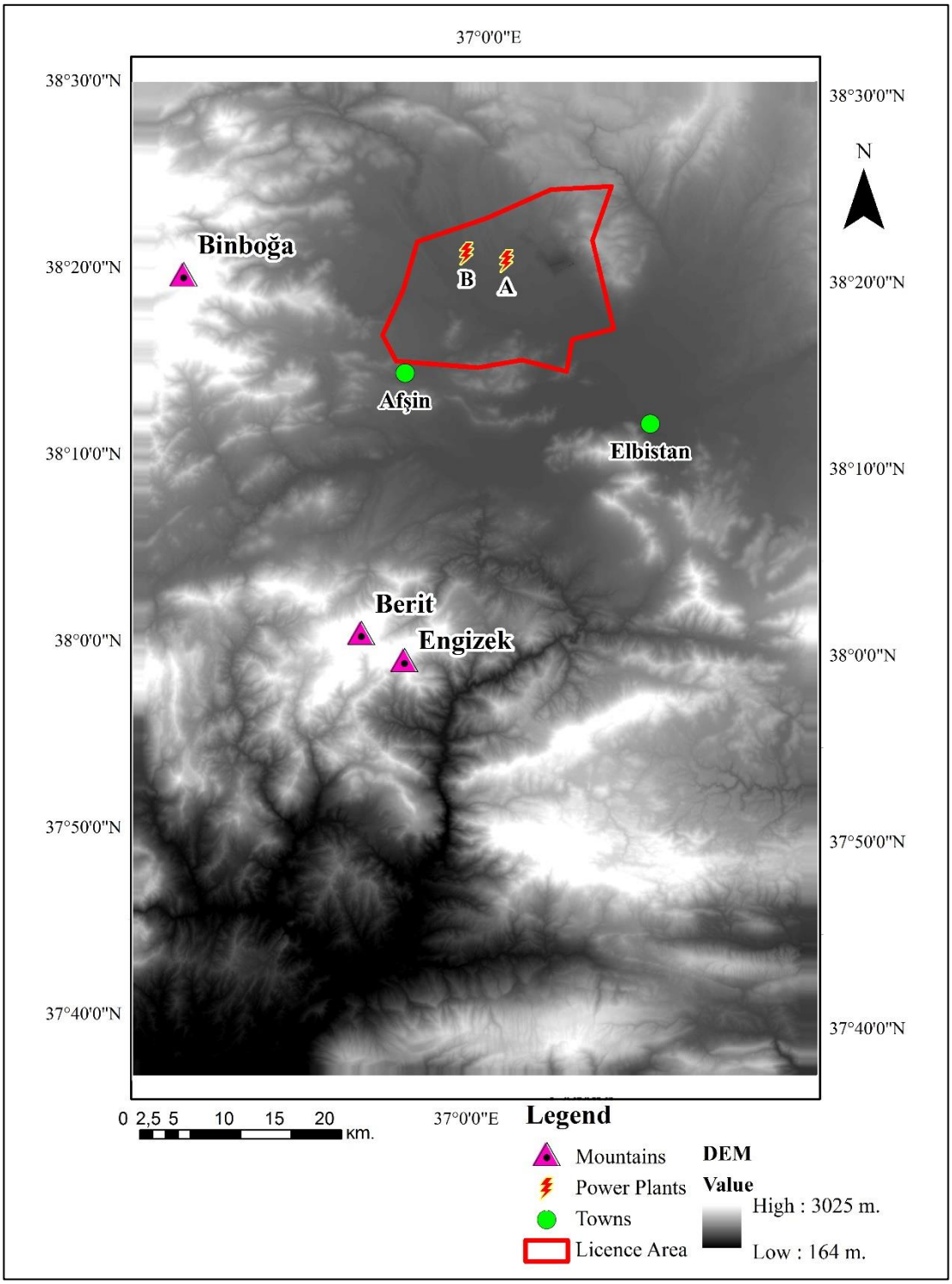

Figure 14. Digital Elevation Model of the mining terrain

In order to perceive the study area better, 3D representation of the DEM was obtained as given in Figure 15. The 3D representation of the Afşin-Elbistan Coal Basin was generated with overlaying study area borders and Landsat OLI image of 2014 as shown in Figure 16.

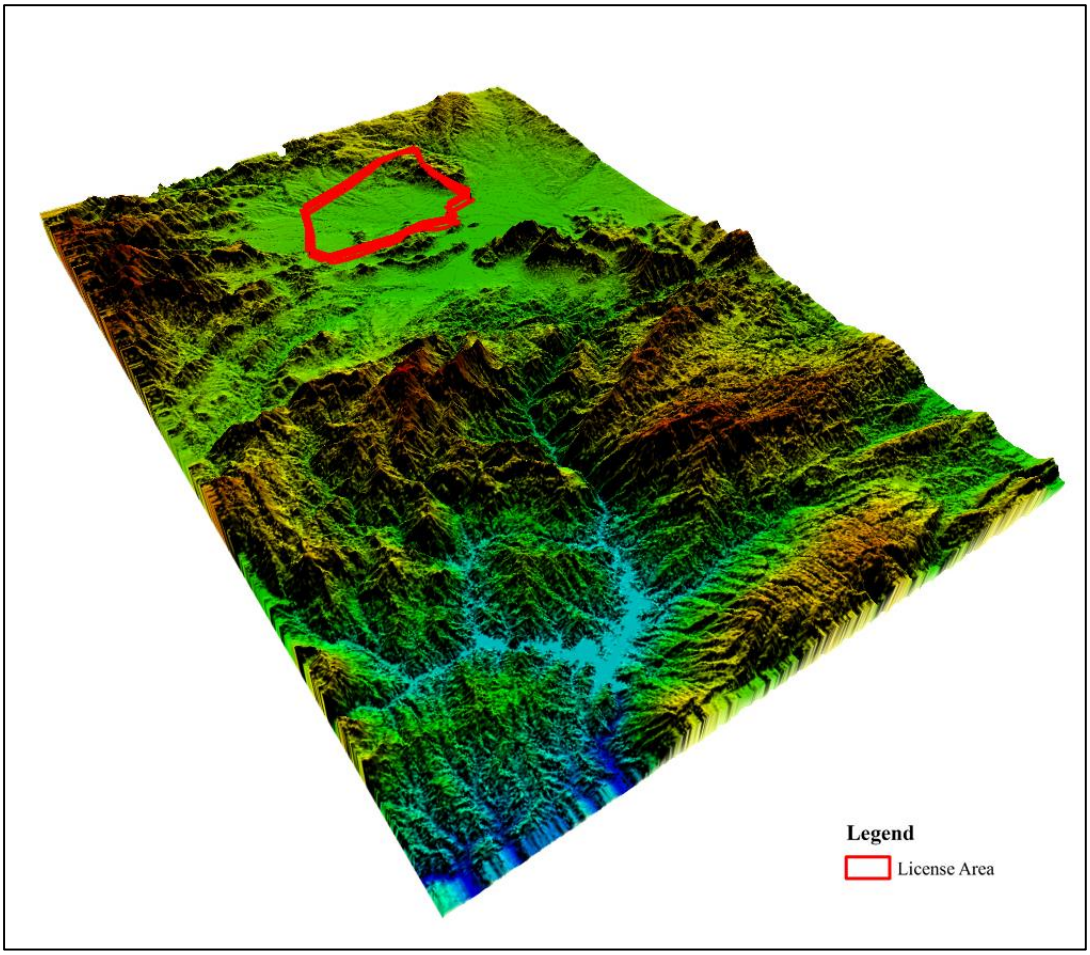

Figure 15. 3D representation of DEM

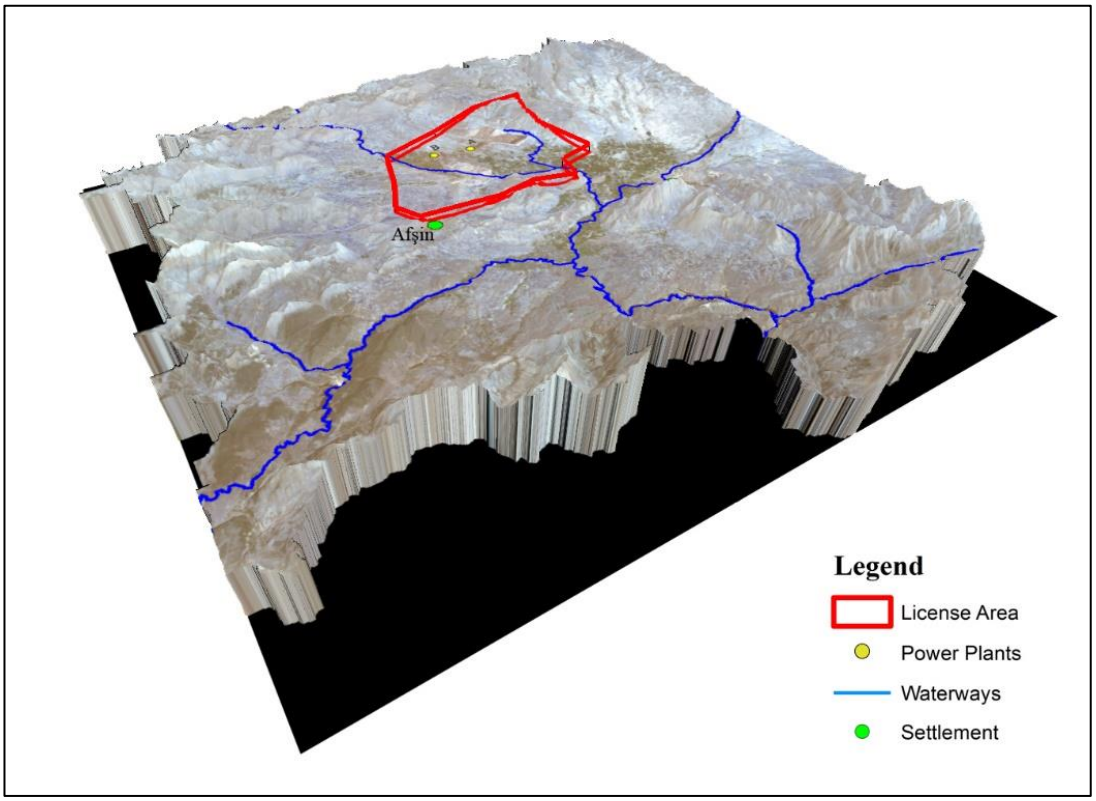

Figure 16. 3D representation of study area

4.3.2 Watershed Generation for Pre-mining and Mining Terrain

Watershed is generated for the purpose of observing the hydrological basins and forms the study area. In order to generate watershed following steps applied on DEMs of pre-mining and mining terrains with the software ArcGIS 10. First, to remove small imperfections in the data, *Fill* function applied to the DEM. Second, to create a raster of flow direction from each cell to its downslope neighbor, *Flow Direction* function applied to the *Fill* raster. Third, to create a raster of accumulated flow into each cell, *Flow Accumulation* function applied to the *Flow Direction* raster. Fourth, to detect pour points by considering highest pour points of the accumulation raster, *Snap Pour Point* function applied to the *Flow Accumulation* raster (Esri, 2010) (Figure 17).

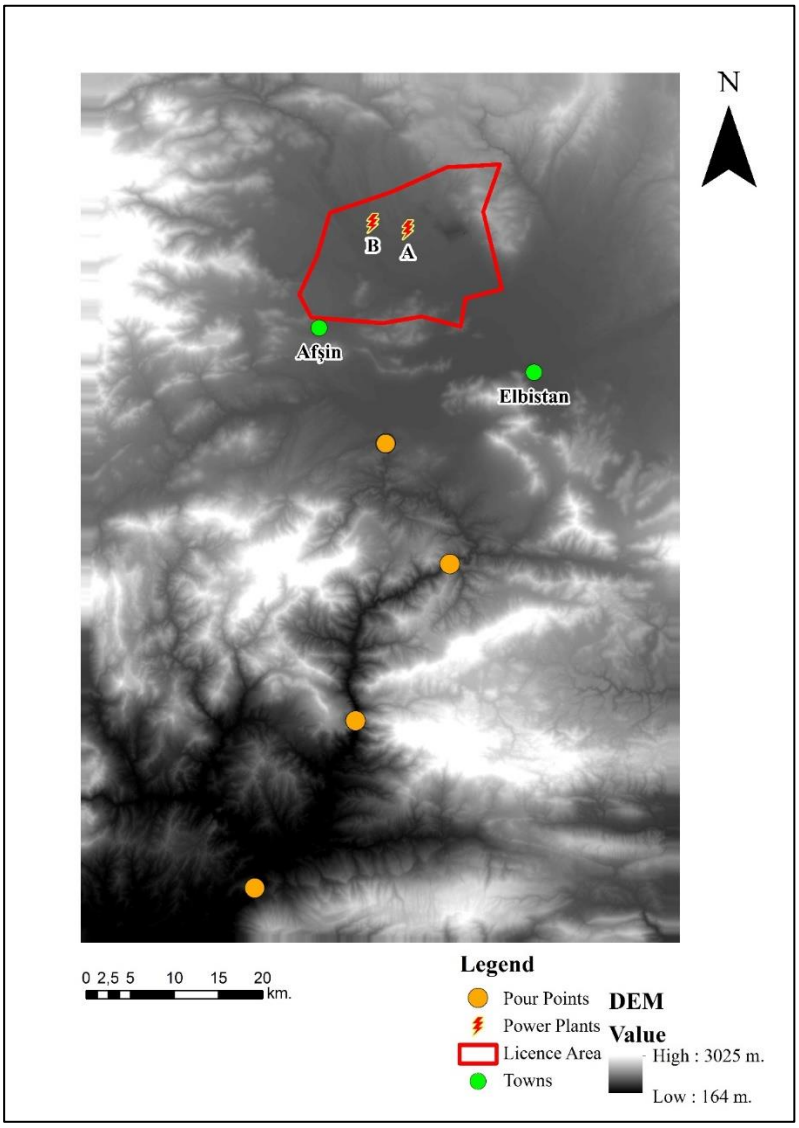

Figure 17. Pour points for watershed analyses

Finally, in order to determine the watershed, *Watershed* function was applied with *Flow Direction* and *Pour Point* layers. All of the steps were applied to the pre-mining and mining DEMs with different pour points and, eight watersheds obtained, four watersheds for pre-mining and four watersheds for mining stages. The generated watersheds can be seen from Figure 18 and Figure 19. Watersheds generated for pre-mining and mining periods were overlaid and no discrepancy was observed. For further analyses, watershed 3 (Figure 20) was chosen to utilize as Afşin-Elbistan Coal Basin.

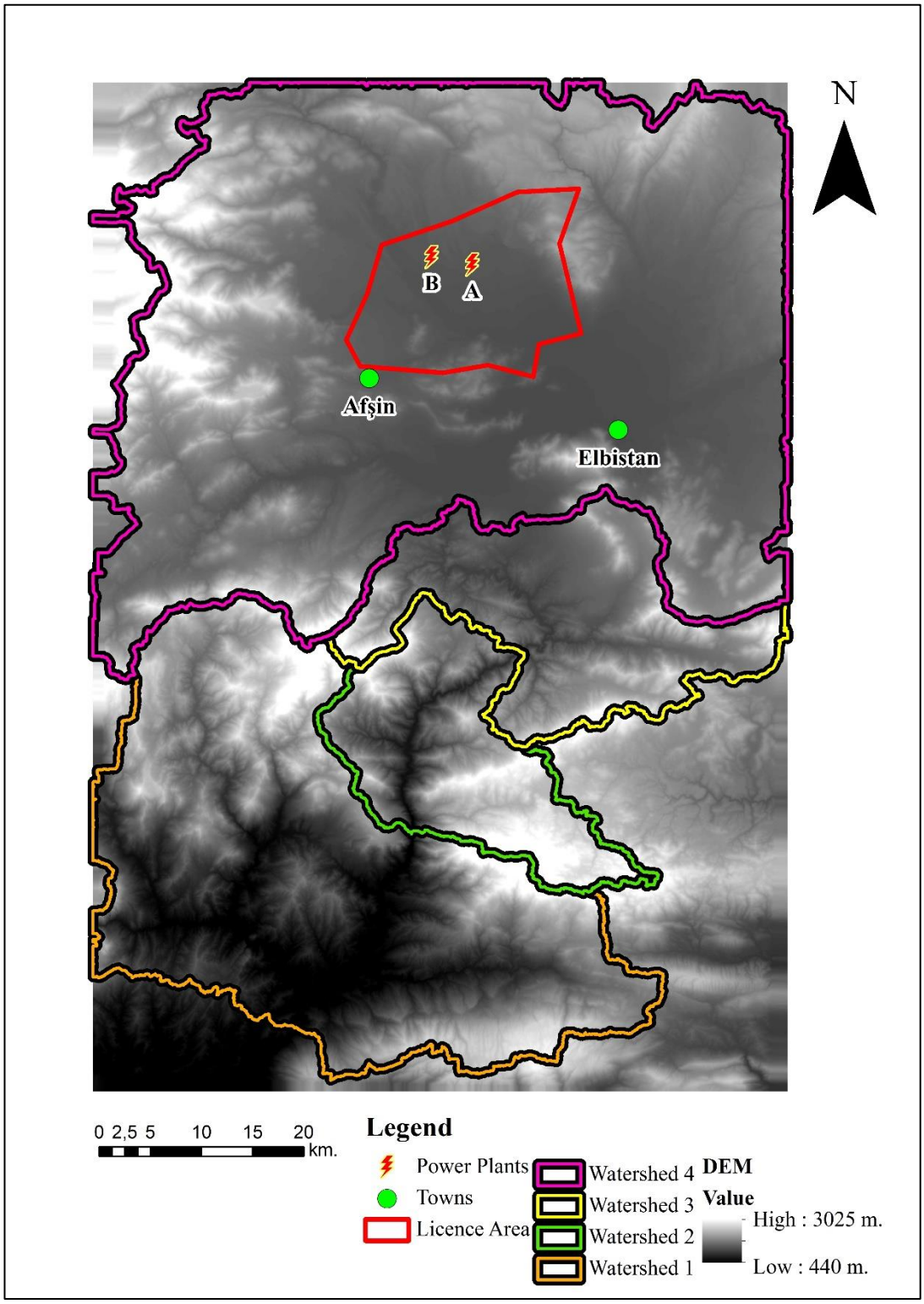

Figure 18. Watersheds of pre-mining terrain

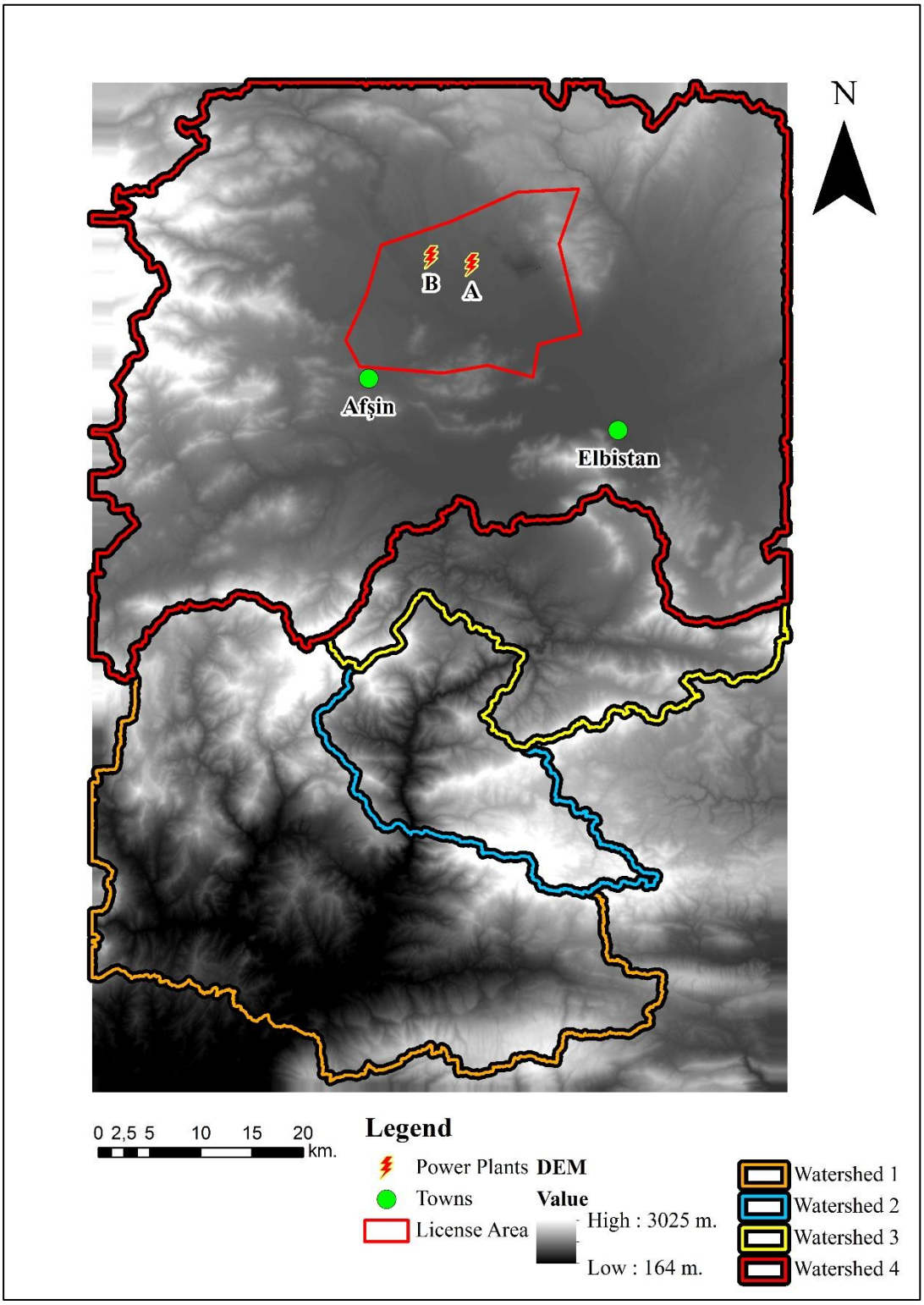

Figure 19. Watersheds of mining terrain

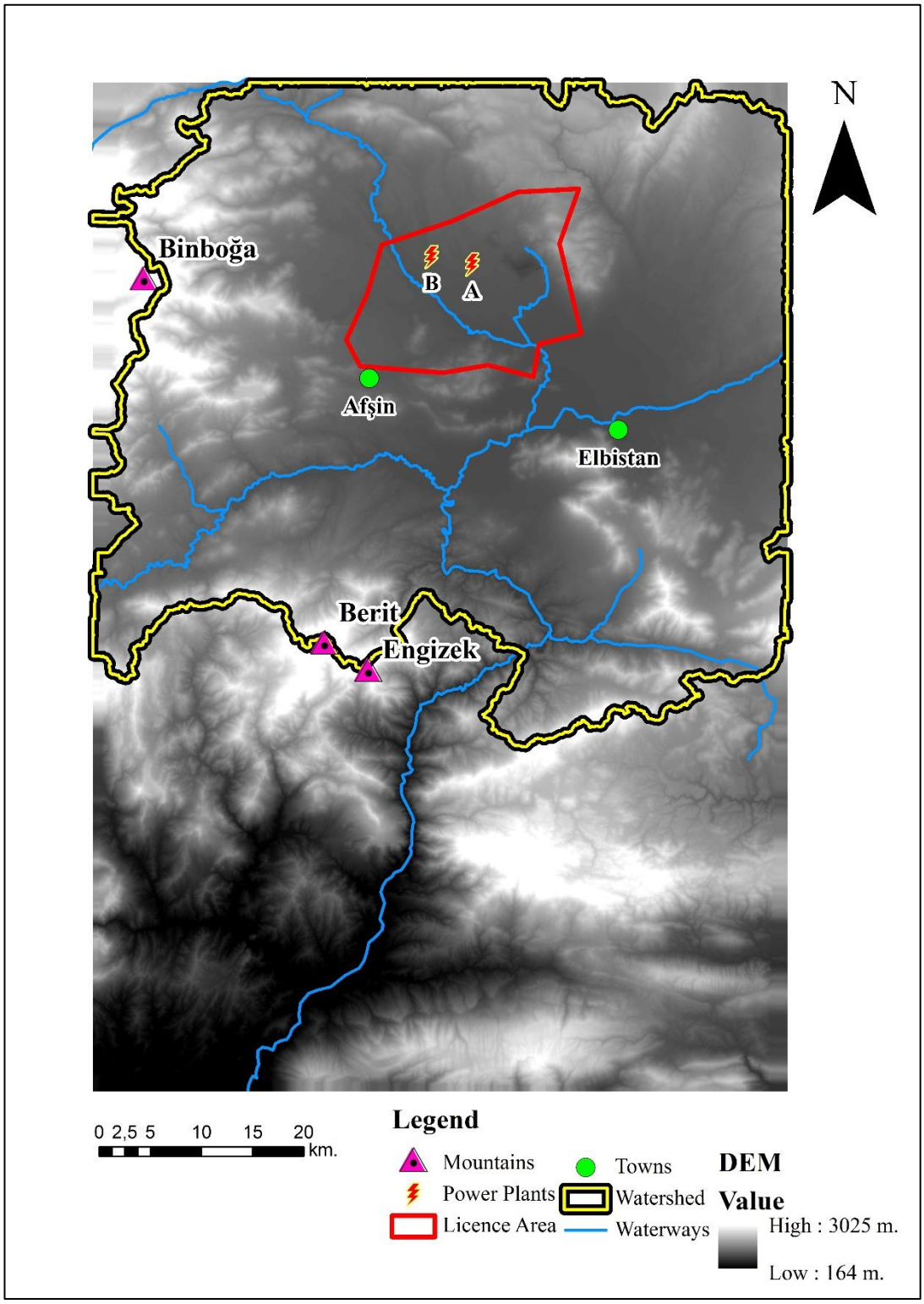

Figure 20. Utilized watershed

4.3.3 Pre-processing of Landsat Satellite Imagery

Before beginning classification analyses, raw images were pre-processed. For Landsat ETM+ imageries, images between years 2003 and 2011 had gaps as seen from Figure 21. Gaps had long triangles starting from the middle of the image and continued through the image. The reason for these gaps is the failure of the scan line corrector of the Landsat imager in May 31 2003. Scan line corrector trimmed the distortions caused by the forward motion of the imager (USGS, 2015).

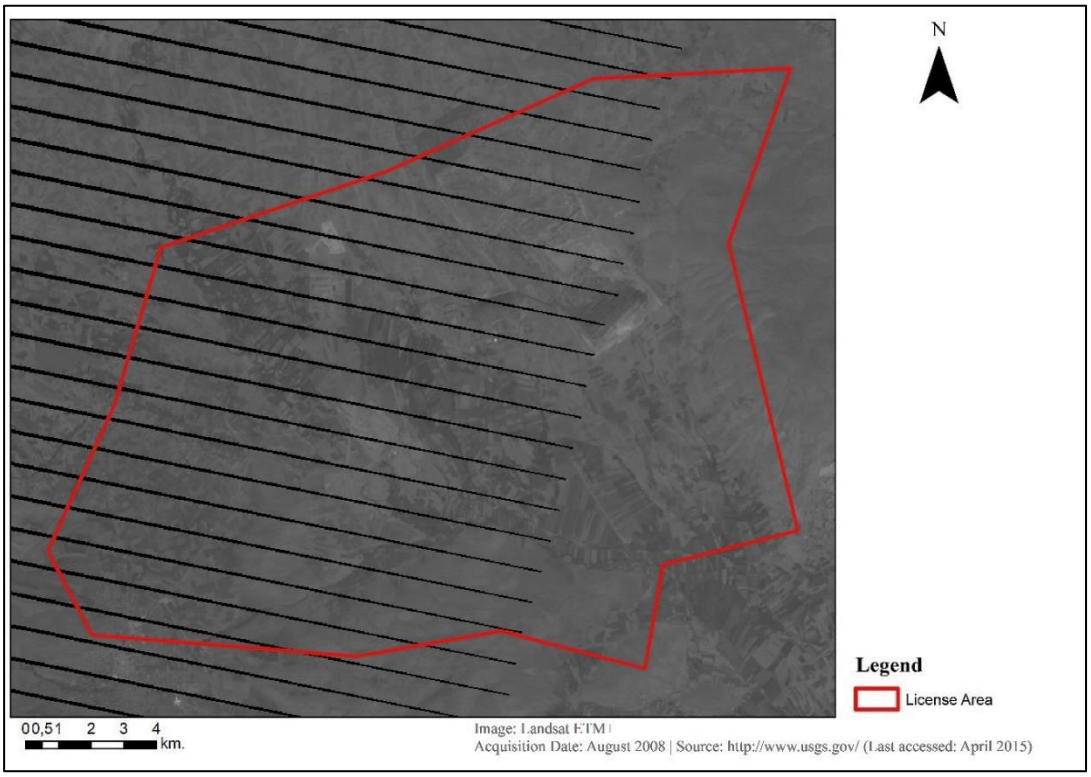

Figure 21. Raw Landsat ETM+ image with gaps

Landsat ETM+ images between the years 2003 and 2011 required further editing due to the scan line corrector failure. The methodology for filling the gaps is published by Scaramuzza, *et al.* (2004) and is developed as a plugin for the ENVI 5.0 by the Yale Centre for Earth Observation (2013). The function is called *landsat_gapfill* and

it was utilized for this study. After applying *landsat_gapfill* function to the images on years 2003, 2005, 2008 and 2011, atmospheric corrections were applied to satellite images. The images without the *landsat_gapfill* processing atmospherically were corrected with the software Geomatica 2014 in trial mode, and the images with *landsat_gapfill* processing were failed for atmospheric correction. Non-morphological filters were applied to the images with *landsat_gapfill* process such as, median filter and mean filter. However, each trail didn't enhance the results. Therefore, all of the images used were non-atmospherically corrected, and preparing training sets for each image in SVM classification had performed the analyses.

Composite Bands, *NDVI*, and *Principal Component Analysis* functions applied to all of the Level 1 GeoTIFF Landsat images taken between the years of 1984 and 2014 with ArcGIS 10 software. Seven classes were determined by using visual examination of images, the data gathered from the field surveys and the Corine map. These classes are:

- Vegetation
- Forest
- Agriculture
- Soil
- Settlement
- Water
- Mine

Vegetation class refers to all the green areas like meadows, parks, etc. Forest class represents the dense forest areas. Agriculture class includes cropland and orchards. Soil corresponds to bare land. Settlement class consists of urban and rural areas with villages, towns and cities. Water class constitutes water bodies like rivers, channels, lake, dam reservoirs, etc. Mine class delineates the areas where surface mining activities are performed. When the images were examined, it was found that six bands, which are blue, green, red, near infrared (NIR), short wave infrared 1 (SWIR1) and short wave infrared 2 (SWIR2) were found to contain most of the

available information for the classes. Hence they were used for the analyses. All of the images were masked out within the boundaries of watershed vector as seen in Figure 22 and the resultant area called as Afşin-Elbistan Coal Basin. Images acquired from USGS website having Level 1 GeoTIFF plus metadata did not require co-registration because all had been resampled with cubic convolution resampling method (USGS, 2015).

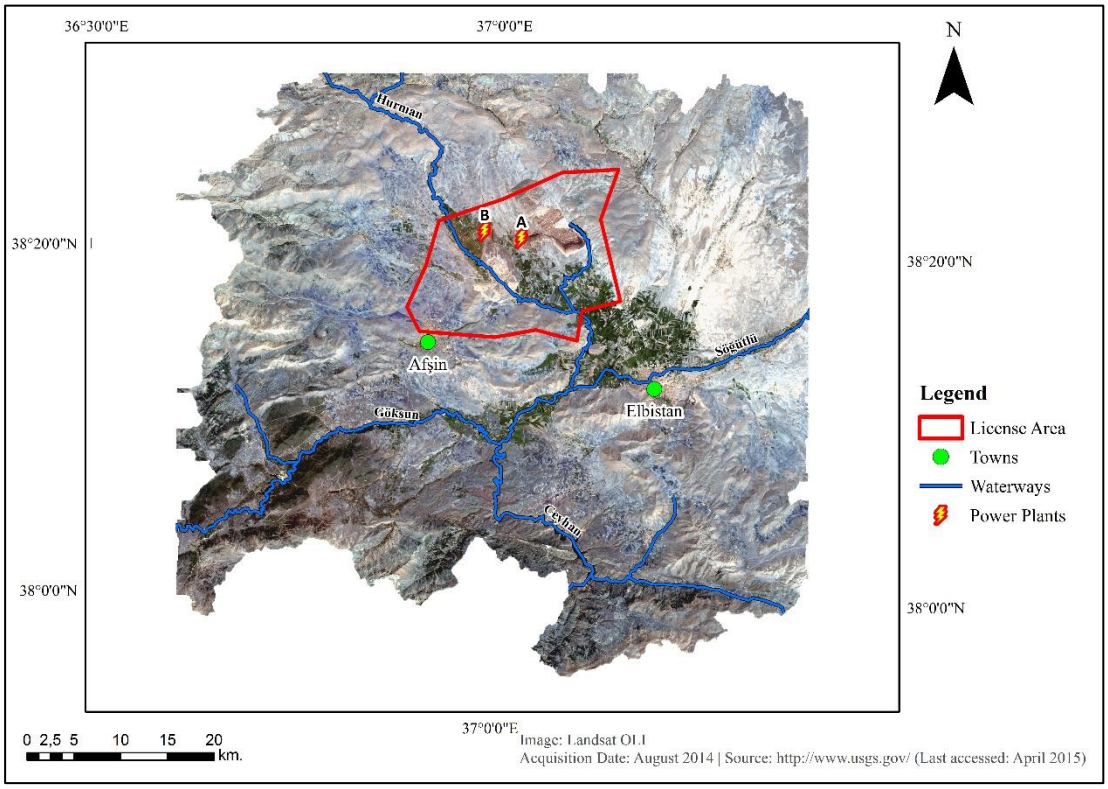

Figure 22. Masked out Landsat image

4.3.4 Image Enhancement

Image enhancement operations were applied to satellite imageries in order to detect the margins between classes. Before the classification analyses, trials had been conducted and it was observed that areas containing active mining operations

presented problems in the classifications. Problems were due to the similarities in spectral signatures of mining area and the other classes, like soil, agriculture, etc. classes (Rathore and Wright, 2007). In order to eliminate this issue, mining area were masked out from all of the images (Figure 23) and analyses were conducted with the masked images.

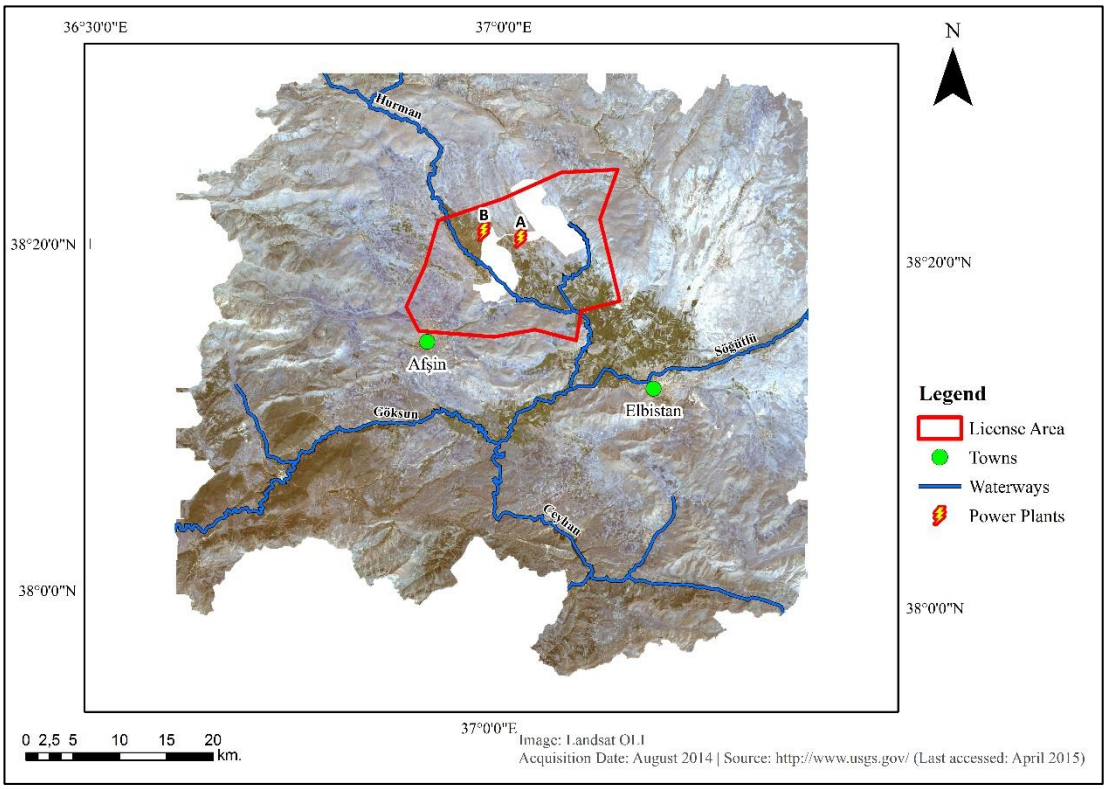

Figure 23. Masked out surface mine area from the year 2014

4.4 Classification Analyses

For the classifications, as mentioned in section 2.2, supervised Support Vector Machine (SVM) classification method was utilized. In order to conduct supervised classifications, sample sets, also called training sets was constructed first. After selection of training sets, supervised classifications were applied to multi-temporal

images for both classification methods, and accuracy assessment calculations were carried out in order to examine the success of classifications.

4.4.1 Training Set Selection

The first step of the supervised classification is choosing the appropriate training sets for the satellite images. As mentioned in section 4.3.3, there were six main classes in the Afşin-Elbistan Coal Basin. Training set selection for SVM classification was performed for each of the satellite images separately as seen between Figure 24 and Figure 32.

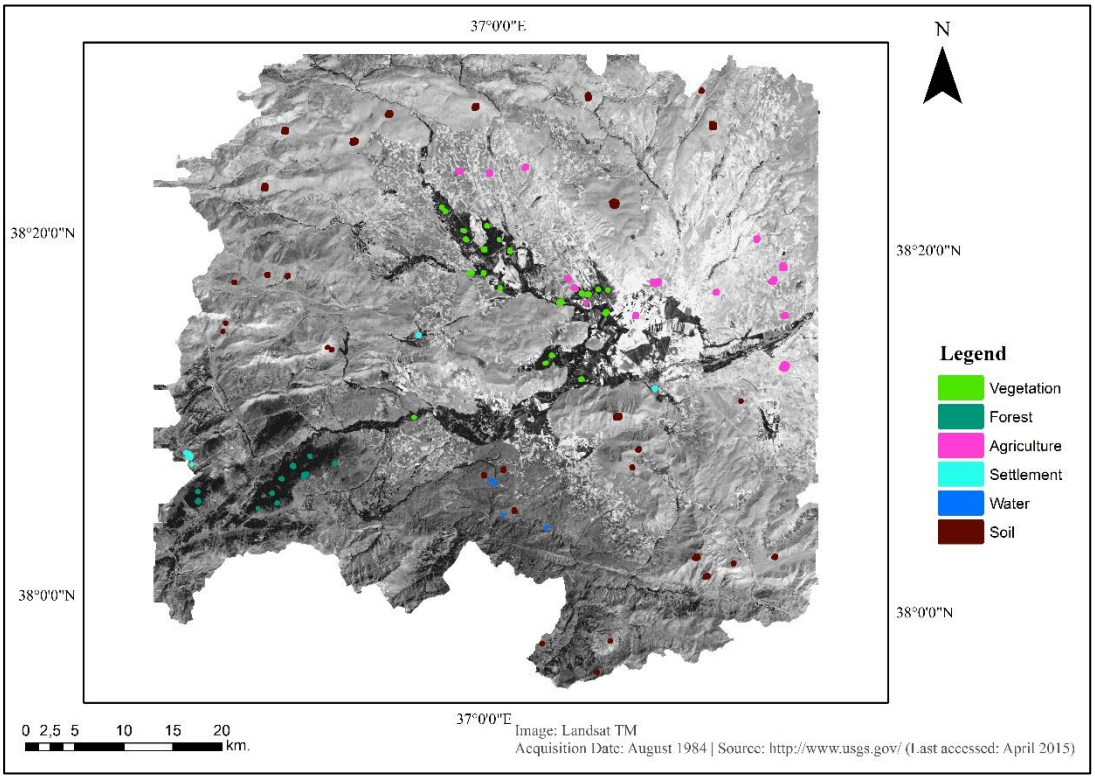

Figure 24. Training sets of SVM classifications for the year 1984

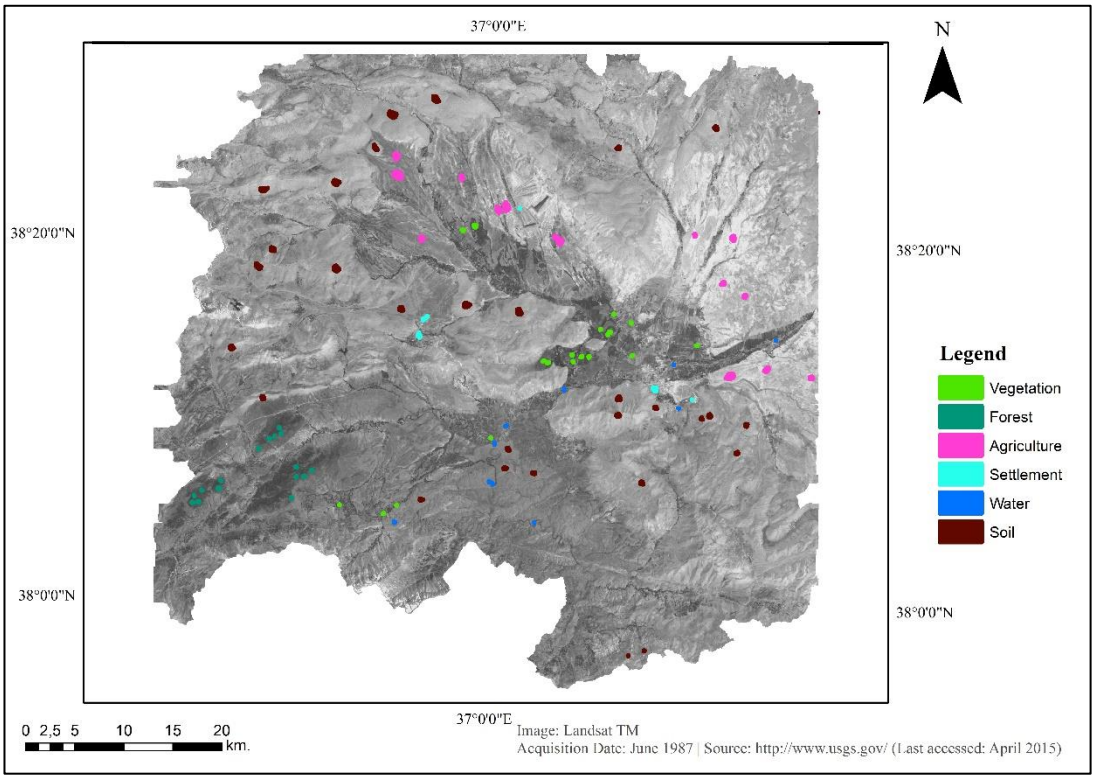

Figure 25. Training sets of SVM classifications for the year 1987

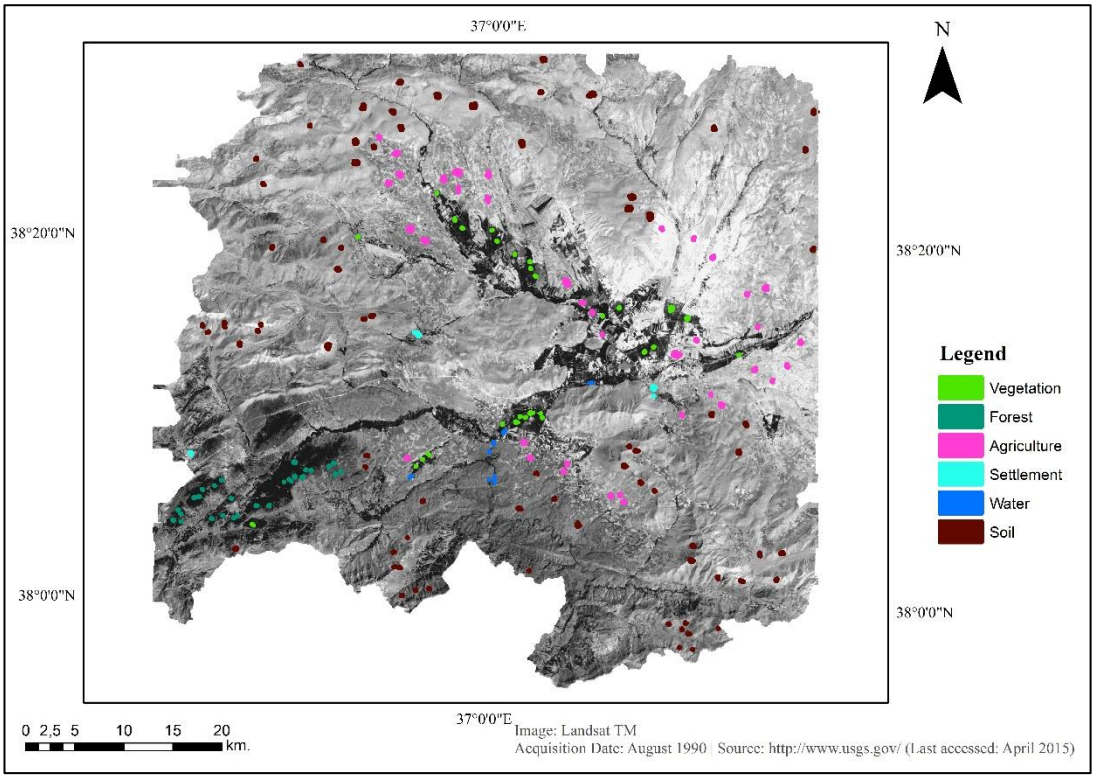

Figure 26. Training sets of SVM classifications for the year 1990

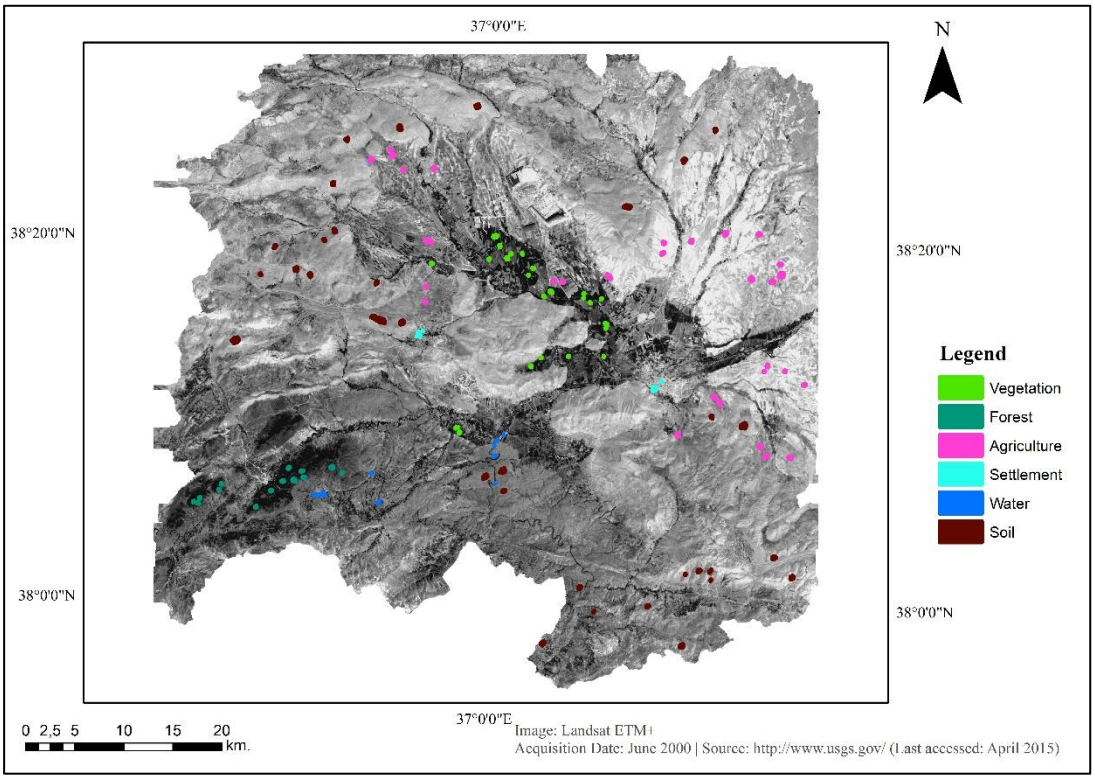

Figure 27. Training sets of SVM classifications for the year 2000

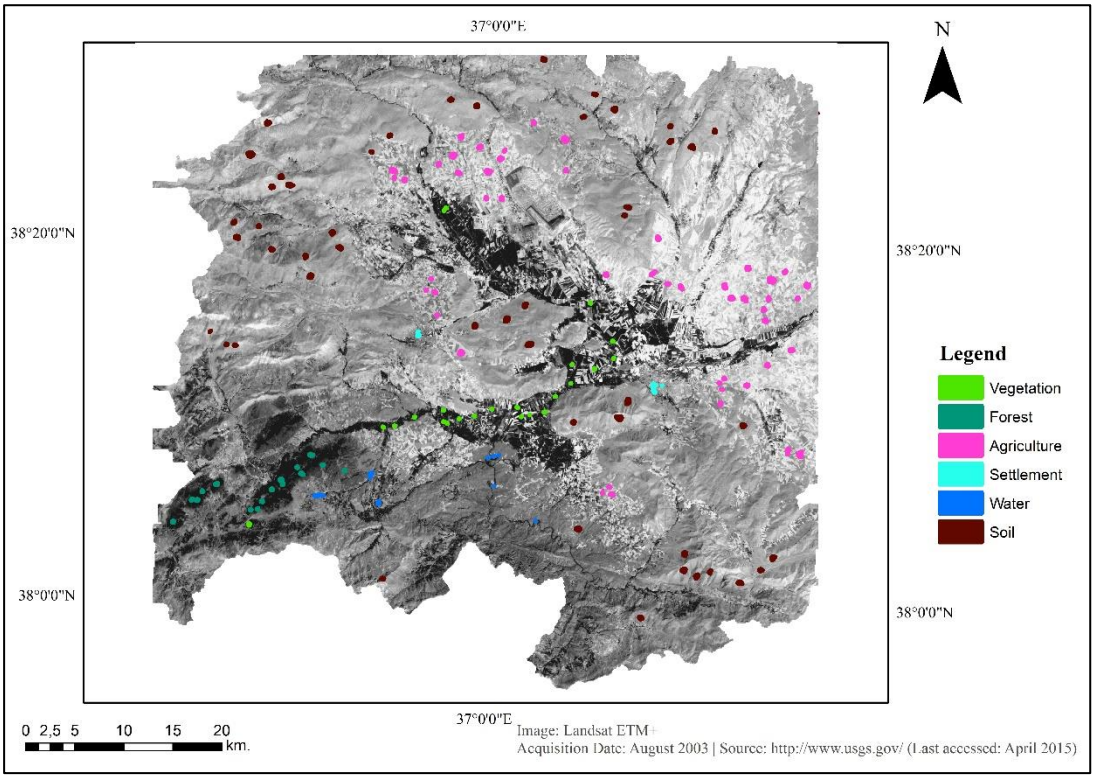

Figure 28. Training sets of SVM classifications for the year 2003

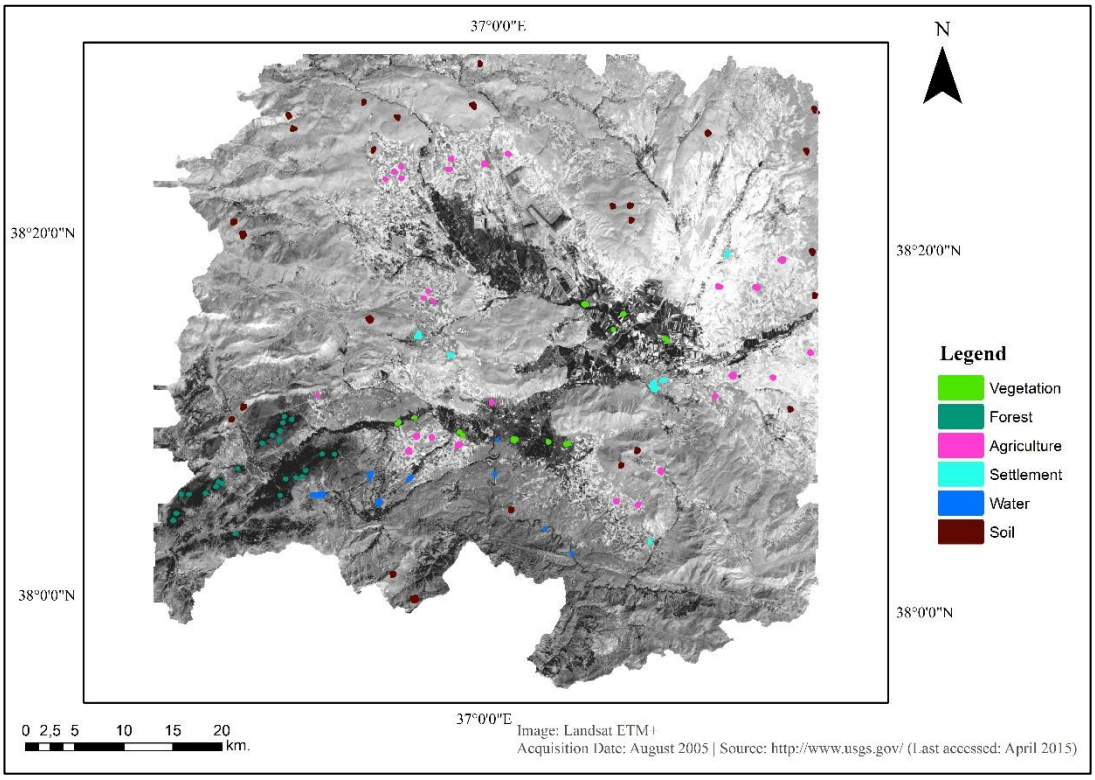

Figure 29. Training sets of SVM classifications for the year 2005

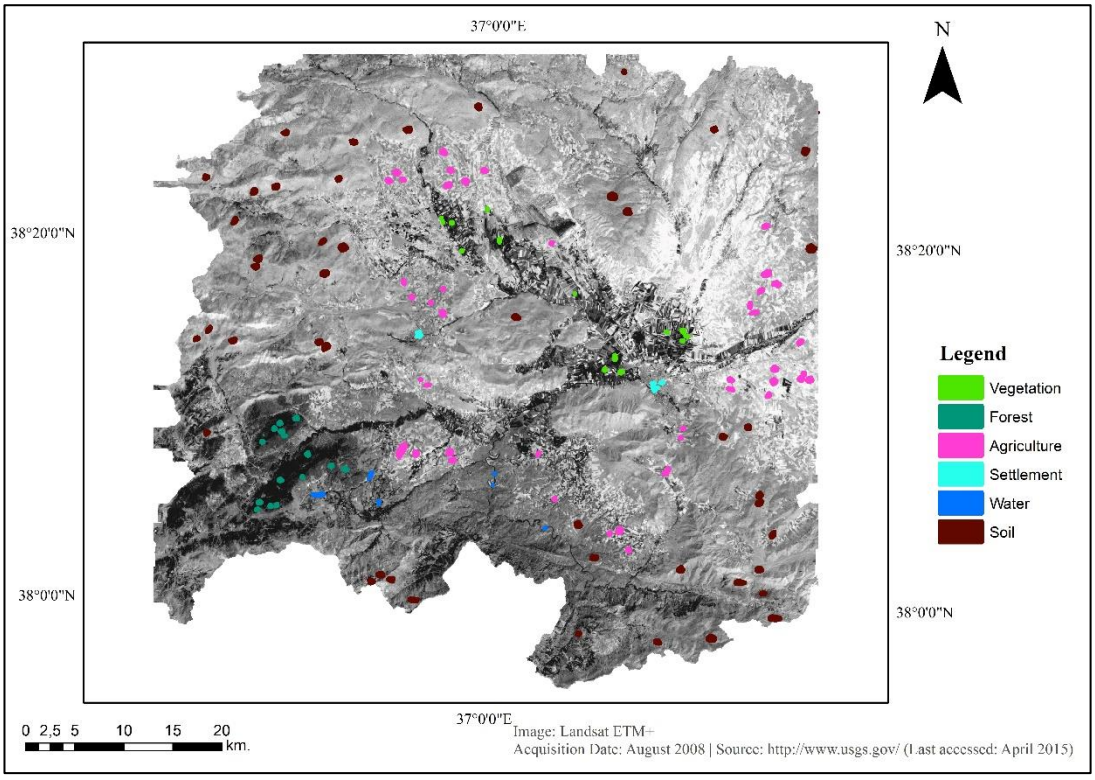

Figure 30. Training sets of SVM classifications for the year 2008

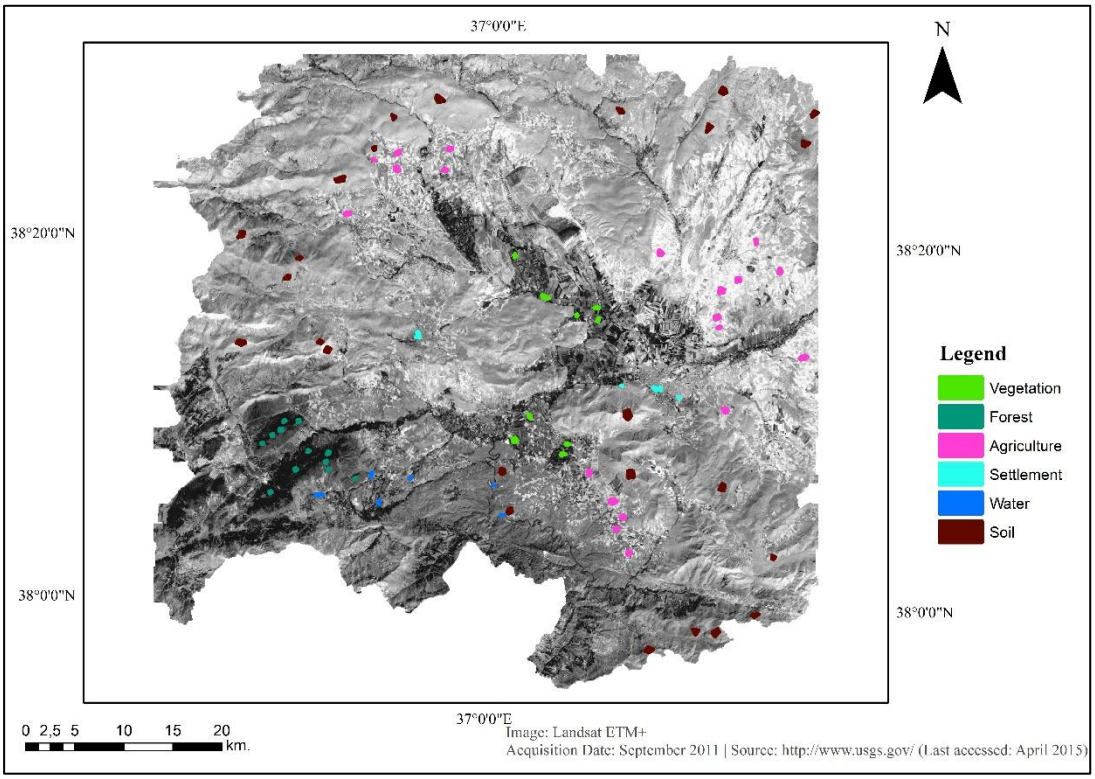

Figure 31. Training sets of SVM classifications for the year 2011

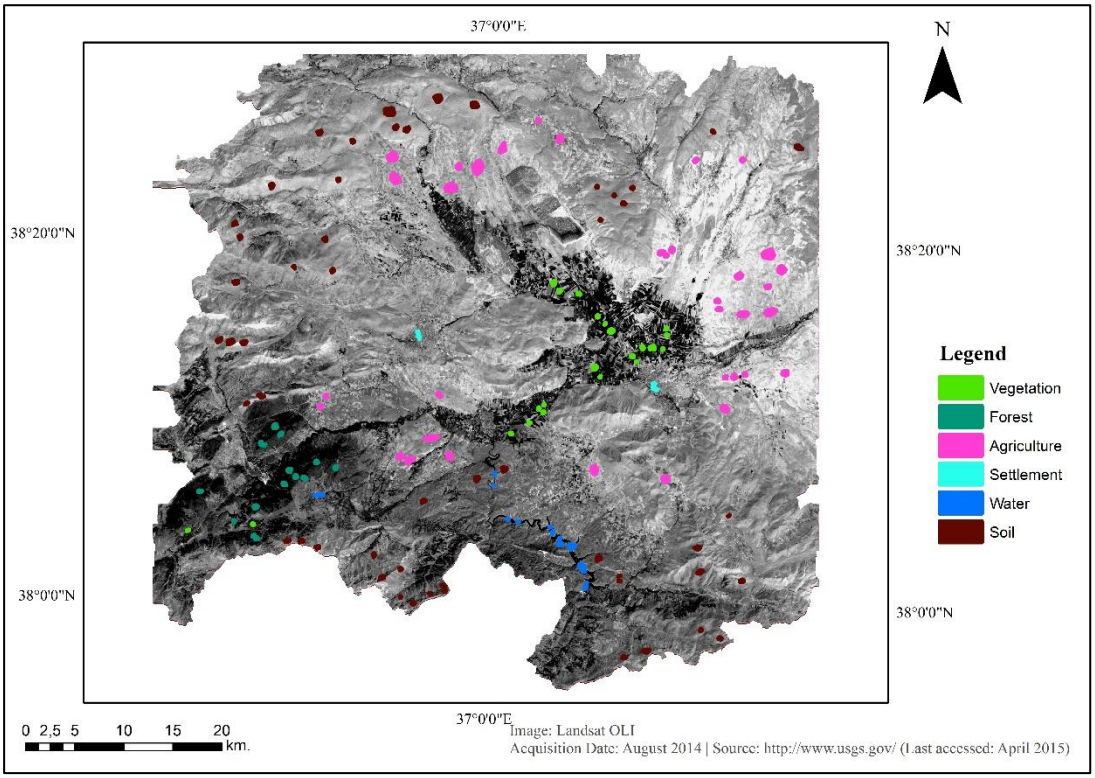

Figure 32. Training sets of SVM classifications for the year 2014

For CDTL classification, one training set is chosen for year 2014 (Figure 33) and other training sets derived from the 2014 training set. In original paper, training sets prepared with machine learning system written in code. The code required could not acquire and generated, thus the training set selection done manually with closest way. Derived training sets arranged with before and after technique. To give an example, absolute value of pre-processed Landsat ETM+ image acquired on 2011 subtracted from the absolute value of pre-processed Landsat OLI image acquired on 2014 with the raster calculator in ArcGIS10 software, and with threshold, gray scale image divided into two groups of changed and unchanged areas which colored as black and white as seen in Figure 34. The differencing is not the prime parameter for the changes as you can see from the Figure 34 because of the differences between the atmospheric effects, the function only decreased the areas to be observed in order to select samples. The difference map, second image that needed training set and first training set overlaid, and second training set derived manually by observing all three layers. Rest of the difference maps can be seen in Appendix B. All of the training sets can be seen between Figure 35 and Figure 42.

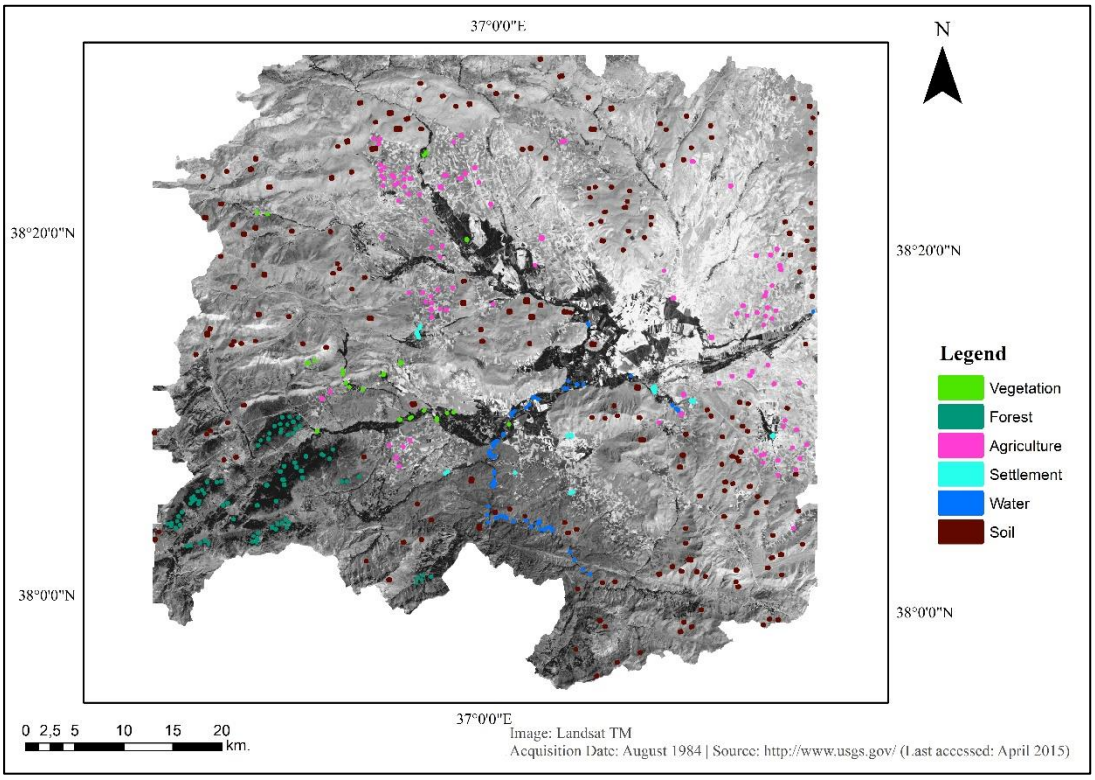

Figure 33. Training set of CDTL classification for the year of 2014

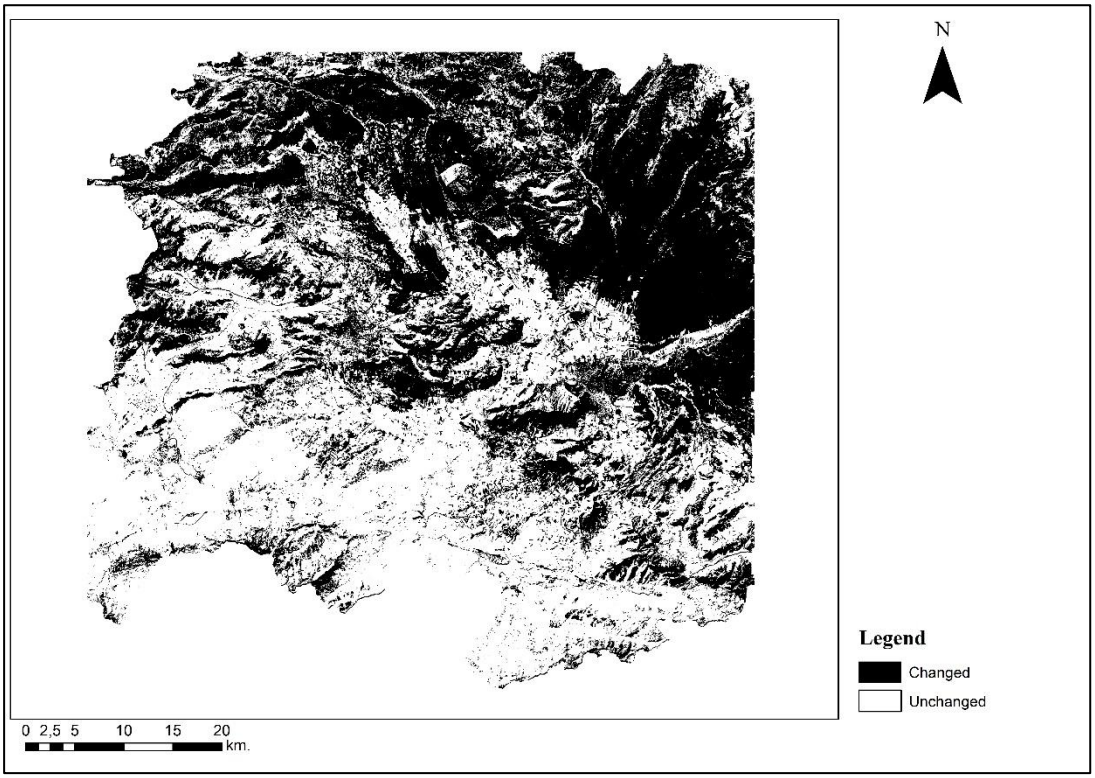

Figure 34. Changed and unchanged areas bewteen the years of 2014 and 2011

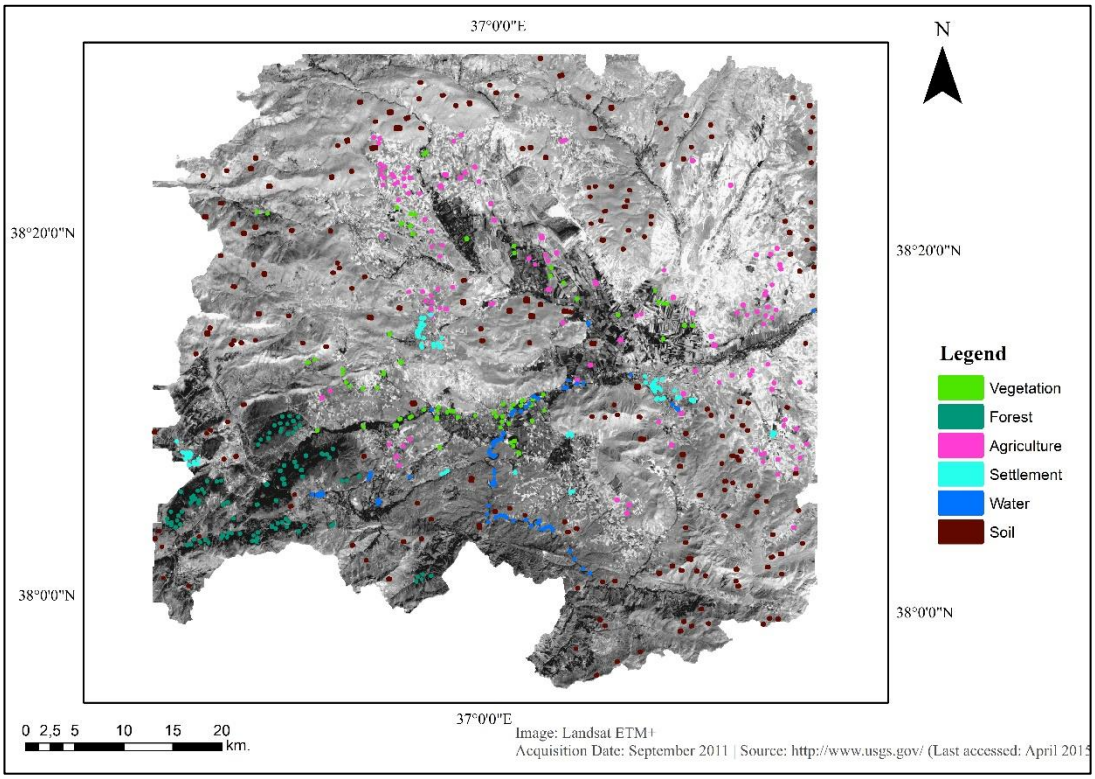

Figure 35. Training set of CDTL classification for the year of 2011

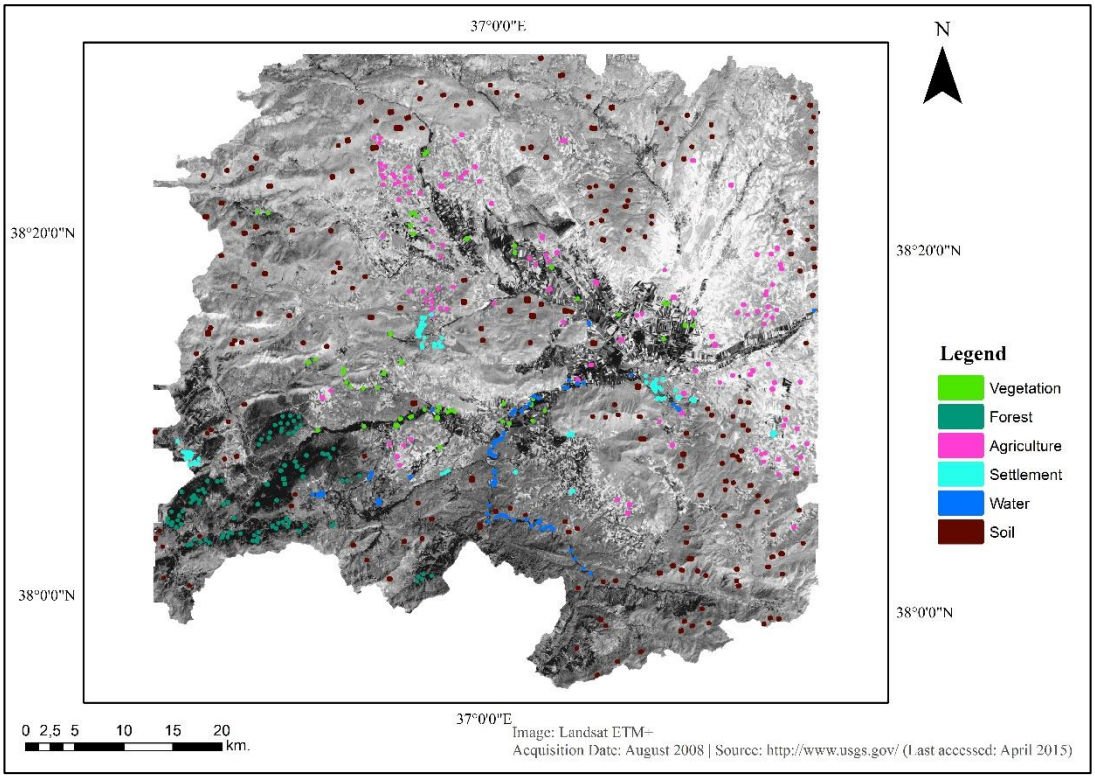

Figure 36. Training set of CDTL classification for the year of 2008

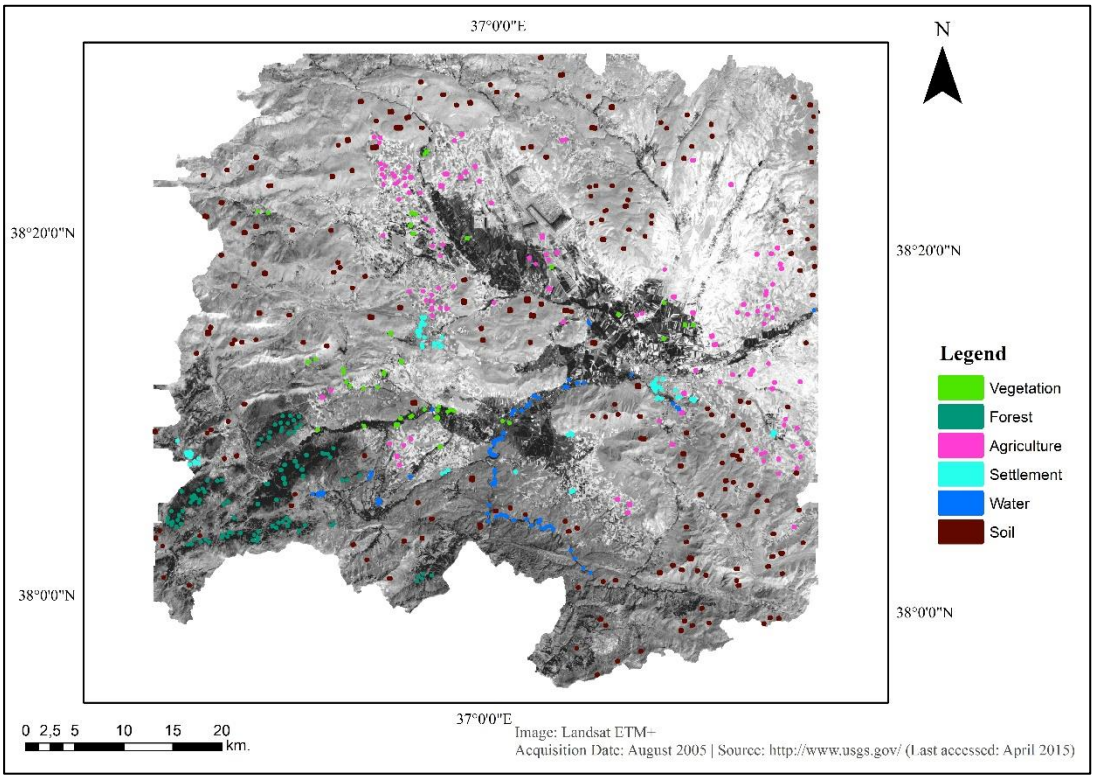

Figure 37. Training set of CDTL classification for the year of 2005

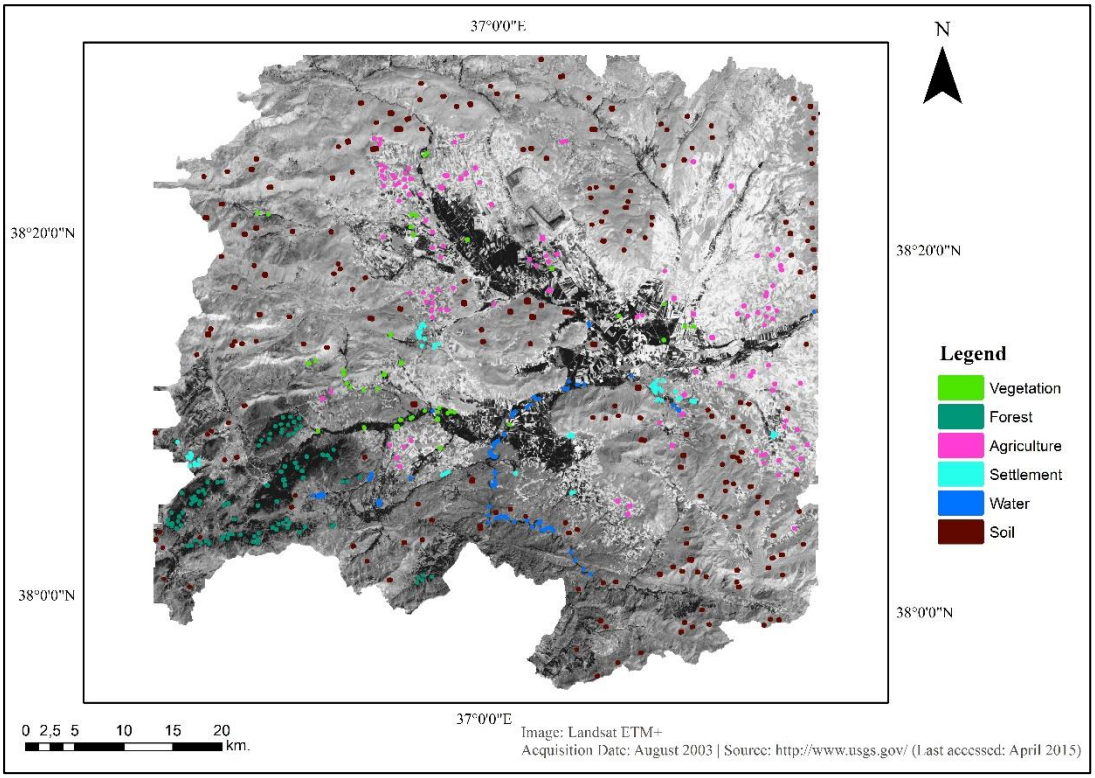

Figure 38. Training set of CDTL classification for the year of 2003

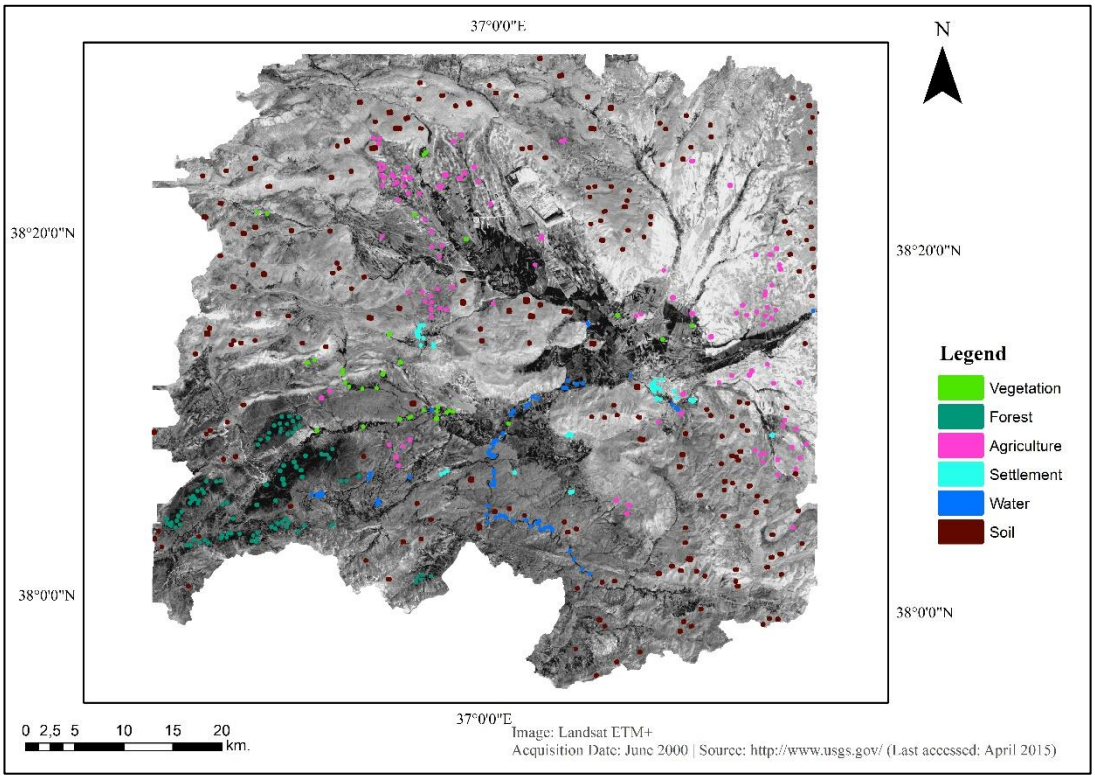

Figure 39. Training set of CDTL classification for the year of 2000

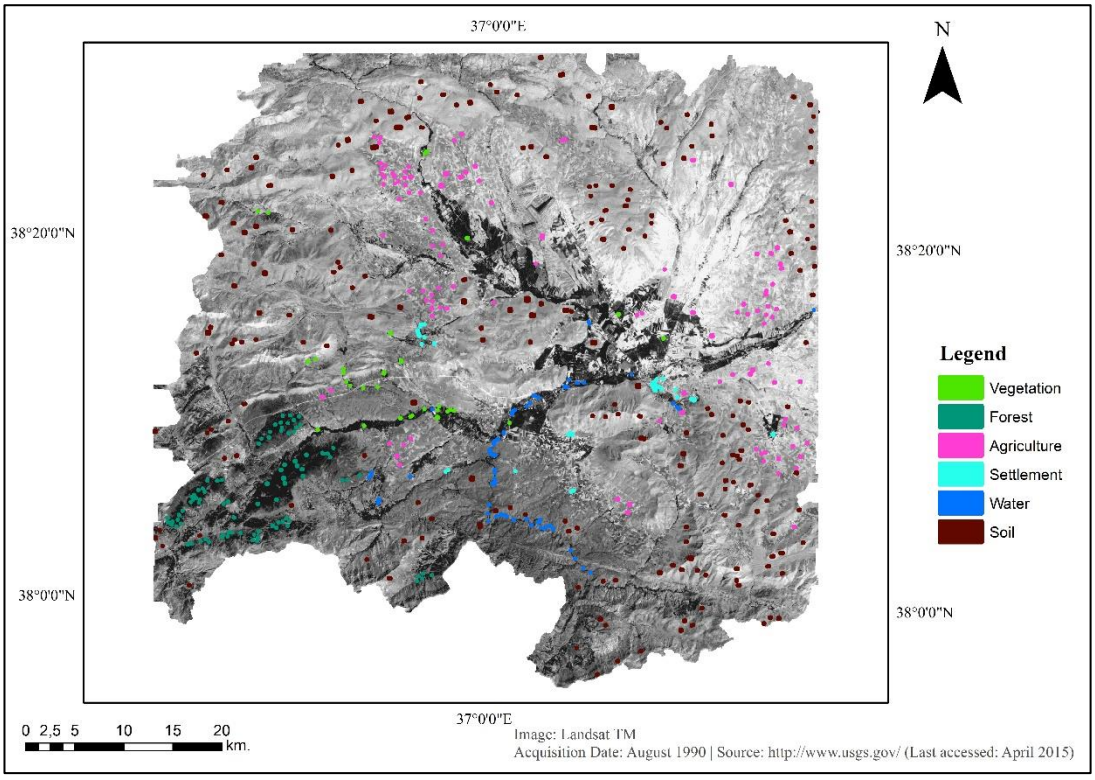

Figure 40. Training set of CDTL classification for the year of 1990

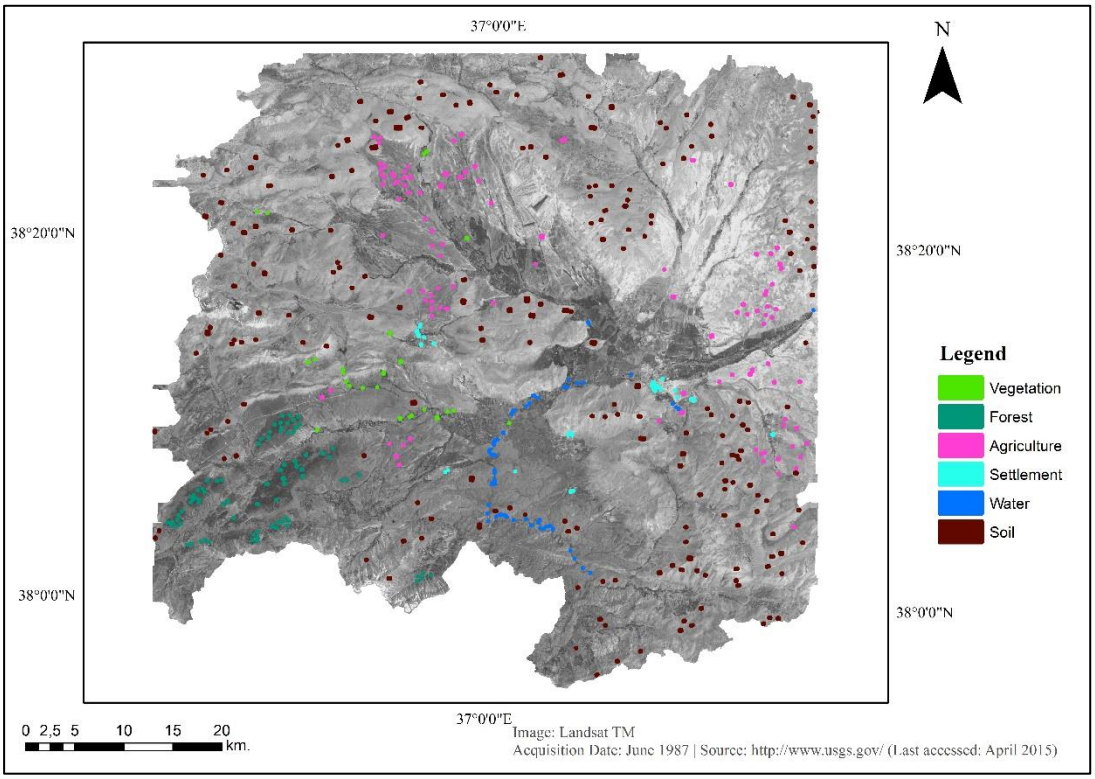

Figure 41. Training set of CDTL classification for the year of 1987

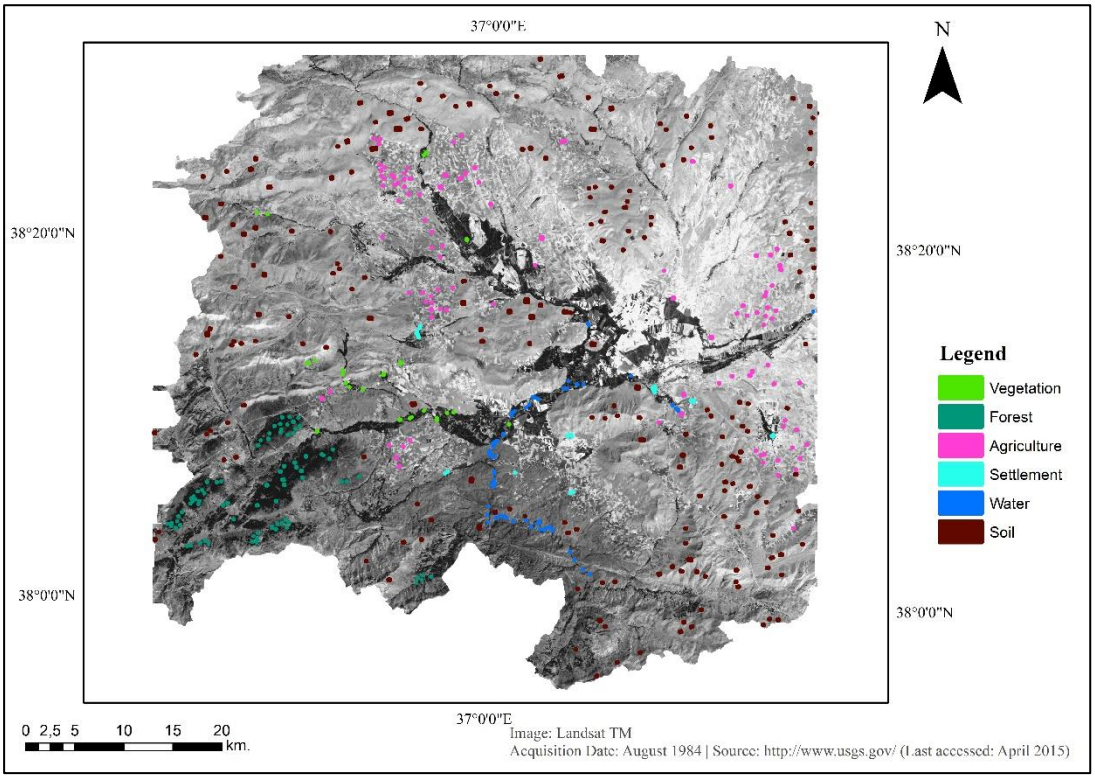

Figure 42. Training set of CDTL classification for the year of 1984

4.4.2 Traditional SVM Classification

The Support Vector Machine (SVM) function was used for each of the nine images with the help of ENVI software. Kernel type for SVM was chosen as *Radial Basis Function*, gamma was taken as 0.167, penalty parameter was 100 and pyramid levels left as 0, all of the parameters can be seen from Figure 43, and classifications can be seen between Figure 44 and Figure 52. Each pixel was counted with respect to their classes and class percentages were calculated.

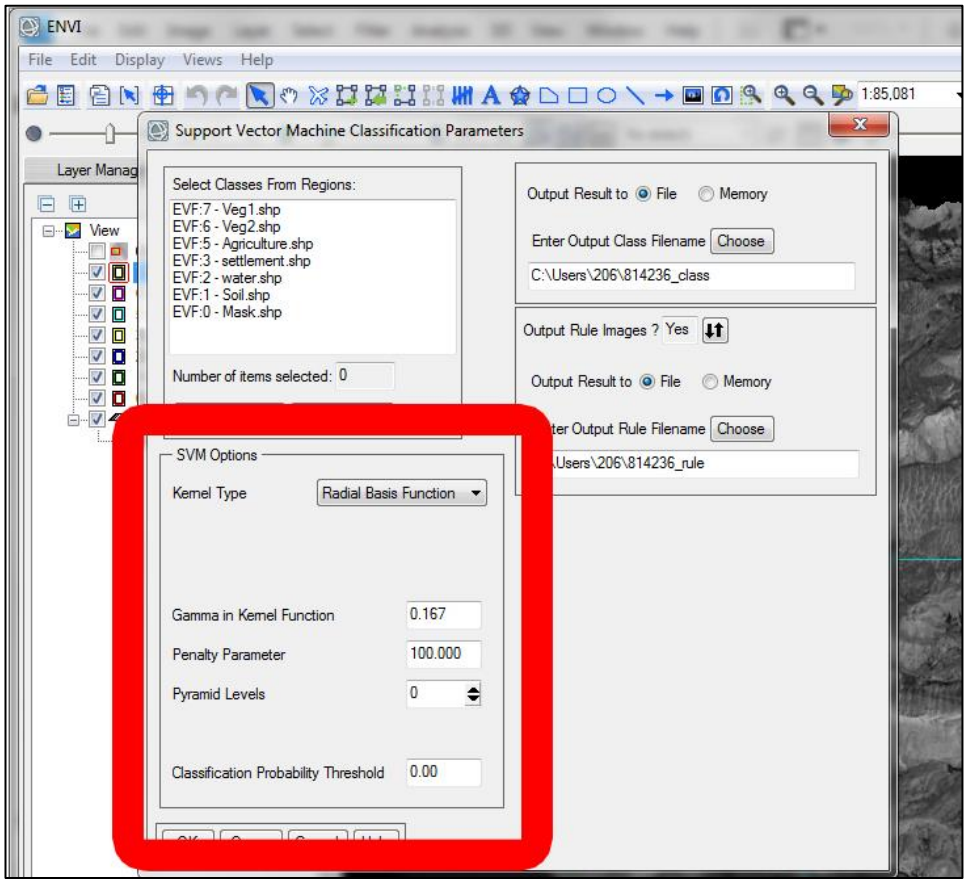

Figure 43. SVM parameters

From the calculations for the classification of 1984 image (Figure 44), percentage of the classes are found to be as: Vegetation is 6.1%, forest is 5.5%, agriculture is 30.3%, settlement is 7.3%, water is 0.1% and soil is 50.4%. The percentage of the mine area is 0.3%. Soil and agriculture are the dominant classes in the classification map of 1984.

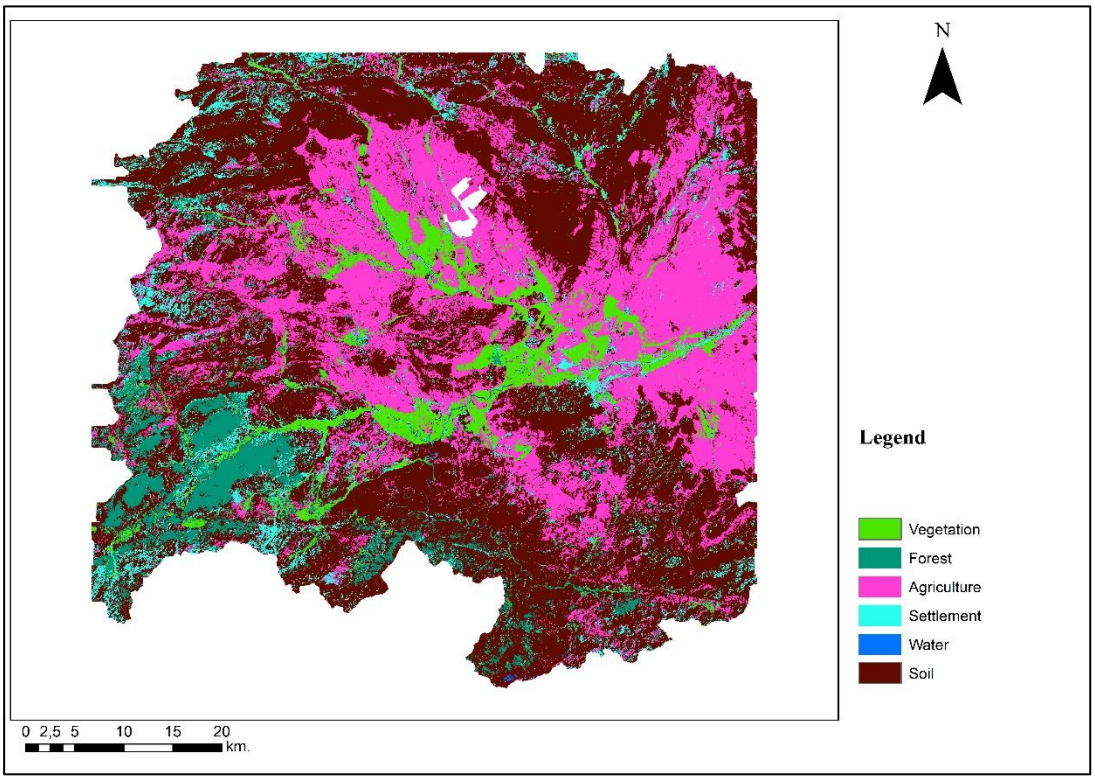

Figure 44. SVM classification of Afşin-Elbistan Coal Basin for year 1984

For the classification of 1987 image (Figure 45), the percentage of the six classes are obtained as: Vegetation is 5.4%, forest is 4.3%, agriculture is 32.5%, settlement is 0.6%, water is 0.5%, soil is 56.2%, and surface mine area is 0.4% of the basin. As seen from Figure 45, soil and agriculture are the dominant classes in the classification. When compared to the classified image of 1984, vegetated lands transforms to soil and agriculture around the mine, settlement decreases in the basin,

vegetation shrinks in the southwest of the basin and forested areas remains unchanged.

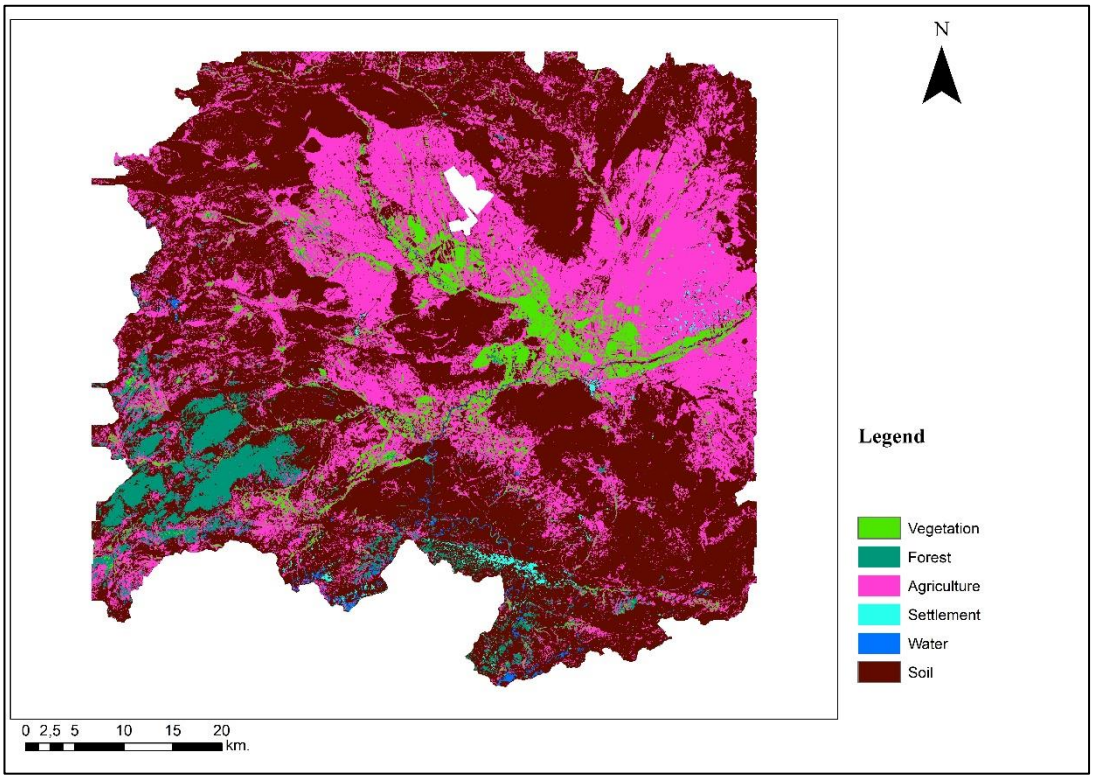

Figure 45. SVM classification of Afşin-Elbistan Coal Basin for year 1987

For the classification of 1990 image (Figure 46), percentage of the six main classes are found to be: Vegetation is 5.3%, forest is 6%, agriculture is 41.9%, settlement is 0.5%, water is 0.3%, soil is 45.6%, and the mine area is 0.5% of the basin. When compared to the classified image of 1987, the transformed vegetated lands of the 1987 image becomes vegetated lands again; the settlement increases in the southeast of the mine, and there is a slight increase in the forested areas.

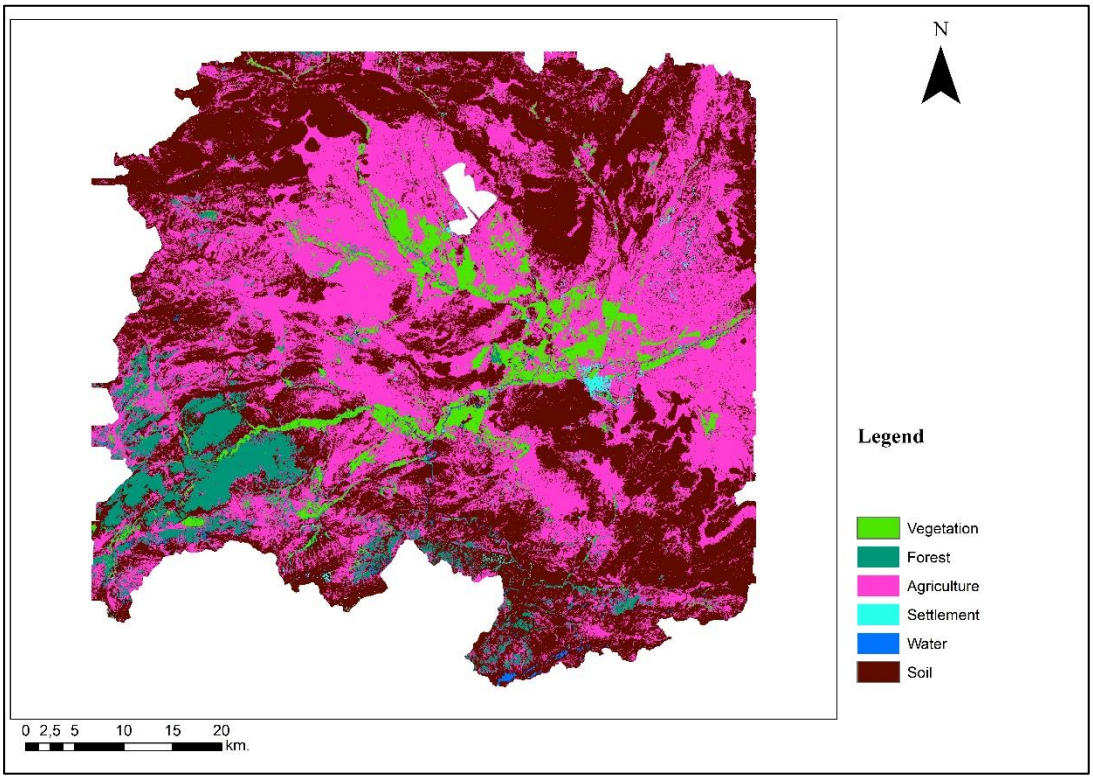

Figure 46. SVM classification of Afşin-Elbistan Coal Basin for year 1990

For the classification of 2000 (Figure 47), percentage of the six main classes were found to be: Vegetation is 5.9%, forest is 4.7%, agriculture is 33%, settlement is 0.5%, water is 0.3%, soil is 54.9%, and the mine area is 0.7% of the basin. When compared to the classified image of 1990, the northwestern parts of the vegetation around the mine transforms to agricultural lands, and settlement and waterways remains unchanged.

For the classification of 2003 (Figure 48), percentage of the main six classes are: Vegetation is 6.2%, forest is 6.2%, agriculture is 18.8%, settlement is 0.6%, water is 0.5%, soil is 65.2%, and the mine area covers 1.1% of the basin. When compared to the classified image of 2000, vegetation is increased with the settlement, forested areas nearly are unchanged, and waterways are dispersed around the basin.

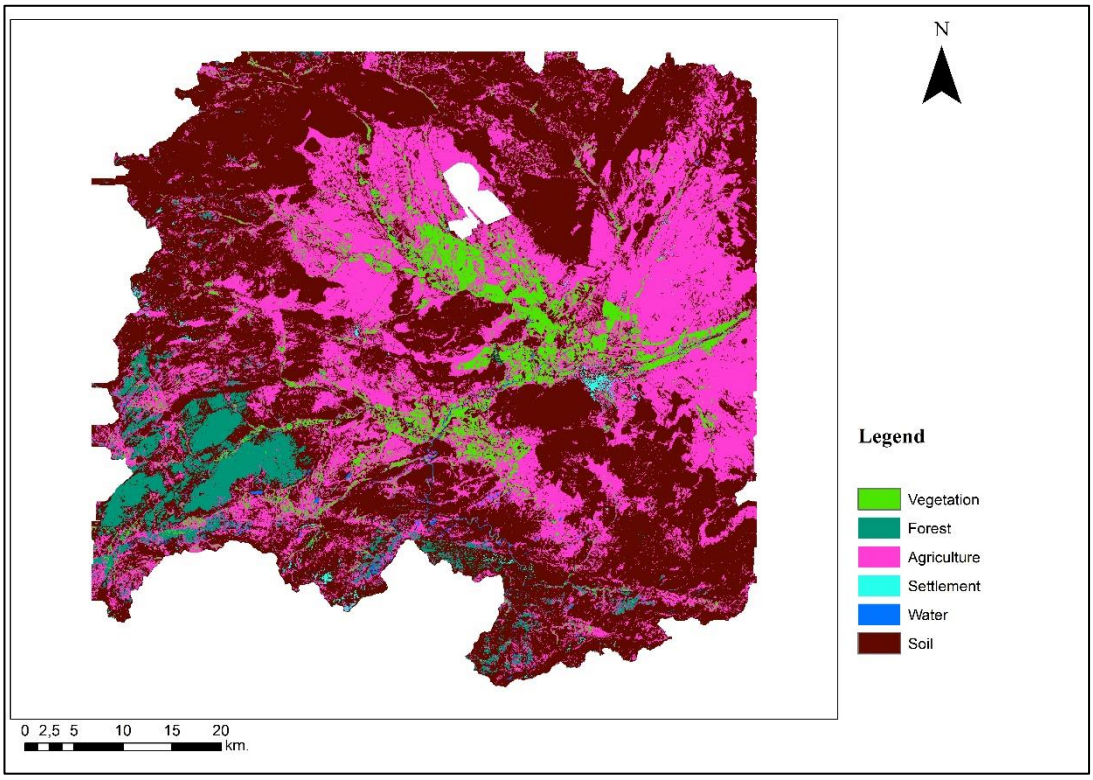

Figure 47. SVM classification of Afşin-Elbistan Coal Basin for year 2000

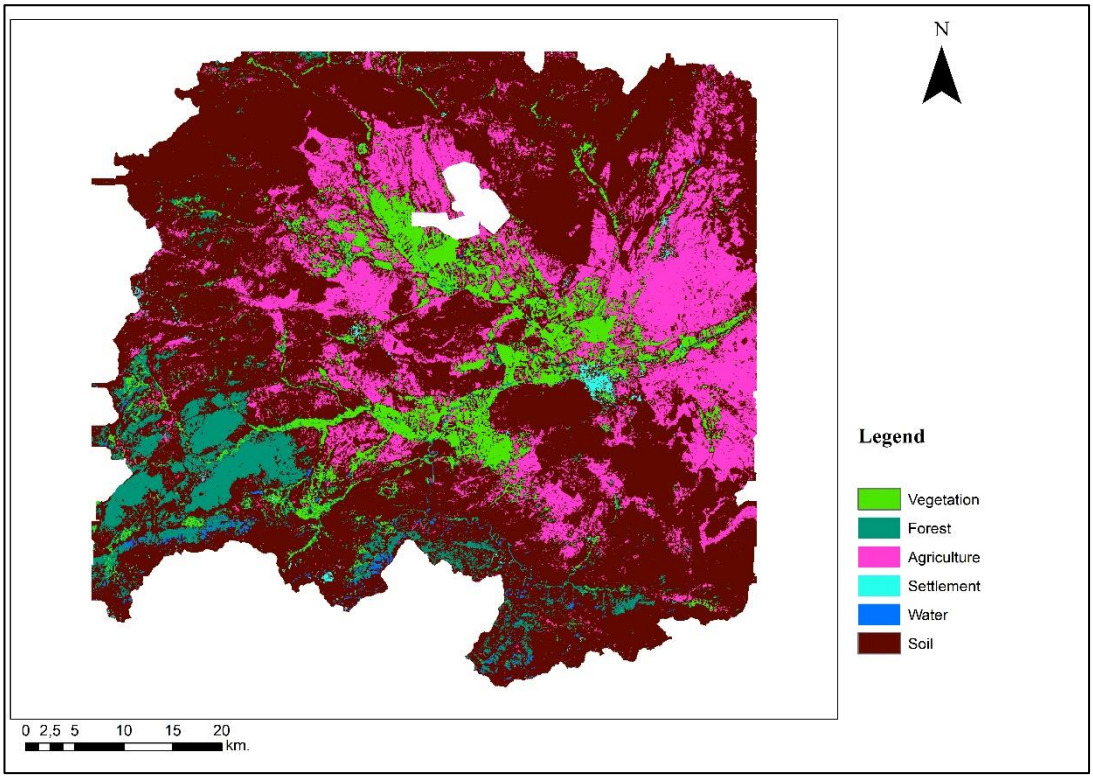

Figure 48. SVM classification of Afşin-Elbistan Coal Basin for year 2003

For the classification of 2005 (Figure 49), percentage of the six classes are: Vegetation is 14.6%, forest is 5%, agriculture is 28.9%, settlement is 1.1%, water is 0.2%, soil is 49.1%, and the mine area covers 1.2% of the basin. When compared to the classified image of 2003, vegetation is increased broadly, especially around the waterways, agriculture is increased as well, new settlement is observed around the northeastern part of the basin, and forested areas are nearly unaltered.

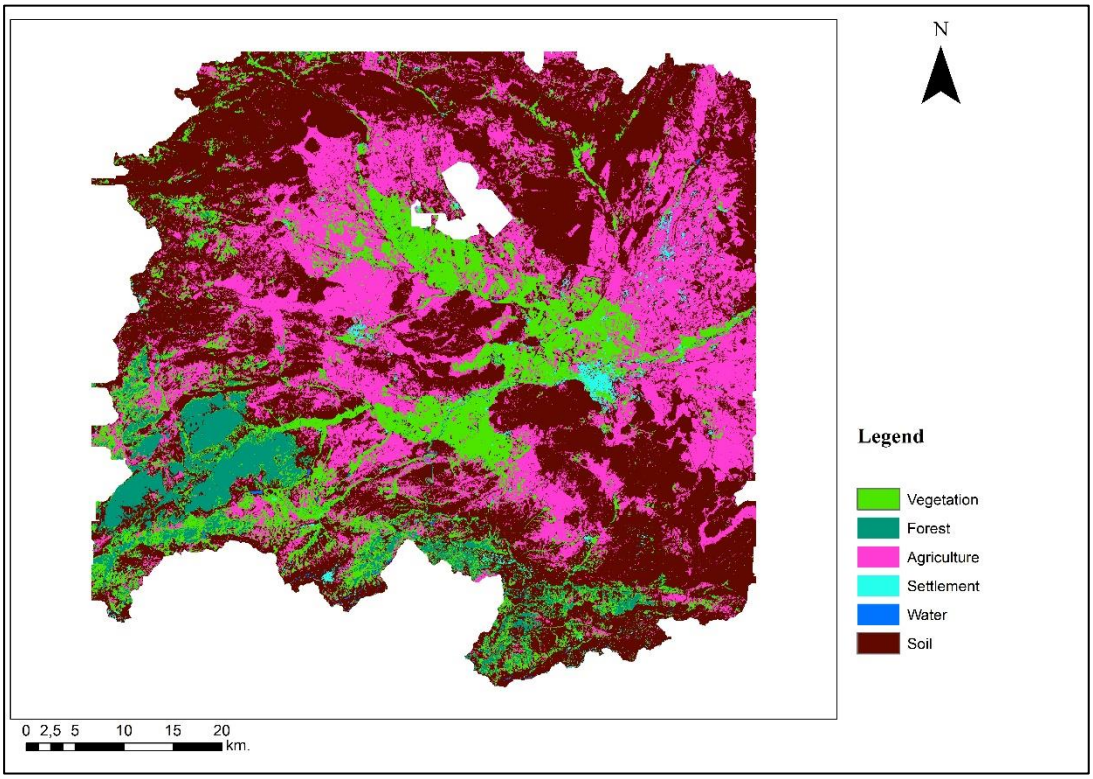

Figure 49. SVM classification of Afşin-Elbistan Coal Basin for year 2005

For the classification of 2008 (Figure 50), percentage of the six main classes are: Vegetation is 5.3%, forest is 8.1%, agriculture is 21.6%, settlement is 0.3%, water is 0.1%, soil is 63.5%, and the mine area covers 1.2% of the basin. When compared to the classified image of 2005, vegetation is decreased, new settlement areas around the northeastern part of the basin from classification of 2005 vanish, this situation may be related to misclassification, and forested areas and waterways are unaltered.

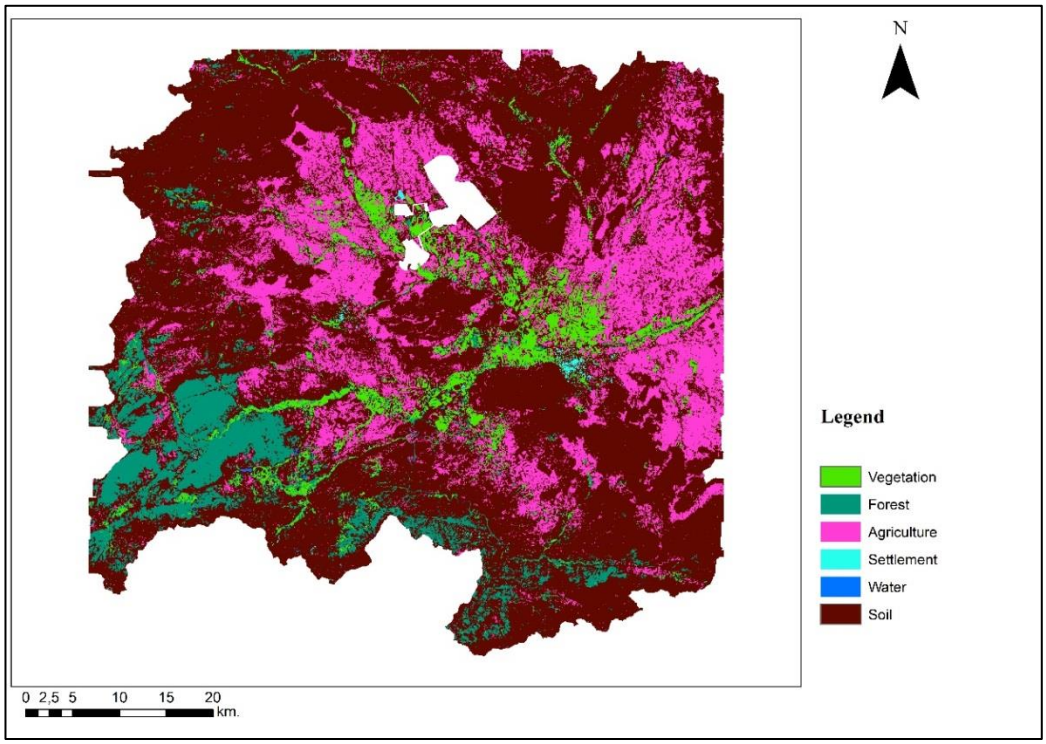

Figure 50. SVM classification of Afşin-Elbistan Coal Basin for year 2008

For the classification of 2011 (Figure 51), percentage of the six classes are: Vegetation is 6.8%, forest is 6%, agriculture is 18.6%, settlement is 0.8%, water is 0.2%, soil is 66.1% and the mine area covers 1.5% of the basin. When compared to the classified image of 2008, there are unclassified areas on the southwestern part of the basin, vegetation is slightly increased, settlement in the southeastern part of the mine increases, and forested areas and waterways are nearly unchanged.

Finally, for the classification of 2014 (Figure 52), percentage of the six main classes are; vegetation 6.3%, forest 8.6%, agriculture 28.5%, settlement 0.3%, water 0.3% and soil is 54.5%. In addition to the classes, the mine area covers 1.5% of the basin. When compared to the classified image of 2011, agriculture increases, settlement nearly disappears, waterways are clearly visible and increased, the reason for the rapid increase may be dam reservoirs being developed due to hydroelectric power plants constructions around the rivers in the basin, and forested areas are slightly increased.

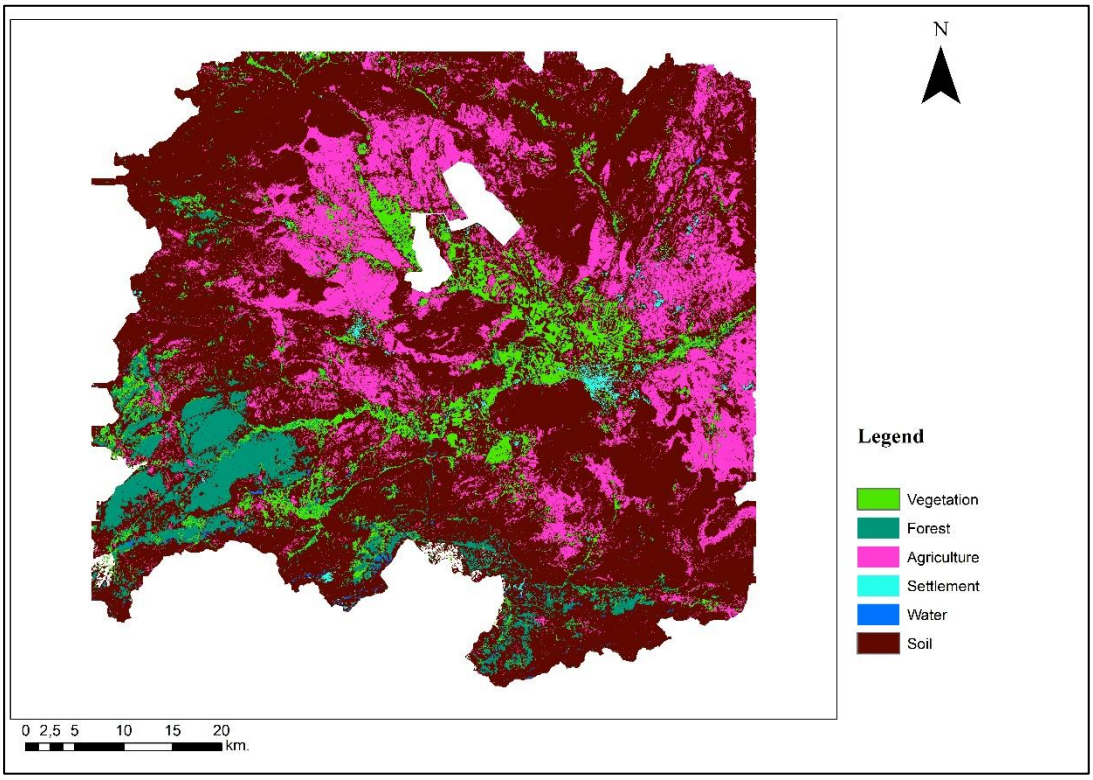

Figure 51. SVM classification of Afşin-Elbistan Coal Basin for year 2011

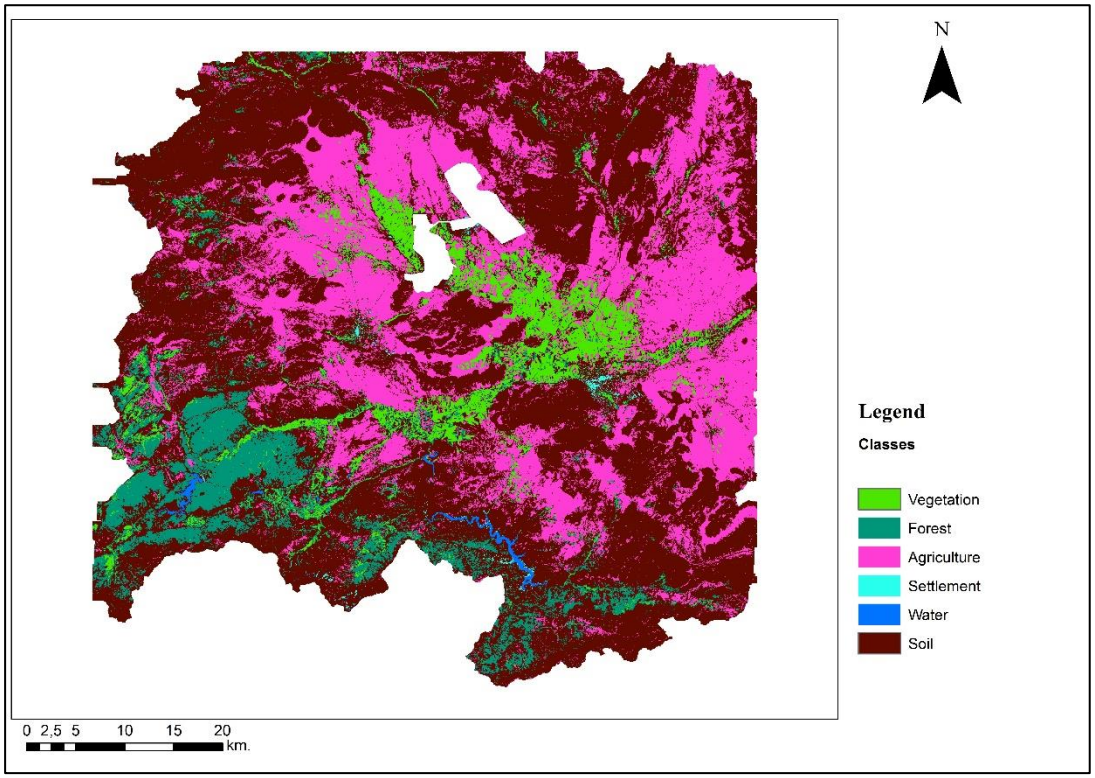

Figure 52. SVM classification of Afşin-Elbistan Coal Basin for year 2014

4.4.3 CDTL Classification

As mentioned in section 2.2, CDTL classification method utilizes SVM function for classifications. SVM step of CDTL classification applied to nine periodically arranged multi-temporal images individually with ENVI software. Kernel type for SVM is chosen as *Radial Basis Function*, gamma is taken as 0.167, penalty parameter is 100 and pyramid levels left as 0, all of the parameters can be seen from Figure 43. Images classified according to six classes, which are vegetation, forest, agriculture, settlement, water and soil. Each pixel had counted with respect to their classes, class percentages are calculated, and the classifications can be seen between Figure 53 and Figure 61.

From the calculations for the classification of 1984 image (Figure 53), percentage of the six classes are: Vegetation is 5.3%, forest is 4.8%, agriculture is 24.0%, settlement is 1.2%, water is 0.3%, soil is 64.1%, and the mine area covers 0.2% of the basin. As seen from Figure 47, soil and agriculture are the dominant classes in the classification.

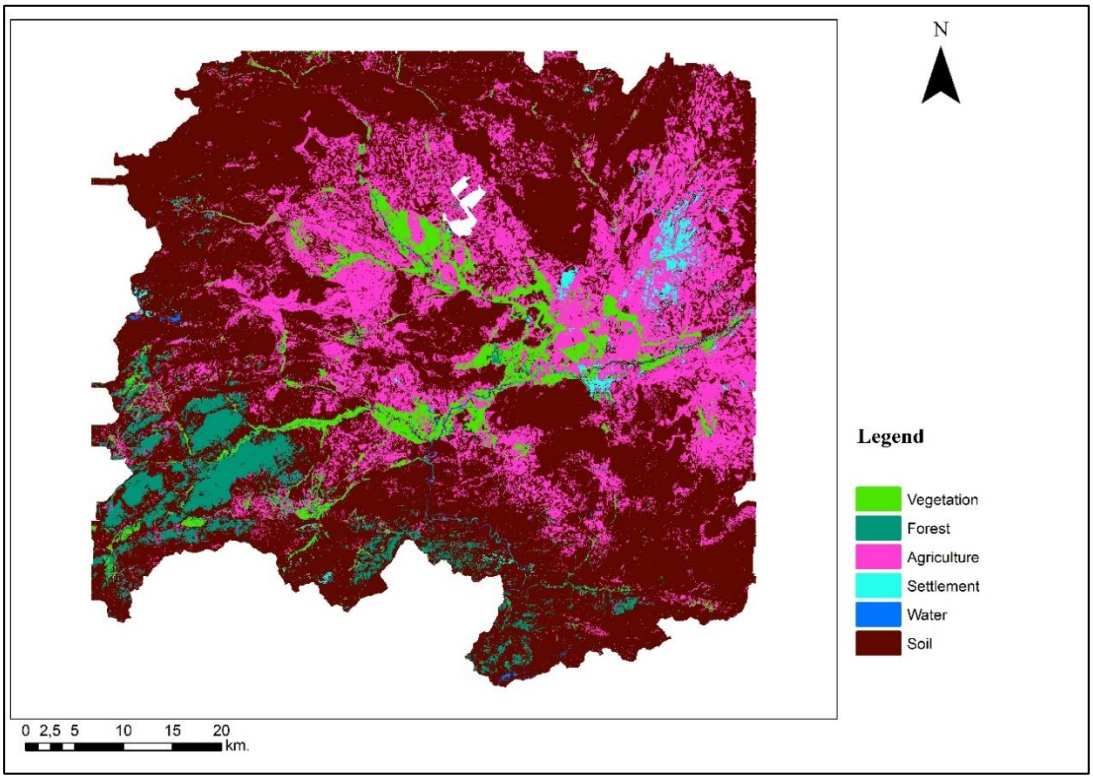

Figure 53. CDTL classification of Afşin-Elbistan Coal Basin for year 1984

For the classification of 1987 (Figure 54), percentages of the six classes are: Vegetation is 7.1%, forest is 3.9%, agriculture is 30.9%, settlement is 0.6%, water is 0.5%, soil is 56.6%, and the mine area covers 0.3% of the basin. When compared to the classified image of 1984, vegetated lands transforms to soil and agriculture around the mine, again vegetation shrinks in the southwest of the basin, settlement decreases, and forested areas are nearly unchanged.

For the classification of 1990 image (Figure 55), percentage of the six classes are: Vegetation is 8.4%, forest is 5.3%, agriculture is 24.6%, settlement is 1.1%, water is 0.3%, soil is 59.9%, and the mine area covers 0.5% of the basin. When compared to the classified image of 1987, transformed vegetated areas of the 1987 image around the cast mine becomes vegetated again, vegetation on the southwestern part of the basin increases, settlement increases in the southeast and the south of the mine, and there is a slight increase on the forested areas.

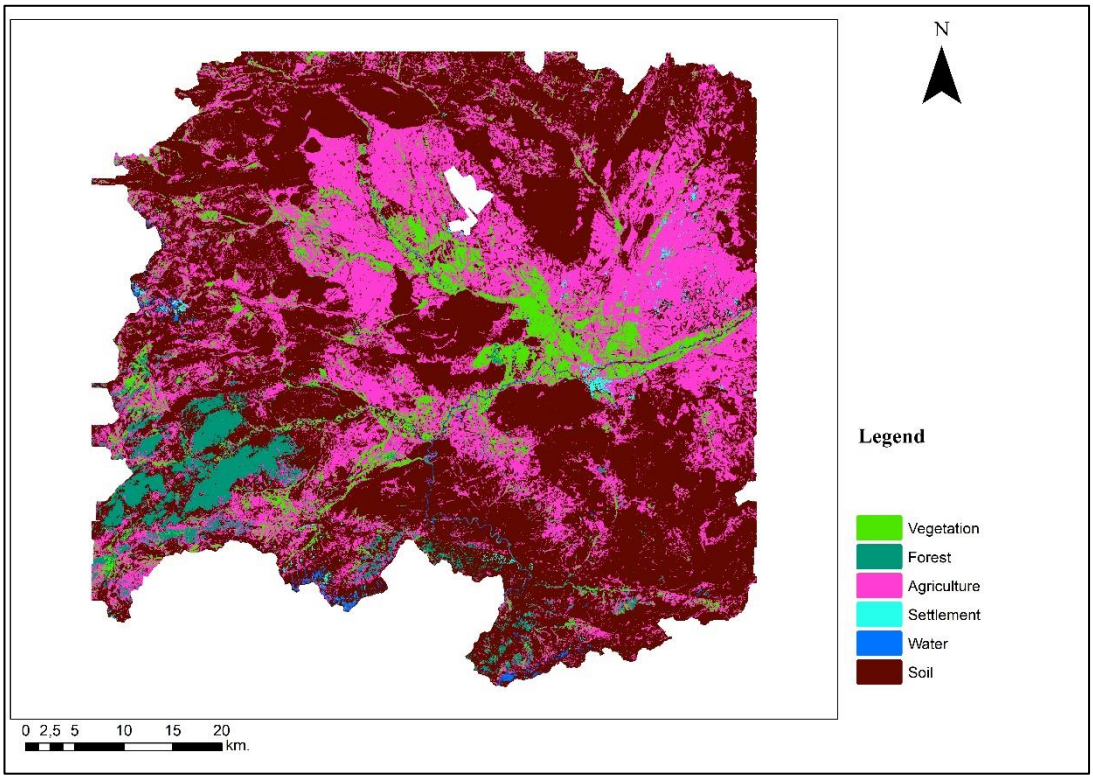

Figure 54. CDTL classification of Afşin-Elbistan Coal Basin for year 1987

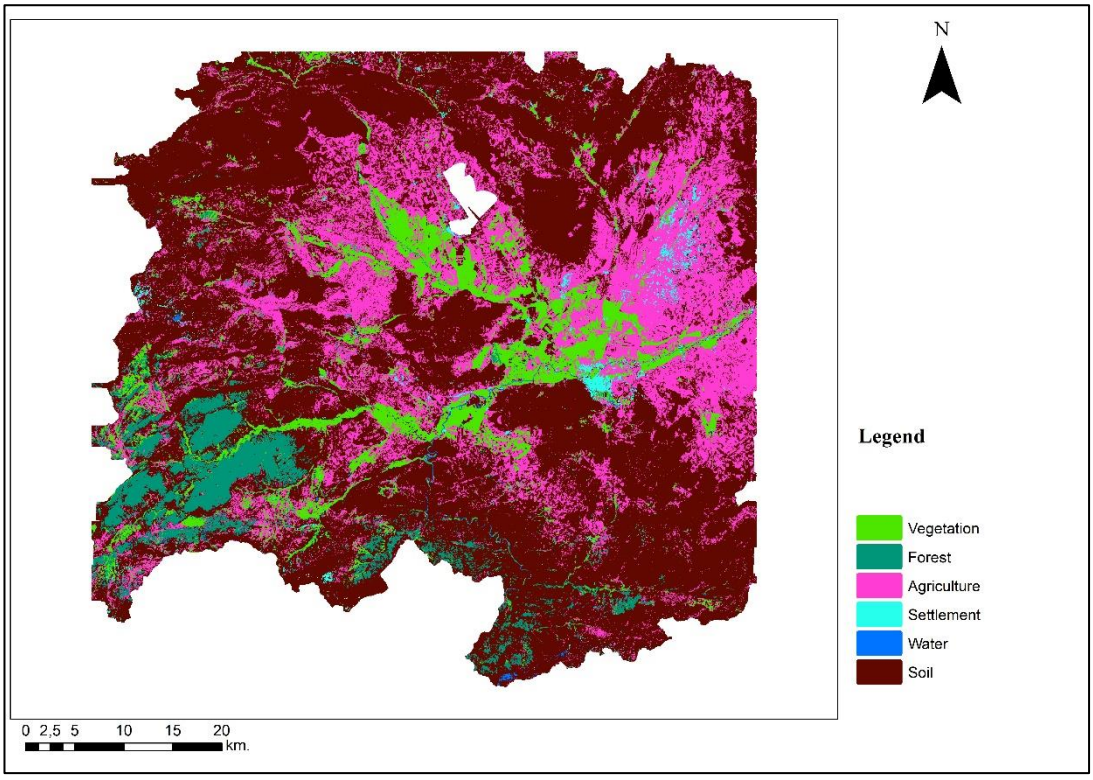

Figure 55. CDTL classification of Afşin-Elbistan Coal Basin for year 1990

For the classification of 2000 image (Figure 56), percentage of the six main classes are: vegetation is 11.2%, forest is 4.4%, agriculture is 23.1%, settlement is 1.7%, water is 0.6%, soil is 58.3%, and the mine area covers 0.7% of the basin. When compared to the thematic map of 1990, the northwestern parts of the agriculture around the mine becomes intact, settlement increases, waterways slightly increases, and forested areas decreases a little.

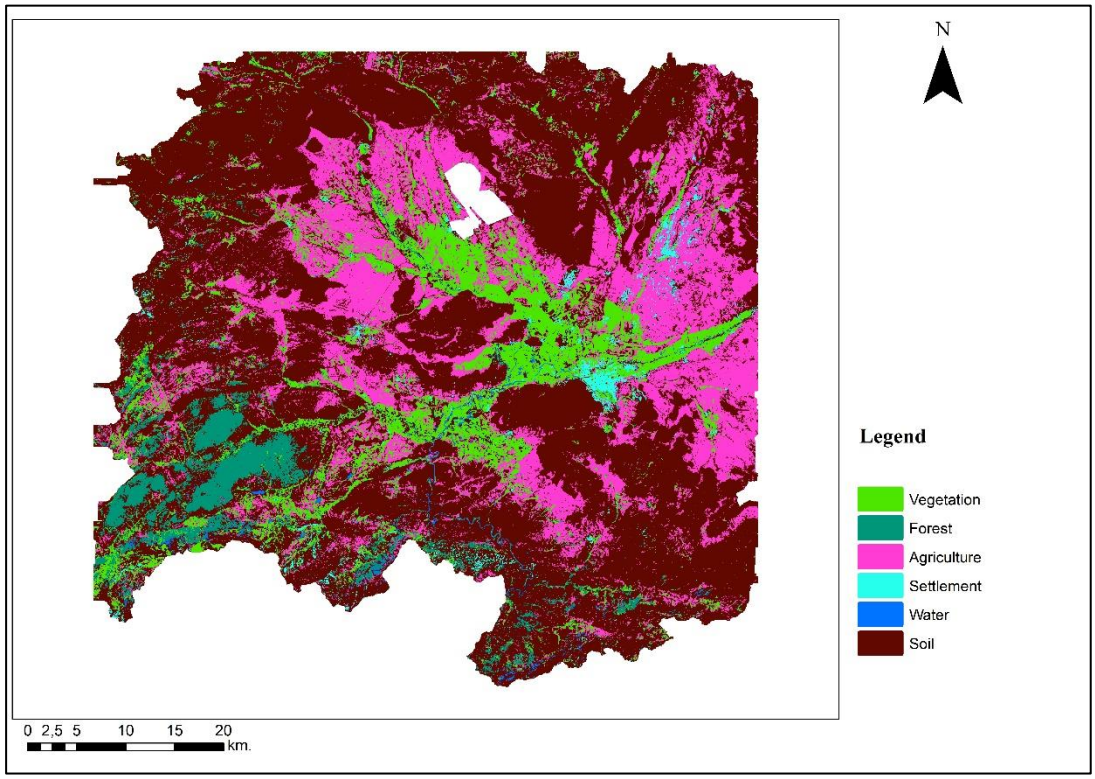

Figure 56. CDTL classification of Afşin-Elbistan Coal Basin for year 2000

For the classification of 2003 image (Figure 57), percentage of the six classes are: Vegetation is 8.8%, forest is 4.6%, agriculture is 24.2%, settlement is 2.4%, water is 0.5%, soil is 58.3%, and the mine area covers 1.1% of the basin. When compared to the classified image of 2000, vegetation slightly decreases, there is a rapid increase in settlement class, this increase may be related to the misclassification of the pixels, forested areas nearly are unchanged, and waterways are dispersed in the basin.

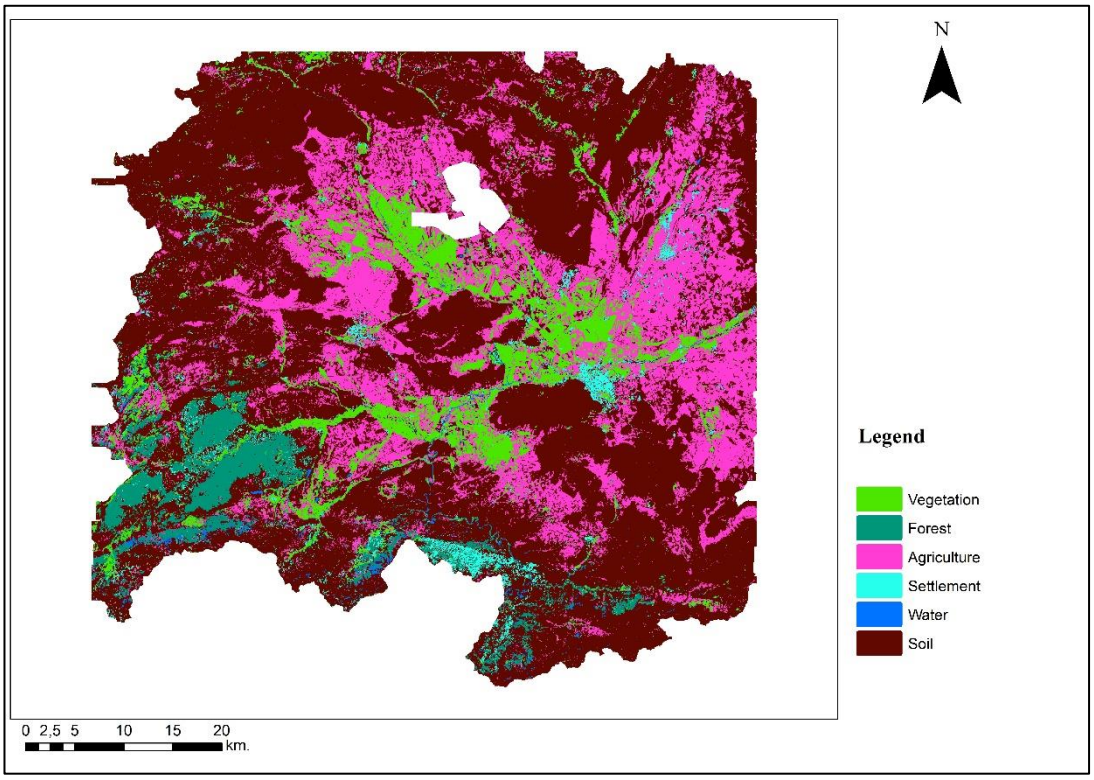

Figure 57. CDTL classification of Afşin-Elbistan Coal Basin for year 2003

For the classification of 2005 (Figure 58), percentage of the classes are: Vegetation is 14.6%, forest is 5%, agriculture is 28.9%, settlement is 1.1%, water is 0.2%, soil is 49.1%, and the mine area covers 1.2% of the basin. When compared to the classified image of 2003, vegetation increases broadly, agriculture increases, settlement decreases, and forested areas are nearly unaltered.

For the classification of 2008 image (Figure 59), percentage of the six classes are: Vegetation is 7%, forest is 4.9%, agriculture is 26.6%, settlement is 2.6%, water is 0.4%, soil is 57.3%, and the mine area covers 1.2% of the basin. When compared to the classified image of 2005, vegetation rapidly decreases, settlement increases, especially in the southwestern part of the mine, forested areas are unaltered, and there is a slight increase in the waterways.

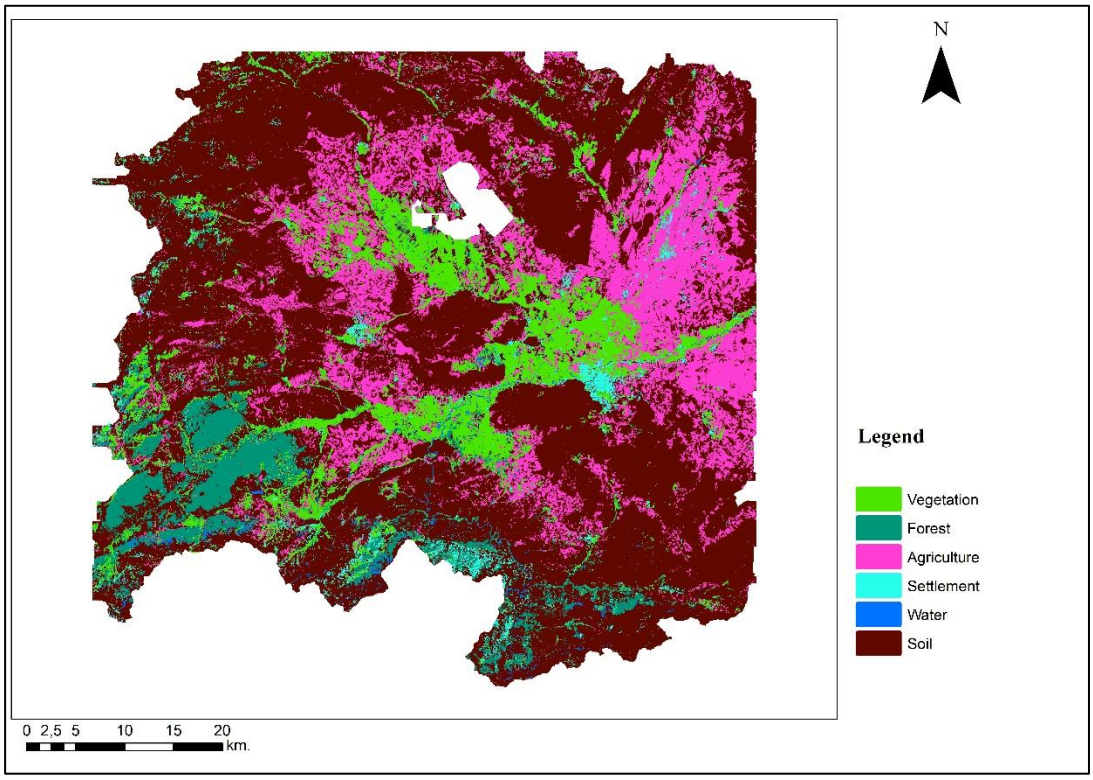

Figure 58. CDTL classification of Afşin-Elbistan Coal Basin for year 2005

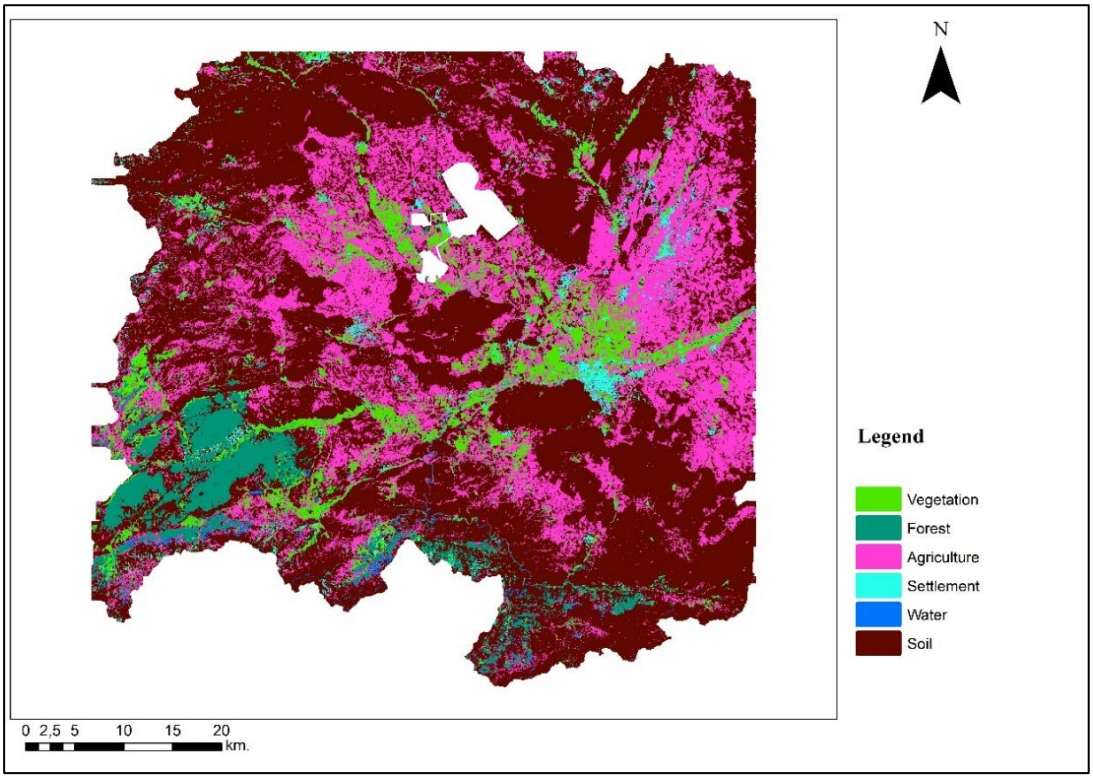

Figure 59. CDTL classification of Afşin-Elbistan Coal Basin for year 2008

For the classification of 2011 image (Figure 60), percentage of the six main classes are: Vegetation is 9.6%, forest is 4.9%, agriculture is 22.3%, settlement is 1%, water is 0.7%, soil is 59.9%, and the mine area covers 1.5% of the basin. When compared to the classified image of 2008, vegetation increases, agricultural lands around the mine transforms into vegetation and decreases mainly, and forested areas and waterways are nearly unchanged.

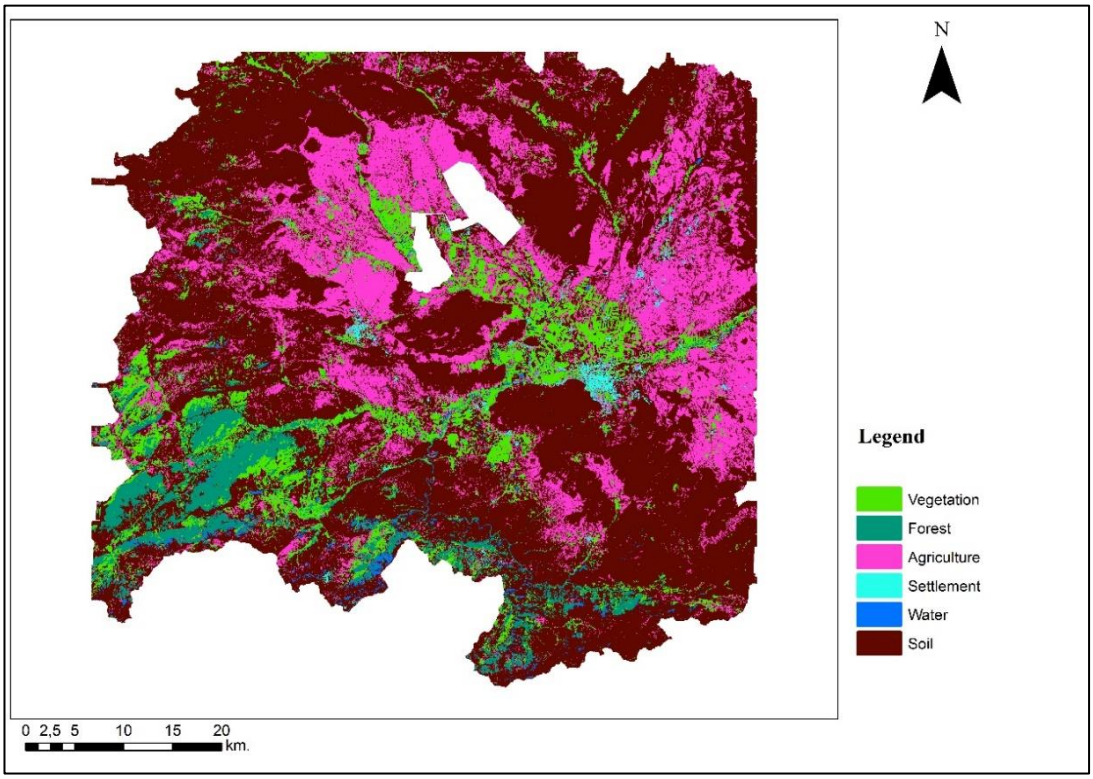

Figure 60. CDTL classification of Afşin-Elbistan Coal Basin for year 2011

Finally for the classification of 2014 image (Figure 61), percentage of the six classes are: Vegetation is 6.1%, forest is 6%, agriculture is 23.6%, settlement is 1.8%, water is 2.2%, soil is 58.9%, and the mine area covers 1.5% of the basin. When compared to the classified image of 2011, there is a slight increase in agriculture. The settlement class increases in the southeastern part of the mine, waterways are clearly visible and increases, the reason for the rapid increase may be the enlarged water

surfaces due to dam reservoirs of hydroelectric power plants in the basin, and forested areas also increase.

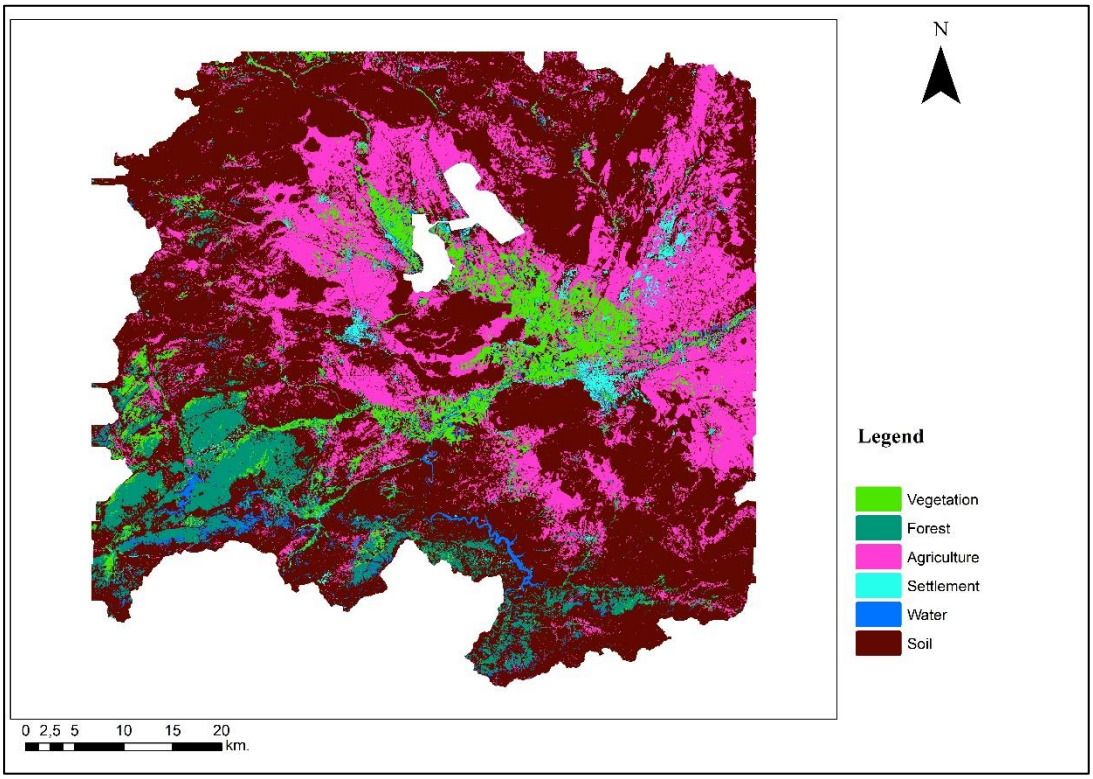

Figure 61. CDTL classification of Afşin-Elbistan Coal Basin for year 2014

4.4.4. Accuracy Assessments

In order to conduct accuracy assessment, approximately 2000 random points are assigned in the classified images using ArcGIS 10 software. As it can be seen from Figure 62, each point represents a pixel on the image. The overall accuracy, i.e.(intersecting pixels/total point number)*100, is calculated by using the matrix in Figure 5.

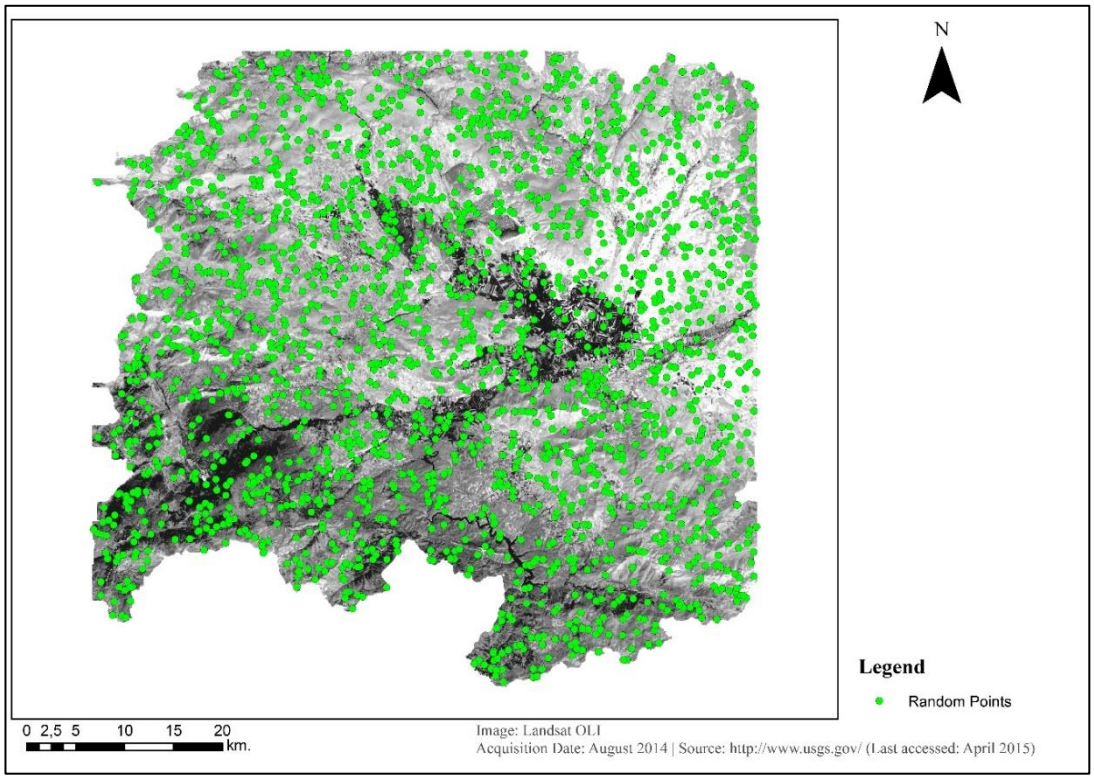

Figure 62. Random points assigned on the image of 2014

Another important accuracy metric is Kappa coefficient, which determines whether the accuracy calculation is valid or not. Calculation of Kappa coefficient can be seen from Figure 63. In Figure 63, the first table is error matrix of a classification with three classes (C1, C2, C3) the second table is prepared to calculate kappa coefficient. It needs two values which are, expected (Ex) and overall accuracy (OA). In order to calculate Ex, cumulative sum (CS) and production matrix (PM) must be found, which are calculated with addition of all the cells and addition of diagonal cells in coefficient calculation table respectively. Dividing PM to CS gives the Ex value and finally Kappa coefficient is calculated as (OA - Ex) / (1 - Ex).

Classification error matrix		Classified Image			
		C1*	C2*	C3*	
Original Image	C1*	x	k	m	OT1*
	C2*	y	l	n	OT2*
	C3*	z	m	o	OT3*
		CT1*	CT2*	CT3*	GT*

Coefficient calculation		Classified Image		
		C1*	C2*	C3*
Original Image	C1*	**CT1xOT1 = P1**	CT2xOT1 = c	CT3xOT1 = e
	C2*	CT1xOT2 = a	**CT2xOT2 = P2**	CT3xOT2 = f
	C3*	CT1xOT3 = b	CT2xOT3 = d	**CT3xOT3 = P3**

Product Matrix = P1 + P2 + P3 = PM
Cumulative Sum = PM + a + b + c + d + e + f = CS
Expected = PM / CS = Ex
Kappa coefficient = (OA* - Ex) / (1 - Ex)

*C = Class, CT = Class Total, OT = Original Total, GT= General Total, OA = Overall Accuracy

Figure 63. Kappa coefficient calculation example

Accuracy Assessments of the SVM Classifications

The number of samples used for the accuracy assessment of 1984 image is 1911. As it can be seen from Table 4, the most unsuccessful class is water with 69.2% producer's accuracy. Overall accuracy is calculated as 86.9% and the Kappa coefficient is 0.79 when these results are compared, the calculation is successful.

The number of samples used for the accuracy assessment of 1987 image is 2057. As it can be seen from Table 5, the most unsuccessful class is forest with 69.3% producer's accuracy. Overall accuracy (OA) is calculated as 86.9% and the Kappa coefficient is 0.78 when these results are compared, the calculation is successful.

Table 4. Error matrix of the classification of year 1984

		CI*								
		F*	V*	A*	S*	M*	So*	W*	Total	UA* (%)
	F*	**106**	1	1	1	0	7	0	116	**91.4**
	V*	7	**125**	0	0	0	0	0	132	**94.7**
	A*	1	4	**525**	1	0	70	0	601	**87.4**
OI*	S*	0	3	0	**32**	0	4	0	39	**82.1**
	M*	0	0	0	0	**10**	0	0	10	**100**
	So*	23	11	107	5	0	**854**	4	1004	**85.1**
	W*	0	0	0	0	0	0	**9**	9	**100**
	Total	137	144	633	39	10	935	13	**1911**	
	PA* (%)	**77.4**	**86.8**	**82.9**	**82.1**	**100**	**91.3**	**69.2**		
	OA: 86.9%, Kappa= 0.79									

*F=Forest, V=Vegetation, A= Agriculture, S=Settlement, M=Mine, So=Soil, W= Water, UA= User's accuracy, PA= Producer's accuracy, OI= Original image, CI= Classified image

Table 5. Error matrix of the classification of year 1987

		CI*								
		F*	V*	A*	S*	M*	So*	W*	Total	UA* (%)
	F*	**79**	2	0	0	0	8	0	89	**88.8**
	V*	8	**91**	8	0	0	7	1	115	**79.1**
	A*	7	9	**588**	2	0	37	0	643	**91.4**
OI*	S*	0	0	0	**28**	0	3	0	31	**90.3**
	M*	0	0	0	0	**12**	0	0	12	**100**
	So*	20	17	127	3	0	**976**	2	1145	**85.2**
	W*	0	0	0	0	0	8	**14**	22	**63.6**
	Total	114	119	723	33	12	1039	17	**2057**	
	PA* (%)	**69.3**	**76.5**	**81.3**	**84.8**	**100**	**93.9**	**82.4**		
	OA: 86.9%, Kappa= 0.78									

*F=Forest, V=Vegetation, A= Agriculture, S=Settlement, M=Mine, So=Soil, W= Water, UA= User's accuracy, PA= Producer's accuracy, OI= Original image, CI= Classified image

The number of samples used for the accuracy assessment of 1990 image is 2056. As it can be seen from Table 6, the most unsuccessful class is forest with 72.9% producer's accuracy. OA is calculated as 84.8% and the Kappa coefficient is 0.76 when these results are compared, the calculation is successful.

Table 6. Error matrix of the classification of year 1990

		CI*							
		F*	V*	A*	S*	M*	So*	W*	Total	UA* (%)
	F*	**97**	9	0	0	0	7	0	113	**85.8**
	V*	3	**105**	1	1	0	4	0	114	**92.1**
	A*	16	7	**699**	2	0	131	0	855	**81.8**
OI*	S*	2	1	1	**22**	0	2	0	28	**78.6**
	M*	0	0	0	0	**12**	0	0	12	**100**
	So*	15	6	95	3	0	**797**	1	917	**86.9**
	W*	0	0	0	0	0	5	**12**	17	**70.6**
	Total	133	128	796	28	12	946	13	**2056**	
	PA* (%)	**72.9**	**82**	**87.8**	**78.6**	**100**	**84.2**	**92.3**		
	OA: 84.8%, Kappa= 0.76									

*F=Forest, V=Vegetation, A= Agriculture, S=Settlement, M=Mine, So=Soil, W= Water, UA= User's accuracy, PA= Producer's accuracy, OI= Original image, CI= Classified image

The number of samples used for the accuracy assessment of 2000 image is 2052. As it can be seen from Table 7, the most unsuccessful class is settlement with 53.1% producer's accuracy. OA is calculated as 87.2% and the Kappa coefficient is 0.79 when these results are compared, the calculation is successful.

The number of samples used for the accuracy assessment of 2003 image is 2059. As it can be seen from Table 8, the most unsuccessful class is settlement with 53.1% producer's accuracy. OA is calculated as 87.7% and the Kappa coefficient is 0.78 when these results are compared, the calculation is successful.

Table 7. Error matrix of the classification of year 2000

		CI*								
		F*	V*	A*	S*	M*	So*	W*	Total	UA* (%)
	F*	**81**	4	0	0	0	8	1	94	**86.2**
	V*	5	**117**	3	0	0	0	0	125	**93.6**
	A*	15	17	**567**	6	0	61	2	668	**84.9**
OI*	S*	0	0	0	**17**	0	2	0	19	**89.5**
	M*	0	0	0	0	**18**	0	0	18	**100**
	So*	34	34	56	9	0	**972**	2	1107	**87.8**
	W*	0	0	0	0	0	2	**19**	21	**90.5**
	Total	135	172	626	32	18	1045	24	**2052**	
	PA* (%)	**60**	**68**	**90.6**	**53.1**	**100**	**93**	**79.2**		
	OA: 87.2%, Kappa= 0.79									

*F=Forest, V=Vegetation, A= Agriculture, S=Settlement, M=Mine, So=Soil, W= Water, UA= User's accuracy, PA= Producer's accuracy, OI= Original image, CI= Classified image

Table 8. Error matrix of the classification of year 2003

		CI*								
		F*	V*	A*	S*	M*	So*	W*	Total	UA* (%)
	F*	**99**	8	1	0	0	10	1	119	**83.2**
	V*	4	**135**	2	0	2	0	0	143	**94.4**
	A*	0	0	**342**	1	0	32	0	375	**91.2**
OI*	S*	0	0	0	**17**	0	3	0	20	**85**
	M*	0	0	0	0	**41**	0	0	41	**100**
	So*	8	14	143	14	0	**1152**	4	1335	**86.3**
	W*	0	0	0	0	0	7	**19**	26	**73.1**
	Total	111	157	488	32	43	1204	24	**2059**	
	PA* (%)	**89.2**	**86**	**70.1**	**53.1**	**95.3**	**95.7**	**79.2**		
	OA: 87.7%, Kappa= 0.78									

*F=Forest, V=Vegetation, A= Agriculture, S=Settlement, M=Mine, So=Soil, W= Water, UA= User's accuracy, PA= Producer's accuracy, OI= Original image, CI= Classified image

The number of samples used for the accuracy assessment of 2005 image is 2035. As it can be seen from Table 9, the most unsuccessful class is forest with 57.7% producer's accuracy. OA is calculated as 80.6% and the Kappa coefficient is 0.71 which indicates a valid accuracy assessment.

Table 9. Error matrix of the classification of year 2005

		CI*							
		F*	V*	A*	S*	M*	So*	W*	Total	UA* (%)
	F*	**75**	8	0	0	0	9	0	92	**81.5**
	V*	13	**231**	5	1	0	34	2	286	**80.8**
	A*	17	15	**455**	5	0	97	0	589	**77.2**
OI*	S*	0	1	2	**17**	0	1	0	21	**81**
	M*	0	0	0	0	**26**	0	0	26	**100**
	So*	25	26	125	5	0	**820**	0	1001	**81.9**
	W*	0	0	0	0	0	4	**16**	20	**80**
	Total	130	281	587	28	26	965	18	**2035**	
	PA* (%)	**57.7**	**82.2**	**77.5**	**60.7**	**100**	**85**	**88.9**		
	OA: 80.60%, Kappa= 0.71									

*F=Forest, V=Vegetation, A= Agriculture, S=Settlement, M=Mine, So=Soil, W= Water, UA= User's accuracy, PA= Producer's accuracy, OI= Original image, CI= Classified image

The number of samples used for the accuracy assessment of 2008 image is 2059. As it can be seen from Table 10, the most unsuccessful class is settlement with 27.3% producer's accuracy. OA is calculated as 87.8% and the Kappa coefficient is 0.79 when these results are compared, the calculation is successful.

The number of samples used for the accuracy assessment of 2011 image is 2041. As it can be seen from Table 11, the most unsuccessful class is forest with 58.5% producer's accuracy. OA is calculated as 80.8% and the Kappa coefficient is 0.70 when these results are compared, the calculation is successful.

Table 10. Error matrix of the classification of year 2008

		CI*								
		F*	V*	A*	S*	M*	So*	W*	Total	UA* (%)
	F*	**132**	5	4	0	0	7	1	149	**88.6**
	V*	4	**103**	1	2	0	0	0	110	**93.6**
	A*	0	2	**376**	4	0	31	0	413	**91**
OI*	S*	0	0	0	**9**	0	1	0	10	**90**
	M*	0	0	0	0	**39**	0	0	39	**100**
	So*	8	18	141	18	0	**1137**	4	1326	**85.7**
	W*	0	0	0	0	0	0	**12**	12	**100**
	Total	144	128	522	33	39	1176	17	**2059**	
	PA* (%)	**91.7**	**80.5**	**72**	**27.3**	**100**	**96.7**	**70.6**		
	OA: 87.8%, Kappa= 0.79									

*F=Forest, V=Vegetation, A= Agriculture, S=Settlement, M=Mine, So=Soil, W= Water, UA= User's accuracy, PA= Producer's accuracy, OI= Original image, CI= Classified image

Table 11. Error matrix of the classification of year 2011

		CI*								
		F*	V*	A*	S*	M*	So*	W*	Total	UA* (%)
	F*	**100**	5	1	0	0	5	0	111	**90.1**
	V*	11	**111**	0	1	0	4	1	128	**86.7**
	A*	3	1	**309**	2	0	51	0	366	**84.4**
OI*	S*	0	0	1	**15**	0	6	0	22	**68.2**
	M*	0	0	0	0	**43**	0	0	43	**100**
	So*	57	58	169	7	0	**1062**	2	1355	**78.4**
	W*	0	0	0	0	0	5	**11**	16	**68.8**
	Total	171	175	480	25	43	1133	14	**2041**	
	PA* (%)	**58.5**	**63.4**	**64.4**	**60**	**100**	**93.7**	**78.6**		
	OA: 80.8%, Kappa= 0.70									

*F=Forest, V=Vegetation, A= Agriculture, S=Settlement, M=Mine, So=Soil, W= Water, UA= User's accuracy, PA= Producer's accuracy, OI= Original image, CI= Classified image

The number of samples used for the accuracy assessment of 2014 image is 2066. As it can seen from Table 12, the most unsuccessful class is settlement with 27.9% producer's accuracy. Overall accuracy is calculated as 89.4% and the Kappa coefficient is 0.83 when these results are compared, the calculation is successful.

Table 12. Error matrix of the classification of year 2014

		CI*								
		F*	V*	A*	S*	M*	So*	W*	Total	UA* (%)
	F*	**146**	13	2	2	0	4	2	169	**86.4**
	V*	2	**130**	0	3	0	0	0	135	**96.3**
	A*	0	0	**516**	4	0	60	0	580	**89**
OI*	S*	0	0	1	**12**	0	1	0	14	**85.7**
	M*	0	0	0	0	**45**	0	0	45	**100**
	So*	21	10	70	22	0	**984**	3	1110	**88.6**
	W*	0	0	0	0	0	0	**13**	13	**100**
	Total	169	153	589	43	45	1049	18	**2066**	
	PA* (%)	**86.4**	**85**	**87.6**	**27.9**	**100**	**93.8**	**72.2**		
	OA: 89.4%, Kappa= 0.83									

*F=Forest, V=Vegetation, A= Agriculture, S=Settlement, M=Mine, So=Soil, W= Water, UA= User's accuracy, PA= Producer's accuracy, OI= Original image, CI= Classified image

Accuracy Assessments of the CDTL Classifications

The number of samples used for the accuracy assessment of 1984 image is 1909. As it can be seen from Table 13, the most unsuccessful class is settlement with 30.8% producer's accuracy. Overall accuracy is calculated as 79.5% and the Kappa coefficient is 0.66 when these results are compared, the calculation is successful.

Table 13. Error matrix of the classification of year 1984

		CI*								
		F*	V*	A*	S*	M*	So*	W*	Total	UA* (%)
OI*	F*	**87**	8	15	0	0	27	0	137	**88.8**
	V*	1	**108**	18	1	0	10	4	142	**93.1**
	A*	1	0	**401**	10	0	221	0	633	**84.4**
	S*	1	0	5	**12**	0	21	0	39	**50**
	M*	0	0	0	0	**10**	0	0	10	**100**
	So*	8	0	36	1	0	**889**	1	935	**76**
	W*	0	0	0	0	0	2	**11**	13	**68.8**
	Total	98	116	475	24	10	1170	16	**1909**	
	PA* (%)	**63.5**	**76.1**	**63.3**	**30.8**	**100**	**95.1**	**84.6**		
	OA: 79.5%, Kappa= 0.66									

*F=Forest, V=Vegetation, A= Agriculture, S=Settlement, M=Mine, So=Soil, W= Water, UA= User's accuracy, PA= Producer's accuracy, OI= Original image, CI= Classified image

The number of samples used for the accuracy assessment of 1987 image is 2057. As it can be seen from Table 14, the most unsuccessful class is forest with 58.6% producer's accuracy. Overall accuracy is calculated as 81.5% and the Kappa coefficient is 0.70 when these results are compared, the calculation is successful.

The number of samples used for the accuracy assessment of 1990 image is 2056. As it can be seen from Table 15, the most unsuccessful class is agriculture with 57.8% producer's accuracy. Overall accuracy is calculated as 77.1% and the Kappa coefficient is 0.63 when these results are compared, the calculation is successful.

Table 14. Error matrix of the classification of year 1987

		CI*								
		F*	V*	A*	S*	M*	So*	W*	Total	UA* (%)
	F*	**65**	11	17	0	0	18	0	111	**86.7**
	V*	1	**104**	13	0	0	14	0	132	**66.2**
	A*	2	38	**518**	5	0	157	0	720	**83.4**
OI*	S*	0	0	2	**22**	0	9	0	33	**75.9**
	M*	0	0	0	0	**12**	0	0	12	**100**
	So*	7	4	71	2	0	**941**	7	1032	**82.4**
	W*	0	0	0	0	0	3	**14**	17	**66.7**
	Total	75	157	621	29	12	1142	21	**2057**	
	PA* (%)	**58.6**	**78.8**	**71.9**	**66.7**	**100**	**91.2**	**82.4**		
	OA: 81.5%, Kappa= 0.70									

*F=Forest, V=Vegetation, A= Agriculture, S=Settlement, M=Mine, So=Soil, W= Water, UA= User's accuracy, PA= Producer's accuracy, OI= Original image, CI= Classified image

Table 15. Error matrix of the classification of year 1990

		CI*								
		F*	V*	A*	S*	M*	So*	W*	Total	UA* (%)
	F*	**80**	27	4	2	0	20	0	133	**88.9**
	V*	2	**115**	6	1	0	4	0	128	**59.9**
	A*	0	40	**460**	7	0	289	0	796	**90.9**
OI*	S*	0	1	2	**21**	0	4	0	28	**55.3**
	M*	0	0	0	0	**12**	0	0	12	**100**
	So*	8	9	34	7	0	**887**	1	946	**73.5**
	W*	0	0	0	0	0	3	**10**	13	**90.9**
	Total	90	192	506	38	12	1207	11	**2056**	
	PA* (%)	**60.2**	**89.8**	**57.8**	**75**	**100**	**93.8**	**76.9**		
	OA: 77.1%, Kappa= 0.63									

*F=Forest, V=Vegetation, A= Agriculture, S=Settlement, M=Mine, So=Soil, W= Water, UA= User's accuracy, PA= Producer's accuracy, OI= Original image, CI= Classified image

The number of samples used for the accuracy assessment of 2000 image is 2047. As it can be seen from Table 16, the most unsuccessful class is forest with 50.8% producer's accuracy. Overall accuracy is calculated as 80.8% and the Kappa coefficient is 0.69 when these results are compared, the calculation is successful.

Table 16. Error matrix of the classification of year 2000

		CI*							
		F*	V*	A*	S*	M*	So*	W*	Total	UA* (%)
	F*	**66**	14	5	0	0	43	2	130	**76.7**
	V*	3	**129**	6	9	0	23	2	172	**57.3**
	A*	8	79	**415**	7	0	113	4	626	**89.8**
OI*	S*	0	0	5	**19**	0	8	0	32	**39.6**
	M*	0	0	0	0	**18**	0	0	18	**100**
	So*	6	3	31	13	0	**989**	3	1045	**84**
	W*	3	0	0	0	0	1	**20**	24	**64.5**
	Total	86	225	462	48	18	1177	31	**2047**	
	PA* (%)	**50.8**	**75**	**66.3**	**59.4**	**100**	**94.6**	**83.3**		
	OA: 80.8%, Kappa= 0.69									

*F=Forest, V=Vegetation, A= Agriculture, S=Settlement, M=Mine, So=Soil, W= Water, UA= User's accuracy, PA= Producer's accuracy, OI= Original image, CI= Classified image

The number of samples used for the accuracy assessment of 2003 image is 2059. As it can be seen from Table 17, the most unsuccessful class is water with 65.4% producer's accuracy. Overall accuracy is calculated as 83.5% and the Kappa coefficient is 0.72 when these results are compared, the calculation is successful.

The number of samples used for the accuracy assessment of 2005 image is 2035. As it can be seen from Table 18, the most unsuccessful class is settlement with 50% producer's accuracy. Overall accuracy is calculated as 78.6% and the Kappa coefficient is 0.67 when these results are compared, the calculation is successful.

Table 17. Error matrix of the classification of year 2003

		CI*								
		F*	V*	A*	S*	M*	So*	W*	Total	UA* (%)
	F*	**73**	15	9	4	0	9	1	111	**83**
	V*	2	**130**	23	2	0	2	0	159	**76**
	A*	0	12	**366**	3	0	107	0	488	**74.7**
OI*	S*	0	2	4	**23**	0	4	0	33	**44.2**
	M*	0	0	0	0	**35**	0	0	35	**100**
	So*	9	12	86	20	0	**1075**	5	1207	**89.6**
	W*	4	0	2	0	0	3	**17**	26	**73.9**
	Total	88	171	490	52	35	1200	23	**2059**	
	PA* (%)	**65.8**	**81.8**	**75**	**69.7**	**100**	**89.1**	**65.4**		
	OA: 83.5%, Kappa= 0.72									

*F=Forest, V=Vegetation, A= Agriculture, S=Settlement, M=Mine, So=Soil, W= Water, UA= User's accuracy, PA= Producer's accuracy, OI= Original image, CI= Classified image

Table 18. Error matrix of the classification of year 2005

		CI*								
		F*	V*	A*	S*	M*	So*	W*	Total	UA* (%)
	F*	**76**	4	4	10	0	35	1	130	**76**
	V*	12	**196**	14	16	0	40	3	281	**91.2**
	A*	0	13	**362**	6	0	206	0	587	**88.5**
OI*	S*	0	0	6	**14**	0	8	0	28	**23.7**
	M*	0	0	0	0	**26**	0	0	26	**100**
	So*	12	2	23	13	0	**909**	6	965	**75.8**
	W*	0	0	0	0	0	1	**17**	18	**63**
	Total	100	215	409	59	26	1199	27	**2035**	
	PA* (%)	**58.5**	**69.8**	**61.7**	**50**	**100**	**94.2**	**94.4**		
	OA: 78.6%, Kappa= 0.67									

*F=Forest, V=Vegetation, A= Agriculture, S=Settlement, M=Mine, So=Soil, W= Water, UA= User's accuracy, PA= Producer's accuracy, OI= Original image, CI= Classified image

The number of samples used for the accuracy assessment of 2008 image is 2059. As it can be seen from Table 19, the most unsuccessful class is settlement with 45.5% producer's accuracy. Overall accuracy is calculated as 78.3% and the Kappa coefficient is 0.64 when these results are compared, the calculation is successful.

Table 19. Error matrix of the classification of year 2008

		CI*								
		F*	V*	A*	S*	M*	So*	W*	Total	UA* (%)
	F*	**77**	32	16	6	0	12	1	144	**91.7**
	V*	3	**96**	23	2	0	4	0	128	**64.4**
	A*	0	9	**362**	8	0	142	0	521	**70.6**
OI*	S*	0	2	4	**15**	0	12	0	33	**21.1**
	M*	0	0	0	0	**39**	0	0	39	**100**
	So*	3	10	107	40	0	**1010**	7	1177	**85.5**
	W*	1	0	1	0	0	1	**14**	17	**63.6**
	Total	84	149	513	71	39	1181	22	**2059**	
	PA* (%)	**53.5**	**75**	**69.5**	**45.5**	**100**	**85.8**	**82.4**		
	OA: 78.3%, Kappa= 0.64									

*F=Forest, V=Vegetation, A= Agriculture, S=Settlement, M=Mine, So=Soil, W= Water, UA= User's accuracy, PA= Producer's accuracy, OI= Original image, CI= Classified image

The number of samples used for the accuracy assessment of 2011 image is 2041. As it can be seen from Table 20, the most unsuccessful class is forest with 44.3% producer's accuracy. Overall accuracy is calculated as 76.6% and the Kappa coefficient is 0.61 when these results are compared, the calculation is successful.

The number of samples used for the accuracy assessment of 2014 image is 2066. As it can be seen from Table 21, the most unsuccessful class is settlement with 62.8% producer's accuracy. Overall accuracy is calculated as 84.1% and the Kappa coefficient is 0.75 when these results are compared, the calculation is successful.

Table 20. Error matrix of the classification of year 2011

		CI*								
		F*	V*	A*	S*	M*	So*	W*	Total	UA* (%)
	F*	**78**	48	10	0	0	37	3	176	**85.7**
	V*	5	**130**	13	2	0	28	1	179	**65.3**
	A*	0	5	**317**	3	0	155	0	480	**68.6**
OI*	S*	0	4	2	**13**	0	6	0	25	**59.1**
	M*	0	0	0	0	**34**	0	0	34	**100**
	So*	7	12	120	4	0	**980**	10	1133	**81.1**
	W*	1	0	0	0	0	2	**11**	14	**44**
	Total	91	199	462	22	34	1208	25	**2041**	
	PA* (%)	**44.3**	**72.6**	**66**	**52**	**100**	**86.5**	**78.6**		
	OA: 76.6%, Kappa= 0.61									

*F=Forest, V=Vegetation, A= Agriculture, S=Settlement, M=Mine, So=Soil, W= Water, UA= User's accuracy, PA= Producer's accuracy, OI= Original image, CI= Classified image

Table 21. Error matrix of the classification of year 2014

		CI*								
		F*	V*	A*	S*	M*	So*	W*	Total	UA* (%)
	F*	**106**	9	5	4	0	26	19	169	**93**
	V*	2	**120**	14	1	0	6	10	153	**91.6**
	A*	0	0	**431**	6	0	151	1	589	**87.1**
OI*	S*	1	2	4	**27**	0	8	1	43	**61.4**
	M*	0	0	0	0	**45**	0	0	45	**100**
	So*	4	0	41	6	0	**995**	3	1049	**83.7**
	W*	1	0	0	0	0	3	**14**	18	**29.2**
	Total	114	131	495	44	45	1189	48	**2066**	
	PA* (%)	**62.7**	**78.4**	**73.2**	**62.8**	**100**	**94.9**	**77.8**		
	OA: 84.1%, Kappa= 0.75									

*F=Forest, V=Vegetation, A= Agriculture, S=Settlement, M=Mine, So=Soil, W= Water, UA= User's accuracy, PA= Producer's accuracy, OI= Original image, CI= Classified image

4.5 Land Use Land Cover Change Detection

LULC change detection between years of 1984 and 2014 for Afşin-Elbistan Coal Basin is performed with *Change Detection* function of ENVI5.0 software. Images with traditional SVM classification and CDTL method are divided into seven pairs of consecutive years, which are 1984-1987, 1987-1990, 1990-2000, 2003-2005, 2005-2008, 2008-2011, and 2011-2014. All of the LULC change maps can be seen between Figure 64 and Figure 79, and change statistics are given between Table 22 and Table 37. From the images, legends indicate changes between the classes from initial year to final year, there are six main classes, which are vegetation, forest, agriculture, settlement, soil, and water. In the tables of change statistics (Table 22-Table 37), *Class Difference* row is the difference in the total number of equivalently classed pixels in two images, computed by subtracting the *Initial State Class Totals* from *Final State Class Totals*. Positive *Class Difference* indicates increase in the class size. Likewise, negative *Class Difference* indicates decrease in class size. For example, in Table 22, agriculture increases by 7.3% and forest decreases by 21.1%, and they are calculated by subtracting initial state pixel count from final state pixel count, then dividing the result with initial state pixel count (ENVI5.0 Help Menu, 2012). The reason of percentage difference between the classification maps and LULC change maps is that mining terrain is included in classification map percentage calculations.

Post-classification change detection with SVM classification

The change map between the years of 1984 and 1987 can be seen from Figure 64. The first class indicates that it belongs to the year 1984, and the second one belongs to year 1987. The observable changes are; agriculture to vegetation (light purple), soil to agriculture (light green), soil to vegetation (light blue) and soil to settlement (dark blue). As it can be seen from Table 22, while vegetation, forest and settlement classes decrease, agriculture, water and soil classes increase. Decrease in settlement is due to the classifications errors in 1984 thematic map, increase in agriculture is related to the increase in vegetation as agricultural lands changes to vegetated lands in resultant change detection map.

Table 22. Change statistics between years 1984 and 1987

		1984					
		Vegetation (%)	Forest (%)	Agriculture (%)	Settlement (%)	Water (%)	Soil (%)
1987	Vegetation (%)	40.7	6.7	5.5	5	0.5	1.1
	Forest (%)	1.6	64.9	0.2	1.8	0	0.9
	Agriculture (%)	41.8	17.9	62.9	28.1	0.2	15.6
	Settlement (%)	0.2	0	0.5	1.5	0.3	0.7
	Water (%)	0.5	0.9	0.1	0.4	91.9	0.6
	Soil (%)	15.2	9.5	30.4	63.2	7	81.1
	Total (%)	100	100	100	100	100	100
	Class Changes (%)	59.3	35.1	37.1	98.5	8.1	18.9
	Class Difference (%)	**-11.3**	**-21.1**	**7.3**	**-91.7**	**534.2**	**11.4**

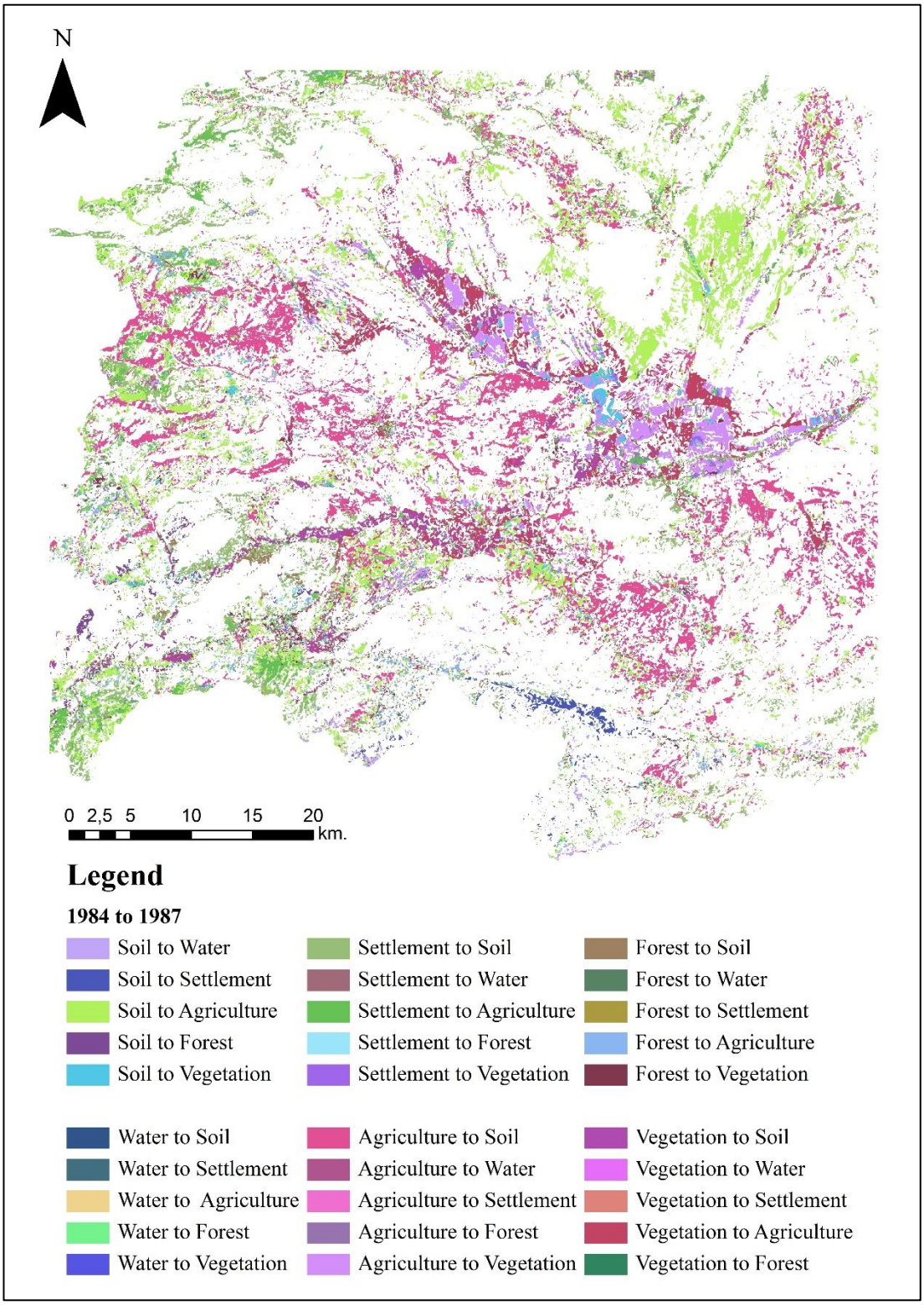

Figure 64. Change map between the years 1984 and 1987

The change map between the years of 1987 and 1990 can be seen from Figure 65. The first class indicates that it belongs to the year of 1987 and the second one belongs to year of 1990. The signifcant changes are; agriculture to vegetation (light purple), soil to agriculture (light green), vegetation to agriculture (maroon), and soil to vegetation (light blue). As it can be seen from Table 23, while vegetation, settlement, water and soil classes are decreasing, forest and agriculture classes increase. Increase in vegetated lands is related to the decrease in agriculture class as both of the classes change into others in the resultant change detection map.

Table 23. Change statistics between years 1987 and 1990

		1987					
		Vegetation (%)	Forest (%)	Agriculture (%)	Settlement (%)	Water (%)	Soil (%)
1990	Vegetation (%)	35.9	2.1	7.2	1.8	5.1	1.5
	Forest (%)	8.6	76.1	3.3	1	7.7	2
	Agriculture (%)	45.7	10.7	70.8	21.3	10.7	28
	Settlement (%)	0.4	0	0.7	15.2	0.7	0.2
	Water (%)	0.3	0.3	0.1	0.3	21.2	0.2
	Soil (%)	8.9	10.8	17.7	60.3	54.2	68
	Total (%)	100	100	100	100	100	100
	Class Changes (%)	64.1	23.9	29.2	84.8	78.8	32
	Class Difference (%)	**-2.8**	**38.1**	**28.8**	**-22.5**	**-46.4**	**-18.8**

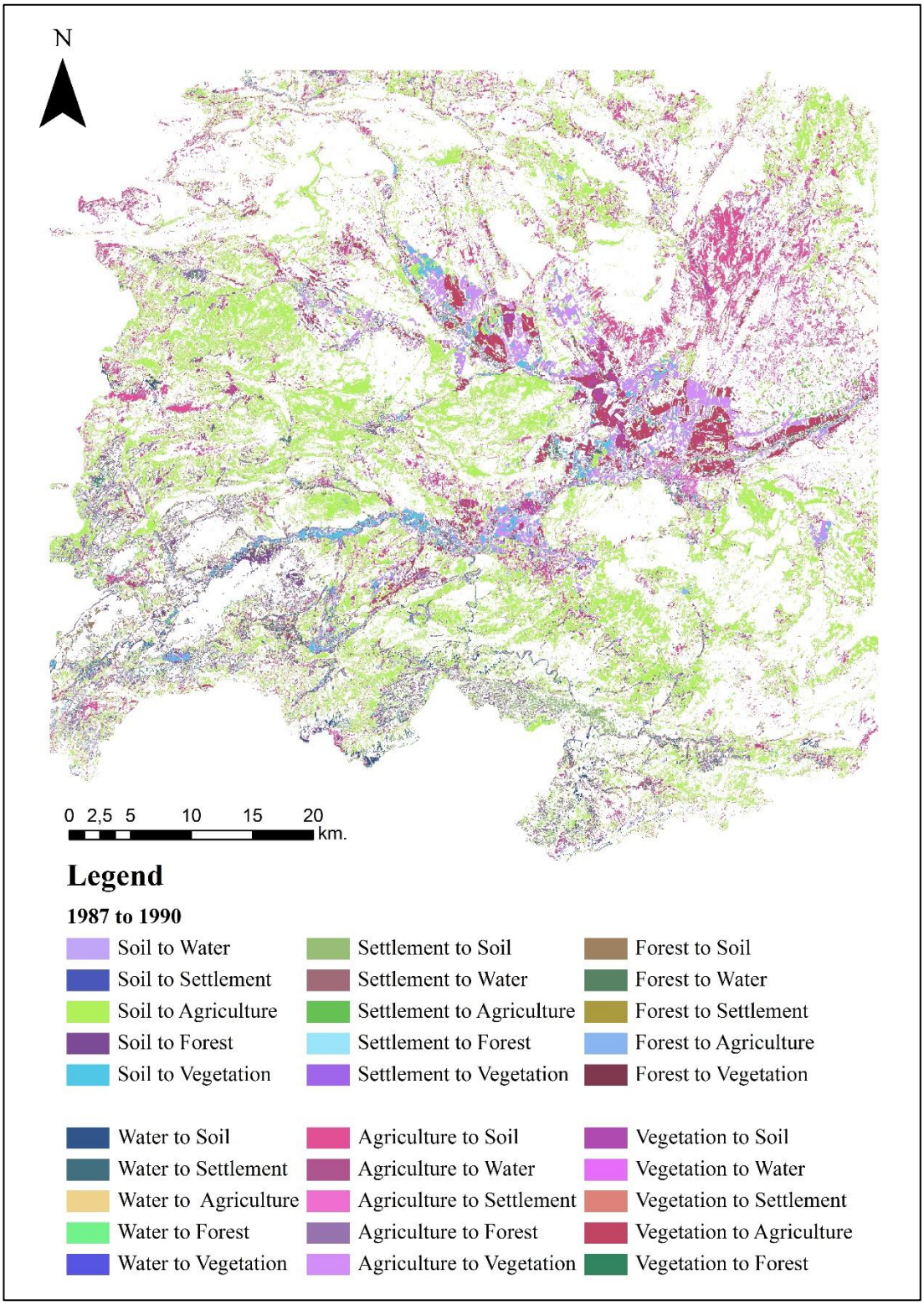

Figure 65. Change map between the years 1987 and 1990

The change map between the years of 1990 and 2000 can be seen from Figure 65. The first class indicates that it belongs to the year of 1990 and the second one belongs to year of 2000. The important changes are; agriculture to vegetation (light purple), agriculture to soil (pink), and soil to vegetation (light blue). From Table 24, forest, agriculture and settlement classes decrease, vegetation, water and soil classes increase. Between years of 1990 and 2000, power plant constructions began; therefore the soil increase can be related to these activities. Vegetated lands increase because, while agricultural lands are left uncultivated, they are detected as vegetated lands.

Table 24. Change statistics between years 1990 and 2000

		1990					
		Vegetation (%)	Forest (%)	Agriculture (%)	Settlement (%)	Water (%)	Soil (%)
2000	Vegetation (%)	49.5	6.7	5.7	3	7.4	1
	Forest (%)	3.2	60	1	0.2	4.4	1.1
	Agriculture (%)	32.5	18.6	59.8	30.7	11.9	10.8
	Settlement (%)	0.3	0.1	0.2	28.8	0.6	0.5
	Water (%)	0.3	0.7	0.1	0.1	23.7	0.3
	Soil (%)	14	14	32.8	36.5	52.1	86.2
	Total (%)	100	100	100	100	100	100
	Class Changes (%)	50.5	40	40.2	71.2	76.3	13.8
	Class Difference (%)	**10.9**	**-21.1**	**-21.2**	**-3.8**	**8.3**	**20.6**

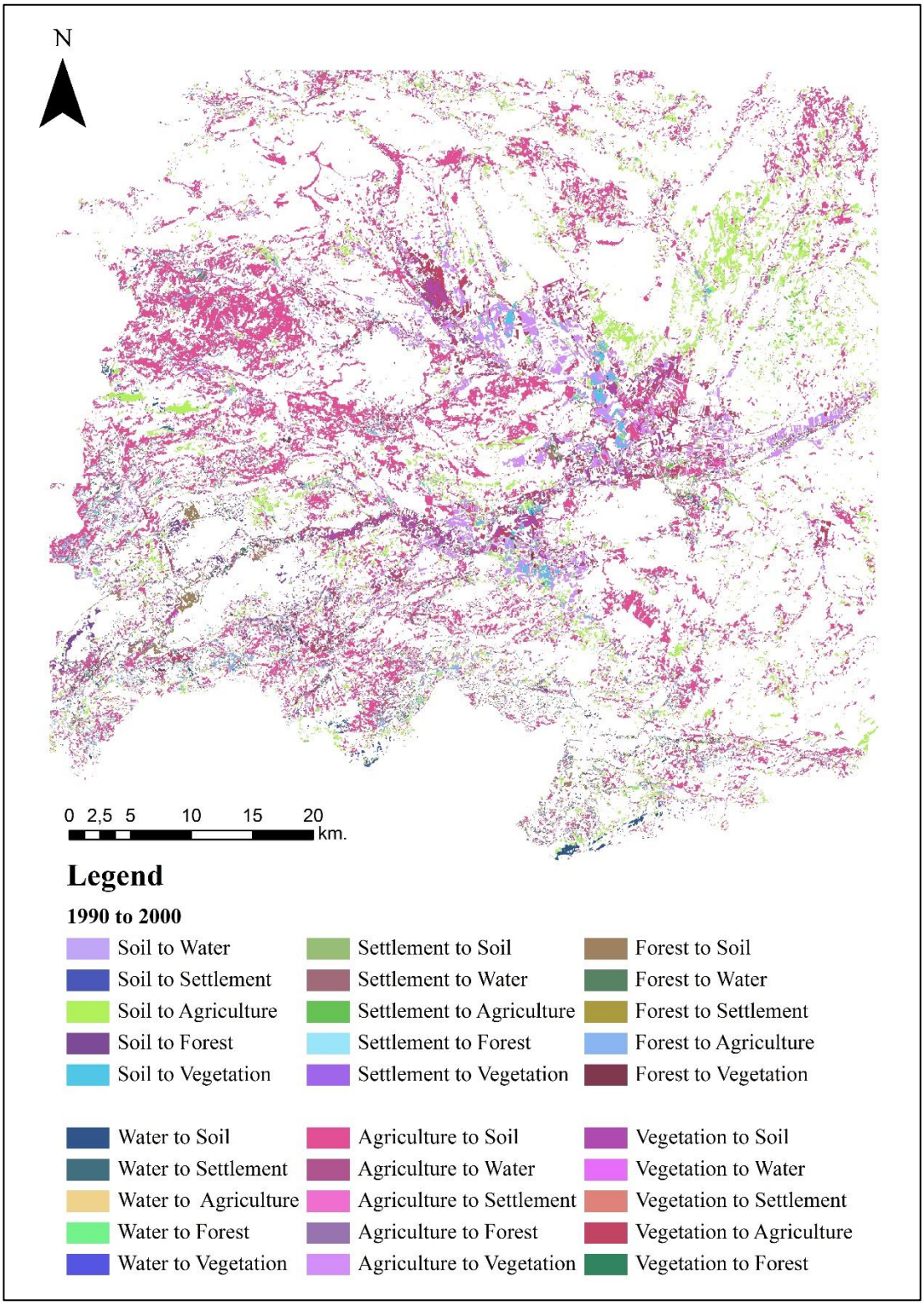

Figure 66. Change map between the years 1990 and 2000

The change map between years 2000 and 2003 can be seen from Figure 67. The first class indicates that it belongs to the year 2000 and second one belongs to year 2003. The important changes are; soil to vegetation (light blue), agriculture to soil (pink), and vegetation to soil (dark purple). From Table 25, while only the agriculture decreased, vegetation, forest, settlement, water and soil classes increased. Between years of 2000 and 2003, construction of power plant B began; therefore the soil increase can be related to these activities. Vegetated lands increase because, while agricultural lands are left uncultivated, they are detected as vegetated lands.

Table 25. Change statistics between years 2000 and 2003

		2000					
		Vegetation (%)	Forest (%)	Agriculture (%)	Settlement (%)	Water (%)	Soil (%)
2003	Vegetation (%)	53.9	4	9.6	3.5	4.9	1.9
	Forest (%)	5.6	84.8	3.7	0.1	4.8	1.1
	Agriculture (%)	13	0.1	46.9	10.1	5.4	5
	Settlement (%)	0.2	0	0.4	52.3	0.3	0.5
	Water (%)	0.4	2.2	0.4	0.2	55.4	0.2
	Soil (%)	27	9	39	33.9	29.3	91.3
	Total (%)	100	100	100	100	100	100
	Class Changes (%)	47	15.3	53.8	48.9	44.6	8.9
	Class Difference (%)	**28.3**	**30.2**	**-43**	**41.5**	**87.9**	**18.7**

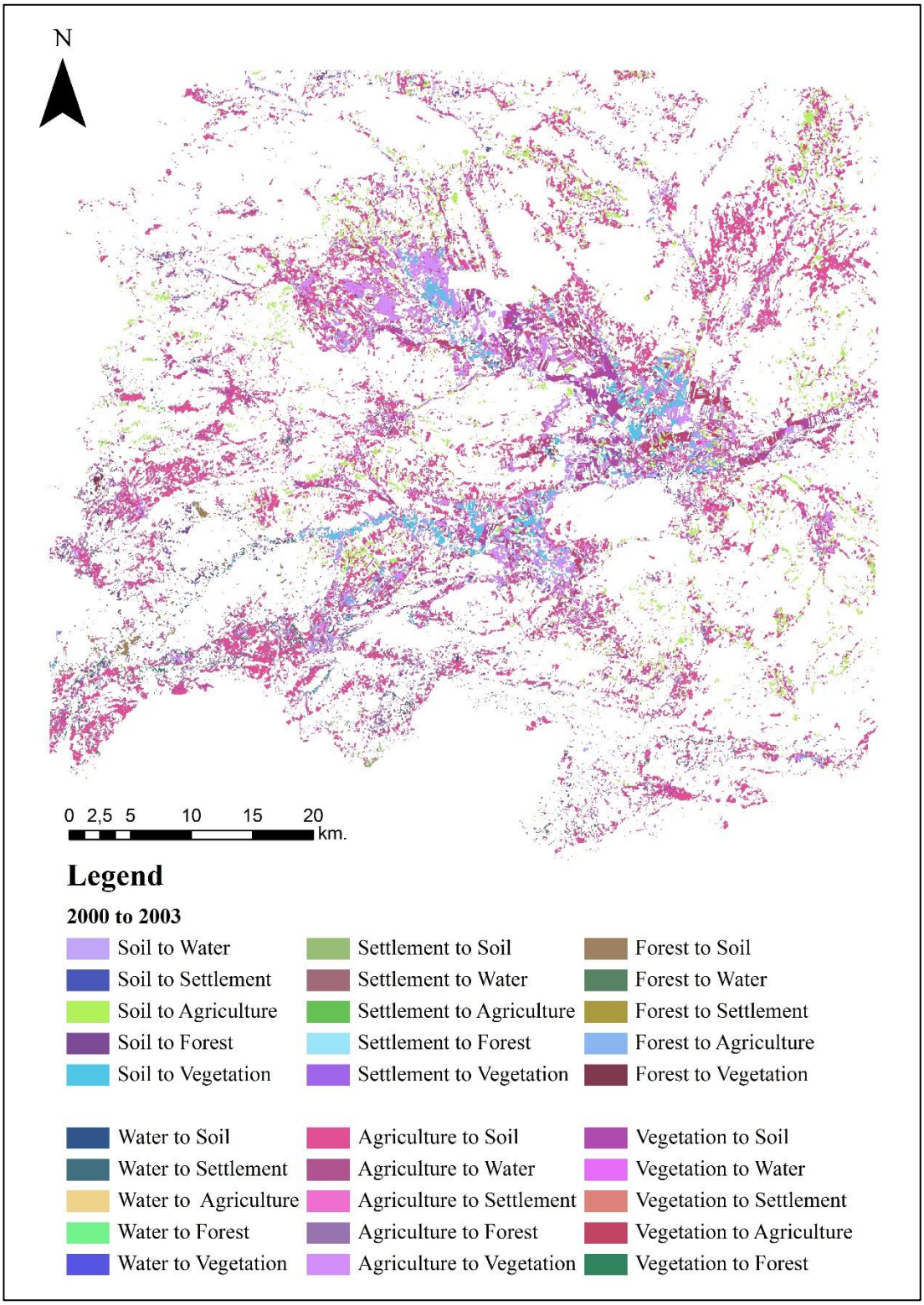

Figure 67. Change map between years 2000 and 2003

The change map between years 2003 and 2005 can be seen from Figure 68. From the legend, first class indicates that it belongs to the year 2003 and second one belongs to year 2005. The observed changes are; soil to vegetation (light blue), soil to agriculture (light green), and agriculture to vegetation (light purple). From Table 26, while forest, water and soil decreased, vegetation, agriculture and settlement increased. Between years of 2003 and 2005, there are no significant changes for mining activities. While barelands transformed to vegetated lands, existing agricultural lands left uncultivated and detected as vegetated lands.

Table 26. Change statistics between years 2003 and 2005

		2003					
		Vegetation (%)	Forest (%)	Agriculture (%)	Settlement (%)	Water (%)	Soil (%)
2005	Vegetation (%)	77.4	28.8	3.3	6.3	32.9	9.5
	Forest (%)	2	66.7	0	0.1	30.3	0.8
	Agriculture (%)	15.7	2.6	81.9	6	1.6	18.5
	Settlement (%)	0.7	0.1	0.7	64.5	0.2	0.9
	Water (%)	0	0	0	0	25.5	0.1
	Soil (%)	4	1.8	14	23.2	9.4	70.2
	Total (%)	100	100	100	100	100	100
	Class Changes (%)	22.6	33.3	18.1	35.5	74.5	29.8
	Class Difference (%)	**94.7**	**-19.8**	**53.6**	**88**	**-64.2**	**-24.8**

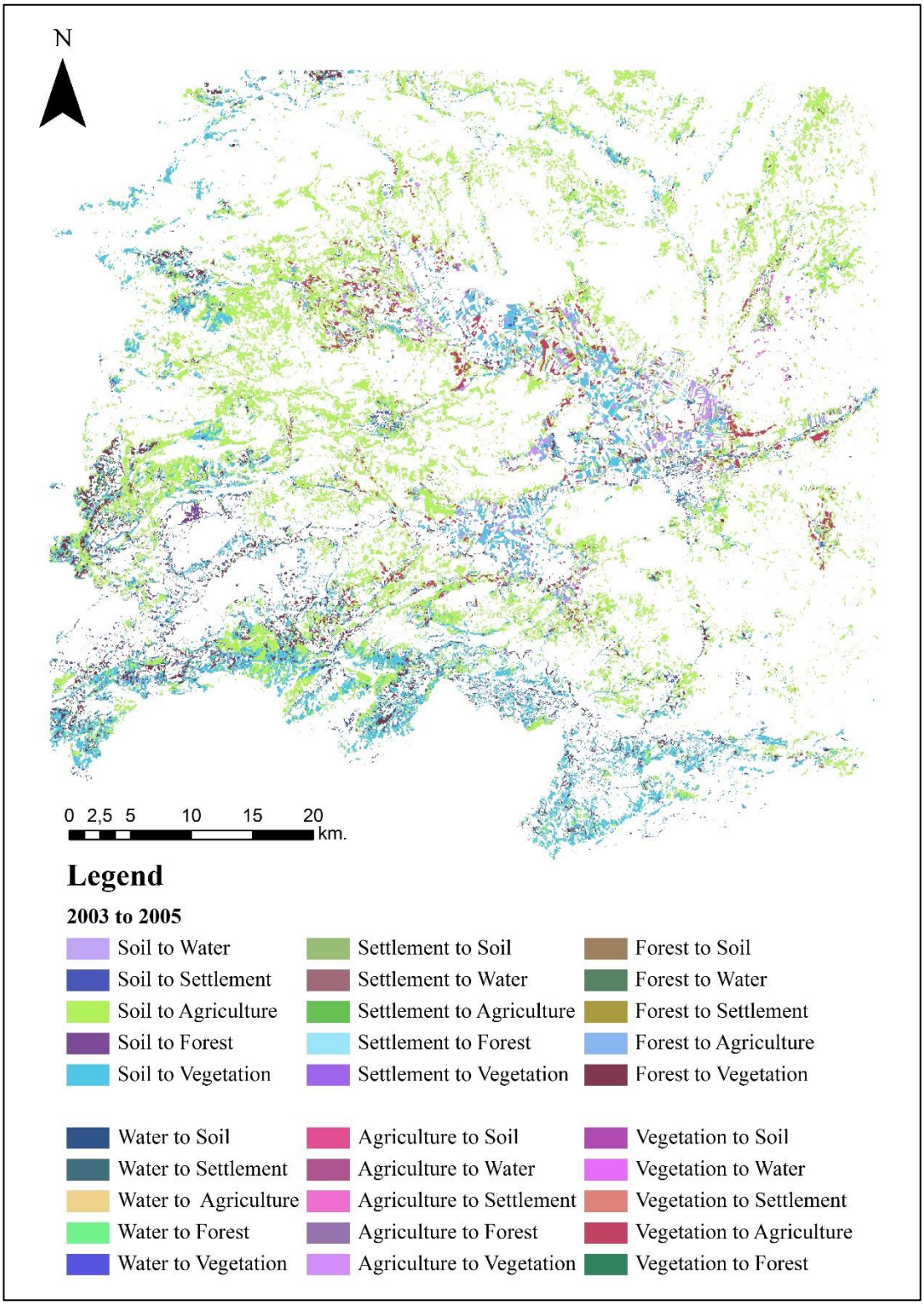

Figure 68. Change map between the years 2003 and 2005

The change map between years 2005 and 2008 can be seen from Figure 69. From the legend, first class indicates that it belongs to the year 2005 and second one belongs to year 2008. The detected changes are; agriculture to vegetation (light purple), vegetation to soil (dark purple), and vegetation to forest (dark green). From Table 27, while vegetation, agriculture, settlement and water decreased, forest and soil increased. Between years of 2005 and 2008, no significant changes for mining activities. There are uncontrolled forestation where vegetated lands are observed as forested areas.

Table 27. Change statistics between years 2005 and 2008

		2005					
		Vegetation (%)	Forest (%)	Agriculture (%)	Settlement (%)	Water (%)	Soil (%)
2008	Vegetation (%)	27.2	2.4	3.2	4.4	4.2	0.4
	Forest (%)	20.1	92.1	1	1	12	0.6
	Agriculture (%)	11.6	0.2	54.1	11.9	2.3	8.3
	Settlement (%)	0.1	0	0.1	16.3	0	0.1
	Water (%)	0	0.1	0	0	21.7	0
	Soil (%)	39.9	5.1	41.5	66.4	59.8	90.5
	Total (%)	100	100	100	100	100	100
	Class Changes (%)	72.8	7.9	45.9	83.7	78.3	9.5
	Class Difference (%)	**-63.8**	**64.3**	**-25.4**	**-75.2**	**-72.2**	**29.4**

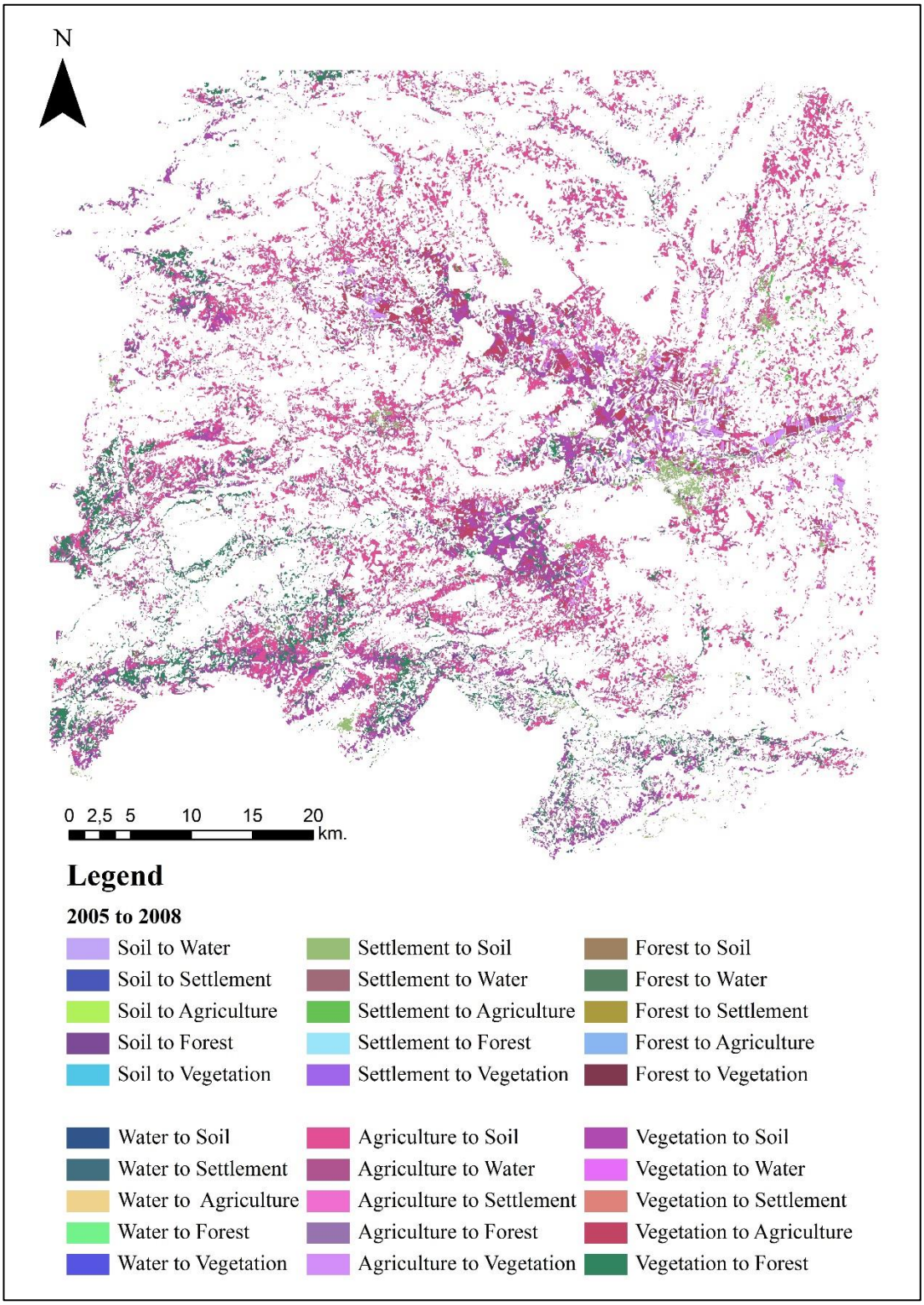

Figure 69. Change map between the years 2005 and 2008

The change map between years 2008 and 2011 can be seen from Figure 70. From the legend, first class indicates that it belongs to the year 2008 and second one belongs to year 2011. The important changes are; agriculture to vegetation (light purple), soil to agriculture (light green), and agriculture to soil (pink). From Table 28, while forest and agriculture decreased, vegetation, settlement, water and soil increased. Between years of 2008 and 2011, mining operations on sector B began and in 2011 a landslide occurred on that sector, therefore soil increase can be related to those activities. There are uncontrolled forestation where vegetated lands are observed as forested areas. Also, existing agricultural lands left uncultivated and detected as vegetated lands.

Table 28. Change statistics between years 2008 and 2011

		2008					
		Vegetation (%)	Forest (%)	Agriculture (%)	Settlement (%)	Water (%)	Soil (%)
2011	Vegetation (%)	57.4	15.6	3.8	1.4	2.1	2.6
	Forest (%)	5.5	68.6	0.1	0.1	7.7	0.6
	Agriculture (%)	5.8	0.8	58	6	0.2	8.9
	Settlement (%)	0.9	0.1	0.6	62.9	0.1	0.7
	Water (%)	0.2	0.5	0	0	82.4	0.2
	Soil (%)	29.1	14.2	36.7	29.4	7.5	86.8
	Total (%)	100	100	100	100	100	100
	Class Changes (%)	42.6	31.4	42.1	37.1	17.6	13.2
	Class Difference	**27.6**	**-22.7**	**-14.1**	**169.8**	**348.9**	**3.8**

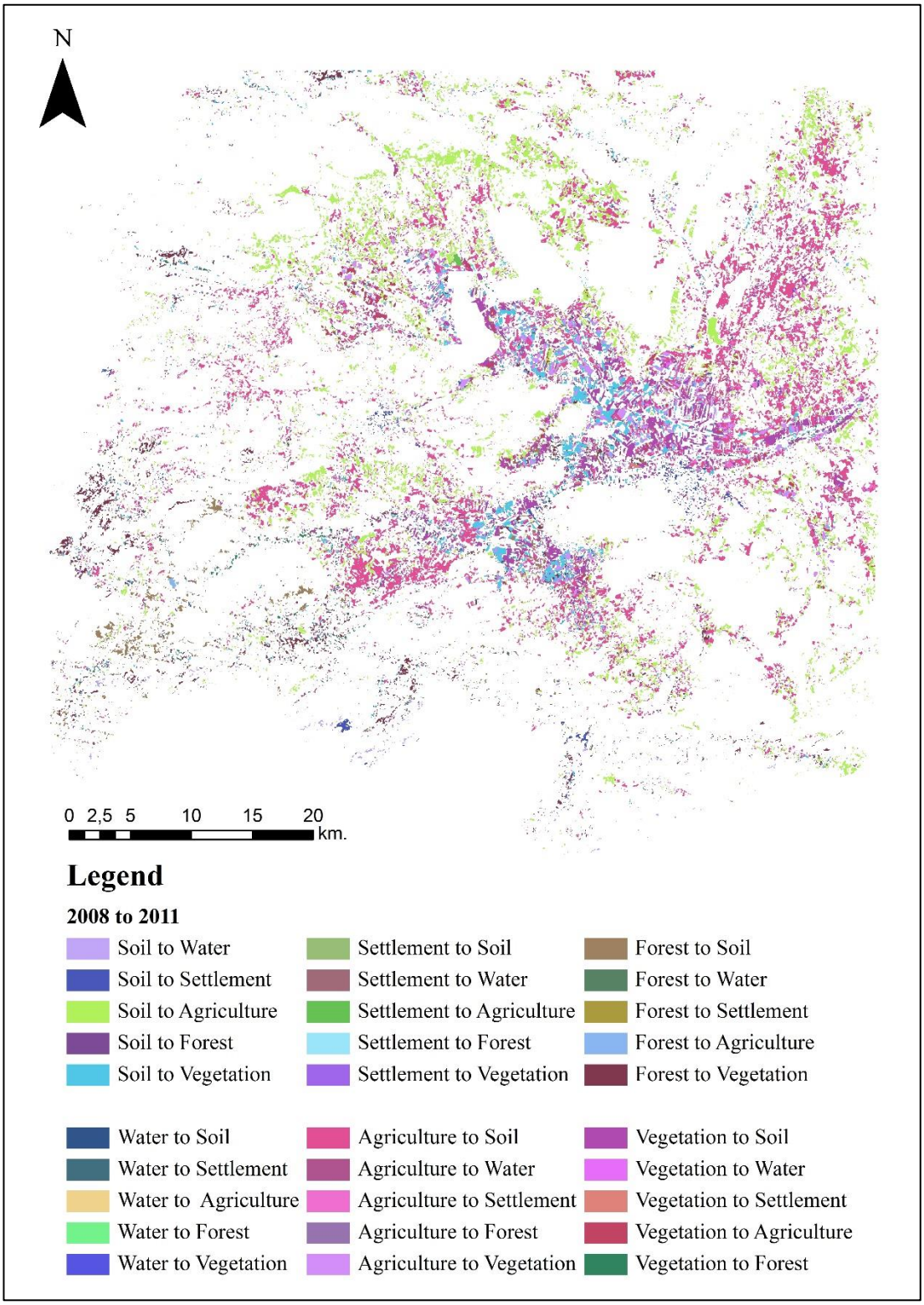

Figure 70. Change map between the years 2008 and 2011

The change map between years 2011 and 2014 can be seen from Figure 71. From the legend, first class indicates that it belongs to the year 2011 and second one belongs to year 2014. The detected changes are; soil to vegetation (light blue), soil to agriculture (light green), and soil to water (light lilac). From Table 29, while vegetation, settlement and soil decreased, forest, agriculture and water increased. Between years of 2011 and 2014, there are no significant changes for mining activities. There are uncontrolled forestation where vegetated lands are observed as forested areas. Also, existing vegetated lands are cultivated and detected as agricultural lands.

Table 29. Change statistics between years 2011 and 2014

		2011					
		Vegetation (%)	Forest (%)	Agriculture (%)	Settlement (%)	Water (%)	Soil (%)
2014	Vegetation (%)	44.8	8.1	2.2	10.2	6.2	3.4
	Forest (%)	20.1	77	0.4	3.3	30.3	3.3
	Agriculture (%)	13.6	0.6	83.3	19.5	1.2	18.1
	Settlement (%)	0.1	0	0	14.6	0.1	0.2
	Water (%)	0.4	0.7	0	0.7	12.4	0.3
	Soil (%)	21	13.6	13.7	51.3	49.8	74.4
	Total (%)	100	100	100	100	100	100
	Class Changes (%)	55.2	23	16.7	85.4	87.6	25.6
	Class Difference (%)	**-6.4**	**36.7**	**53.9**	**-65.9**	**27.7**	**-17.3**

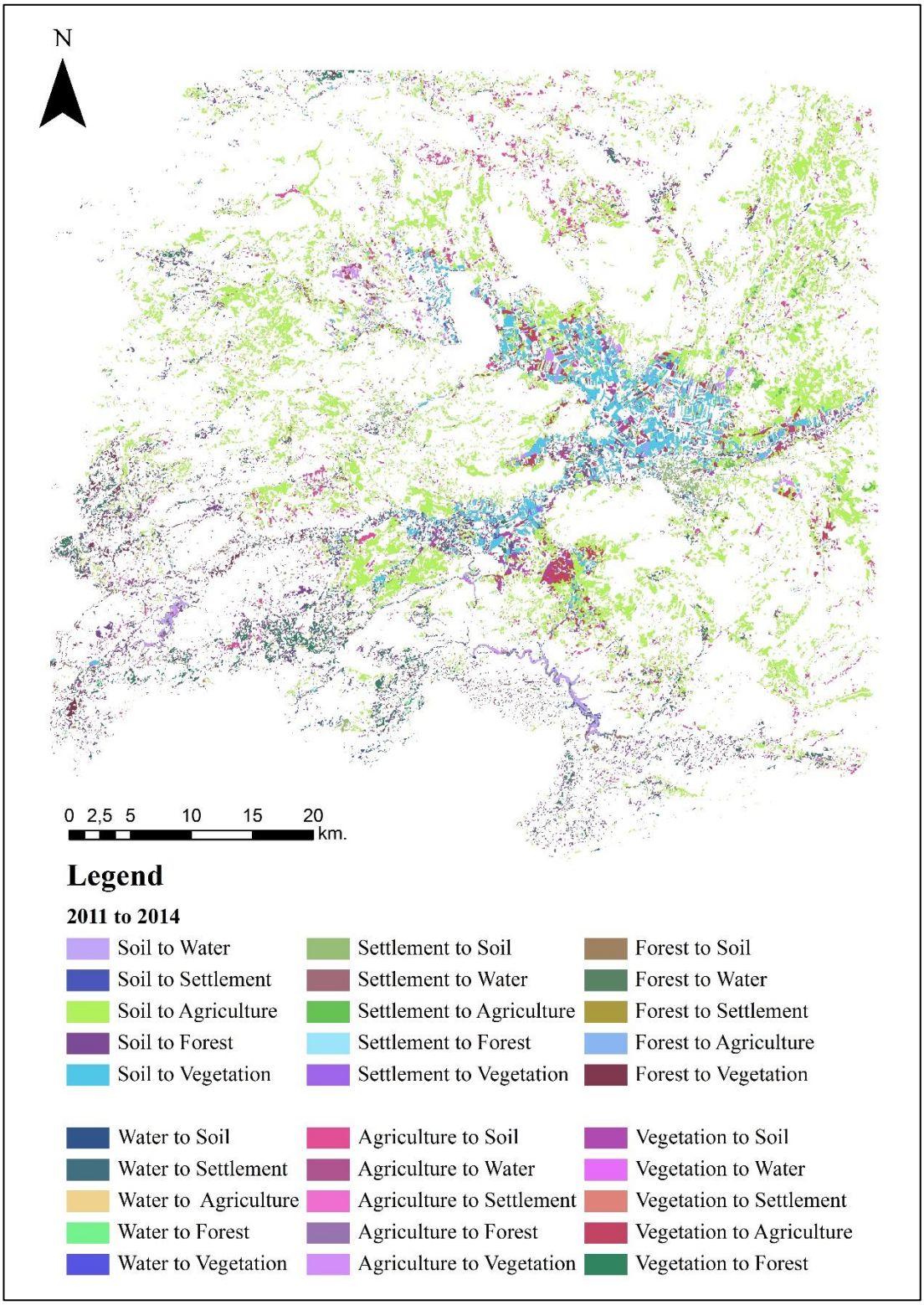

Figure 71. Change map between the years 2011 and 2014

Post-classification change detection with CDTL method

The change map between the years 1984 and 1987 can be seen from Figure 72. The first class indicates that it belongs to the year 1984 and second one belongs to year 1987. The observable changes are; soil to agriculture (orange), agriculture to vegetation (cyan), agriculture to soil (purple), and vegetation to agriculture (light orange). As seen from the Table 30, while forest, settlement and soil classes decreased, vegetation, agriculture and water classes increased. Increase in agriculture is related to the increase in vegetation as agricultural lands changes to vegetated lands in resultant change detection map.

Table 30. Change statistics between years 1984 and 1987

		1984					
		Vegetation (%)	Forest (%)	Agriculture (%)	Settlement (%)	Water (%)	Soil (%)
1987	Vegetation (%)	50.7	9.7	10.6	3.3	9.6	2.2
	Forest (%)	2	68.9	0.7	0	2.6	0.6
	Agriculture (%)	34.7	12.2	62.2	64.2	13.1	19.9
	Settlement (%)	0.2	0	0.6	19.1	0.7	0.3
	Water (%)	0.3	0.2	0	0.5	51.6	0.5
	Soil (%)	12	9	25.9	12.9	22.3	76.6
	Total (%)	100	100	100	100	100	100
	Class Changes (%)	49.3	31.1	37.9	80.9	48.4	23.5
	Class Difference	**35.9**	**-18.6**	**28.9**	**-53.5**	**59.6**	**-11.8**

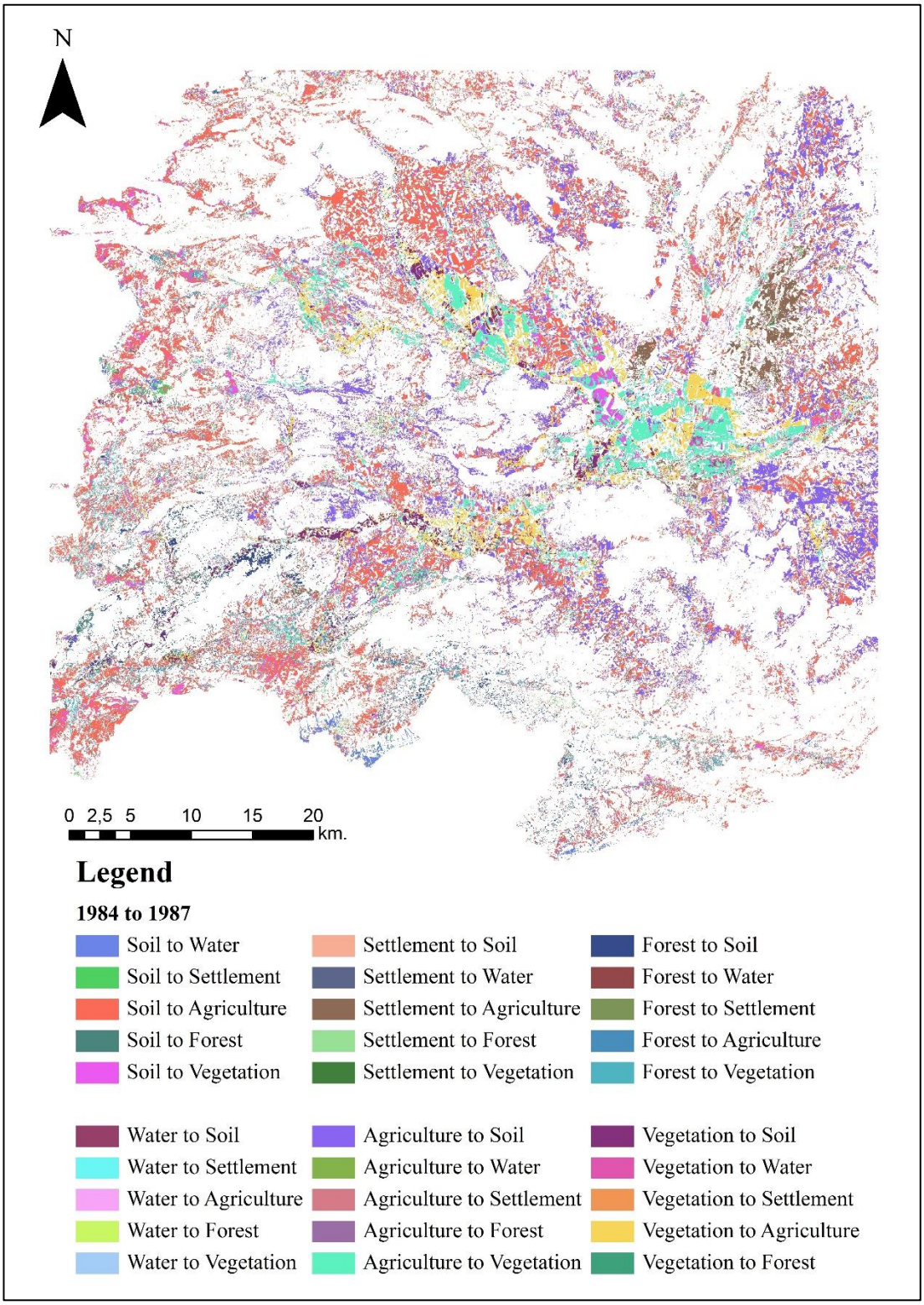

Figure 72. Change map between the years 1984 and 1987

The change map between the years of 1987 and 1990 can be seen from Figure 73. The first class indicates that it belongs to the year of 1987 and the second one belongs to year of 1990. The significant changes are; agriculture to soil (purple), agriculture to vegetation (cyan), vegetation to agriculture (light orange) and vegetation to soil (dark purple). As seen from Table 31, while agriculture and water classes decreased, vegetation, forest, settlement and soil classes increased. Increase in vegetated lands is related to the decrease in agriculture class as both of the classes change into others in the resultant change detection map.

Table 31. Change statistics between years 1987 and 1990

		1987					
		Vegetation (%)	Forest (%)	Agriculture (%)	Settlement (%)	Water (%)	Soil (%)
1990	Vegetation (%)	46.8	5.2	11.2	4.1	13.5	2.4
	Forest (%)	4.7	78.7	2.7	0.3	3.3	1.8
	Agriculture (%)	29	3.3	49.5	27.3	4.5	12.3
	Settlement (%)	1	0.1	1.5	37.3	3.2	0.6
	Water (%)	0.5	0.3	0.2	0.7	16.8	0.1
	Soil (%)	18	12.4	34.9	30.3	58.7	82.8
	Total (%)	100	100	100	100	100	100
	Class Changes (%)	53.2	21.3	50.6	62.8	83.3	17.2
	Class Difference	**18.3**	**34.1**	**-20.6**	**90.2**	**-45.8**	**5.9**

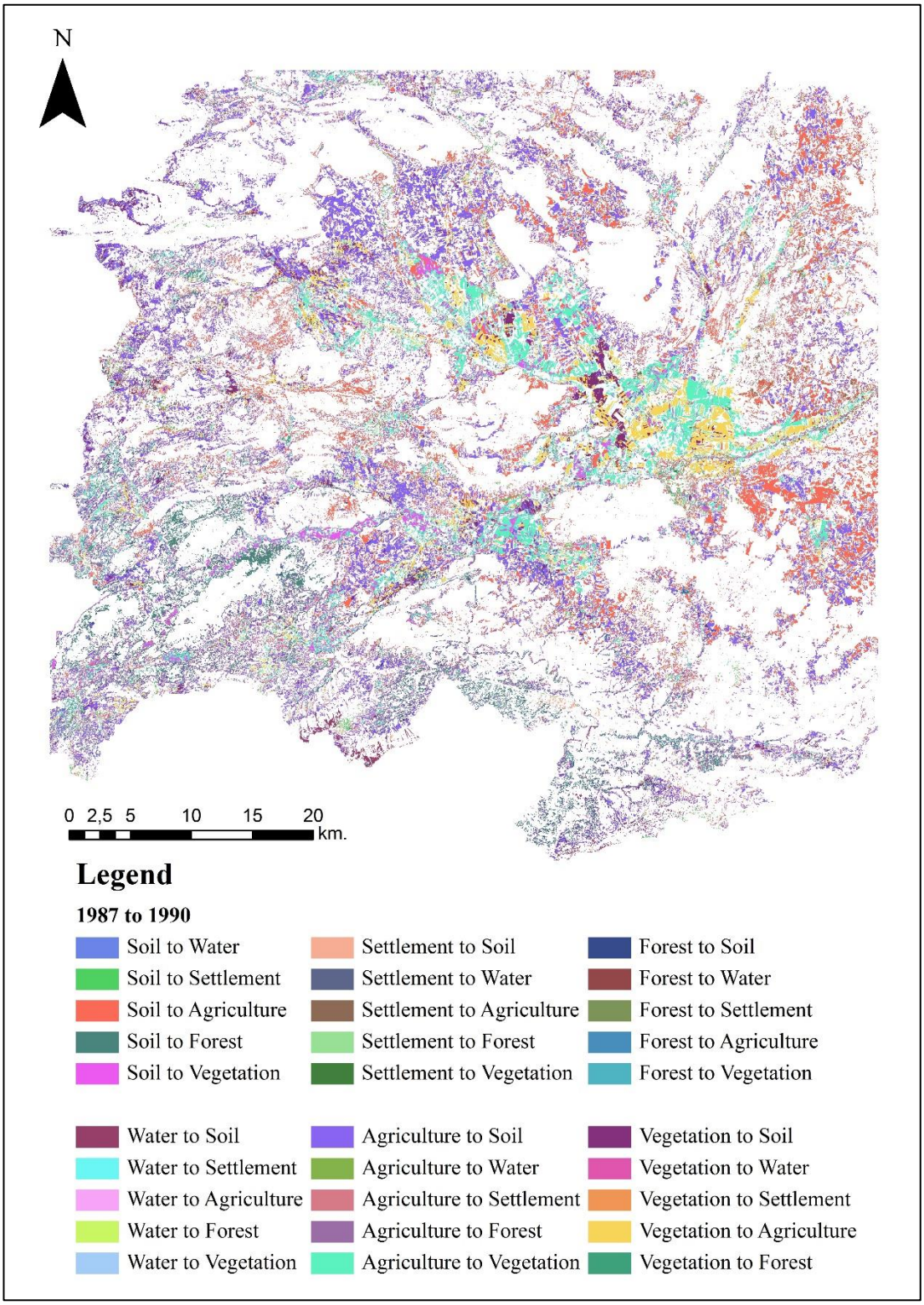

Figure 73. Change map between the years 1987 and 1990

The change map between the years of 1990 and 2000 can be seen from Figure 74. The first class indicates that it belongs to the year of 1990 and the second one belongs to year of 2000. The important changes are; agriculture to soil (purple), agriculture to vegetation (cyan), soil to agriculture (orange), and forest to soil (dark blue). From Table 32, forest, agriculture and soil classes decreased, and vegetation, water and settlement classes increased. Between years of 1990 and 2000, power plant constructions began; therefore the settlement increase can be related to these activities. Vegetated lands increase because, while agricultural lands are left uncultivated, they are detected as vegetated lands.

Table 32. Change statistics between years 1990 and 2000

		1990					
		Vegetation (%)	Forest (%)	Agriculture (%)	Settlement (%)	Water (%)	Soil (%)
2000	Vegetation (%)	62.1	8.6	13.6	9.8	23.2	3.4
	Forest (%)	3.3	63.9	0.7	0.2	5.4	1
	Agriculture (%)	13.6	5.2	57.2	18.7	3.1	12.3
	Settlement (%)	2.3	0.3	2.3	38.9	3.4	0.8
	Water (%)	1.7	1.1	0.3	0.5	32.8	0.5
	Soil (%)	16.9	20.8	25.9	31.8	32.1	81.8
	Total (%)	100	100	100	100	100	100
	Class Changes (%)	37.9	36.1	42.9	61.2	67.2	18.2
	Class Difference	**32.8**	**-16.2**	**-6.1**	**51.9**	**138.2**	**-2.6**

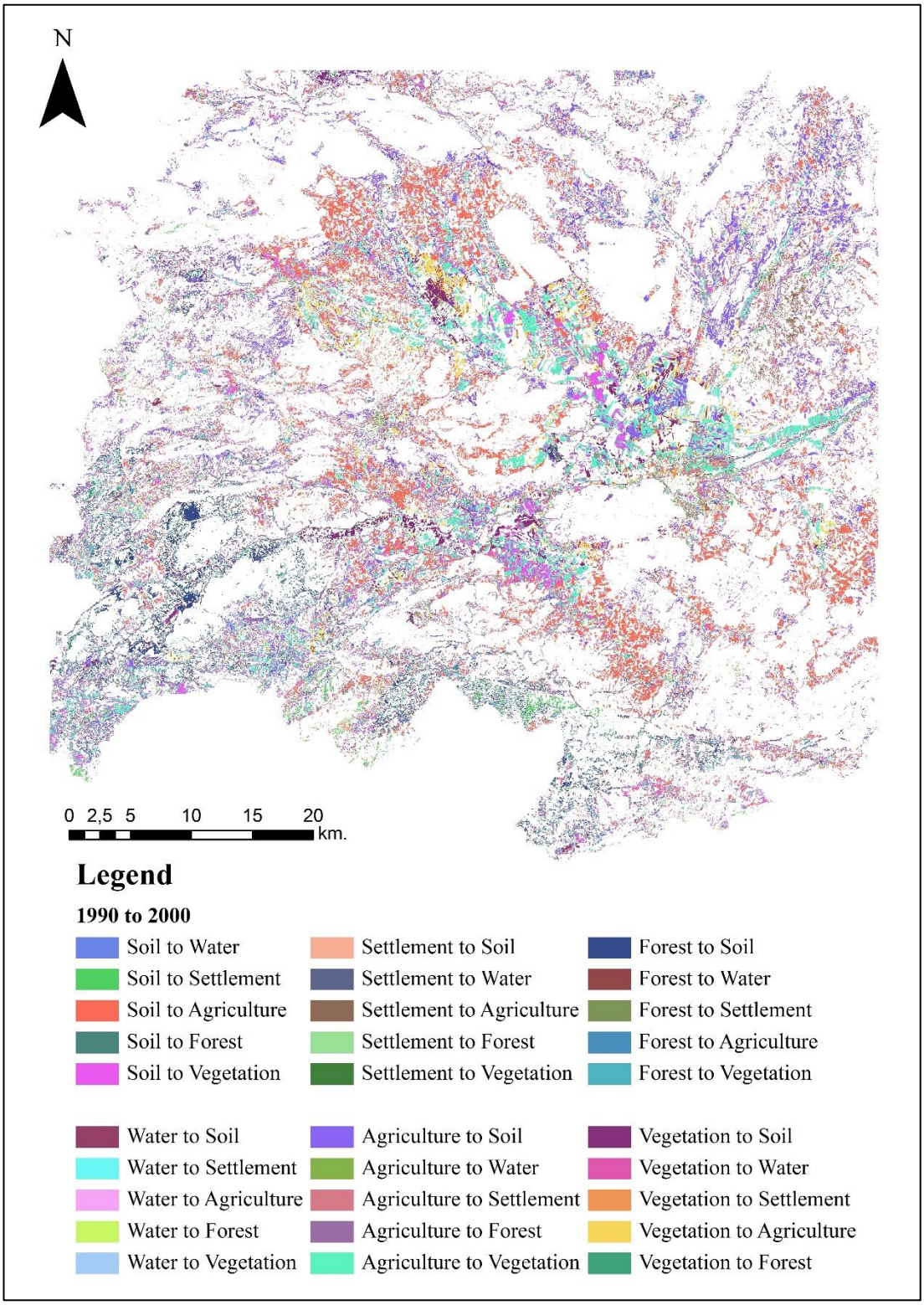

Figure 74. Change map between the years 1990 and 2000

The change map between years 2000 and 2003 can be seen from Figure 75. The first class indicates that it belongs to the year 2000 and second one belongs to year 2003. The important changes are; soil to settlement (light green), agriculture to soil (purple), agriculture to vegetation (cyan), vegetation to agriculture (light orange), and vegetation to soil (dark purple). From Table 33, while vegetation and water decreased, forest, agriculture, settlement classes increased, and changes on soil did not effect its increase and/or decrease. Existing vegetated lands are cultivated and detected as agricultural lands. Therefore, while vegetation is decreased, agricultural lands are increased.

Table 33. Change statistics between years 2000 and 2003

		2000					
		Vegetation (%)	Forest (%)	Agriculture (%)	Settlement (%)	Water (%)	Soil (%)
2003	Vegetation (%)	48.3	5.5	6.6	10.9	14.7	2.3
	Forest (%)	3.7	79.5	0.5	0.1	8.7	0.9
	Agriculture (%)	29	3.7	66.6	22.2	14.5	8.6
	Settlement (%)	2.3	1.5	1.1	40.9	1.3	2
	Water (%)	0.3	1.6	0.1	0.1	35.1	0.2
	Soil (%)	15.6	8.2	24.3	24.8	25.5	85.7
	Total (%)	100	100	100	100	100	100
	Class Changes (%)	51.7	20.5	33.4	59.2	64.9	14.3
	Class Difference	**-21.5**	**5.1**	**5.1**	**47.5**	**-24.8**	**0**

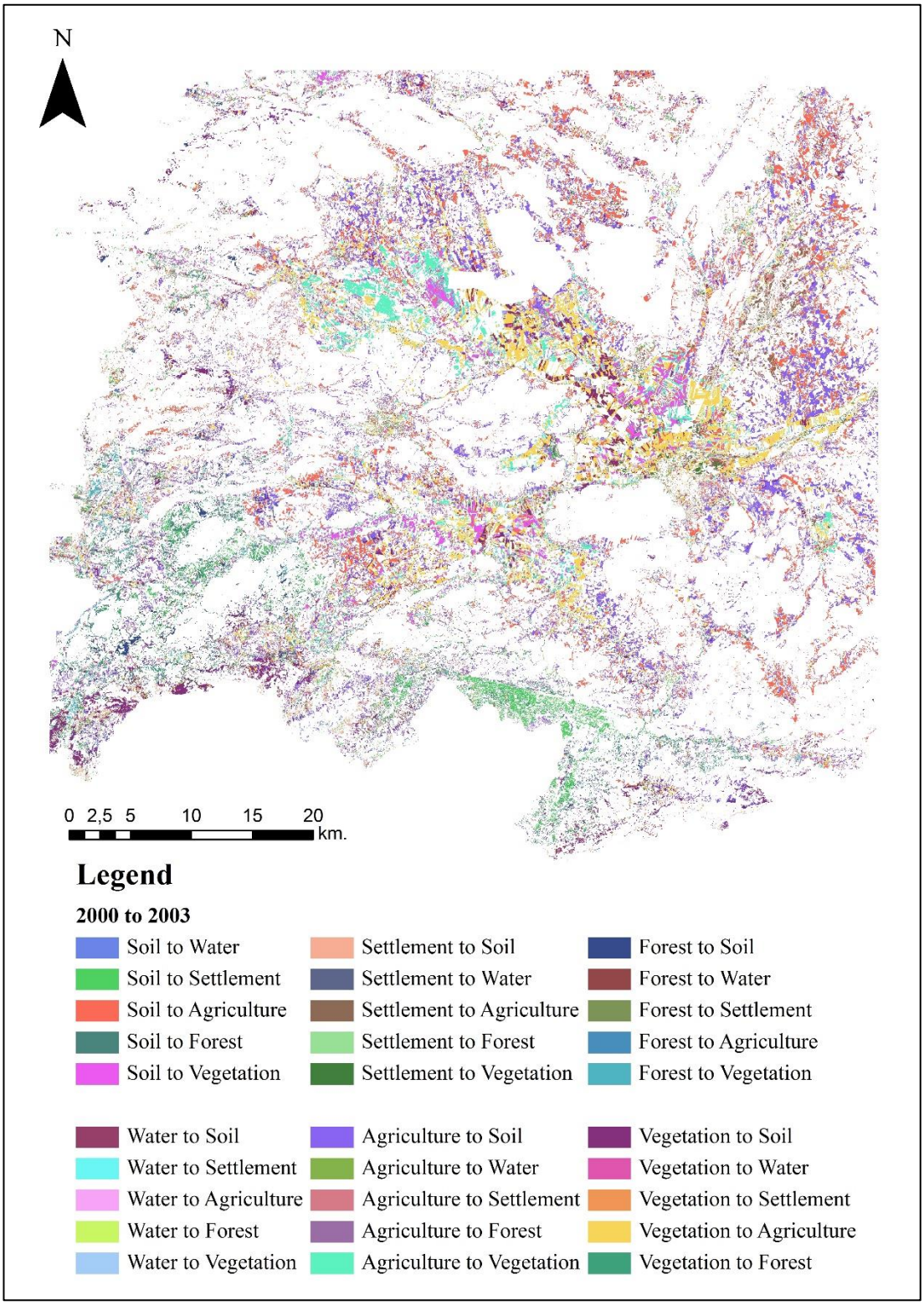

Figure 75. Change map between the years 2000 and 2003

The change map between years 2003 and 2005 can be seen from Figure 76. The first class indicates that it belongs to the year 2003 and second one belongs to year 2005. The observed changes are; agriculture to soil (purple), agriculture to vegetation (cyan), and forest to vegetation (light blue). From Table 34, while only agriculture decreased, all the other classes are increased. Between years of 2003 and 2005, there are no significant changes for mining activities. Existing agricultural lands left uncultivated and detected as vegetated lands.

Table 34. Change statistics between years 2003 and 2005

		2003					
		Vegetation (%)	Forest (%)	Agriculture (%)	Settlement (%)	Water (%)	Soil (%)
2005	Vegetation (%)	73.2	6.9	10	13	7.3	1.7
	Forest (%)	5.1	88	1.4	8.4	24	0.8
	Agriculture (%)	10.7	0.6	62.9	8.7	2.1	5.9
	Settlement (%)	2.2	0.9	1.3	45.5	1.1	2.1
	Water (%)	0.5	0.5	0.2	0.2	54.6	0.2
	Soil (%)	8.2	3.1	24.1	24.2	10.9	89.3
	Total (%)	100	100	100	100	100	100
	Class Changes (%)	26.8	12	37.1	54.5	45.4	10.7
	Class Difference	**19.9**	**21.3**	**-17.8**	**17.7**	**6**	**1.9**

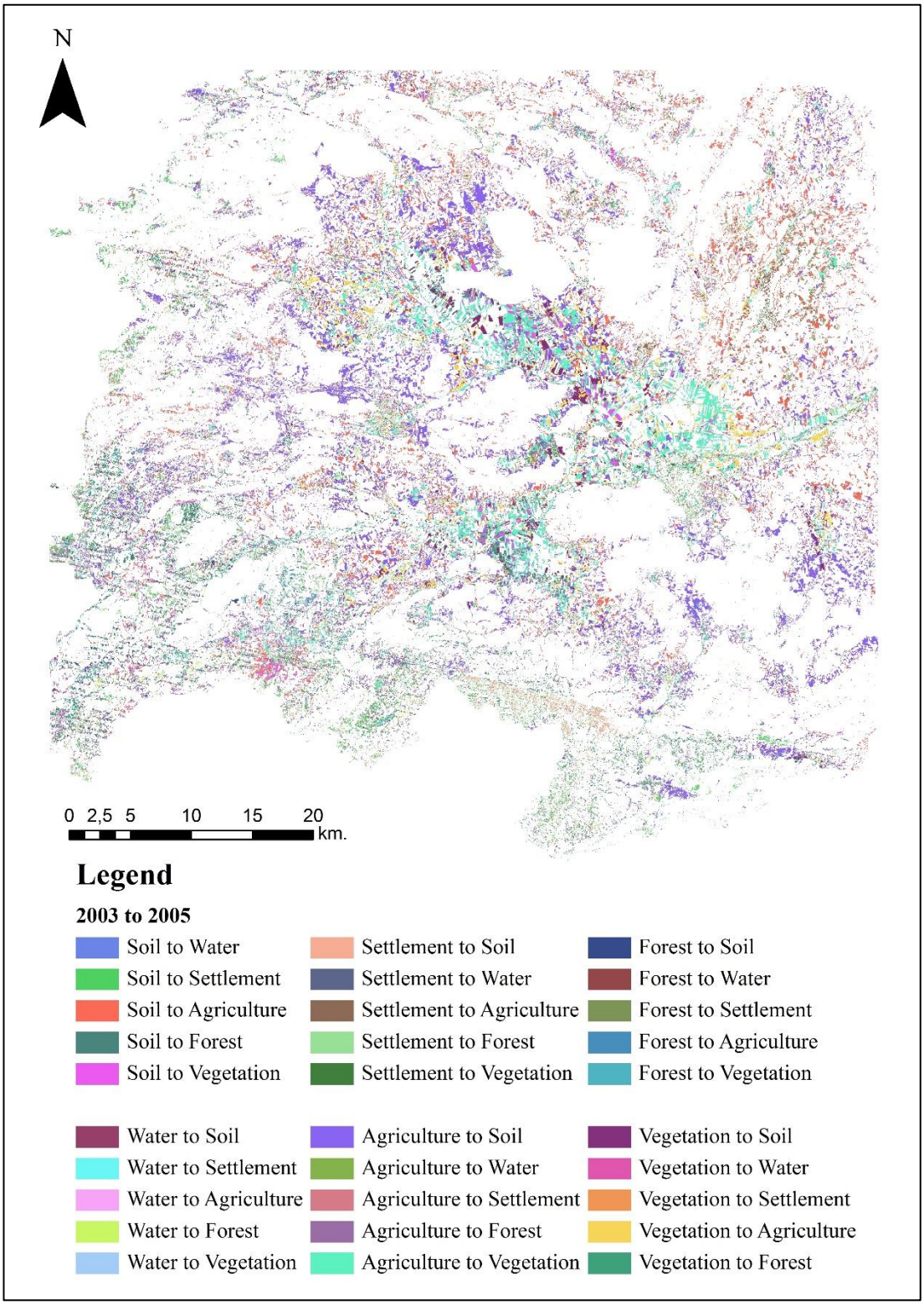

Figure 76. Change map between the years 2003 and 2005

The change map between years 2005 and 2008 can be seen from Figure 77. The first class indicates that it belongs to the year 2005 and second one belongs to year 2008. The detected changes are; agriculture to soil (purple), vegetation to agriculture (light orange), vegetation to soil (dark purple), and soil to agriculture (orange). From Table 35, while vegetation, forest, settlement, water and soil decreased, only agriculture increased. Between years of 2005 and 2008, no significant changes for mining activities. Existing vegetated lands are cultivated and detected as agricultural lands. Therefore, while vegetation is decreased, agricultural lands are increased.

Table 35. Change statistics between years 2005 and 2008

		2005					
		Vegetation (%)	Forest (%)	Agriculture (%)	Settlement (%)	Water (%)	Soil (%)
2008	Vegetation (%)	48.1	8.4	4.1	7.8	4.8	0.7
	Forest (%)	2.2	75.2	0.1	3.7	5.5	0.4
	Agriculture (%)	31.1	9.1	63.1	24.7	25.9	15.8
	Settlement (%)	4.5	0.4	2.1	31.8	0.3	1.3
	Water (%)	0.2	1.5	0	0	41.3	0.1
	Soil (%)	12.4	5.4	30.3	31.9	22.1	81.7
	Total (%)	100	100	100	100	100	100
	Class Changes (%)	51.9	24.8	36.9	68.2	58.7	18.3
	Class Difference	**-33.3**	**-13.1**	**33.6**	**-8.4**	**-28.2**	**-3.7**

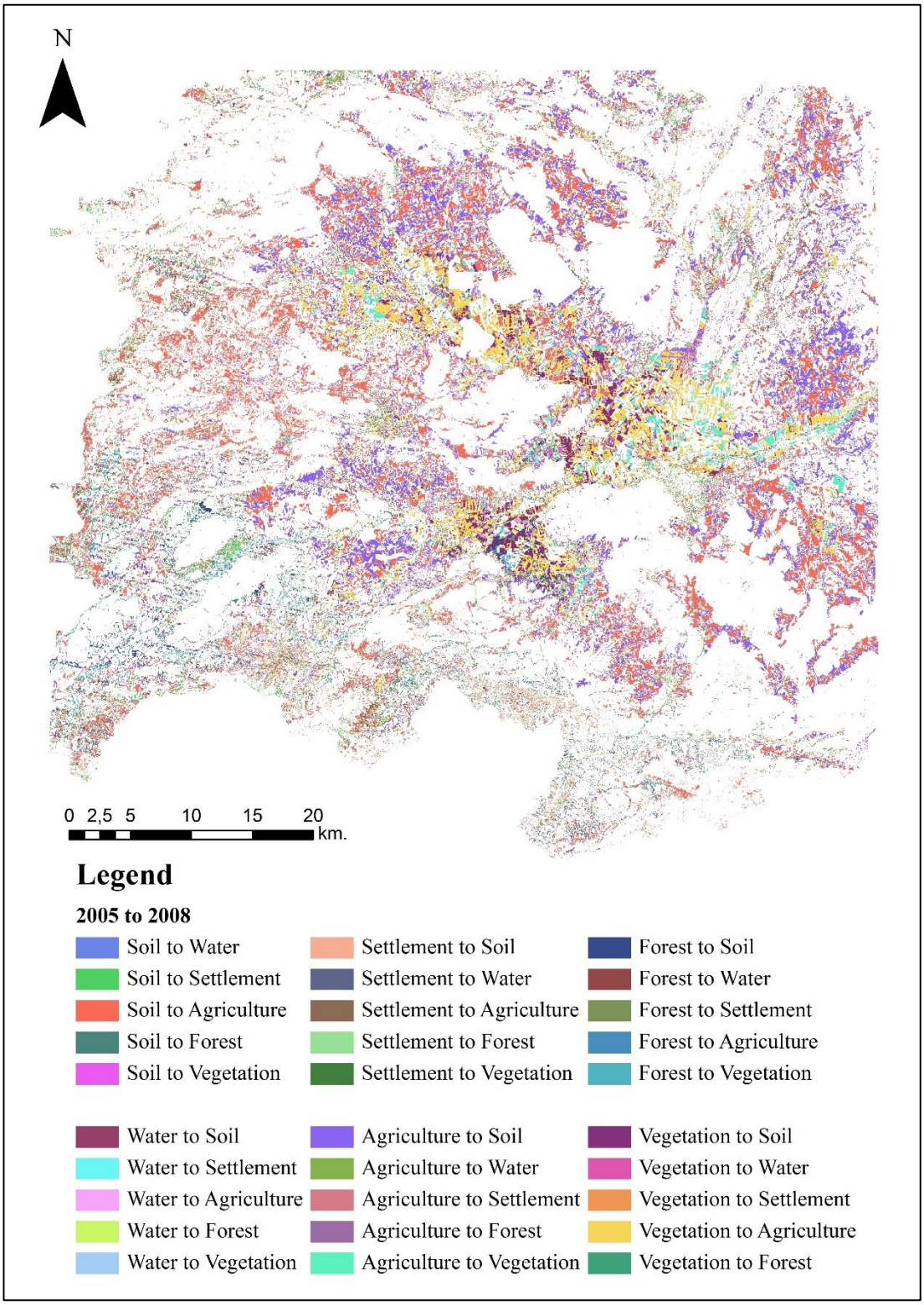

Figure 77. Change map between the years 2005 and 2008

The change map between years 2008 and 2011 can be seen from Figure 78. The first class indicates that it belongs to the year 2008 and second one belongs to year 2011. The detected changes are; agriculture to soil (purple), forest to vegetation (blue), soil to agriculture (orange), and agriculture to vegetation (cyan). From Table 36, while settlement and agriculture decreased, vegetation, forest, water and soil increased. Between years of 2008 and 2011, mining operations on sector B began and in 2011 a landslide occurred on that sector, therefore soil increase can be related to those activities. Also, existing agricultural lands left uncultivated and detected as vegetated lands.

Table 36. Change statistics between years 2008 and 2011

		2008					
		Vegetation (%)	Forest (%)	Agriculture (%)	Settlement (%)	Water (%)	Soil (%)
2011	Vegetation (%)	64.8	19.3	9.1	21.2	2.3	2
	Forest (%)	6.1	74.7	1.9	0.4	22.4	0.4
	Agriculture (%)	12.9	0.7	55.2	18.6	2	10.8
	Settlement (%)	1.1	0	0.8	18.7	0.1	0.3
	Water (%)	0.4	0.9	0.7	0.2	64.5	0.4
	Soil (%)	13.8	4.2	31.3	40.7	8.5	85.9
	Total (%)	100	100	100	100	100	100
	Class Changes (%)	35.2	25.3	44.8	81.3	35.5	14.1
	Class Difference	**37.1**	**1**	**-16.2**	**-62.7**	**104.5**	**4.6**

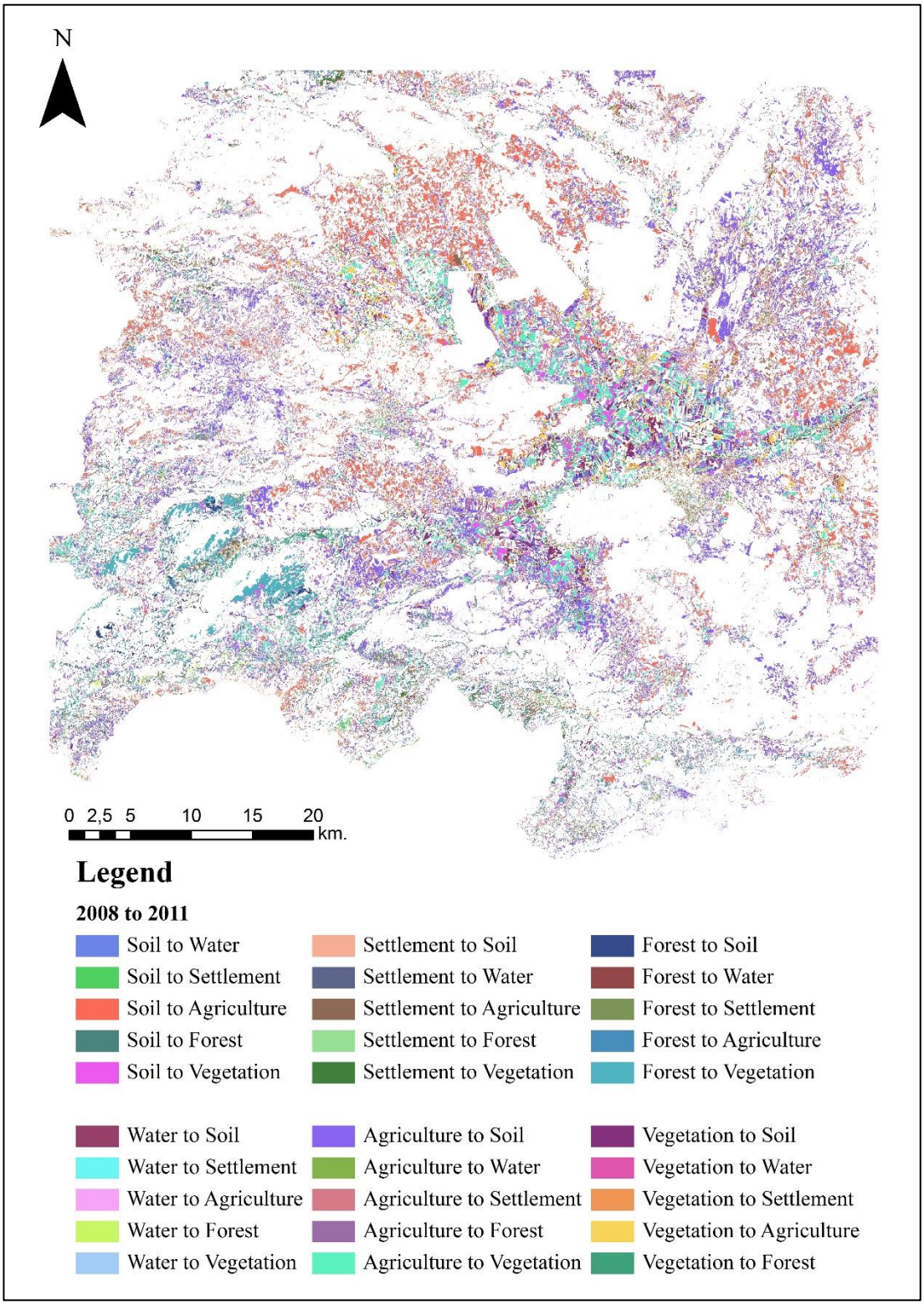

Figure 78. Change map between the years 2008 and 2011

The change map between years 2011 and 2014 can be seen from Figure 79. The first class indicates that it belongs to the year 2011 and second one belongs to year 2014. The detected changes are; agriculture to soil (purple), vegetation to forest (dark green), soil to water (dark blue), and soil to agriculture (orange). From Table 37, while vegetation and soil decreased, forest, agriculture, settlement and water increased. Between years of 2011 and 2014, there are no significant changes for mining activities. There are uncontrolled forestation where vegetated lands are observed as forested areas. Also, existing vegetated lands are cultivated and detected as agricultural lands.

Table 37. Change statistics between years 2011 and 2014

		2011					
		Vegetation (%)	Forest (%)	Agriculture (%)	Settlement (%)	Water (%)	Soil (%)
2014	Vegetation (%)	35.9	7.2	4.3	9.3	5.8	1.9
	Forest (%)	15	72.3	0.5	0.9	15	1.2
	Agriculture (%)	14.8	0.7	68	15.6	2.9	11.3
	Settlement (%)	3.2	0.3	1.9	45.5	0.9	0.9
	Water (%)	6.9	6.5	1.2	5.2	29.1	1.1
	Soil (%)	24	13	23.9	23.2	46.3	83.3
	Total (%)	100	100	100	100	100	100
	Class Changes (%)	64.1	27.7	32	54.5	70.9	16.7
	Class Difference	**-36.9**	**21.4**	**5.8**	**79.3**	**194**	**-1.7**

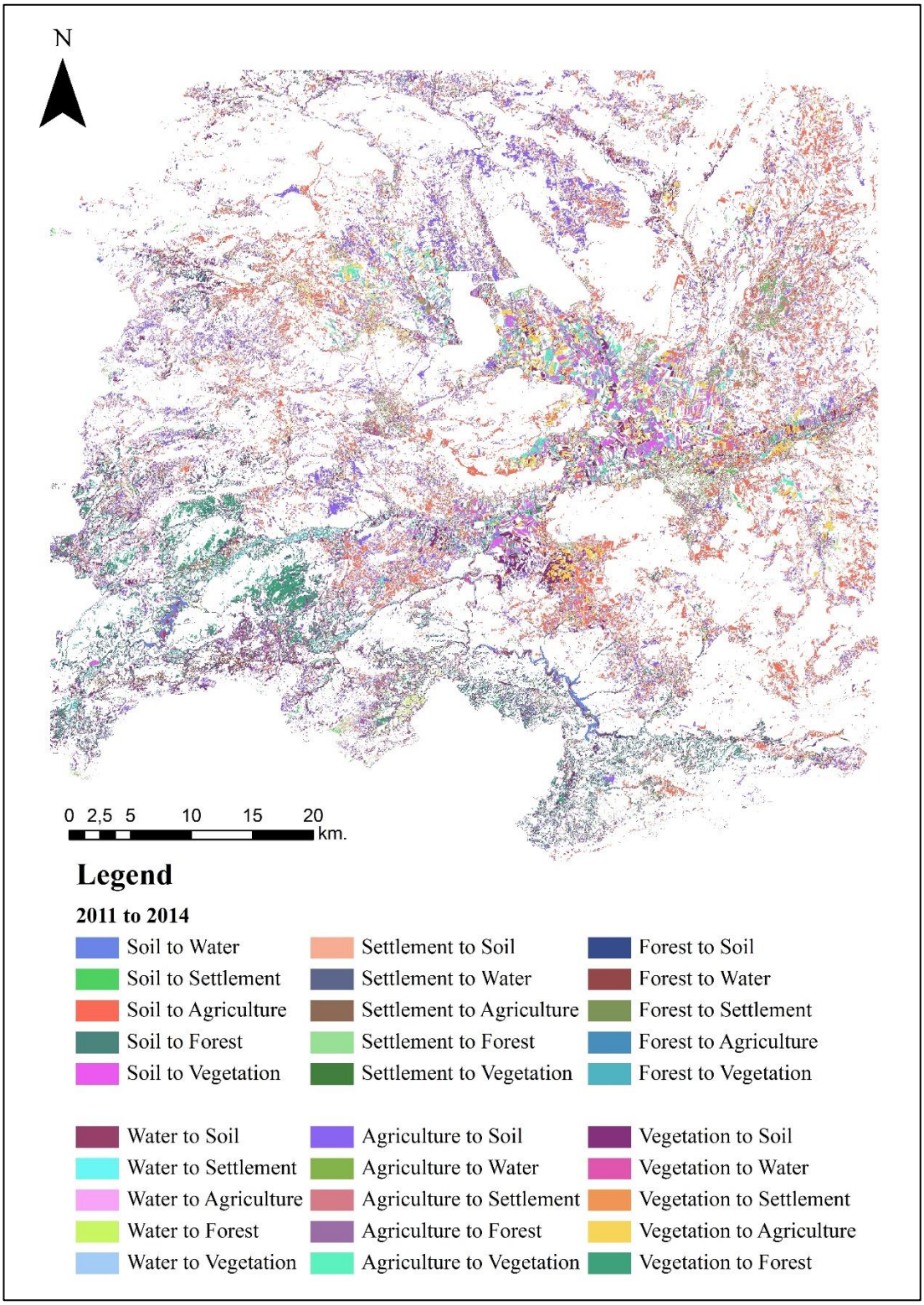

Figure 79. Change map between the years 2011 and 2014

4.6 Results and Discussions

In this study, LULC change detection of Afşin-Elbistan Coal Basin is studied with two classification methods. The methods, SVM and CDTL, are used for comparing their performance. The results of these analyses are listed below:

1. Using DEMs, band combinations of satellite images and the collected data in the field studies, the determined LULC classes are vegetation, forest, agriculture, settlement, soil, water and mine. Mine class is masked out from the images due to its mixing with other classes.
2. When the images are examined visually, six bands, which are blue, green, red, near infrared (NIR), short wave infrared 1 (SWIR1) and short wave infrared 2 (SWIR2) are found to contain the most available information for the classes, and are utilized for the analyses.
3. LULC maps are obtained with respect to the selected classes by using the two classification techniques. The overall accuracies are compared to each other. As it can be seen from Figure 80, traditional SVM classification technique has higher overall accuracies than CDTL classification method for each year. However, the differences are not considerably high. The highest difference is obtained with 9.8% for the 2008 image. The difference is maninly because of the misclassifications of settlement and forest classes. For traditional SVM classification, true pixel numbers for forest and settlement are 132 and 9 respectively, while for the CDTL classification the numbers are 77 and 15, respectively. Also water has higher producer's accuracy for CDTL than traditional SVM classification for the 2008 image. When the other years are compared, numbers usually changes between the classification techniques. The reason for the higher accuracy in water class for 2008 image is the training set which includes detailed water class labeling for CDTL classification.

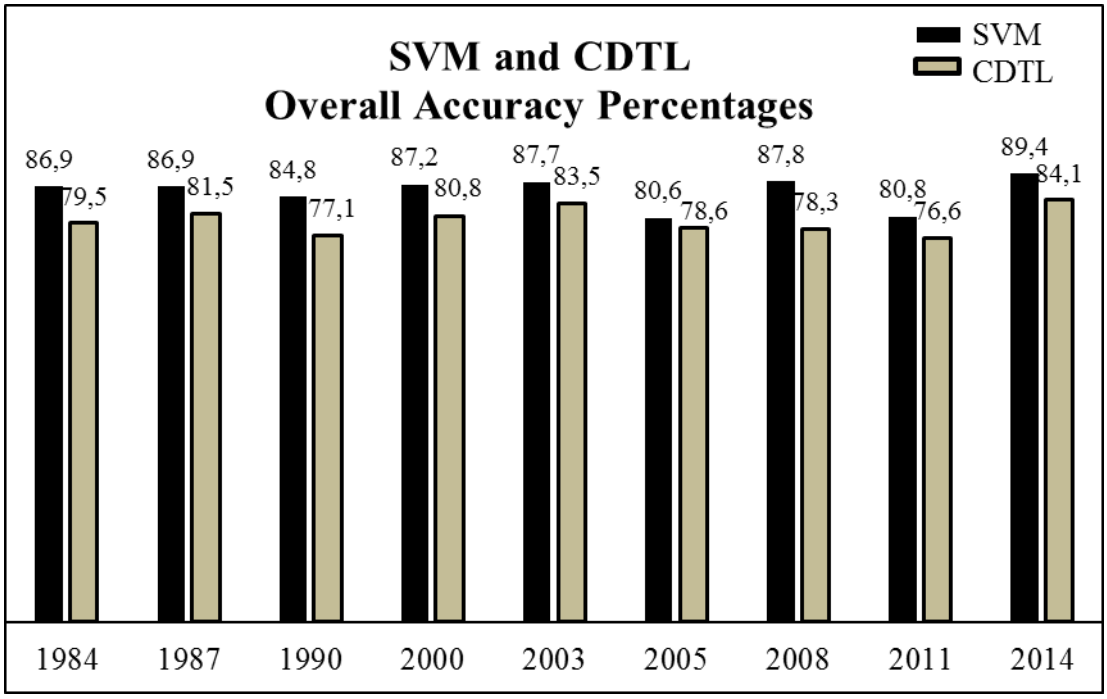

Figure 80. Overall Accuracy comparison for SVM and CDTL classification methods

4. In addition to comparison of the overall accuracies, producer's accuracies (PA) of the classifications for each class are compared. The results are given in Appendix C. Specific class performances of the classification methods based on producer's accuracies (PA) are listed in Table 38. The results show that traditional SVM classification method is more effective for forest, vegetation, agriculture and settlement classes, while CDTL method is effective for soil and water classes for large-area classification.
5. LULC change detection with SVM classification between images of 1984 and 2014 for the Afşin-Elbistan Coal Basin is performed for each year and the resultant LULC change image between years 1984 and 2014 can be seen from Figure 81. The map reveals that the vegetation increases by 3.2%, forest increases by 55.9%, agriculture decreases by 5.9%, settlement decreases by 96.2%, water increases by 289.9% and soil increases by 8.2% between the years 1984 and 2014.

Table 38. Producer's accuracy (PA) comparison of classifications for each year

		PA			PA			PA	
Year	**Class**	**SVM**	**CDTL**	**Year**	**SVM**	**CDTL**	**Year**	**SVM**	**CDTL**
1984	Forest	77.4	63.5	**2000**	60.0	50.8	**2008**	91.7	53.5
	Vegetation	86.8	76.1		68.0	75.0		80.5	75.0
	Agriculture	82.9	63.3		90.6	66.3		72.0	69.5
	Settlement	82.1	30.8		53.1	59.4		27.3	45.5
	Soil	91.3	95.1		93.0	94.6		96.7	85.8
	Water	69.2	84.6		79.2	83.3		70.6	82.4
1987	Forest	69.3	58.6	**2003**	89.2	65.8	**2011**	58.5	44.3
	Vegetation	76.5	78.8		86.0	81.8		63.4	72.6
	Agriculture	81.3	71.9		70.1	75.0		64.4	66.0
	Settlement	84.8	66.7		53.1	69.7		60.0	52.0
	Soil	93.9	91.2		95.7	89.1		93.7	86.5
	Water	82.4	82.4		79.2	65.4		78.6	78.6
1990	Forest	72.9	60.2	**2005**	57.7	58.5	**2014**	86.4	62.7
	Vegetation	82.0	89.8		82.2	69.8		85.0	78.4
	Agriculture	87.8	57.8		77.5	61.7		87.6	73.2
	Settlement	78.6	75.0		60.7	50.0		27.9	62.8
	Soil	84.2	93.8		85.0	94.2		93.8	94.9
	Water	92.3	76.9		88.9	94.4		72.2	77.8

6. LULC change detection with CDTL method between years of 1984 and 2014 for Afşin-Elbistan Coal Basin is performed for each year and the resultant LULC change image between years of 1984 and 2014 can be seen from Figure 82. The map reveals that the vegetation increases by 15.9%, forest increases by 24.3%, agricultural lands decrease by 1.6%, settlement increases by 42.8%, water increases by 608.1% and soil decreases by 8.1% between the years of 1984 and 2014.

7. When change detection statistics of years of 1984 and 2014 for both methods are compared, big differences between results are observed as seen from Table 39. When investigating the classification maps of both classes, these differences are not visible as seen in the statistics. Vegetation, forest and water increase, and agriculture decrease for both methods. Soil increases in the resultant post-classification change-detection map with SVM classification, meanwhile decreasing in the resultant post-classification change-detection map with CDTL method. Likewise, settlement decreases for post-classification change-detection map with SVM classification, while increasing for post-classification change-detection map with CDTL method. The difference between the percentages are significant. The maximum difference is observed for the water class as 318.2%, and the minimum difference is obtained for the agriculture class as 4.3%.
8. During the the investigation of classification performances by using the change detection maps, the following change values are taken into count due to the least amount of accuracy values obtained in the classifications: Change in water by 608.1% and soil by 8.1% are significant between years of 1984 and 2014 because of classification performance of CDTL technique, and change in vegetation by 3.2%, forest by 55.9%, agriculture by 5.9% and settlement by 96.2% are significant between years of 1984 and 2014 because of classification performance of traditional SVM method.

Table 39. Change statistics comparison of both methods

1984 to 2014	SVM (%)	CDTL(%)
Vegetation (%)	**3.2**	15.9
Forest (%)	**55.9**	24.3
Agriculture (%)	**-5.9**	-1.6
Settlement (%)	**-96.2**	42.8
Water (%)	289.9	**608.1**
Soil (%)	8.2	**-8.1**

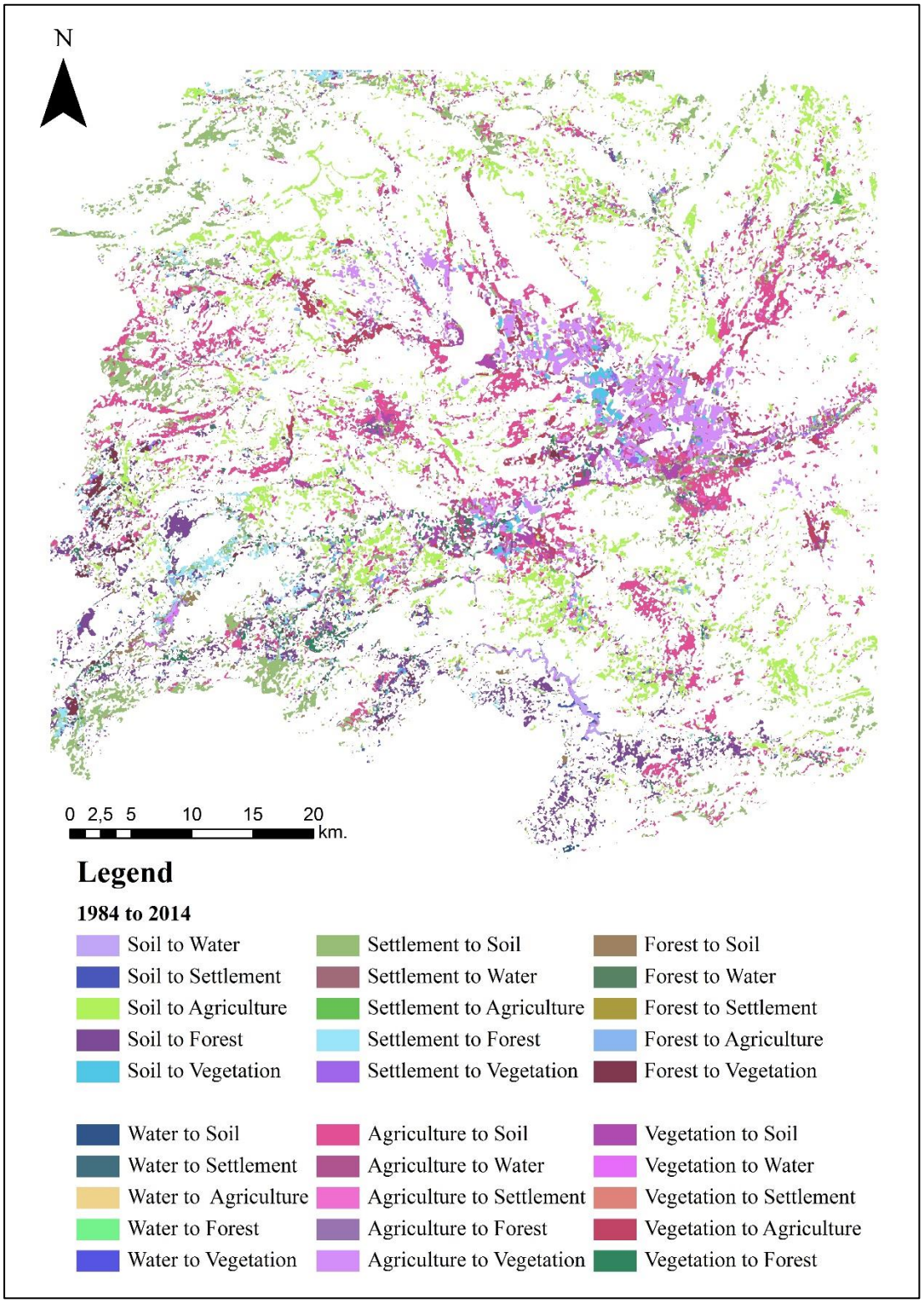

Figure 81. LULC change-detection with SVM between years 1984 and 2014

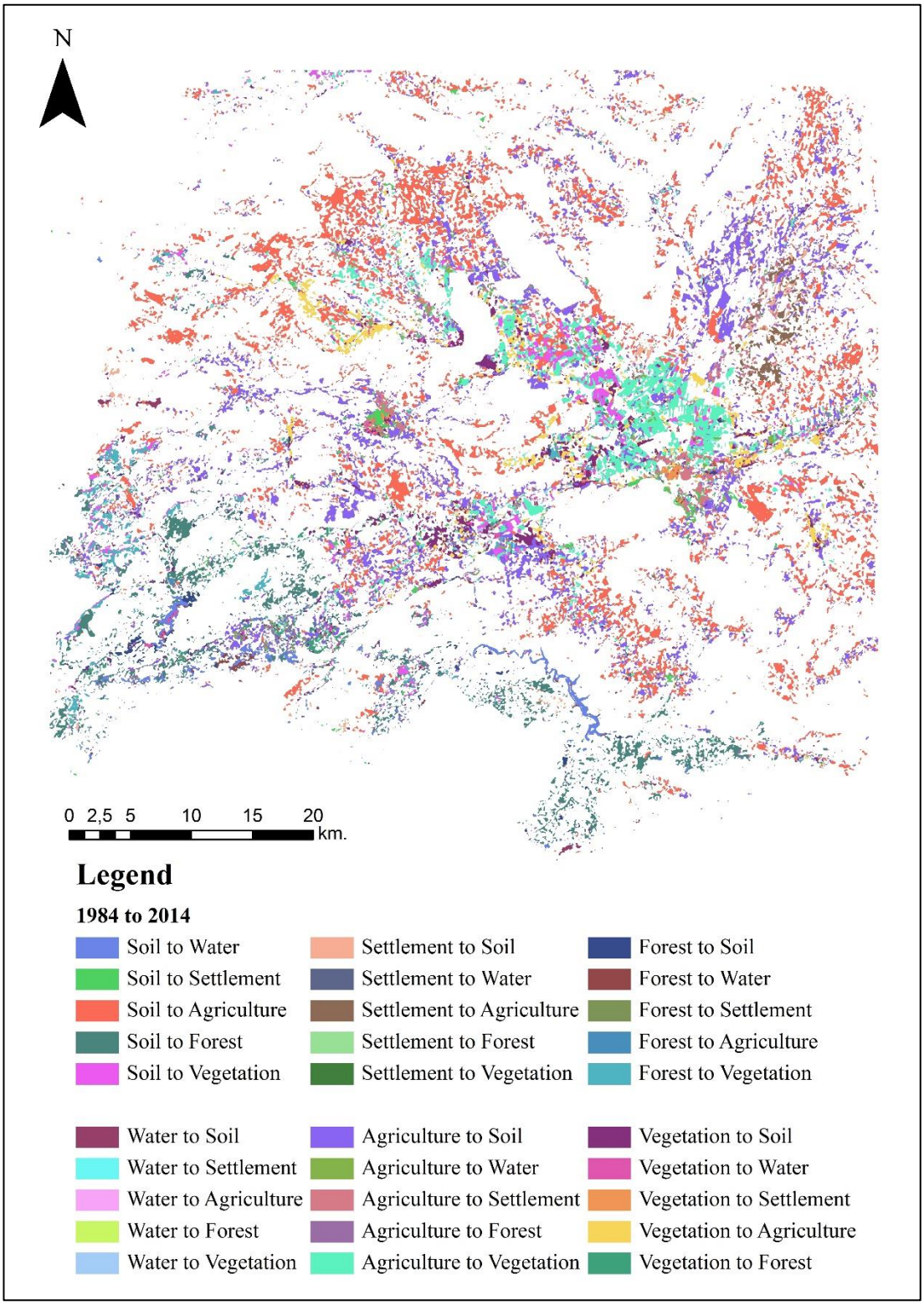

Figure 82. LULC change-detection with CDTL between years 1984 and 2014

CHAPTER 5

CONCLUSIONS AND RECOMMENDATIONS

Surface coal mining is one of the most disturbing activities for the environment. These activities threaten the economical, social and biological value of the surrounding environment. While the awareness about impacts of surface mining increased, monitoring became more and more important. Remote Sensing (RS) and Geographic Information Systems (GIS) play a central role in monitoring the effected areas caused by the surface mining activities. Capability of management of large remotely sensed data, wide range analysis options and visualizing the end-product make RS and GIS utilization a must for the LULC change detection, impact assessment, reclamation and rehabilitation studies.

Utilization of post-classification change detection with CDTL algorithm in this study is a first for monitoring the surface coal mine impacts on environment of Afşin-Elbistan Coal Basin. Updating LULC cover maps for large-areas such as the study area is a necessity to minimize the effects of the surface mine activities.

LULC maps for nine periodical years (1984, 1987, 1990, 2000, 2003, 2008, 2011, 2014) and the corresponding change maps are extracted. The change maps demonstrate the severity of settlement and agriculture decrease on the basin. The study area is a relatively large area and the classes investigated are primary classes, which are vegetation, forest, agriculture, soil, water, and settlement. This study

intends to perform broad change analysis of the basin, for the further studies, only the license area can be analyzed with more than six LULC classes. A proper reclamation plan can be proposed with the new results, and this plan can be visualized and shared with the decision makers, stakeholders, and local people. Also, this case study can be transformed to investigate changes on vegetated lands, waterways, and agricultural activities in Afşin-Elbistan Coal Basin.

LULC maps for nine periodical years and the corresponding LULC change detection maps of Afşin-Elbistan Coal Basin are successfully analyzed and quantified based on remotely sensed images of Landsat images. When the results from change detection between thematic maps of years 1984 and 2014, and change detection maps for other pairs of years are examined, agriculture and vegetation classes usually transform into another. The main reason for this change is decrease in agricultural areas in the basin. The decrease in agricultural lands can be attributed to various interrelated dynamic factors in the basin. However, two important parameters that may lead to decrease in agricultural activities are notable. The first one is the ash from the power plant A, which has old filters on funnels. The ashes are transported by winds and cover the land and the crop, which degrade the crop yield. The second important parameter is land expropriation and resettlement due to mining activities, where the majority of the resettled population has been started to live in urban areas leaving the agricultural activities. As mentioned before, the fouth biggest plain in Turkey is in Elbistan, therefore the decrease in agricultural lands is a negative impact on the economic status of the area, where mining activities have some contribution to it. This fact is validated also by the field surveys, in which it was observed that most of the residents inside the license area left their agricultural lands and moved to work in other towns. Increase in forest class is observed outside of the license area. Settlement class increases between the images of years 1984 and 2014, which is mainly due to classification errors related to the settlement class in 1984 thematic map. In order to overcome this error, post-classification change detection is utilized for 1987 and 2014 thematic maps, and the same difference is observed again. Therefore, post-classification change detection maps for 1984 and 2014 thematic

maps are taken into account. However, results are not interpreted due to large classification errors. The high increase in water bodies is notable, which is mainly due to formation of dam reservoirs for hydroelectric power plant activities in the Basin. In addition, hybrid post-classification change detection with two different classification algorithms can be utilized in the future with best performances of classifiers for each individual class.

While this study is the first one on detecting the LULC changes in Afşin-Elbistan Coal Basin, it will be a base for further studies on rehabilitation planning for the site, and several other studies. There are other sectors in the basin that are planned for extraction with ongoing agricultural activities, where the methodology used in the thesis can be adopted. For the sectors with abandoned mining activities, erosion factor should also be considered in reclamation planning in order to stabilize the slopes, and to maintain ecology and biology of the area in equilibrium. Moreover, people living inside the license area whom are continuing their activities near the mine pose great threat and they should be evacuated properly to designated settlement areas.

Image processing results indicate that Landsat satellite imagery could not supply sufficient detail due to its resolution (30x30 m) for monitoring only the license area. For further researches, remotely sensed data having higher spatial and spectral properties should be utilized in order to obtain more detailed classification maps.

In conclusion, traditional SVM classification and CDTL classification techniques are both effective classification techniques, SVM classification is more reliable than CDTL method because of higher accuracies, and CDTL is more preferable for multi-date classification analyses because of its time efficiency. In order to increase accuracy of CDTL method, samples for training set should be selected carefully. Post-classification LULC change detection maps for both classification methods are compared and excessive differences between the difference maps is observed. These differences mostly occur due to the different sample sets, therefore selection of training sets for each individual classification method is crucial for the analyses.

Finally, utilization of remotely sensed data is a must for the determining LULC change detection of surface mining activities instead of costly methods.

REFERENCES

Adams, J. B., Sabol, D., Kapos, V., Filho, R. A., Roberts, D. A., Smith, M. O., & Gillespie, A. R. (1995). Classification of multispectral images based on fractions of endmembers: application to land-cover change in the Brazilian Amazon. *Remote Sensing of Environment, 52*, 137-154.

Anderson, J. R., Hardy, E. E., Roach, J. T., & Witmer, R. E. (1978). *A Land Use and Land Cover Classification System for use with Remote Sensor Data.* U.S. Department of the Interior.

Aspinall, R. J., & Hill, M. J. (1997). Land cover change: a method for assessing the reliability of land cover changes measured from remotely-sensed data. *Proceedings of the International Geoscience and Remote Sensing Symposium* (pp. 269-271). Singapore: GARSS '97.

Bandibas, J. C. (1998). Combining the spectral and spatial signature of information classes using artificial neural network based classifier for remote sensing of spatially heterogeneous land-use/land cover system in the tropics. *19th Asian Conference on Remote Sensing.* Philippine. Retrieved February 10, 2015, from http://www.a-a-r-s.org/aars/proceeding/ACRS1998/Papers/DIP98-2.htm

Bascetin, A. (2006). A decision support system using analytical hierarchy process (AHP) for the optimal environmental reclamation of an open-pit mine. *Environmental Geology, 52*, 663-672.

Boser, B. E., Guyon, I. M., & Vapnik, V. N. (1992). A Training Algorithm for Optimal Margin Classifiers. *Proceedings of the Fifth Annual Workshop on Computational Learning Theory* (pp. 144-152). Pittsburgh: ACM Press.

Brown, M., Gunn, S. R., & Lewis, H. G. (1999). Support vector machines for optimal classification and spectral unmixing. *Ecological Modelling, 120*, 167-179.

Bryne, G. F., Crapper, P. F., & Mayo, K. K. (1980). Monitoring land cover change by principal component analysis of multitemporal Landsat data. *Remote Sensing of Environment, 10*, 175-184.

Burrough, P. A., & McDonnell, R. A. (1998). *Principles of Geographical Information Systems.* Wiltshire: Oxford University Press.

Chatterjee, R. S., Roy, J., & Bhattacharya, A. K. (1996). Mapping geological features of the Jharia coalfield from Landsat-5 TM data. *International Journal of Remote Sensing, 17*(16), 3257-3270.

Chen, J., Gong, P., He, C., Pu, R., & Shi, P. (2003). Land use land cover change detection using improved change vector analysis. *Photogrammetric Engineering and Remote Sensing, 69*(4), 369-379.

Coker, A. E. (1977). The application of remote sensing technology to assess the effects of and monitor change in coal mining in Easter Tenessee. *First Annual William Symposium*, (pp. 173-176). Falls Church.

Collins, G. W. (1991). Monitoring environmental quality: derelict and degraded land survey. *Conference on Remote Sensing of the Environment*, (pp. 95-105). Birmingham.

Collins, J. B., & Woodcock, C. E. (1994). Change Detection Using the Gramm-Schmidt Transformation Applied to Mapping Forest Mortality. *Remote Sensing Environment, 50*, 267-279.

Collins, J. B., & Woodcock, C. E. (1996). An assessment of several linear change detection techniques for mapping forest mortality using multitemporal Landsat TM data. *Remote Sensing of Environment, 56*, 66-77.

Coppin, P., Nackaerts, K., Queen, L., & Brewer, K. (2001). Operational monitoring of green biomass change for forest management. *Photogrammetric Engineering and Remote Sensing, 67,* 603-611.

Cortes, C., & Vapnik, V. (1995). Support-Vector Networks. *Machine Learning, 20,* 273-297.

Demir, B., Bovolo, F., & Bruzzone, L. (2012). Updating Land-Cover Maps by Classification of Image Time Series: A Novel Change-Detection-Driven Transfer Learning Approach. *IEEE Transactions on Geoscience and Remote Sensing, 51*(1), 300-312.

Demirel, N., Emil, M. K., & Düzgün, H. Ş. (2010). Surface coal mine area monitoring using multi-temporal high-resolution satellite imagery. *International Journal of Coal Geology, 86,* 3-11.

Department of Environment (DoE). (1987). *Handling Geographic Information.* London: HMSO.

Dimyati, M., Muzino, K., Kobayashi, S., & Kitamura, T. (1996). An analysis of land use/cover change using the combination of MSS Landsat and land use map-a case study in Yogyakarta, Indonesia. *International Journal of Remote Sensing, 17,* 931-944.

Düzgün, Ş., & Demirel, N. (2011). *Remote Sensing of the Mine Environment.* Taylor & Francis Group.

Electricity Generation Company of Turkish Republic. (2014). *Electricity Generation Company 2014 Annual Report*. Retrieved May 11, 2015, from http://www.euas.gov.tr/Documents/YILLIKRAPOR_2014.pdf

Emil, M. K. (2010). Land Degradation Assessment for an abandoned coal mine with geospatial information technologies. *M.Sc. Thesis*. Ankara, Turkey: METU Mining Engineering Department.

ENVI5.0 Help Menu. (2012). Exelis Visual Information Solutions.

Erener, A. (2010). Remote sensing of vegetation health for reclaimed areas of Seyitömer open cast coal mine. *International Journal of Coal Geology, 86*, 20-26.

Esri. (2010). ArcGIS10 Desktop Help.

European Environment Agency. (1995). *CORINE Land Cover*. Retrieved August 15, 2015, from http://www.eea.europa.eu/publications/COR0-landcover

Fauzi, A., Hussin, Y. A., & Weir, M. (2001). A comparison between neural networks and maximum likelihood remotely sensed data classifiers to detect tropical rain logged-over forest in Indonesia. *22nd Asian Conference on Remote Sensing.* Singapore: Asian Association on Remote Sensing.

Foody, G. M. (2001). Monitoring the magnitude of land-cover change around the southern limits of the Sahara. *Photogrammetric Engineering and Remote Sensing, 67*, 841-847.

Governor's Office of Kahramanmaraş. (2014). *Governor's Office of Kahramanmaraş*. Retrieved May 11, 2015, from http://kahramanmaras.gov.tr/CografiYapi.aspx

Green, K., Kempka, D., & Lackey, L. (1994). Using Remote Sensing to Detect and Monitor Land-Cover and Land-Use Change. *Photogrammetric Engineering and Remote Sensing, 60*(3), 331-337.

Hame, T., Heiler, I., & Miguel-Ayanz, J. S. (1998). An unsupervised change detection and recognition system for forestry. *International Journal of Remote Sensing, 19*, 1079-1099.

Henrico County. (1997). *Geographic Information Systems*. Retrieved June 2015, from http://henrico.us/gis/

Hsu, C.-W., Chang, C.-C., & Lin, C.-J. (2010, April 15). *A Practical Guide to Support Vector Classification.* Retrieved June 2015, from http://www.csie.ntu.edu.tw/~cjlin/papers/guide/guide.pdf

Ingebritsen, S. E., & Lyon, R. J. (1985). Principal component analysis of multitemporal image pairs. *International Journal of Remote Sensing, 6,* 687-696.

Jensen, J. (1996). *Introductory digital image processing. A remote sensing perspective* (2nd ed.). New Jersey: Prentice Hall.

Jensen, J. R., Cowen, D. J., Althausen, J. D., Naumalani, S., & Weatherbee, O. P. (1993). An evaluation of coast watch change detection protocol in South Carolina. *Photogrammetric Engineering and Remote Sensing, 59,* 1039-1046.

Jha, C. S., & Unni, N. V. (1994). Digital change detection of forest conversion of dry tropical forest region. *International Journal of Remote Sensing, 15,* 2543-2552.

Johnson, R. D. (1994). Change vector analysis for disaster assessment: a case study of Hurricane Andrew. *Geocarto International, 1,* 41-45.

Johnson, R. D., & Kasischke, E. S. (1998). Change vector analysis: a technique for the multitemporal monitoring of land cover and condition. *International Journal of Remote Sensing, 19,* 411-426.

Kauth, R. J., & Thomas, G. (1976). The tasseled cap-a graphic description of the spectral-temporal development of agricultural crops as seen by Landsat. *Symposium on Machine Processing of Remotely Sensed Data* (pp. 4 B-41-4 B-51). West Lafayette: Purdue University.

Kavzoglu, T., & Colkesen, I. (2009). A kernel functions analysis for support vector machines for land cover classification. *International Journal of Applied Earth Observation and Geoinformation, 11,* 352-359.

Lambin, E. F. (1996). Change detection at multiple temporal scales: seasonal and annual variation in landscape variables. *Photogrammetric Engineering and Remote Sensing, 62,* 931-938.

Latifovic, R., Fytas, K., J. C., & Paraszczak, J. (2005). Assessing land cover change resulting from large surface mining development. *International Journal of Applied Earth Observation and Geoinformation, 7,* 29-48.

Lillesand, T. M., Kiefer, R. W., & Chipman, J. W. (2004). *Remote Sensing and Image Interpretation.* :John Wiley & Sons.

Lu, D., Mausel, P., Brondízio, E., & Moran, E. (2004). Change detection techniques. *International Journal of Remote Sensing, 25*(12), 2365-2401.

Macleod, R. D., & Congalton, R. G. (1998). A quantitative comparison of change-detection algorithms for monitoring eelgrass from remotely sensed data. *Photogrammetric Engineering and Remote Sensing, 64*(3), 207-2016.

Manu, A., Twumasi, Y. A., & Coleman, T. L. (2004). Application of Remote Sensing and GIS Technologies to Assess the Impact of Surface Mining at Tarkwa, Ghana. *Geoscience and Remote Sensing Symposium. 1*, pp. 572-574. Anchorage: IEEE.

Mas, J. F. (1999). onitoring land-cover changes: a comparison of change detection techniques. *International Journal of Remote Sensing, 20*, 139-152.

Mather, P. M. (2004). *Computer Processing of Remotely-sensed Images.* John Wiley & Sons.

Mert, B. A. (2010). The Research of the Possibilities of the use of Geographical Information Systems and Global Positioning Systems on the Mining Activities in the Afşin-Elbistan Coal Field. *PhD Thesis*. Adana: Çukurova University.

Miller, A. B., Bryant, E. S., & Birnie, R. W. (1998). An analysis of land cover changes in the northern forest of New England using multitemporal Landsat MSS data. *International Journal of Remote Sensing, 19*, 245-265.

Ministry of Environment and Urbanization. (2011). *Kahramanmaraş Province Environmental Status Report in Turkish*. Retrieved May 11, 2015, from http://www.csb.gov.tr/turkce/dosya/ced/icdr2011/kmaras_icdr2011.pdf

Muchoney, D. M., & Haack, B. N. (1994). Change Detection for Monitoring Forest Defoliation. *Photogrammetric Engineering and Remote Sensing, 60*(10), 1243-1251.

Munyati, C. (2000). Wetland change detection on the Kafue Flats, Zambia, by classification of a multitemporal remote sensing image dataset. *International Journal of Remote Sensing, 21*, 1787-1806.

NASA. (2000, August 30). *Earth Observatory*. Retrieved February 2, 2015, from http://earthobservatory.nasa.gov/Features/MeasuringVegetation/printall.php

Pamukçu, C., & Simsir, F. (2006). Example of Reclamation Attempts at a set of Quarries Located in İzmir. *Journal of Mining Science, 42*(3), 304-308.

Parks, N. F., & Petersen, G. W. (1987). High Resolution Remote Sensing of Spatially and Spectrally Complex Coal Surface Mines of Central Pennsylvania: A Comparison between Simulated SPOT MSS and Landsat-5 Thematic Mapper. *Photogrammetric Engineering and Remote Sensing, 53*(4), 415-420.

Petit, C. C., & Lambin, E. F. (2001). Integration of multi-source remote sensing data for land cover change detection. *International Journal of Geographical Information Science, 15*, 785-803.

Petit, C., Scudder, T., & Lambin, E. (2001). Quantifying processes of land-cover change by remote sensing: resettlement and rapid land-cover change in southeastern Zambia. *International Journal of Remote Sensing, 22*, 3435-3456.

Poyatos, R., Latron, J., & Llorens, P. (2003). Land Use and Land Cover Change After Agricultural Abandonment. *Mountain Research and Development, 23*(4), 362-368.

Prakash, A., & Gupta, R. P. (1998). Land-use mapping and change detection in a coal mining area - a case study in the Jharia coalfield, India. *International Journal of Remote Sensing, 19*(3), 391-410.

Radeloff, V. C., Mladenoff, D. J., & Boyce, M. S. (1999). Detecting jack pine budworm defoliation using spectral mixture analysis: separating effects from determinants. *Remote Sensing of Environment, 69*, 156-169.

Rathore, C. S., & Wright, R. (2007). Monitoring environmental impacts of surface coal mining. *International Journal of Remote Sensing, 14*(6), 1021-1042.

Ridd, M. K., & Liu, J. (1998). A comparison of four algorithms for change detection in an urban environment. *Remote Sensing of Environment, 63*, 95-100.

Roberts, D. A., Batista, G. T., Pereira, J. L., Waller, E. K., & Nelson, B. W. (1998). Change identification using multitemporal spectral mixture analysis: applications in eastern Amazonia. *Remote Sensing Change Detection: Environmental Monitoring Methods and Applications*, 137-161.

Scaramuzza, P., Micijevic, E., & Chander, G. (2004). *U.S. Geological Survey*. Retrieved December 8, 2014, from USGS Landsat Missions: http://landsat.usgs.gov/documents/SLC_Gap_Fill_Methodology.pdf

Schmidt, H., & Glaesser, C. (1998). Multitemporal analysis of satellite data and their use in the monitoring of the enviromental impacts of open cast lignite mining areas in Eastern Germany. *International Journal of Remote Sensing, 19*(12), 2245-2260.

Schoppmann, M. W., & Tyler, W. A. (1996). Chernobyl revisited: monitoring change with change vector analysis. *Geocarto International, 11*, 13-27.

Sengupta, M. (1993). *Enviromental Impacts of Mining.* CRC Press.

Seto, K. C., Woodcock, C. E., Song, C., Huang, X., Lu, J., & Kaufmann, R. K. (2002). Monitoring land-use change in the Pearl River Delta using Landsat TM. *International Journal of Remote Sensing, 23,* 1985-2004.

Singh, A. (1986). Change detection in the tropical forest environment of northeastern India using Landsat. In M. J. Eden, & J. T. Parry, *Remote Sensing and Tropical Land Management* (pp. 237-254). New York: J. Wiley.

Singh, A. (2010). Review Article Digital change detection techniques using remotely-sensed data. *International Journal of Remote Sensing, 10*(6), 989-1003.

Siwe, R. N., & Koch, B. (2008). Change vector analysis to categorise land cover change processes using the tasselled cap as biophysical indicator. *Enviromental Monitoring and Assesment, 145,* 227-235.

Sohl, T. L. (1999). Change Analysis in the United Arab Emirates: An Inverstigation of Techniques. *Photogrammetric Engineering and Remote Sensing, 65*(4), 475-484.

The Yale Center for Earth Observation. (2013). *Yale University Center for Earth Observation*. Retrieved December 10, 2014, from http://www.yale.edu/ceo/Documentation/Landsat_ETM_Gap_Fill.pdf

Tso, B., & Mather, P. M. (2009). *Classification Methods for Rometely Sensed Data.* Taylor & Francis Gorup.

U.S. Energy Information Administration. (2012). *International Energy Statistics*. Retrieved February 10, 2015, from http://www.eia.gov/cfapps/ipdbproject/iedindex3.cfm?tid=1&pid=7&aid=1&cid=TU,&syid=2008&eyid=2012&unit=TST

U.S. Geological Survey. (2014). *EarthExplorer*. Retrieved September 3, 2014, from USGS: http://earthexplorer.usgs.gov/

U.S. Geological Survey. (2015, January 15). *U.S. Department of the Interior*. Retrieved February 2, 2015, from U.S. Geological Survey: http://phenology.cr.usgs.gov/ndvi_foundation.php

U.S. Geological Survey. (2015). *USGS*. Retrieved September 2, 2014, from Landsat: http://landsat.usgs.gov/band_designations_landsat_satellites.php

Ustin, S. L., Roberts, D. A., & Hart, Q. J. (1998). Seasonal vegetation patterns in a California coastal savanna derived from Advanced Visible/Infrared Imaging Spectrometer (AVIRIS) data. *Remote Sensing Change Detection: Environmental Monitoring Methods and Applications*, 163-180.

Woodcock, C. E., Macomber, S. A., Pax-Lenney, M., & Cohen, W. B. (2001). Monitoring large areas for forest change using Landsat: generalization across space, time and Landsat sensors. *Remote Sensing of Environment, 78*, 194-203.

World Coal Institute. (2009). *The Coal Resource: A Comprehensive Overview of Coal.* World Coal Institute.

Yaylacı, E. D. (2015). A Sustainability Assesment Framework for Evaluation of Coal Mining Sector Plans in Afşin-Elbistan Coal Basin with a Special Emphasis on Land Disturbance. *Ph.D. Thesis*. Ankara: Middle East Technical University.

APPENDIX A

Table A1. Specifications of Landsat imagery used (USGS, 2015)

Landsat 5 TM	**Bands**	**Wavelength (micrometers)**	**Resolution (meters)**
	Band 1	0.45-0.52	30
	Band 2	0.52-0.60	30
	Band 3	0.63-0.69	30
	Band 4	0.76-0.90	30
	Band 5	1.55-1.75	30
	Band 6	10.40-12.50	120* (30)
	Band 7	2.08-2.35	30
	Bands	**Wavelength (micrometers)**	**Resolution (meters)**
Landsat 7 ETM+	Band 1	0.45-0.52	30
	Band 2	0.52-0.60	30
	Band 3	0.63-0.69	30
	Band 4	0.77-0.90	30
	Band 5	1.55-1.75	30
	Band 6	10.40-12.50	60 * (30)
	Band 7	2.09-2.35	30
	Band 8	.52-.90	15
Landsat 8 OLI	**Bands**	**Wavelength (micrometers)**	**Resolution (meters)**
	Band 1 - Coastal aerosol	0.43 - 0.45	30
	Band 2 - Blue	0.45 - 0.51	30
	Band 3 - Green	0.53 - 0.59	30
	Band 4 - Red	0.64 - 0.67	30
	Band 5 - Near Infrared (NIR)	0.85 - 0.88	30
	Band 6 - SWIR 1	1.57 - 1.65	30
	Band 7 - SWIR 2	2.11 - 2.29	30
	Band 8 - Panchromatic	0.50 - 0.68	15
	Band 9 - Cirrus	1.36 - 1.38	30
	Band 10 - Thermal Infrared 1	10.60 - 11.19	100 * (30)
	Band 11 - Thermal Infrared 2	11.50 - 12.51	100 * (30)

Figure A1. Landsat imageries used in analyses

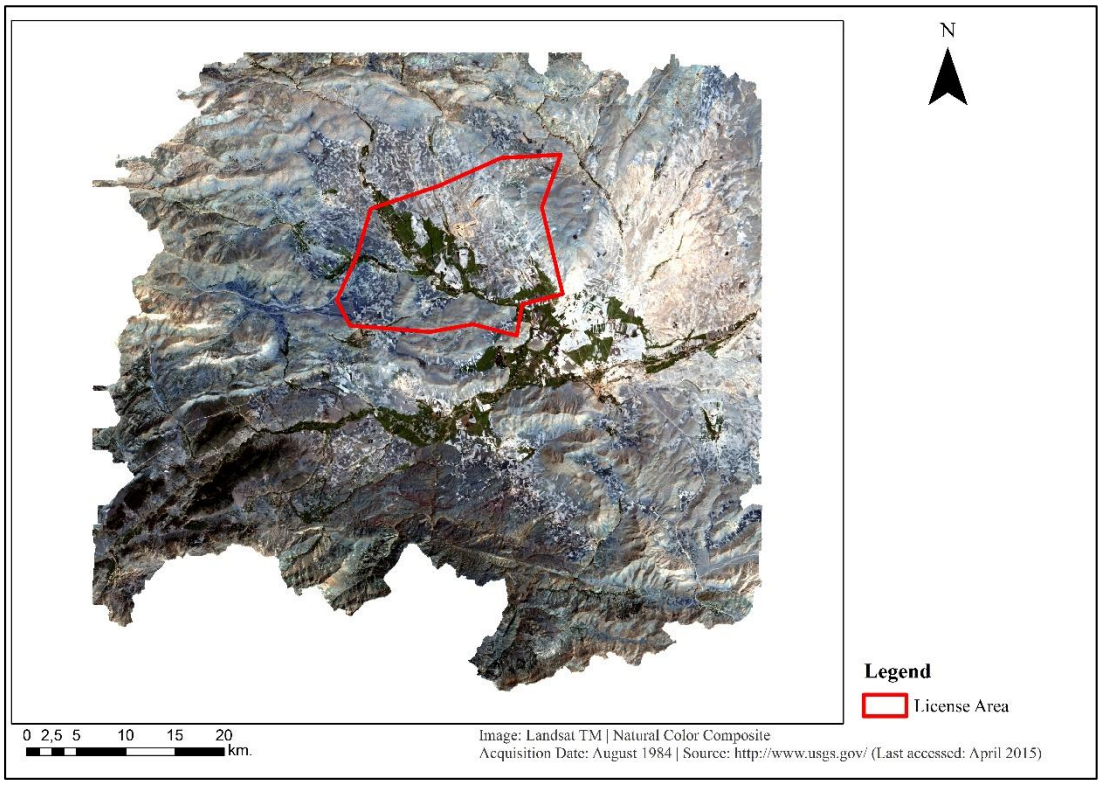

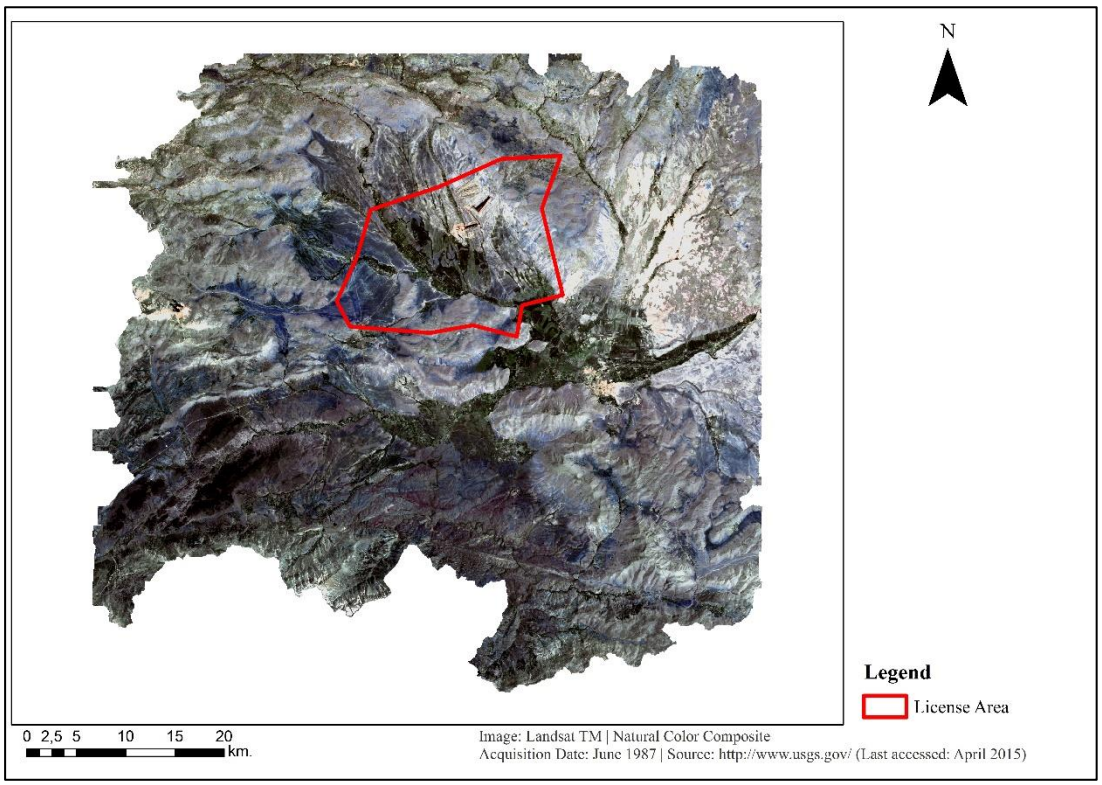

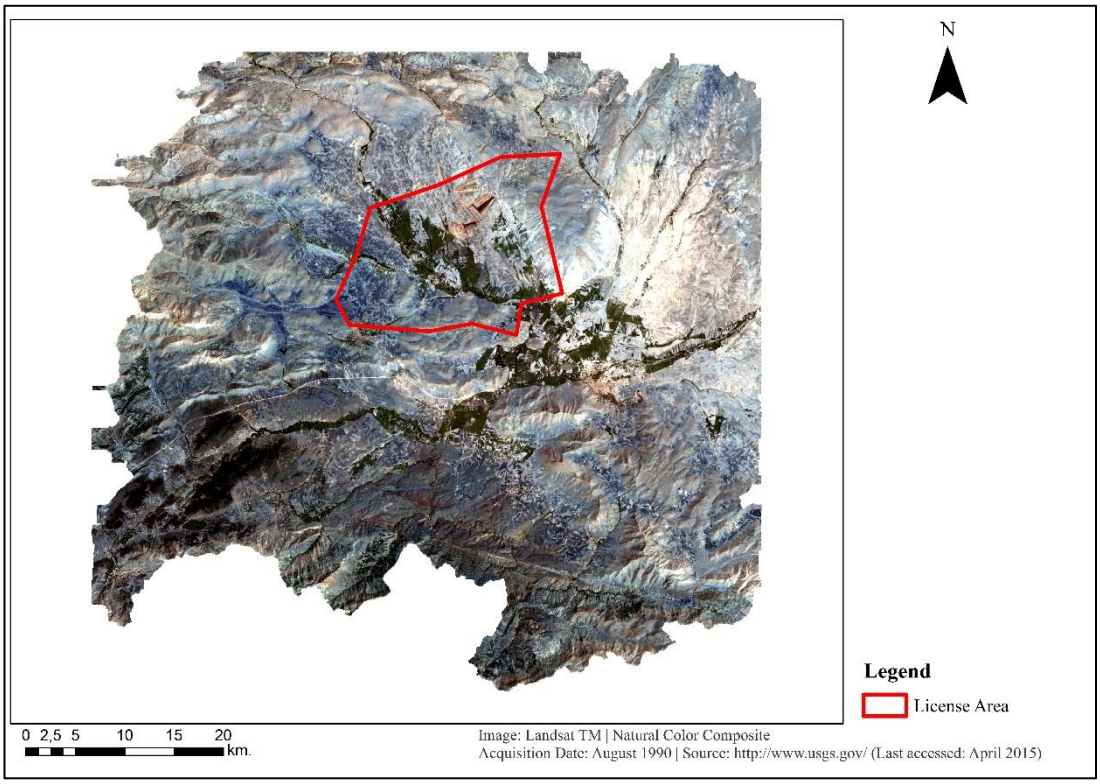

Image: Landsat TM | Natural Color Composite
Acquisition Date: August 1990 | Source: http://www.usgs.gov/ (Last accessed: April 2015)

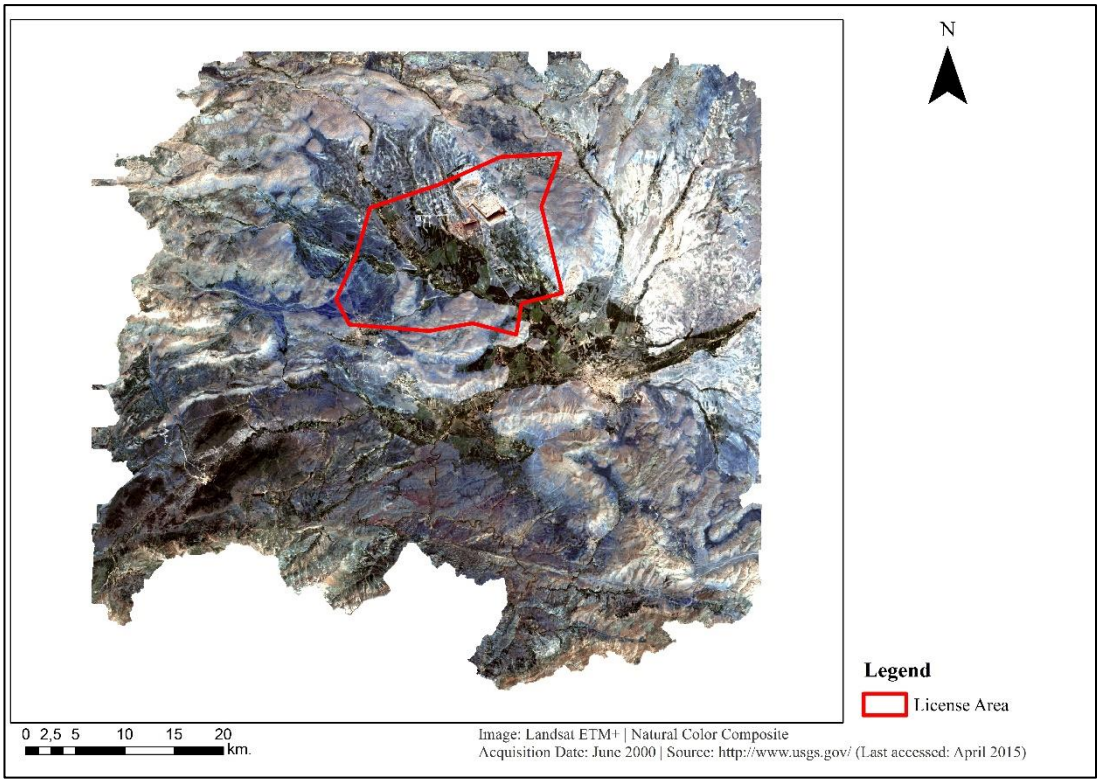

Image: Landsat ETM+ | Natural Color Composite
Acquisition Date: June 2000 | Source: http://www.usgs.gov/ (Last accessed: April 2015)

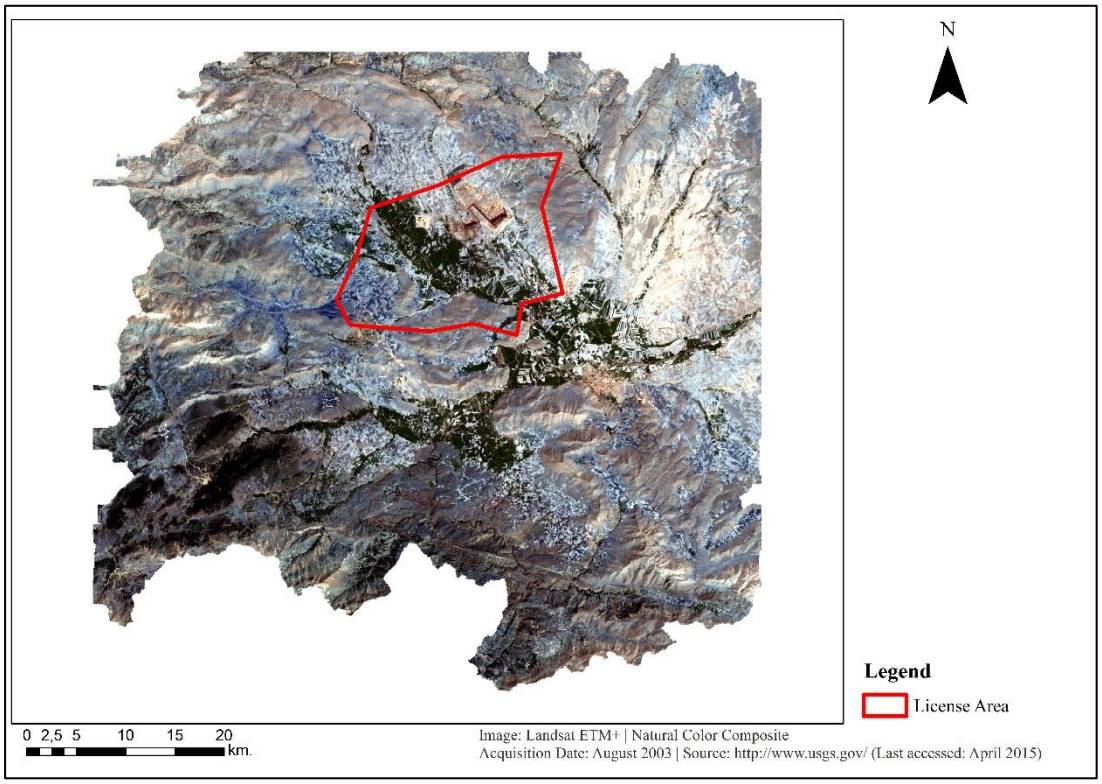
N
Legend
License Area
0 2,5 5 10 15 20
km.
Image: Landsat ETM+ | Natural Color Composite
Acquisition Date: August 2003 | Source: http://www.usgs.gov/ (Last accessed: April 2015)

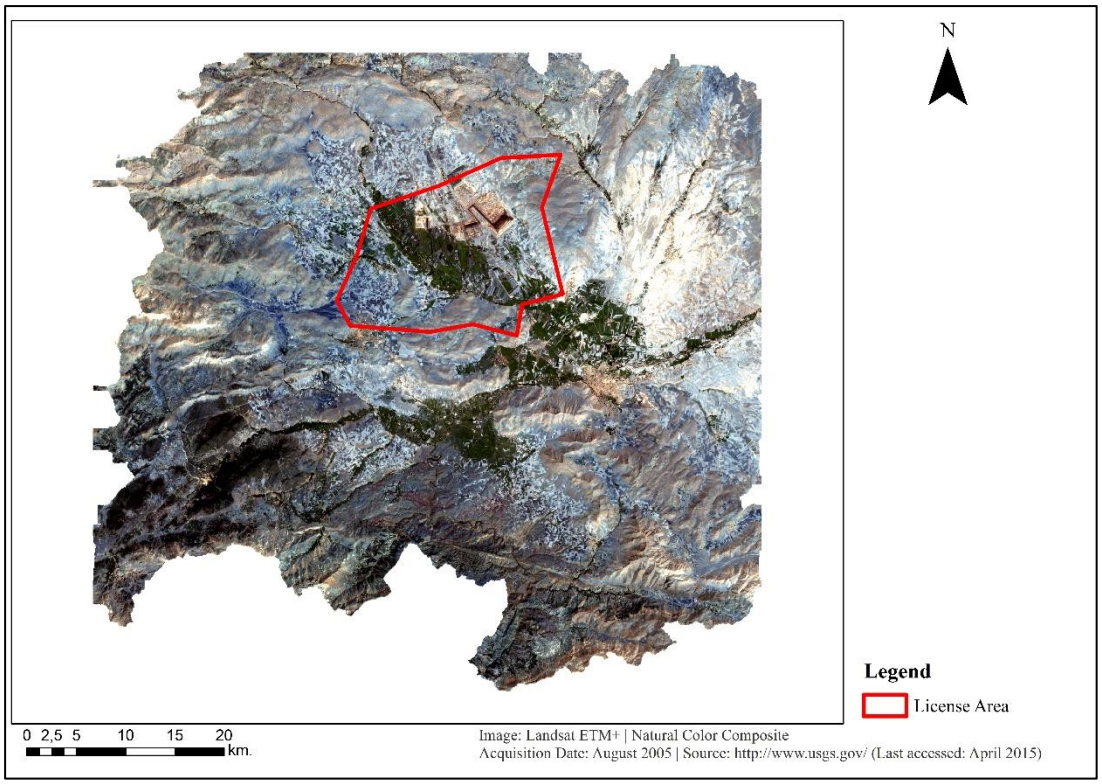
N
Legend
License Area
0 2,5 5 10 15 20
km.
Image: Landsat ETM+ | Natural Color Composite
Acquisition Date: August 2005 | Source: http://www.usgs.gov/ (Last accessed: April 2015)

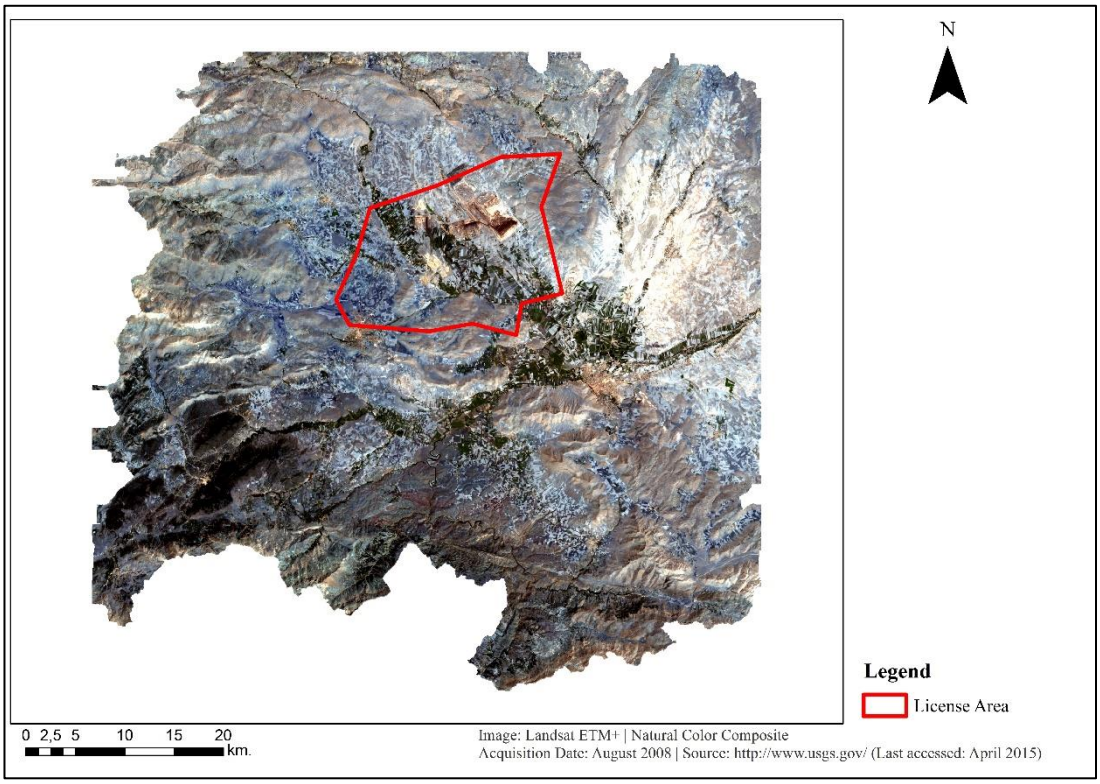
N
Legend
License Area
0 2,5 5 10 15 20
km.
Image: Landsat ETM+ | Natural Color Composite
Acquisition Date: August 2008 | Source: http://www.usgs.gov/ (Last accessed: April 2015)

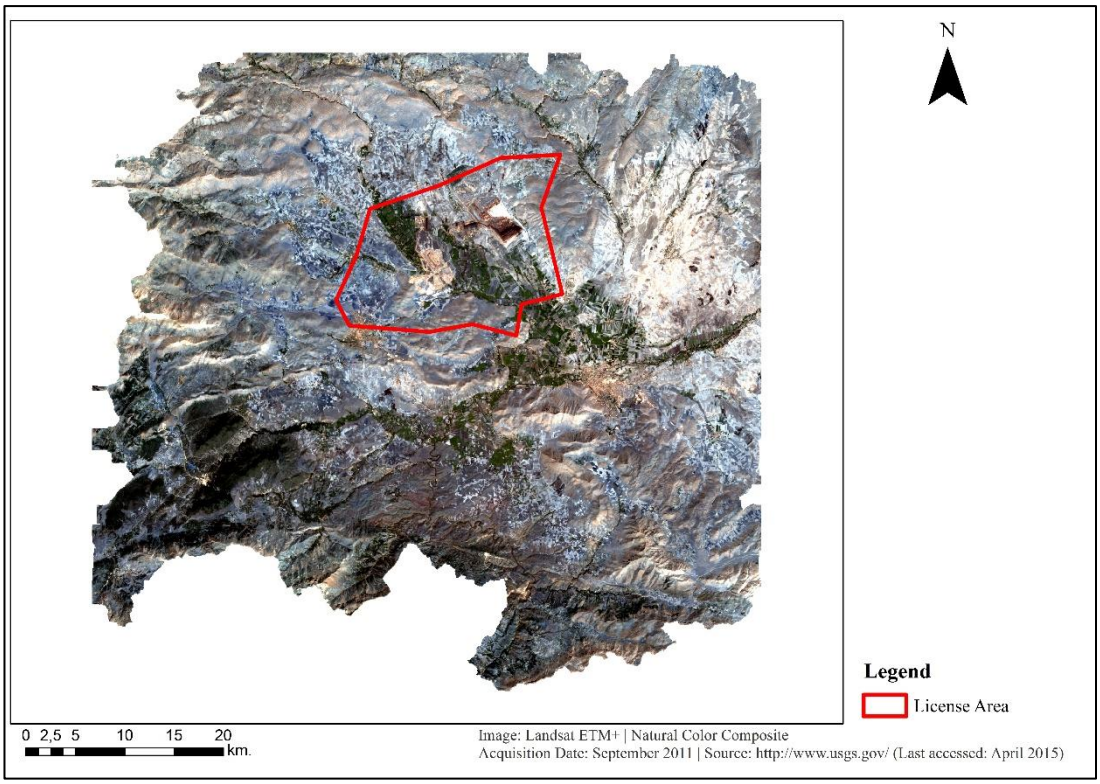
N
Legend
License Area
0 2,5 5 10 15 20
km.
Image: Landsat ETM+ | Natural Color Composite
Acquisition Date: September 2011 | Source: http://www.usgs.gov/ (Last accessed: April 2015)

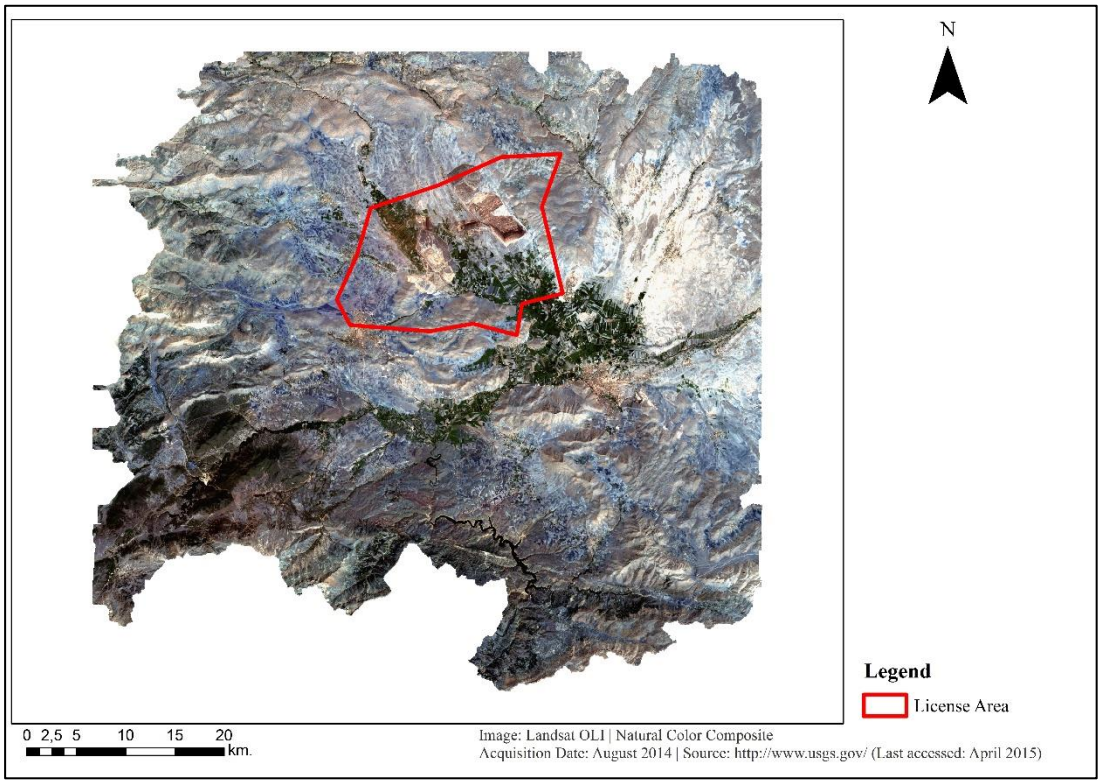
N
Legend
License Area
0 2,5 5 10 15 20
km.
Image: Landsat OLI | Natural Color Composite
Acquisition Date: August 2014 | Source: http://www.usgs.gov/ (Last accessed: April 2015)

APPENDIX B

Figure B1. Difference maps from the year 1984 to 2014 periodically

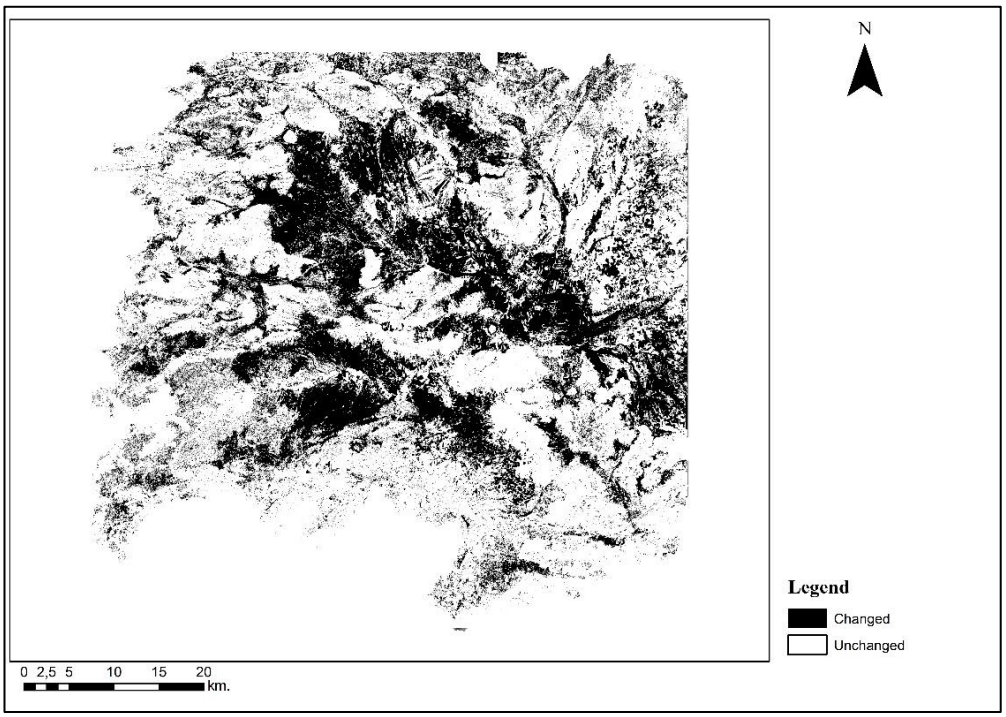

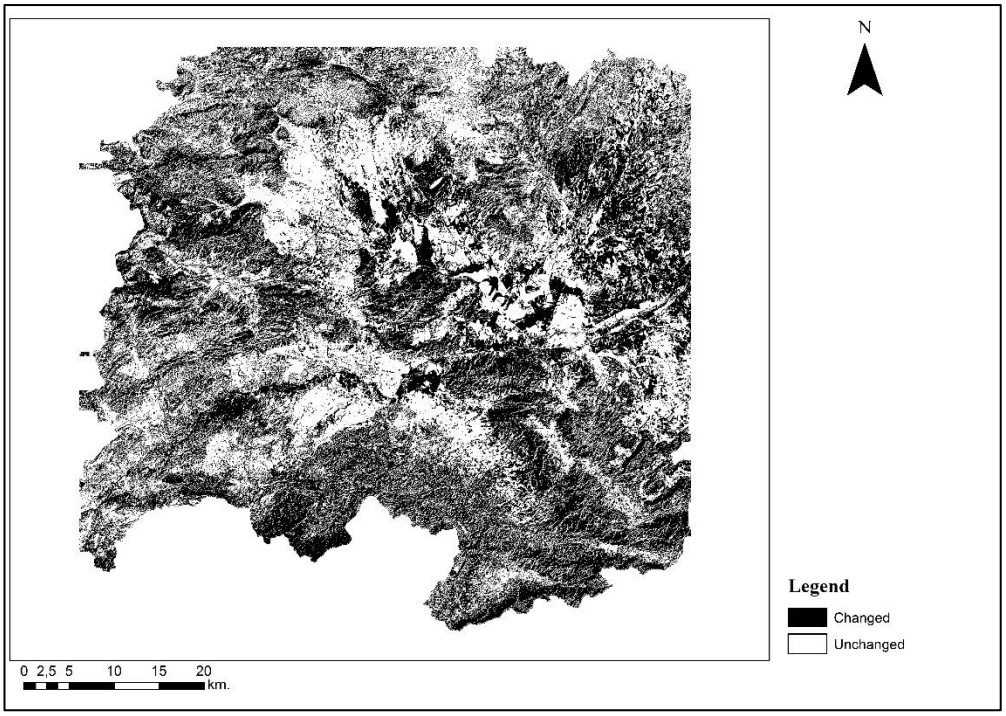

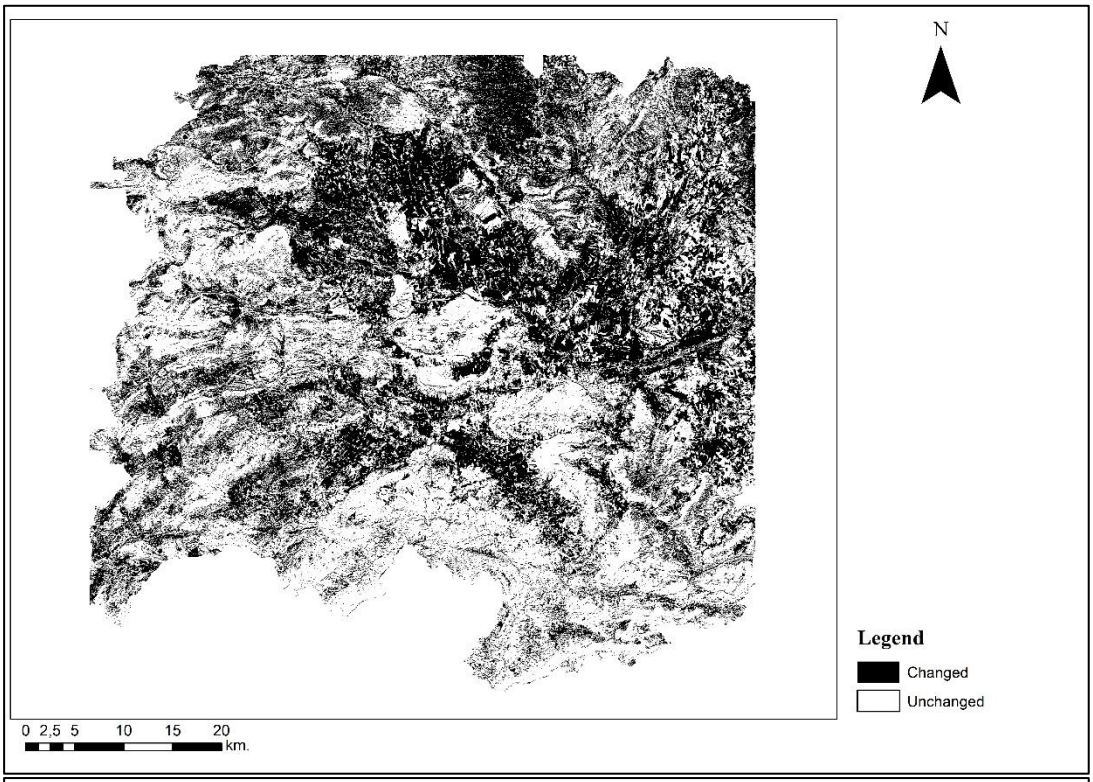
N
Legend
Changed
Unchanged
0 2,5 5 10 15 20
km.

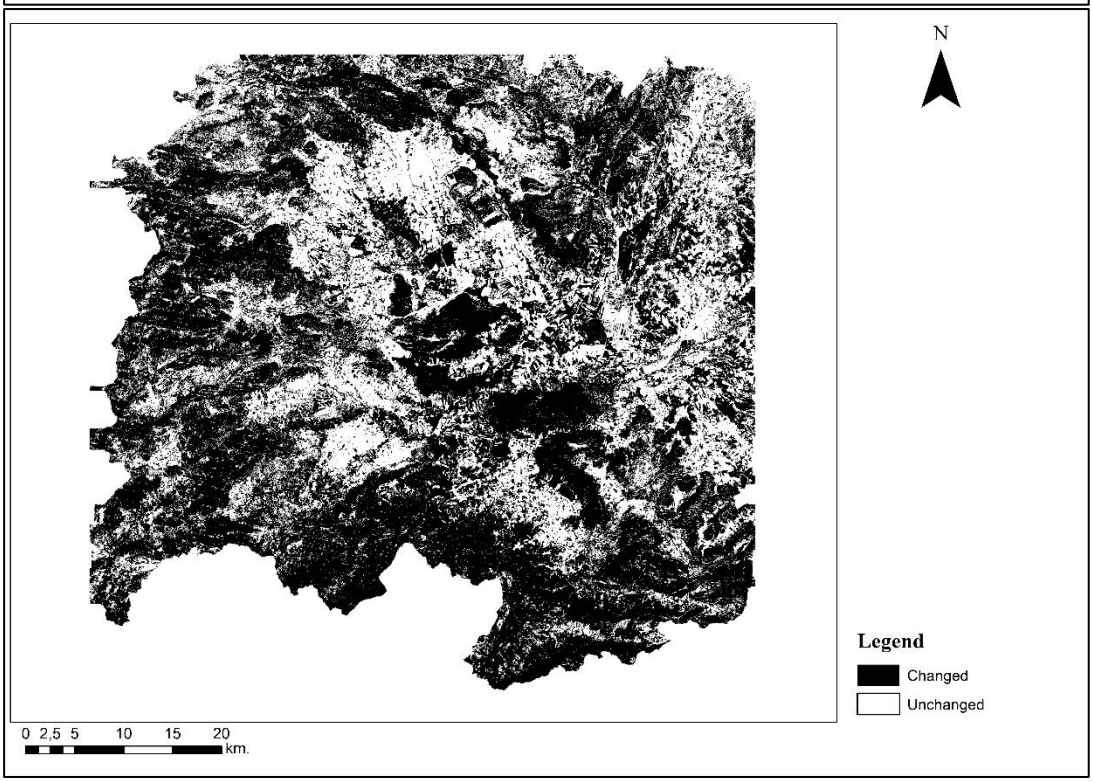
N
Legend
Changed
Unchanged
0 2,5 5 10 15 20
km.

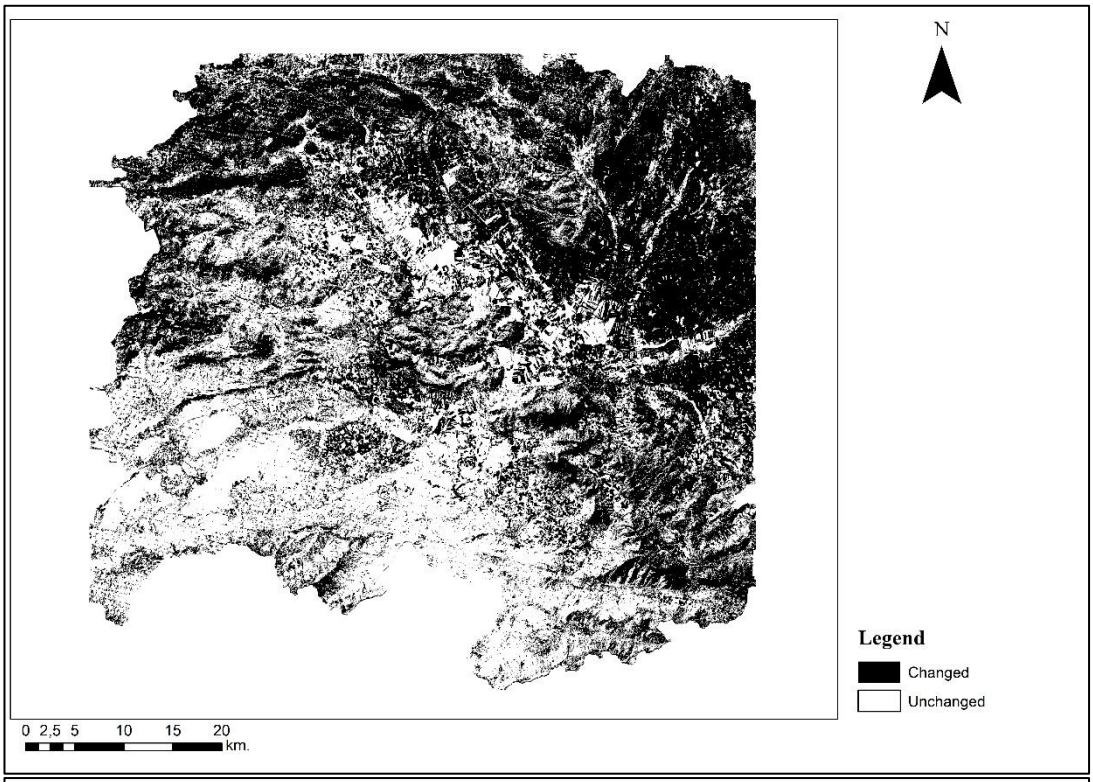
N
Legend
Changed
Unchanged
0 2,5 5 10 15 20
km.

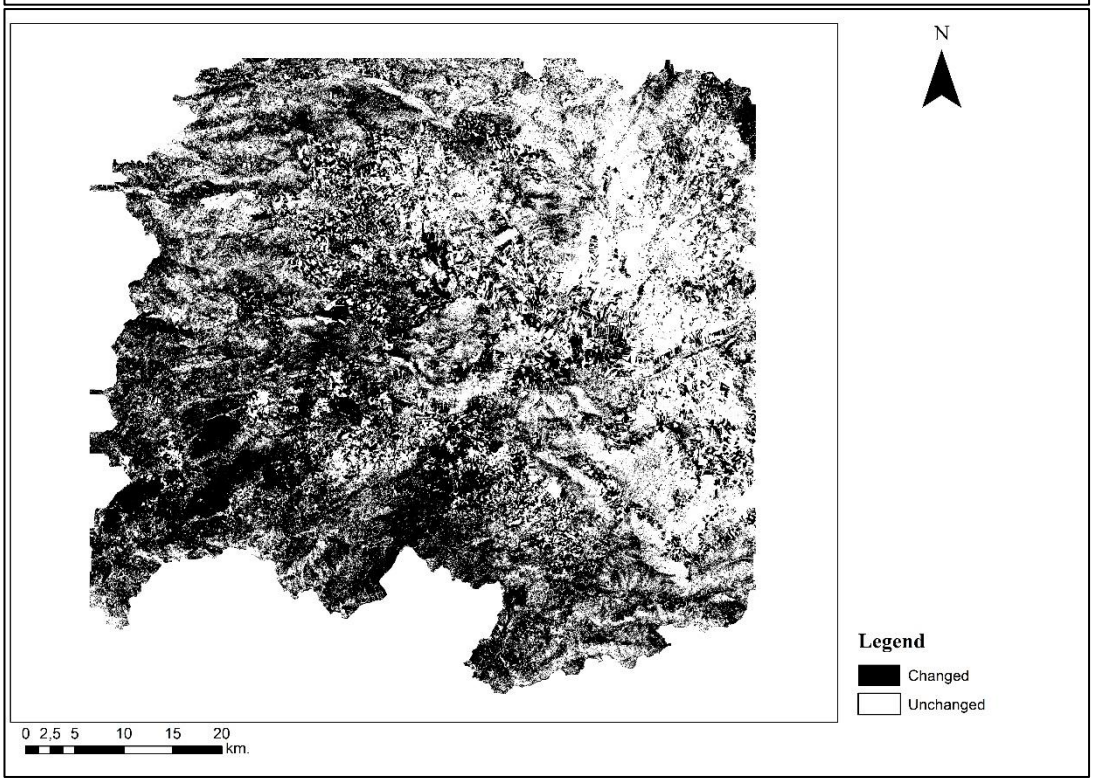
N
Legend
Changed
Unchanged
0 2,5 5 10 15 20
km.

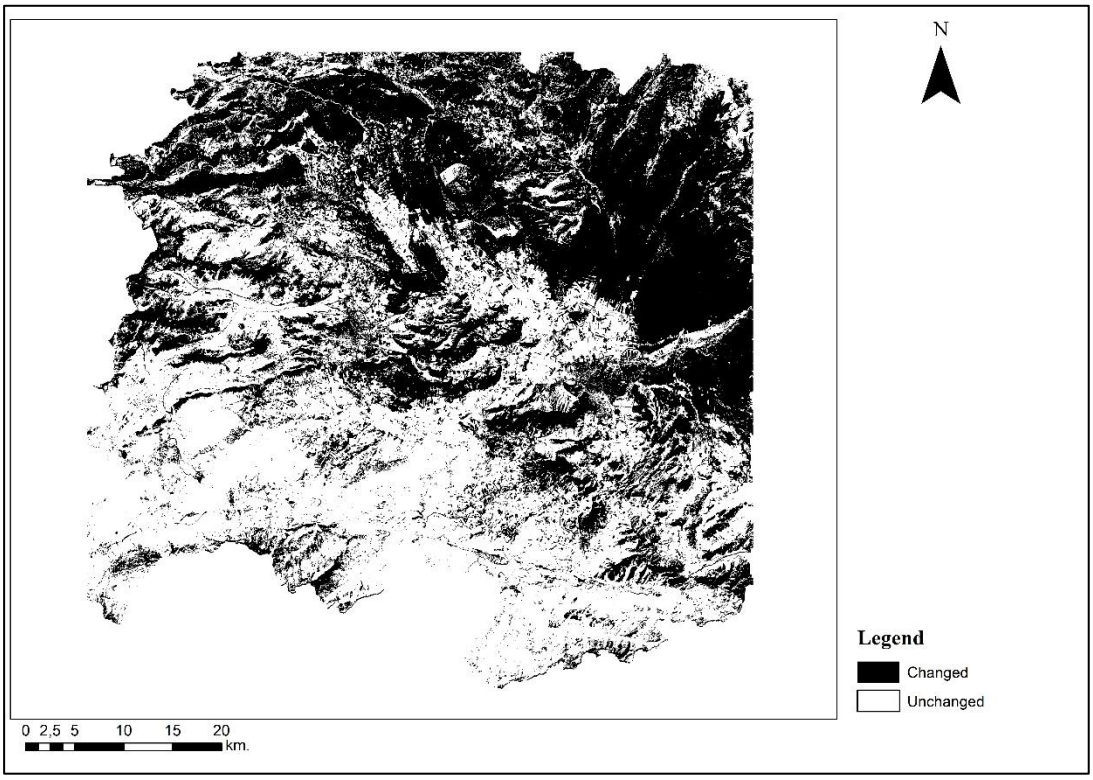
N
Legend
Changed
Unchanged
0 2,5 5 10 15 20
km.

APPENDIX C

Figure C1. Producer's Accuracy comparison between SVM and CDTL classifications for each years

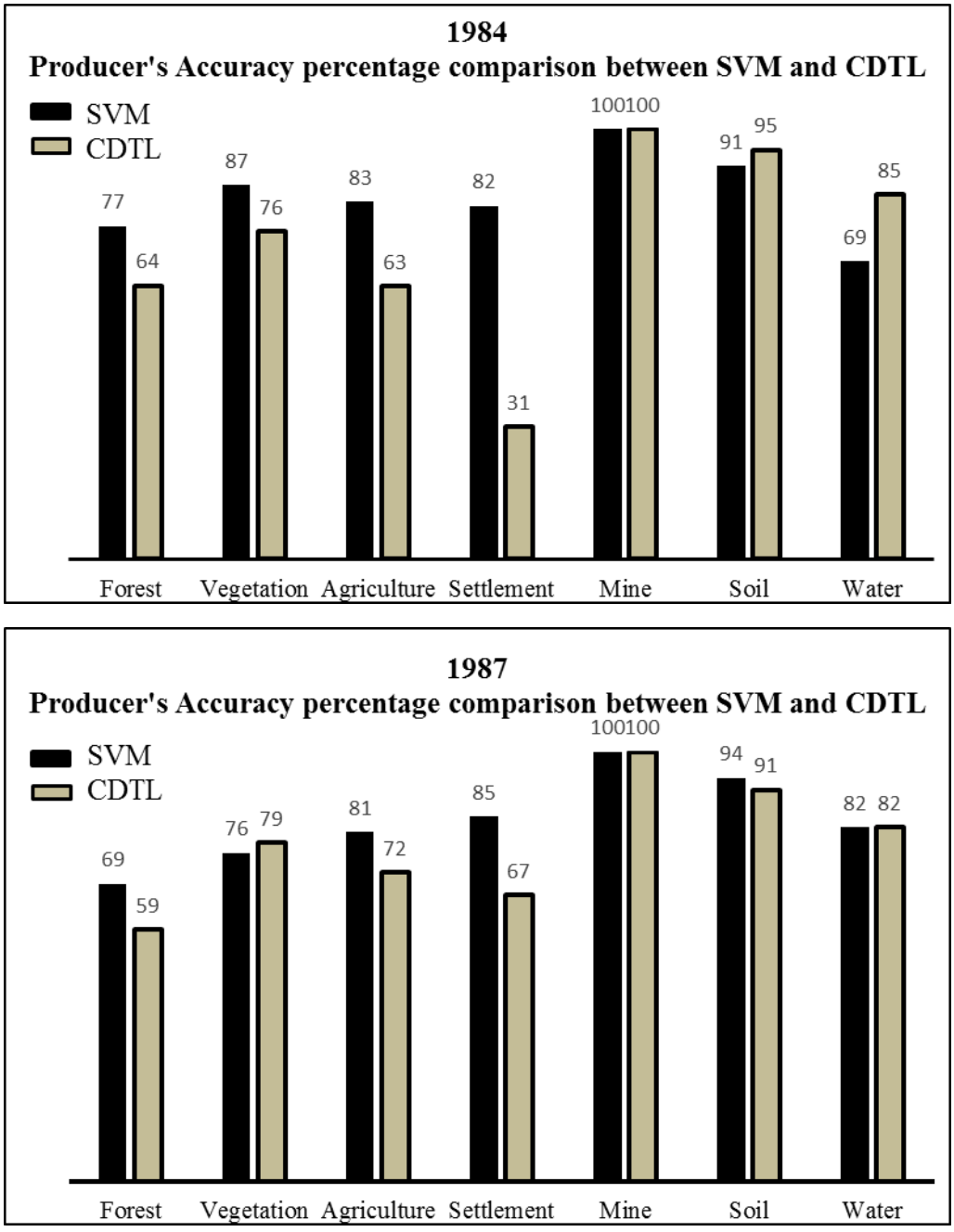

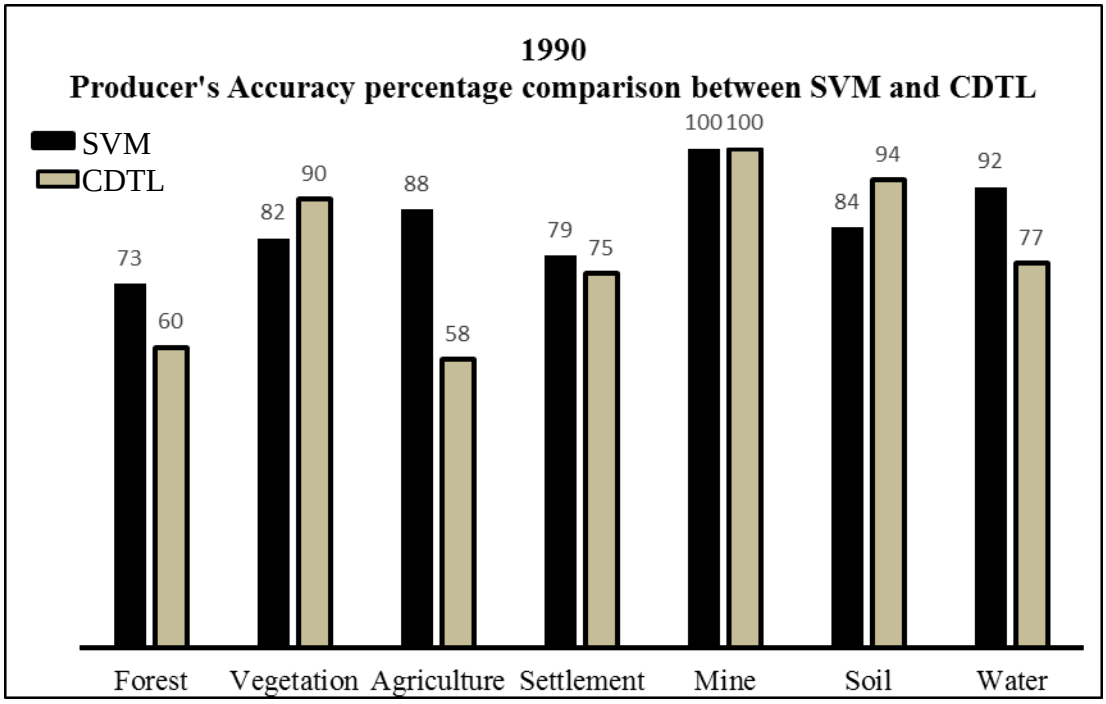
1990
Producer's Accuracy percentage comparison between SVM and CDTL
SVM
CDTL
73
60
82
90
88
58
79
75
100
100
84
94
92
77
Forest
Vegetation
Agriculture
Settlement
Mine
Soil
Water

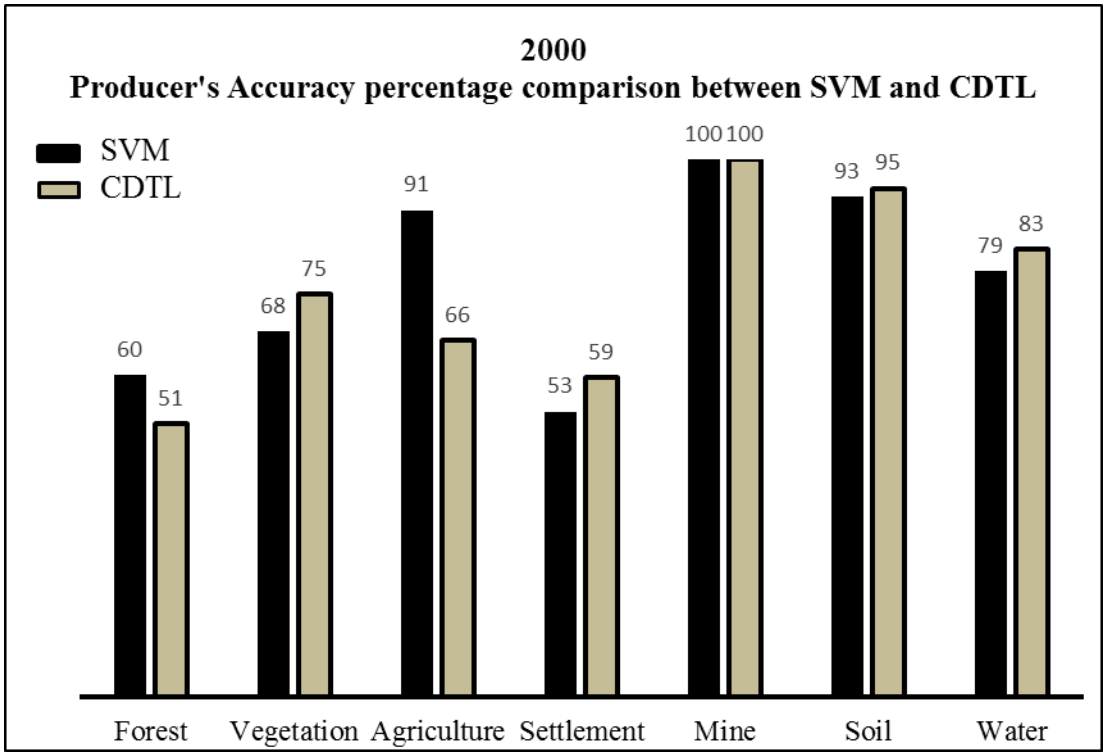
2000
Producer's Accuracy percentage comparison between SVM and CDTL
SVM
CDTL
60
51
68
75
91
66
53
59
100
100
93
95
79
83
Forest
Vegetation
Agriculture
Settlement
Mine
Soil
Water

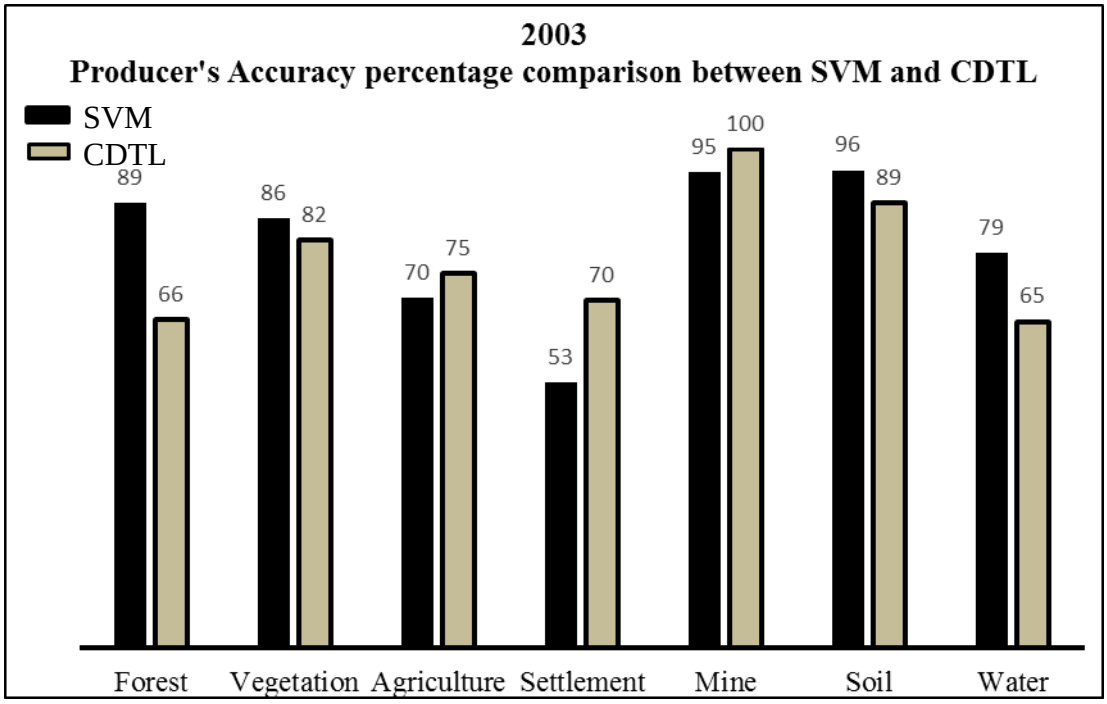
2003
Producer's Accuracy percentage comparison between SVM and CDTL
SVM
CDTL
89
66
86
82
70
75
53
70
95
100
96
89
79
65
Forest
Vegetation
Agriculture
Settlement
Mine
Soil
Water

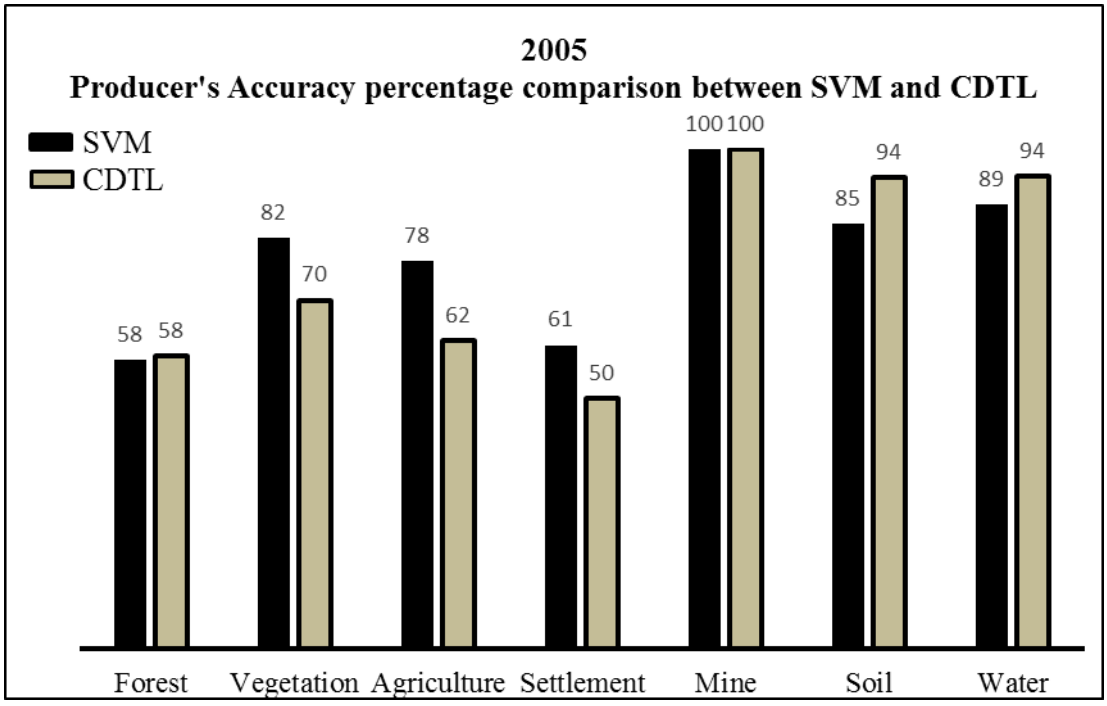
2005
Producer's Accuracy percentage comparison between SVM and CDTL
SVM
CDTL
58
58
82
70
78
62
61
50
100
100
85
94
89
94
Forest
Vegetation
Agriculture
Settlement
Mine
Soil
Water

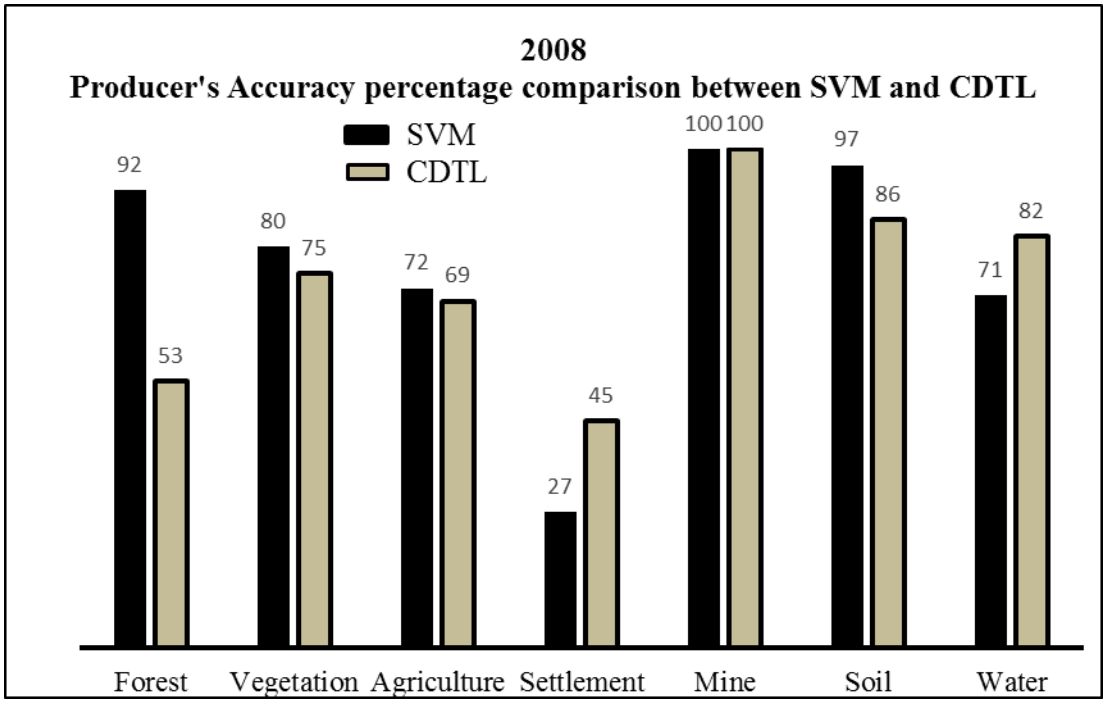
2008
Producer's Accuracy percentage comparison between SVM and CDTL
SVM
CDTL
92
53
80
75
72
69
27
45
100 100
97
86
71
82
Forest
Vegetation
Agriculture
Settlement
Mine
Soil
Water

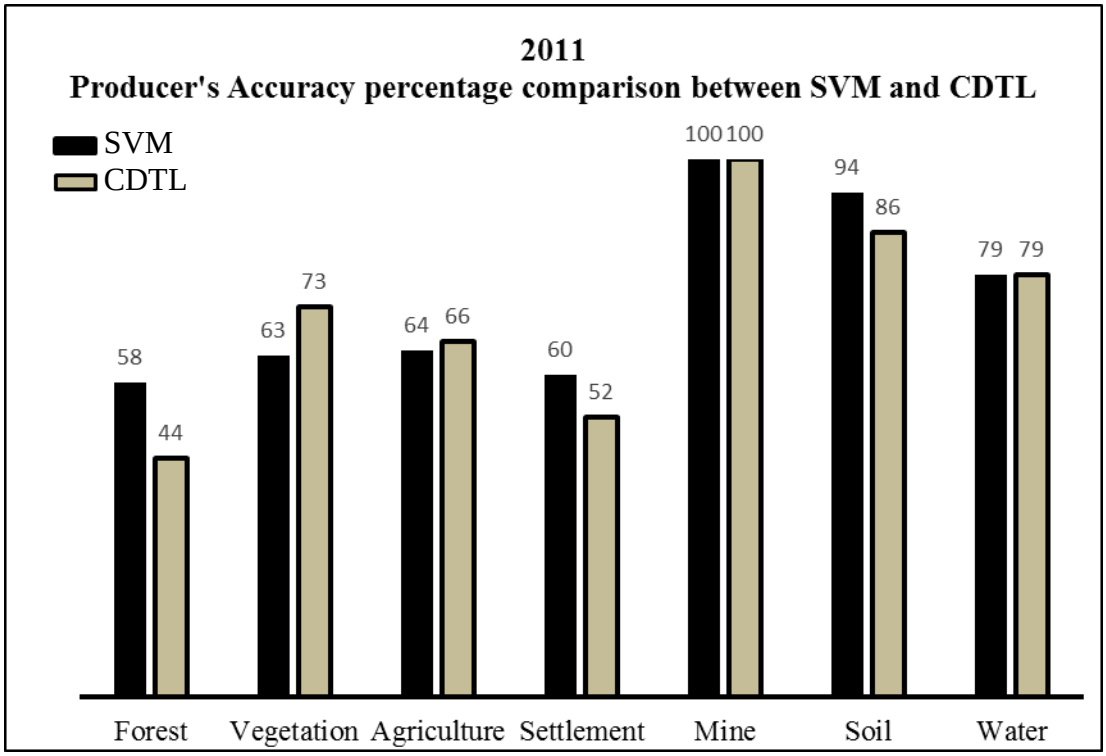
2011
Producer's Accuracy percentage comparison between SVM and CDTL
SVM
CDTL
58
44
63
73
64
66
60
52
100 100
94
86
79 79
Forest
Vegetation
Agriculture
Settlement
Mine
Soil
Water

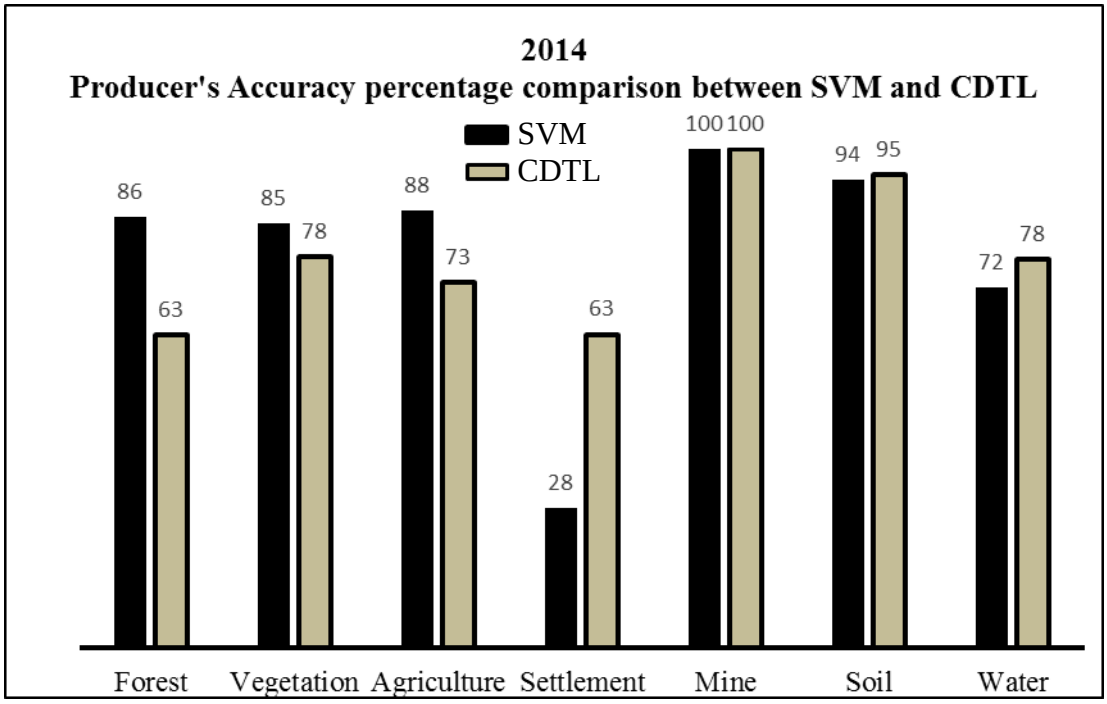
2014
Producer's Accuracy percentage comparison between SVM and CDTL
SVM
CDTL
86
63
85
78
88
73
28
63
100
100
94
95
72
78
Forest
Vegetation
Agriculture
Settlement
Mine
Soil
Water